



Universiteit  
Leiden  
The Netherlands

## **Clustering: a rational design principle for potentiated antibody therapeutics**

Oostindie, S.C.

### **Citation**

Oostindie, S. C. (2022, May 18). *Clustering: a rational design principle for potentiated antibody therapeutics*. Retrieved from <https://hdl.handle.net/1887/3304220>

Version: Publisher's Version

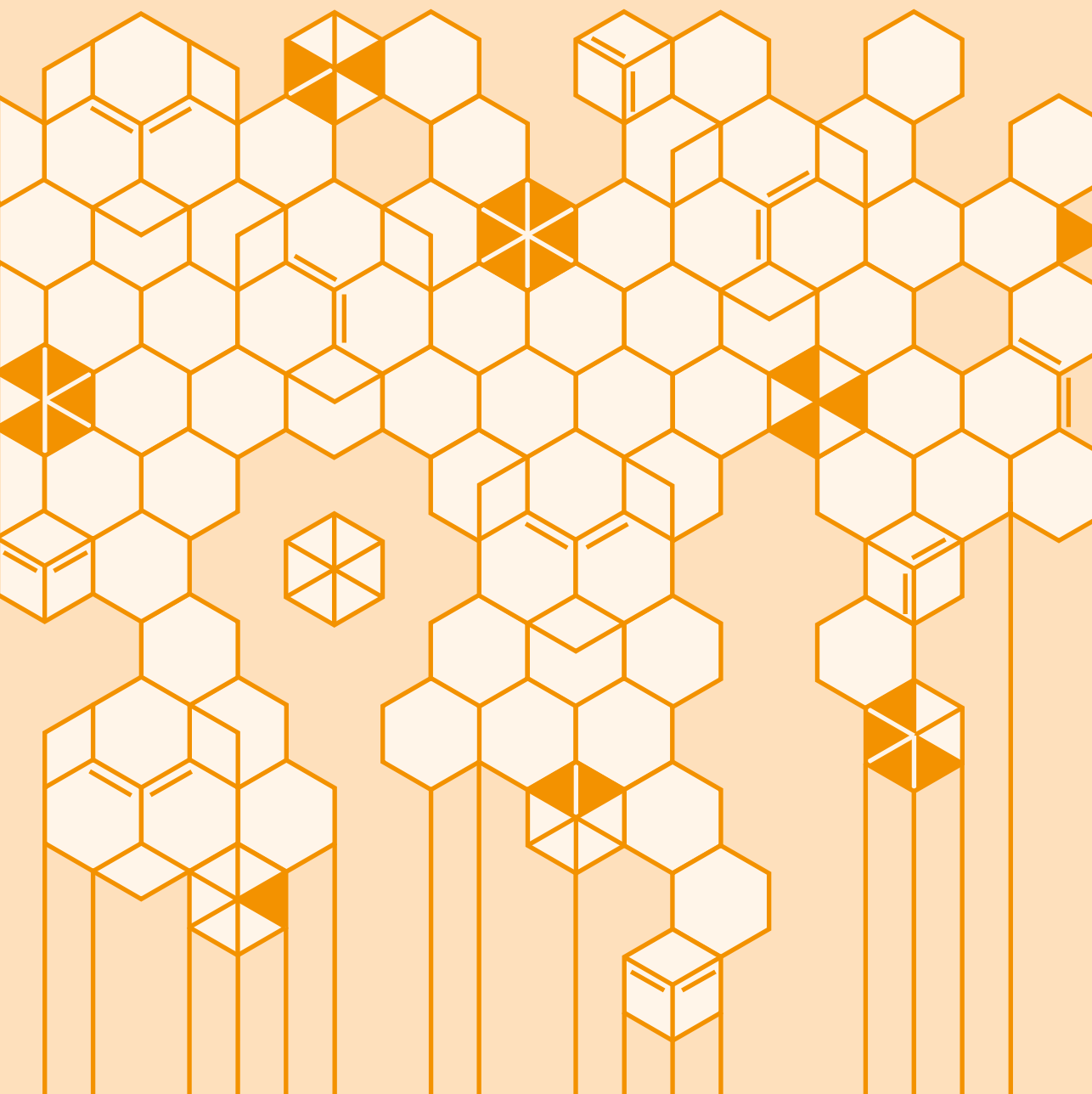
License: [Licence agreement concerning inclusion of doctoral thesis in the Institutional Repository of the University of Leiden](#)

Downloaded from: <https://hdl.handle.net/1887/3304220>

**Note:** To cite this publication please use the final published version (if applicable).

SIMONE C. OOSTINDIE

CLUSTERING: A RATIONAL  
DESIGN PRINCIPLE FOR  
POTENTIATED ANTIBODY  
THERAPEUTICS



CLUSTERING: A RATIONAL DESIGN PRINCIPLE FOR  
POTENTIATED ANTIBODY THERAPEUTICS

**Cover art**

Simone C. Oostindie  
Joost Bakker

**Production**

Joost Bakker,  
SCICOMVISUALS, Amsterdam, The Netherlands

**Design & Dtp**

De vliegende kiep,  
Amsterdam, The Netherlands

**Printed by**

Ipskamp Printing, Enschede

ISBN/EAN: 978 94 6421 572 4

Proefschrift Universiteit Leiden,  
Faculteit Geneeskunde  
© 2021, Simone Charlotte Oostindie,  
The Netherlands

Dit proefschrift werd mede  
mogelijk gemaakt met financiële  
steun van Genmab

# CLUSTERING: A RATIONAL DESIGN PRINCIPLE FOR POTENTIATED ANTIBODY THERAPEUTICS

## PROEFSCHRIFT

Ter verkrijging van  
de graad van doctor aan de Universiteit Leiden,  
op gezag van rector magnificus prof.dr.ir. H. Bijl,  
volgens besluit van het college voor promoties  
te verdedigen op woensdag 18 mei 2022  
klokke 15:00 uur

## DOOR

**Simone Charlotte Oostindie**

Geboren te Delft  
in 1990

**Promotor**

Prof. Dr. P.W.H.I. Parren

**Co-promotor**

Dr. E.C.W. Breij, Genmab, Utrecht

**Promotiecommissie**

Prof. Dr. J.G. Borst

Prof. Dr. T.W.J. Huizinga

Dr. L.A. Trouw

Prof. Dr. A.B. van Spriel,

    Radboud Universitair Medisch Centrum,

    Nijmegen

Dr. G. Vidarsson,

    Sanquin Research, and Landsteiner Laboratory,

    Amsterdam Universitair Medisch Centrum,

    Universiteit van Amsterdam

**VOOR PAULUS**





# TABLE OF CONTENTS

Chapter 1	Aim and outline of this thesis	9
Chapter 2	CD20 and CD37 antibodies synergize to activate complement by Fc-mediated clustering	17
Chapter 3	DuoHexaBody-CD37 <sup>®</sup> , a novel biparatopic CD37 antibody with enhanced Fc-mediated hexamerization as a potential therapy for B-cell malignancies	51
Chapter 4	Potent preclinical efficacy of DuoHexaBody-CD37 in B-Cell malignancies	83
Chapter 5	Therapeutic IgG antibody combinations acting as Bio-Logic AND gates	97
Chapter 6	Avidity in antibody effector functions and biotherapeutic drug design	135
Chapter 7	General discussion	179
	Summary	191
	Samenvatting in het Nederlands	193
	Dankwoord	197
	Publications	199
	Abbreviations	200
	Curriculum Vitae	202

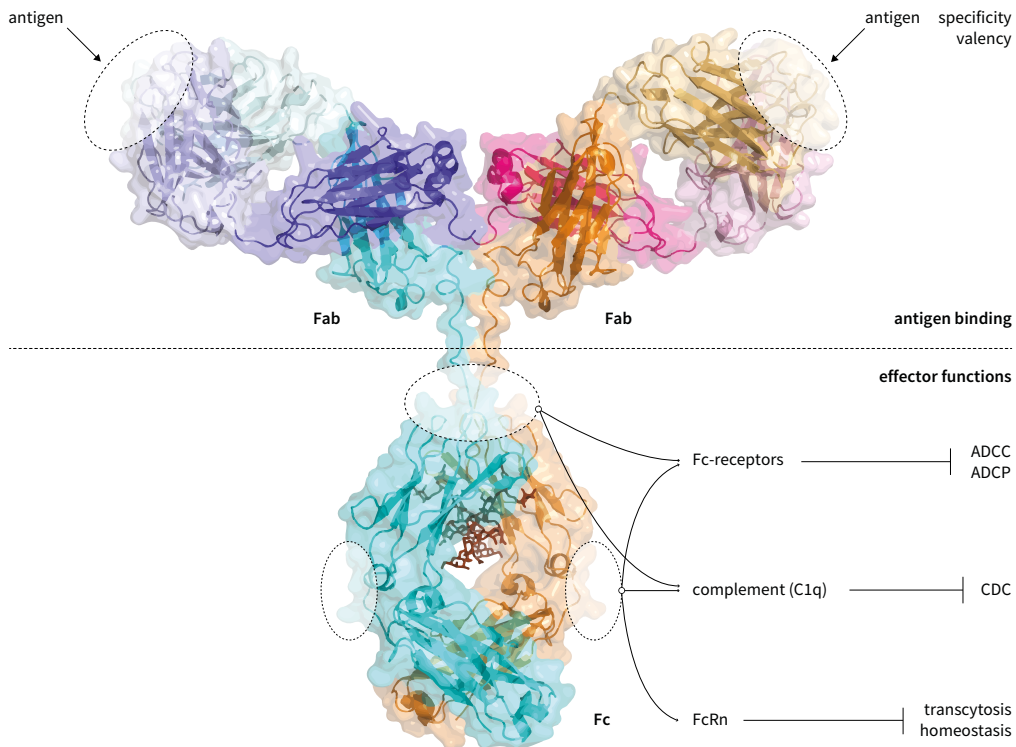


# 1

## AIM AND OUTLINE OF THIS THESIS

For centuries, the field of medicine was dominated by the belief in a Greek theory suggesting that all disease was caused by an imbalance of the four 'humors': black bile, yellow bile, phlegm and blood. It was not until the 19<sup>th</sup> century that this view was challenged by Ilya Metchnikoff, Emil Behring and Shibasaburo Kitasato<sup>2</sup>. Metchnikoff discovered that phagocytic cells could respond to injury in starfish and other invertebrates, while Behring and Kitasato reported that something in the blood of mice immunized with diphtheria and tetanus toxins seemed to mediate antitoxic activity. These observations shifted the paradigm towards a separation of the immune system into two branches: cellular immunity, for which protection is mediated by cells and humoral immunity, for which protection is mediated by substances in the humors, or body fluids. The substances present in the humors were later identified as antibodies produced by B lymphocytes, amongst other macromolecules such as complement components.

In humans, there are five classes of antibodies, or immunoglobulins (Ig) – IgA, IgD, IgE, IgG and IgM, of which IgG is the most abundant comprising of up to 75% of serum Ig. IgG, consisting of four subclasses (IgG1-4), is the main immunoglobulin class used as therapeutic agent. The general structure of IgG molecules is similar amongst subclasses, each consisting of a Fab domain with two Fab arms and an Fc domain (Figure 1). Structural differences between subclasses are mainly found in the hinge region, which confers the flexibility of the molecule, and accounts for a large part of the variation in effector function activation observed between subclasses. The Fab domain is responsible for highly specific antigen recognition and consists of two Fab-arms with identical binding sites that may bind simultaneously (bivalent) or alternately (monovalent) to target antigen(s). The Fc domain is involved in binding complement or Fc receptors (FcRs) present on immune cells and is

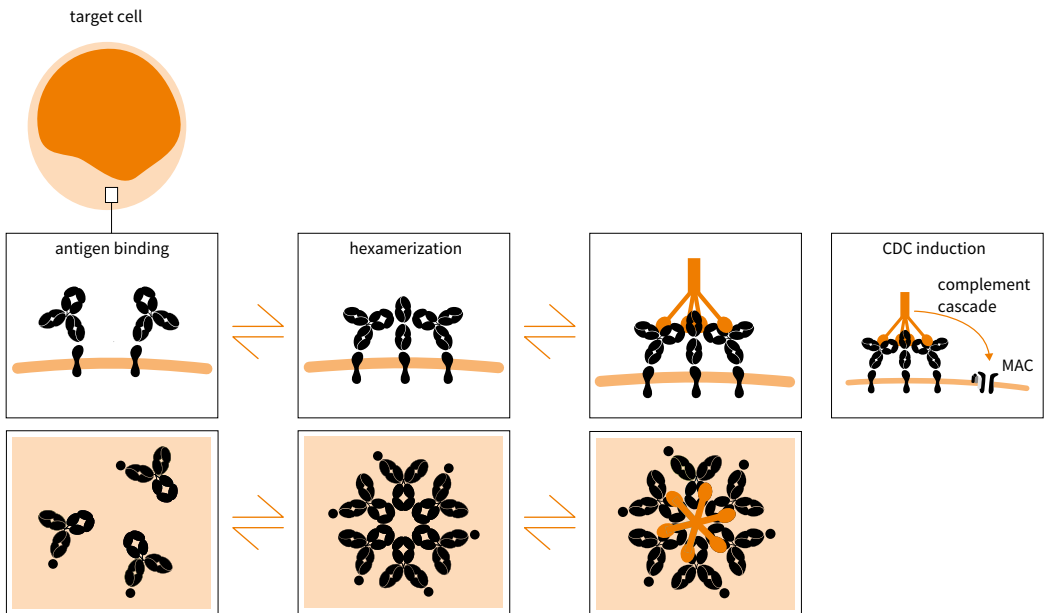


▲ **Figure 1**  
**IgG antibody structural and functional characteristics.**

thereby capable of activating a variety of effector functions including complement-dependent cytotoxicity (CDC), antibody-dependent cellular cytotoxicity (ADCC) and antibody-dependent cellular phagocytosis (ADCP). The Fc-region also contains a binding site for the neonatal Fc receptor (FcRn) that regulates serum half-life of IgG through transcytosis, or bidirectional transport across polarized cellular membranes.

Due to their high specificity and capacity to initiate a range of effector functions, antibodies are widely used as therapeutics for treatment of cancer, infectious diseases and autoimmunity. Antibody-based therapy evolved from passive immunization using polyclonal antisera to the discovery the hybridoma technique that allowed for the stable and controlled generation of monoclonal antibodies (mAbs) of single origin and specificity<sup>3,4</sup>. Although the success of mAb-based therapeutics is illustrated by over 100 antibodies having been granted marketing approval to date, disease heterogeneity and plasticity drive resistance to targeted therapies, demonstrating the continuous need for novel and more efficacious drugs<sup>5,6</sup>. A key feature shared by many high-

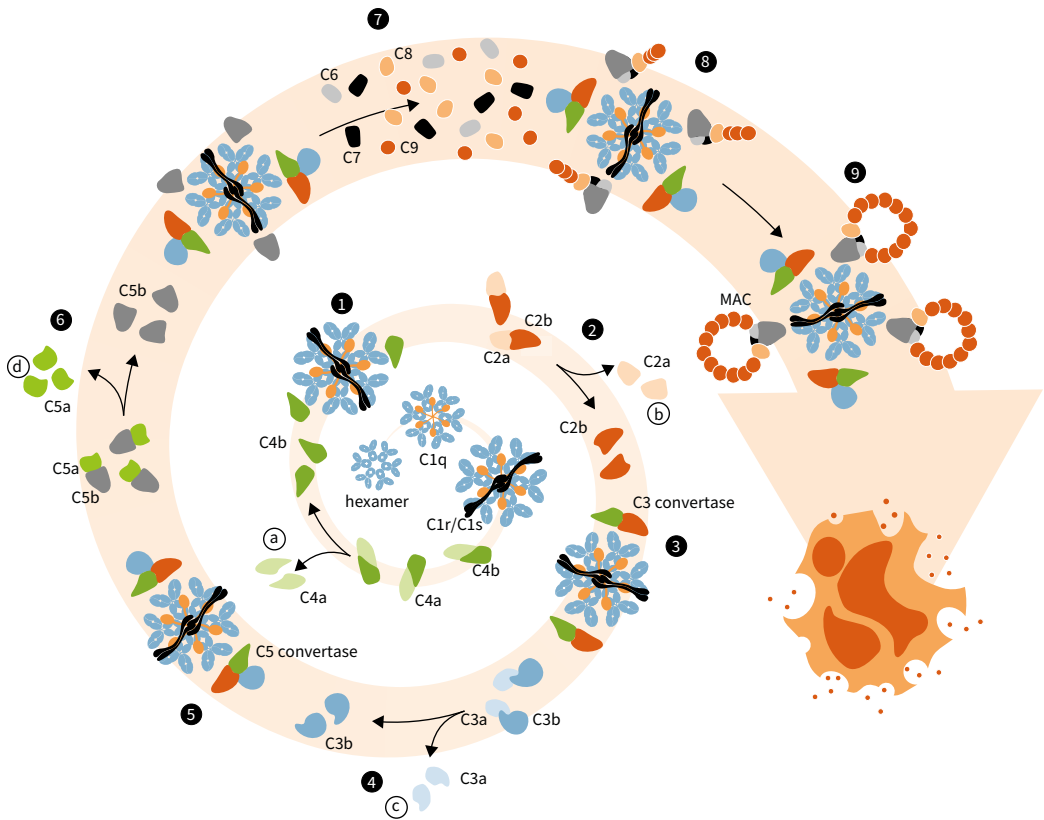
ly efficacious therapeutic antibodies including, amongst others, rituximab, ofatumumab, daratumumab, cetuximab and trastuzumab, is their capacity to engage the immune system and initiate effector functions. It is generally acknowledged that a single binding interaction between an antibody and antigen is generally not sufficient to successfully activate effector functions. Instead, antibody-mediated effector function activation often requires multi-valent target binding and cell surface clustering to effectively recruit immune effector molecules or cells of the immune system. For example, ADCC and ADCP are initiated through crosslinking of clustered antibody Fc domains with Fc gamma receptors (FcγRs) expressed on immune effector cells such as natural killer (NK) cells, macrophages and neutrophils. Furthermore, while it has long been recognized that membrane-bound antibodies or immune complexes can induce CDC through the so-called classical complement pathway, it was discovered more recently that this pathway is optimally activated by cell-bound IgGs organized into ordered hexameric clusters through non-covalent Fc-Fc interactions (Figure 2)<sup>7</sup>. Hexameric IgG clusters efficiently bind and activate complement factor C1, consisting of a hexavalent C1q subunit and associated proteases C1r and C1s, thereby triggering a series of enzymatic events at the cell surface that ultimately kill the cell (Figure 3)<sup>8</sup>.



▲ **Figure 2**

**The biology of IgG hexamerization and complement activation.**

Cell-bound IgGs organize into ordered hexameric clusters through non-covalent Fc-Fc interactions, thereby facilitating efficient C1q binding and activation of the complement cascade. Complement activation results in induction of complement-dependent cytotoxicity (CDC) through the formation of the membrane attack complex (MAC). Upper panels: side view, lower panels: top view.



▲ **Figure 3**

**Schematic overview of the classical complement pathway.**

Cell-bound IgGs organize into ordered hexameric clusters, thereby providing an optimal docking site for the hexavalent C1q subunit and associated proteases C1r and C1s that together form C1 complex. (1-4) Activated C1 complex cleaves C4 and C2 into fragments to form C3 convertase (C4b2b - according to old terminology, C2a and C4b2a<sup>1</sup>), which subsequently cleaves complement component C3 into C3a and C3b. (5) High density cell surface deposition of C3b results in association of C3b with existing C3 convertase to form C5 convertase (C4b3b2b). (6-8) Proteolysis of C5 by C5 convertase produces C5b, which triggers the terminal phase of complement activation by binding C6, C7, C8 and multiple copies of C9. (9) C5b-9 together form lytic pores in the cell membrane termed membrane attack complexes (MACs), which eventually kill the cell. (A-D) Proteolysis of complement components throughout the cascade generates small byproducts (anaphylatoxins) with potent chemoattractant properties, and opsonins that recruit and activate immune effector cells.

In natural biology, an effective immune response often involves multiple distinct antibodies originating from multiple B-cell clones, also referred to as polyclonal antibodies, which all bind specific structures, or antigens expressed on the pathogenic target. Importantly, a polyclonal antibody response often yields antibodies having the capacity to recognize multiple (non-overlapping) epitopes on a single antigen, thereby allowing for sufficient target occupancy and high local density of IgG Fc domains to enable clustering-dependent initiation of effector functions. Polyclonal antibodies therefore provide an advantage to the immune system compared to mAbs, which are of single origin and react against a single antigen or antigenic epitope. The single

antigen or epitope specificity of mAbs can strongly influence effector function activation. For example, many mAbs have a weak intrinsic ability to trigger the complement cascade and induce CDC. Multiple studies have shown that the lack of CDC activity by mAbs can be overcome by combining mAbs that recognize non-overlapping epitopes on a single antigen, suggesting that a certain level of ordered clustering via self-assembling Ig Fc domains is required prior to activation<sup>9-14</sup>.

The importance of antibody clustering in driving efficient effector function activation is becoming increasingly recognized, as is demonstrated by a broad spectrum of novel engineering strategies that leverage antibody clustering mechanisms to boost 'classical' as well as novel or 'designed' effector functions. In the context of 'classical' effector functions, antibody-mediated CDC can be improved by single point mutations in the IgG Fc domain that increase intermolecular Fc-Fc interactions upon binding to membrane-bound targets, thereby facilitating enhanced IgG hexamer formation and C1q binding<sup>7,15</sup>. Moreover, Fc domain engineering may also promote novel or 'designed' effector functions typically not obtainable using conventional mAbs. Enhancing IgG hexamerization was shown to allow the possibility of using monoclonal antibodies to induce hyper clustering of tumor necrosis factor receptor superfamily (TNFRSF) cell surface receptors including death receptor 5 (DR5) and OX40, resulting in increased agonistic activity<sup>11,16</sup>. Such engineering approaches illustrate the relevance of antibody clustering mechanisms in efficient effector function activation. The aim of this thesis was to further explore the role of antibody clustering in the mechanisms of action and design of effective antibody-based therapeutics. This research provides insight into the importance of 'ordered clustering' in antibody function and how this knowledge may directly translate into novel antibody-based therapeutics.

Previous research studying the molecular events governing complement activation demonstrated that antibody clustering or hexamerization after target binding to the cell surface is essential for optimal binding of C1q and efficient activation of the proteolytic cascade of complement<sup>7</sup>. In **Chapter 2**, we expanded on this observation and addressed the question whether multiple antibodies targeting different cell surface receptors are capable of cooperatively engaging in complement activation by forming mixed (hetero-) hexameric clusters on the cell surface.

Further building on the knowledge that enhancing intermolecular Fc-Fc interactions through single point mutations, such as E430G, in the Fc domain can increase antibody hexamerization and complement activation<sup>15</sup>, led us to explore the use of such mutations for the design of novel therapeutic antibodies with enhanced potency. In **Chapter 3**, we describe the generation and

characterization of DuoHexaBody-CD37, a novel CD37-targeting antibody for the treatment of B-cell malignancies, which potentially activates complement through a combination of dual epitope targeting and enhanced hexamerization. The preclinical activity of this antibody molecule was further studied *ex vivo* in primary tumor cells derived from patients with various B-cell malignancies, as described in **Chapter 4**. The potent preclinical anti-tumor activity observed *in vitro*, *ex vivo* and *in vivo* in a broad spectrum of B-cell malignancies provided the preclinical rationale to advance this molecule into clinical development and initiate a first-in-human clinical trial (NCT04358458).

Based on the observation that antibodies targeting different membrane receptors can hetero-oligomerize into mixed hexameric complexes upon antigen binding (**Chapter 2** of this thesis), we further explored whether IgG antibody pairs could be engineered to act as Boolean logic AND gates selectively activated after hetero-oligomerization in **Chapter 5**. Logic AND gates, originating from electrical engineering, can convert a combination of input signals into outputs according to the laws of Boolean algebra. Fc-domain engineered IgG antibody pairs were designed to integrate two antibody binding signals into a functional response output only on cells or surfaces co-expressing both antibody targets, thereby enabling the creation of antibody-based therapeutics with improved safety and efficacy.

Understanding the relationship between antibody structure and function and more specifically, how antibodies interact with their target, has proven to be essential in the design of next-generation antibody-based therapeutics. The crucial role of antibody (-mediated) clustering in successful effector function activation has become more apparent in recent years. In **Chapter 6** we reviewed (therapeutic) antibody effector mechanisms, with particular emphasis how antibody (-mediated) clustering impacts functional response. We further described how tuning of antibody clustering can serve as a design basis for engineering to increase the functional activity of novel antibody-based therapeutics and provided an overview of current translational efforts regarding clustering-based antibody concepts in the clinic.

Finally, a general discussion summarizing the key findings of this thesis is provided in **Chapter 7**. The relevance of these findings are discussed in the context of the past, present and future landscape of antibody-based therapeutics.



# REFERENCES

1. Bohlson SS, Garred P, Kemper C, Tenner AJ. Complement Nomenclature—Deconvoluted. *Front Immunol* 2019; **10**(1308).
2. Silverstein AM. Cellular versus humoral immunology: a century-long dispute. *Nat Immunol* 2003; **4**(5): 425-8.
3. Behring, Kitasato. Ueber das Zustandekommen der Diphtherie-Immunität und der Tetanus-Immunität bei Thieren. *Dtsch Med Wochenschr* 1890; **16**(49): 1113-4.
4. Köhler G, Milstein C. Continuous cultures of fused cells secreting antibody of predefined specificity. *Nature* 1975; **256**(5517): 495-7.
5. Kaplon H, Muralidharan M, Schneider Z, Reichert JM. Antibodies to watch in 2020. *MAbs* 2020; **12**(1): 1703531.
6. <https://www.antibodysociety.org/resources/approved-antibodies/>.
7. Diebolder CA, Beurskens FJ, de Jong RN, et al. Complement is activated by IgG hexamers assembled at the cell surface. *Science* 2014; **343**(6176): 1260-3.
8. Ugurlar D, Howes SC, de Kreuk B-J, et al. Structures of C1-IgG1 provide insights into how danger pattern recognition activates complement. *Science* 2018; **359**(6377): 794.
9. Klausz K, Berger S, Lammerts van Bueren JJ, et al. Complement-mediated tumor-specific cell lysis by antibody combinations targeting epidermal growth factor receptor (EGFR) and its variant III (EGFRvIII). *Cancer Sci* 2011; **102**(10): 1761-8.
10. Macor P, Mezzananza D, Cossetti C, et al. Complement activated by chimeric anti-folate receptor antibodies is an efficient effector system to control ovarian carcinoma. *Cancer Res* 2006; **66**(7): 3876-83.
11. Overdijk MB, Strumane K, Beurskens FJ, et al. Dual epitope targeting and enhanced hexamerization by DR5 antibodies as a novel approach to induce potent anti-tumor activity through DR5 agonism. *Mol Cancer Ther* 2020.
12. Peschiera I, Giuliani M, Giusti F, et al. Structural basis for cooperativity of human monoclonal antibodies to meningococcal factor H-binding protein. *Commun Biol* 2019; **2**(1): 241.
13. Rijkers M, Schmidt D, Lu N, et al. Anti-HLA antibodies with complementary and synergistic interaction geometries promote classical complement activation on platelets. *Haematologica* 2019; **104**(2): 403-16.
14. Schütze K, Petry K, Hambach J, et al. CD38-Specific Biparatopic Heavy Chain Antibodies Display Potent Complement-Dependent Cytotoxicity Against Multiple Myeloma Cells. *Front Immunol* 2018; **9**: 2553-.
15. de Jong RN, Beurskens FJ, Verploegen S, et al. A Novel Platform for the Potentiation of Therapeutic Antibodies Based on Antigen-Dependent Formation of IgG Hexamers at the Cell Surface. *PLoS Biol* 2016; **14**(1): e1002344.
16. Zhang D, Goldberg MV, Chiu ML. Fc Engineering Approaches to Enhance the Agonism and Effector Functions of an Anti-OX40 Antibody. *J Biol Chem* 2016; **291**(53): 27134-46.



# CD20 AND CD37 ANTIBODIES SYNERGIZE TO ACTIVATE COMPLEMENT BY FC-MEDIATED CLUSTERING

Simone C. Oostindie,<sup>1,2,@</sup> Hilma J. van der Horst,<sup>3</sup> Margaret A. Lindorfer,<sup>4</sup>  
Erika M. Cook,<sup>4</sup> Jillian C. Tupitza,<sup>4</sup> Clive S. Zent,<sup>5</sup> Richard Burack,<sup>5</sup> Karl R. VanDerMeid,<sup>5</sup>  
Kristin Strumane,<sup>1</sup> Martine E. D. Chamuleau,<sup>3</sup> Tuna Mutis,<sup>3</sup> Rob N. de Jong,<sup>1</sup>  
Janine Schuurman,<sup>1</sup> Esther C. W. Breij,<sup>1</sup> Frank J. Beurskens,<sup>1</sup> Paul W. H. I. Parren,<sup>2,6</sup>  
and Ronald P. Taylor<sup>4,@</sup>

Haematologica 2019 Sep;104(9):1841-1852.

- 1 Genmab, Utrecht, The Netherlands;
  - 2 Department of Immunohematology and Blood Transfusion, Leiden University Medical Center, Leiden, The Netherlands;
  - 3 Department of Hematology, Amsterdam University Medical Center, Amsterdam, The Netherlands;
  - 4 Department of Biochemistry and Molecular Genetics, University of Virginia School of Medicine, Charlottesville, Virginia, USA;
  - 5 Wilmot Cancer Institute, University of Rochester Medical Center, Rochester, New York, USA;
  - 6 Lava Therapeutics, Utrecht, The Netherlands;
- @ Corresponding author

### Corresponding authors

**Simone C. Oostindie**, Genmab, Uppsalalaan 15, 3584CT, Utrecht, The Netherlands; e-mail: [sio@genmab.com](mailto:sio@genmab.com); and **Ronald P. Taylor**, Department of Biochemistry and Molecular Genetics, Box 800733, University of Virginia School of Medicine, Charlottesville, Virginia, 22908, USA; e-mail: [rpt@virginia.edu](mailto:rpt@virginia.edu)

### Acknowledgements

The authors would like to thank Joost Bakker (SCICOMVISUALS) for designing Figure 7.

## ABSTRACT

CD20 monoclonal antibody therapies have significantly improved the outlook for patients with B-cell malignancies. However many patients acquire resistance, demonstrating the need for new and improved drugs. We previously demonstrated that the natural process of antibody hexamer formation on targeted cells allows for optimal induction of complement-dependent cytotoxicity. Complement-dependent cytotoxicity can be potentiated by introducing a single point mutation such as E430G in the IgG Fc domain that enhances intermolecular Fc-Fc interactions between cell-bound IgG molecules, thereby facilitating IgG hexamer formation. Antibodies specific for CD37, a target that is abundantly expressed on healthy and malignant B cells, are generally poor inducers of complement-dependent cytotoxicity. Here we demonstrate that introduction of the hexamerization-enhancing mutation E430G in CD37-specific antibodies facilitates highly potent complement-dependent cytotoxicity in chronic lymphocytic leukemia cells *ex vivo*. Strikingly, we observed that combinations of hexamerization-enhanced CD20 and CD37 antibodies cooperated in C1q binding and induced superior and synergistic complement-dependent cytotoxicity in patient-derived cancer cells compared to the single agents. Furthermore, CD20 and CD37 antibodies colocalized on the cell membrane, an effect that was potentiated by the hexamerization-enhancing mutation. Moreover, upon cell surface binding, CD20 and CD37 antibodies were shown to form mixed hexameric antibody complexes consisting of both antibodies each bound to their own cognate target, so-called hetero-hexamers. These findings give novel insights into the mechanisms of synergy in antibody-mediated complement-dependent cytotoxicity and provide a rationale to explore Fc-engineering and antibody hetero-hexamerization as a tool to enhance the cooperativity and therapeutic efficacy of antibody combinations.

# INTRODUCTION

Monoclonal antibodies (mAbs) have become the backbone of treatment regimens for several cancer indications. The chimeric immunoglobulin (Ig) G1 CD20 mAb rituximab was the first mAb approved for clinical use in cancer therapy. CD20 is expressed on more than 90% of mature B cells and rituximab is widely used to treat B-cell malignancies.<sup>1-3</sup> However, many patients do not experience complete remission or acquire resistance to rituximab treatment, thereby demonstrating the need for improved mAb therapeutics or alternative tumor-targeting strategies.<sup>4-6</sup>

mAbs employ various mechanisms to eliminate cancer cells, such as induction of programmed cell death or Fc-mediated effector functions, including antibody-dependent cell-mediated cytotoxicity (ADCC), antibody-dependent cellular phagocytosis (ADCP) and complement-dependent cytotoxicity (CDC), which can be increased by Fc engineering.<sup>7</sup> ADCC and ADCP, for example, can be enhanced by improving Fc $\gamma$ R binding through Fc glyco-engineering or amino acid modifications.<sup>8-11</sup> Likewise, C1q binding and CDC can be increased by amino acid substitutions in Fc domains.<sup>12,13</sup> CDC is initiated when membrane-bound antibodies bind the hexavalent C1q molecule, which together with C1r and C1s forms the C1 complex, the first component of the classical complement pathway. C1 activation triggers an enzymatic cascade that leads to covalent attachment of opsonins to target cells, and the generation of potent chemo attractants, anaphylatoxins and membrane attack complexes (MACs).<sup>14</sup> IgG antibodies bound to cell surface antigens assemble into ordered hexamers, providing high avidity docking sites to which C1 binds and is activated.<sup>15</sup> IgG hexamer formation and complement activation can be enhanced by single point mutations in IgG Fc domains, such as E430G, which increase interactions between Fc domains of cell-bound IgG.<sup>16</sup> The hexamerization-enhanced (Hx) CD20-targeting mAb 7D8 displayed strongly enhanced CDC of B cells from patients with chronic lymphocytic leukemia (CLL), which often demonstrate complement resistance due to low CD20 and high membrane complement regulatory protein (mCRP) expression.<sup>16-18</sup>

In polyclonal antibody responses, antibodies against distinct epitopes or antigens are thought to cooperate resulting in increased effector functions against target cells. This increase can be mimicked in mAb combinations or cocktails. For example, monoclonal EGFR antibodies do not induce CDC *in vitro*, but combinations of mAbs against multiple EGFR epitopes induced potent CDC.<sup>19,20</sup>

CD37, which is abundantly expressed on B cells, represents a promising therapeutic target for the treatment of B-cell malignancies.<sup>21,22</sup> Currently known CD37 mAbs in clinical development however, are generally poor inducers of CDC.<sup>23-27</sup> Here we show that introducing Hx mutations into CD37 mAbs strongly potentiated CDC of CLL cells, and that combinations of CD20 and CD37 targeting mAbs could further enhance CDC of tumor cell lines and primary patient cells. We investigated the mechanism behind the synergistic CDC activity of CD20 and CD37 mAbs, and found that the mAb combinations activate complement cooperatively. The two mAbs formed mixed hexameric antibody complexes consisting of both antibodies each bound to their cognate targets, which we termed hetero-hexamers. The concept of hetero-hexamer formation and the use of Fc-Fc interaction enhancing mutations could serve as a tool to enhance cooperativity, and thereby the tumor killing capacity, of mAb combinations.

# METHODS

## Cells

Daudi, Raji and WIL2-S B-lymphoma cell lines were obtained from the American Type Culture Collection (ATCC no. CCL-213, CCL-86 and CRL-8885 respectively). All primary patient cells used in this study were obtained after written and informed consent and stored using protocols approved by the institutional review boards in accordance with the declaration of Helsinki (see Online Supplementary Methods).

## Antibodies and reagents

mAbs IgG1-CD20-7D8, IgG1-CD20-11B8, IgG1-CD37 clone 37.3 and IgG1-gp120 were recombinantly produced at Genmab.<sup>18,28-30</sup> The HIV-1 gp120 mAb b12 was used to determine assay background signal. Mutations to enhance or inhibit Fc-Fc interactions were introduced in expression vectors encoding the antibody heavy chain by gene synthesis (GeneArt). Rituximab (MabThera<sup>®</sup>), ofatumumab (Arzerra<sup>®</sup>) and obinutuzumab (Gazyvaro<sup>®</sup>) were obtained from the pharmacy (UMC Utrecht). See Online Supplementary Methods for details on reagents used.

## CDC assays

CDC assays with CLL patient cells were performed with human complement as described.<sup>31</sup> CDC assays with B-lymphoma cell lines and patient-derived B-lymphoma cells were performed using 100,000 target cells incubated (45 minutes at 37 °C) with a mAb concentration series and pooled normal human serum (NHS, 20% final concentration) as a complement source. Killing was calculated as the percentage of propidium iodide (PI) or 7-AAD positive cells determined by flow cytometry. See Online Supplementary Methods for details on cell markers used to define cell populations.

## Expression analysis

Expression levels of cellular markers were determined using an indirect immunofluorescence assay (QIFIKIT<sup>®</sup>, Agilent Technologies) according to the manufacturer's instructions (see online Supplementary Methods).

## C1q binding and CDC efficacy

Daudi cells ( $3 \times 10^6$  cells/mL) were incubated with 10 µg/mL mAb and a concentration series of purified human C1q for 45 minutes at 37 °C. After washing, cells were incubated with FITC-labeled rabbit anti-human C1q antibody for 30 minutes at 4 °C and analyzed on a FACS Canto II flow cytometer (BD Biosciences, CA, USA). The efficiency of C1q binding and subsequent CDC was



assessed as described above using fixed mAb concentrations, a concentration series of purified C1q and 20% C1q depleted serum.

### **Confocal microscopy**

Raji cells were opsonized with A488 labeled Hx-CD20-7D8 and A594 labeled Hx-CD37 mAbs (2.5 µg/mL final concentrations), and incubated for 15 minutes at room temperature. After washing, cells were placed on a poly-D lysine-coated slide and images were captured with a Zeiss AxioObserver LSM 700 microscope using plan-Apochromat 63X/1.40 Oil DIC M27 objective lenses and acquired/processed using Zen software.

### **Förster Resonance Energy Transfer (FRET) analysis**

Proximity-induced FRET was determined by measuring energy transfer between cells incubated with A555-conjugated donor and A647-conjugated acceptor mAbs using flow cytometry (see Online Supplementary Methods). The dynamic range of FRET analysis by flow cytometry was determined using control mAbs, as specified in Supplementary Figure 1.

### **Data processing and statistical analyses**

All values are expressed as the mean ± standard deviation of at least two independent experiments. Graphs were generated and analyzed using GraphPad Prism 7.0 (CA, USA). Differences between two groups were analyzed using paired Student's t-test with two-tailed 95% confidence intervals and between more groups by paired or unpaired one-way ANOVA followed by a Tukey post-hoc multiple comparisons test. Significant differences are indicated as: \*p < 0.05, \*\*p < 0.01, \*\*\*p < 0.001 and \*\*\*\*p < 0.0001. See Online Supplementary Methods for details on synergy and colocalization analysis.

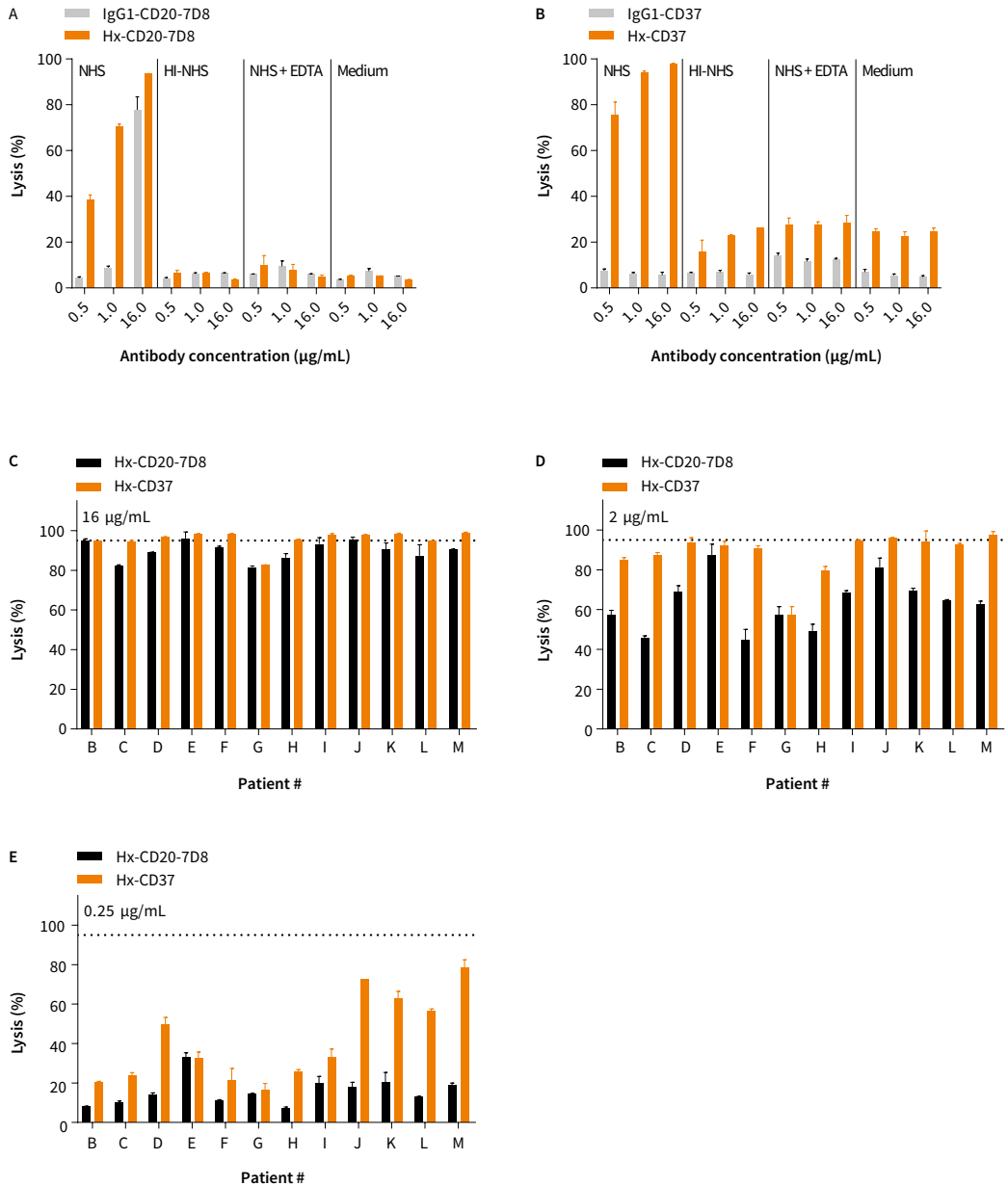
# RESULTS

## **Hexamerization-enhancing mutations in CD20 and CD37 mAbs substantially enhance CDC of CLL B cells**

We previously reported increased CDC with engineered mAbs containing Hx mutations in the Fc domain.<sup>15,16</sup> We therefore investigated whether introducing the Hx mutation E430G into the CD37 chimeric IgG1 mAb 37.3 could potentiate CDC in B cells isolated from CLL patients and compared this to the CD20 mAb IgG1-CD20-7D8 with and without a Hx mutation. Wild-type (WT) IgG1-CD20-7D8 promoted considerable CDC of CLL B cells and CDC was increased by the E430G mutation (Figure 1A). While WT IgG1-CD37 efficiently binds to CLL B cells, it was ineffective at inducing CDC (Figure 1B; Supplementary Figure 2), in contrast to Hx-CD37 (Figure 1B). For both Hx-CD20-7D8 and Hx-CD37, high levels of cell killing largely required active complement, since CDC was almost absent in heat-inactivated NHS, NHS supplemented with EDTA or medium alone (Figure 1 A-B). Background killing of cells from patient A mediated by Hx-CD37 in the absence of complement was slightly higher than expected. However, in C1q-depleted serum, background killing was 16%, compared to 6% for cells reacted with Hx-CD20-7D8. Background killing in C1q-depleted serum for 6 other CLL patient samples averaged 13% and 14% for cells reacted with Hx-CD20-7D8 and Hx-CD37, respectively. Reaction in NHS increased CDC to averages of 91% and 95%, respectively. Introduction of the Hx mutation E430G into CD20 and CD37 mAbs did not affect pharmacokinetic profiles and binding to FcRn (data not shown).<sup>16</sup> At the highest concentration (16 µg/mL) Hx-CD37 induced ≥ 95% CDC of tumor B cells for 9 out of 12 patients (Figure 1C). At concentrations of 0.25 and 2 µg/mL, Hx-CD37 generally demonstrated higher potency than Hx-CD20-7D8 (Figure 1D-E), which may be explained by higher expression levels of CD37 (approximately 2-fold) in the majority of CLL samples (Supplementary Figure 3A-B).

## **CD20 and CD37 mAbs synergistically induce CDC of malignant B cells**

We investigated the CDC activity of combinations of WT CD20 and WT CD37 mAbs, using two different CD20 mAbs. The ability to activate complement represents a key distinction between type I CD20 mAbs which mediate strong CDC and type II CD20 mAbs, which only mediate weak CDC.<sup>32</sup> The effect of combining WT type I CD20 mAb 7D8 or WT type II CD20 mAb 11B8 with WT CD37 mAb on CDC was assessed using Daudi cells. As expected, WT IgG1-CD20-7D8 showed potent CDC activity (96.6% cell lysis), whereas WT IgG1-CD37 did not induce CDC (Figure 2A). The combination of WT IgG1-CD20-7D8 and WT IgG1-CD37 did not demonstrate enhanced CDC. However, while neither WT IgG1-CD20-11B8 nor WT IgG1-CD37 induced CDC as single agents, the combination



▲ **Figure 1**

**Hexamerization-enhancing mutations in CD20 and CD37 mAbs substantially enhance CDC of CLL B cells.**

(A-B) CDC of B cells obtained from patient A with CLL. Cells were opsonized with different concentrations of CD20 mAb 7D8 as wild type (IgG1-CD20-7D8) or with a hexamerization-enhancing mutation (Hx-CD20-7D8) (A); or CD37 mAb 37.3 as wild type (IgG1-CD37) or with a hexamerization-enhancing mutation (Hx-CD37) (B) in the presence of 50% pooled normal human serum (NHS), heat-inactivated (HI) NHS, NHS + EDTA or medium. Representative examples of three replicate experiments are shown. (C-E) CDC of B cells obtained from 12 different CLL patients (patient B-M). CLL B cells were opsonized with 16 µg/mL (C), 2 µg/mL (D) or 0.25 µg/mL (E) Hx-CD20-7D8 or Hx-CD37. The dashed line represents 95% cell lysis. CDC induction is expressed as the percentage lysis determined by the fraction of TO-PRO-3 positive cells and data shown are mean and standard deviation (SD) of duplicate measurements.

promoted strong lysis of approximately 60% (Figure 2B). Minimal cell lysis was observed in experiments with heat-inactivated serum, indicating that that cell killing was largely dependent on complement (Supplementary Figure 4).

We additionally examined whether combinations of CD20 and CD37 mAbs with Hx mutations also showed cooperativity in CDC by testing mAb combinations using a full dose-response matrix (8x8 serial dilution grid) based on the EC50 values of the single mAbs. Surprisingly, both Hx-CD20-7D8 and Hx-CD20-11B8 in combination with Hx-CD37 showed enhanced CDC of Daudi cells compared to the single agents (Figure 2C, Supplementary Figure 5A). We next assessed whether the observed combination effect was synergistic using the Loewe additivity-based combination index (CI) score calculated by CompuSyn, whereby effects were categorized as synergistic (CI < 1), additive (CI = 1) or antagonistic (CI > 1).<sup>33</sup> The Loewe additivity-based model assumes synergy when the effect of a drug combination is higher than the effect of a drug combined with itself, and takes into account both the potency and the shape of the dose-effect curve of each drug in the dose-response matrix. Synergy was observed for both Hx-CD20-7D8 and Hx-CD20-11B8 when combined with Hx-CD37, with average CI values of 0.37 and 0.31 (effective dose - ED95), respectively (Figure 2D, Supplementary Figure 5B, Supplementary Table 1). At the lower tested mAb concentrations, synergy was more profound (lower CI values) for combinations of Hx-CD37 with type II CD20 mAb-derived Hx-CD20-11B8 than with type I CD20 mAb-derived Hx-CD20-7D8.

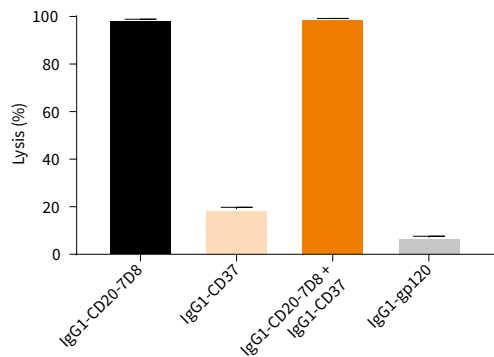
In addition to Daudi cells, we used two other B-cell lines expressing various levels of CD20 and CD37 to further examine the cooperativity in CDC between combinations of Hx-CD37 with Hx-CD20 mAbs or with clinically validated CD20 mAbs. Across all B-cell lines tested, enhanced CDC activity was observed for

**Figure 2** ▶

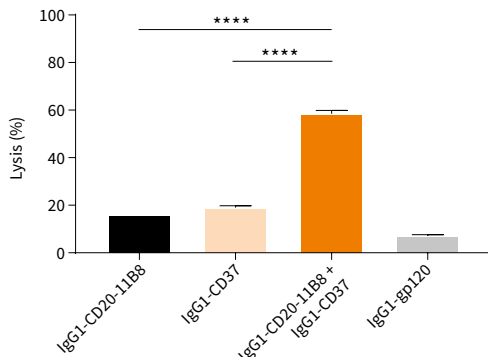
**CD20 and CD37 mAbs synergistically induce CDC of malignant B cells.**

(A-B) CDC on Daudi cells opsonized with 30 µg/mL WT type I CD20 mAb 7D8 (IgG1-CD20-7D8) (A) or type II CD20 mAb 11B8 (IgG1-CD20-11B8) (B), CD37 mAb 37.3 (IgG1-CD37), or a combination thereof (15 + 15 µg/mL) in the presence of 20% NHS. CDC induction is expressed as the percentage lysis determined by the fraction of propidium iodide (PI)-positive cells. Data shown are mean and SD of triplicate measurements. (C) 8 x 8 CDC dose response matrix plot for the combination of hexamerization-enhanced CD37 mAb Hx-CD37 (0-0.8 µg/mL) with hexamerization-enhanced CD20 mAb Hx-CD20-11B8 (0-8 µg/mL), tested on Daudi cells and categorized as a color gradient from green (0% lysis) to yellow (50% lysis) to red (100% lysis). HIV gp120-specific mAb b12 (IgG1-gp120) was used as a negative control human mAb. (D) Loewe additivity-based Combination index (CI) values calculated by CompuSyn for the CDC dose response matrix as described in (C) and categorized as synergistic (<1, red), additive (1, white) and antagonistic (>1, blue). Representative examples of two replicate experiments are shown. (E) CDC and CD37 expression analysis on Daudi, Raji and WIL2-S cells. For the CDC assay, cells were opsonized with Hx-CD37 (10 µg/mL), different CD20 mAb variants (10 µg/mL) or combinations thereof (10 + 10 µg/mL). Data show the mean of nine replicates collected from three independent experiments. Expression levels were determined using QIFIKIT analysis. The number of antibody molecules per cell was calculated from the antibody-binding capacity (mean fluorescence intensity - MFI) normalized to a calibration curve, according to the manufacturer's guidelines. Expression data show the mean of four replicates collected from two independent experiments.

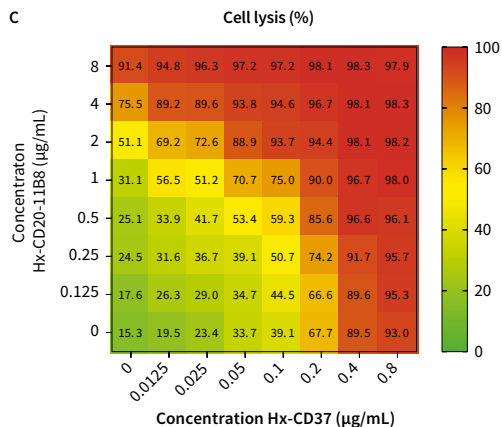
**A**



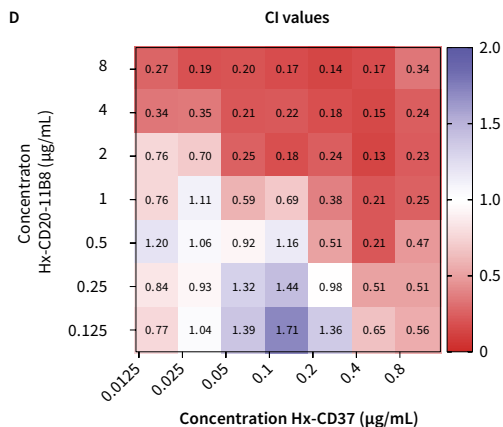
**B**



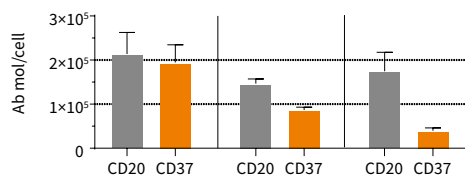
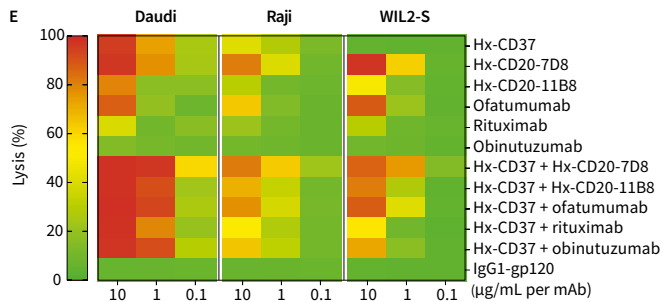
**C**



**D**



**E**



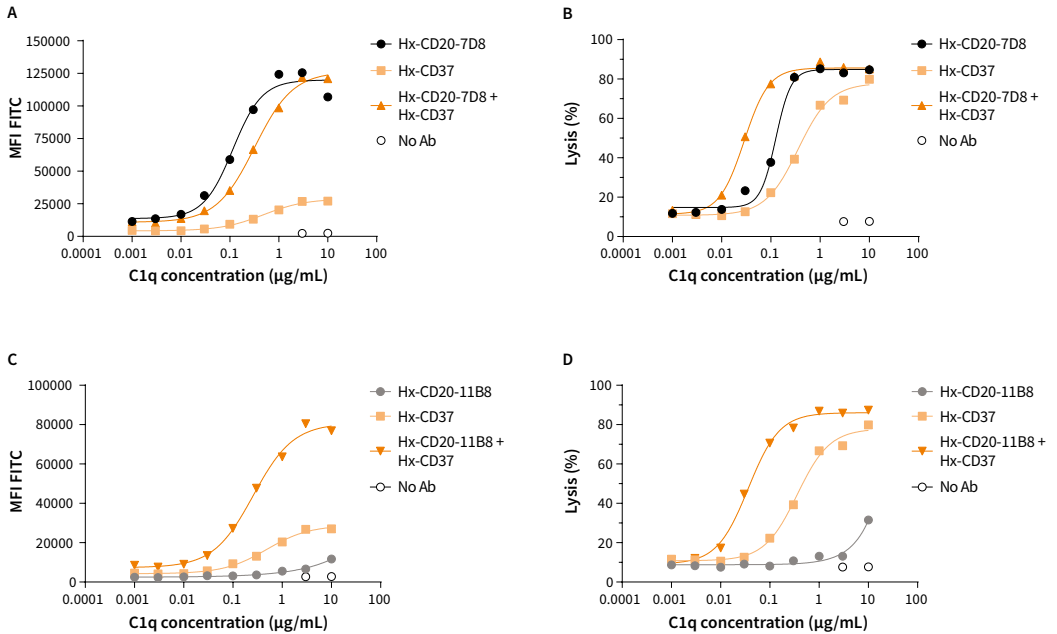
combinations of Hx-CD37 with Hx-CD20 mAbs, as well as for combinations of Hx-CD37 with ofatumumab, rituximab and obinutuzumab (Figure 2E). Even in WIL2-S cells expressing low levels of CD37, a combination of Hx-CD37 with obinutuzumab induced 72% lysis, whereas the single agents induced only 5% and 10% lysis respectively. Despite high single agent activity of Hx-CD37 and Hx-CD20 mAbs at 10 µg/mL (per mAb) in Daudi cells, the cooperativity between Hx-CD37 and Hx-CD20 mAbs became apparent at the lower mAb concentrations.

### **Enhanced binding and use of C1q by combinations of hexamerization-enhanced CD20 and CD37 mAbs**

We hypothesized that the observed synergy in CDC between Hx-CD20 and Hx-CD37 mAbs resulted from more efficient use of complement proteins, starting with binding of C1q. Therefore, we determined whether combinations of Hx-CD20 and Hx-CD37 differed in their C1q binding capacity. We incubated Daudi cells with fixed mAb concentrations and titrated C1q, and measured C1q binding and the concentration of C1q required to induce CDC, referred to here as CDC efficacy. Hx-CD20-7D8 already induced efficient C1q binding as a single agent, while Hx-CD37 showed limited C1q binding (Figure 3A). Combinations of Hx-CD20-7D8 and Hx-CD37 did not significantly increase C1q binding. However, the combination showed higher CDC efficacy as demonstrated by the lower EC<sub>50</sub> value in the C1q dose-response curves compared to the single mAbs (0.03 µg/mL for the combination versus 0.12 µg/mL for Hx-CD20-7D8 and 0.34 µg/mL for Hx-CD20-11B8) (Figure 3B). In contrast to the results with the type I CD20 mAb-derived variant, combining type II CD20 mAb-derived Hx-CD20-11B8 with Hx-CD37 resulted in increased C1q binding compared to the single mAbs, as well as increased CDC efficacy (Figure 3C-D). Collectively, these data suggest that combinations of both type I and type II CD20 mAb-derived Hx-CD20 mAbs with Hx-CD37 mAbs activate complement more effectively.

### **CD20 and CD37 mAbs colocalize on B cells**

Confocal microscopy was used to determine whether the CD20- and CD37-specific antibodies associate on the cell surface upon target binding. Cell-bound Hx variants of CD20 mAb 7D8 and CD37 mAb 37.3 were detected using A488 and A594 fluorescent labeling, respectively, and antibody colocalization was quantified by calculating spatial overlap (Manders' coefficients) between the two fluorescent labels. The merged A488/A594 image showed that membrane-bound Hx-CD20 and Hx-CD37 mAbs indeed colocalized on the surface of Raji cells (Figure 4A), which was confirmed by quantitative analysis, giving Manders' Coefficients of M<sub>1</sub>=0.805 (fraction of image 1 overlapping image 2) and M<sub>2</sub>=0.751 (fraction of image 2 overlapping image 1).



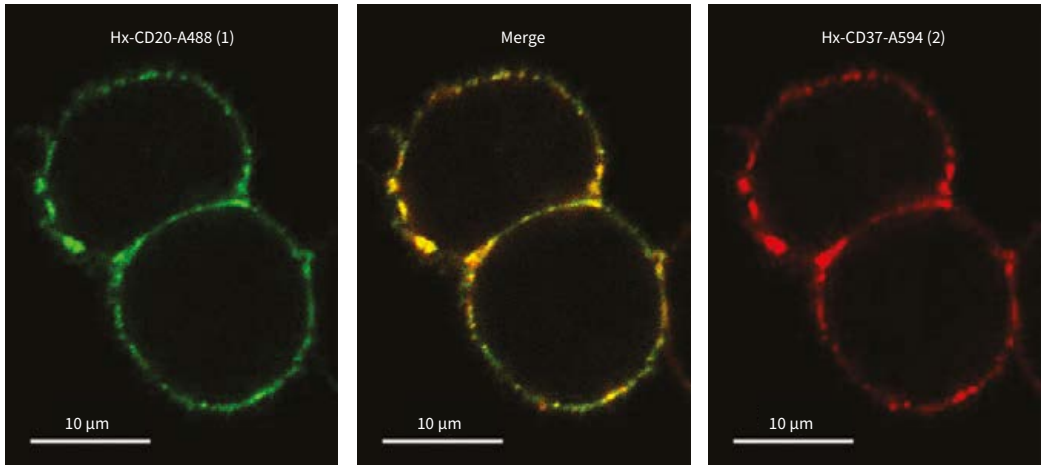
▲ **Figure 3**

**Enhanced binding and use of C1q by combinations of hexamerization-enhanced CD20 and CD37 mAbs.**

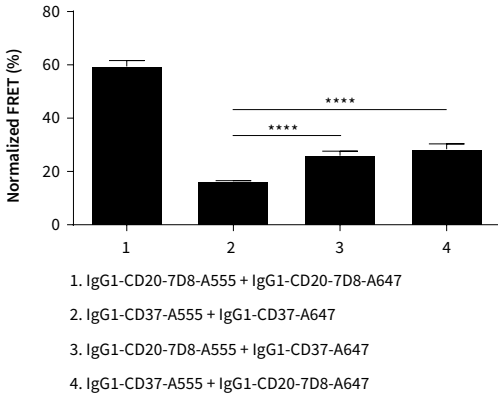
The capacity to bind C1q (A, C) and the efficiency to bind C1q and promote CDC (B, D) was assessed using Daudi cells opsonized with 10 μg/mL of hexamerization-enhanced variants of type I CD20 mAb-derived Hx-CD20-7D8 (A-B) or type II CD20 mAb-derived Hx-CD20-11B8 (C-D), CD37 mAb 37.3-derived Hx-CD37, or a combination thereof (5 + 5 μg/mL). Binding was detected using a FITC-labeled rabbit anti-human C1q secondary antibody and is expressed as MFI. CDC induction was assessed in C1q-depleted serum by calculating the percentage of PI-positive cells as determined by flow cytometry. Representative examples of three replicate experiments are shown.

Colocalization of cell-bound CD20 and CD37 mAbs was further examined by directly assessing molecular proximity using fluorescence resonance energy transfer (FRET) analysis. We examined FRET on Daudi cells between WT and Hx variants of CD20 and CD37 mAbs alone and in combination. Consistent with its CDC activity (Figure 2A), WT IgG1-CD20-7D8 induced high FRET, which suggests antibody hexamer formation (Figure 4B). WT IgG1-CD20-11B8 did not demonstrate proximity-induced FRET (Figure 4C), and WT IgG1-CD37 induced approximately 15% FRET (Figure 4B-C). Introducing a Hx mutation resulted in increased FRET levels for each of the single agents, indicating that enhancing Fc-Fc interactions increases mAb colocalization at the cell surface ( $P < 0.0001$ , Figure 4D-E). Introduction of the Hx mutation did not affect target binding (data not shown), thereby excluding the possibility that increased FRET would be due to more mAbs being available on the cell surface. Combinations of WT IgG1-CD20-7D8 and WT IgG1-CD37 induced approximately 30% FRET, which was increased compared to the WT IgG1-CD37 single mAb ( $P < 0.0001$ , Figure 4B). Combinations of WT IgG1-CD20-11B8 and WT IgG1-

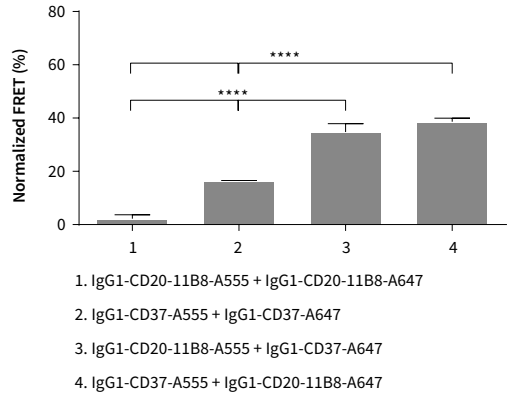
A



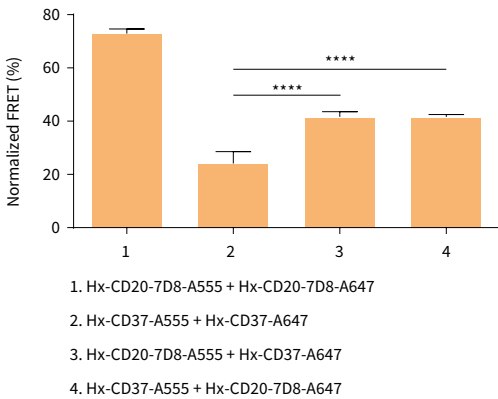
B



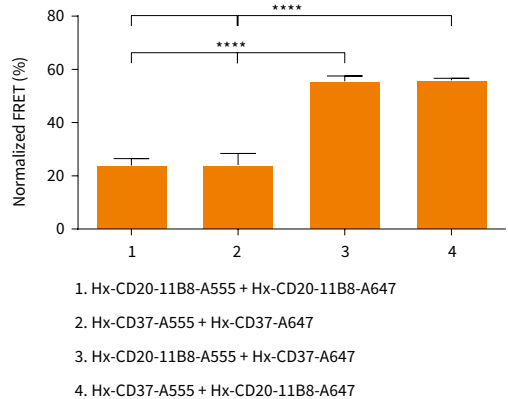
C



D



E





#### ◀ Figure 4

##### **CD20 and CD37 mAbs colocalize on B cells.**

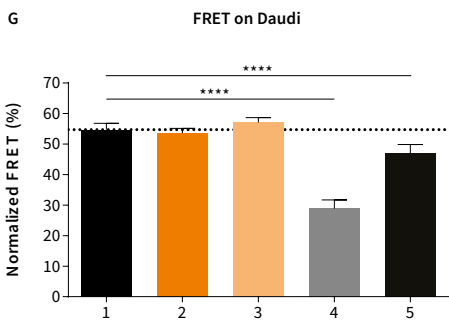
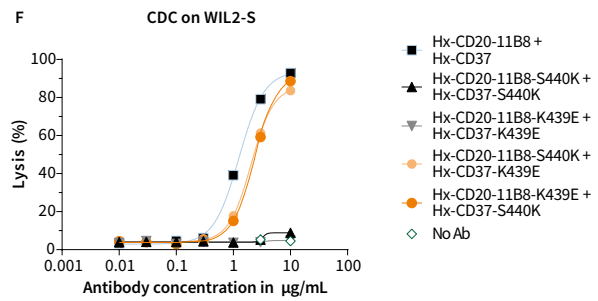
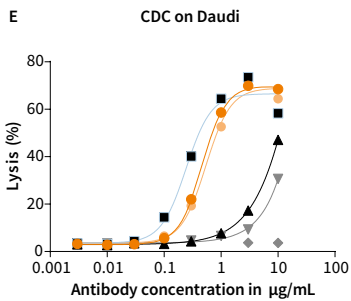
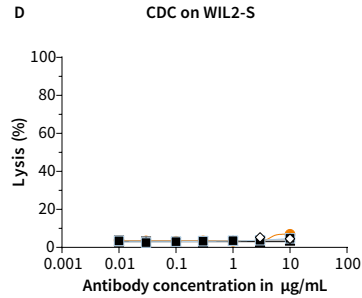
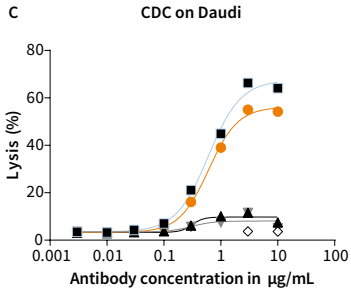
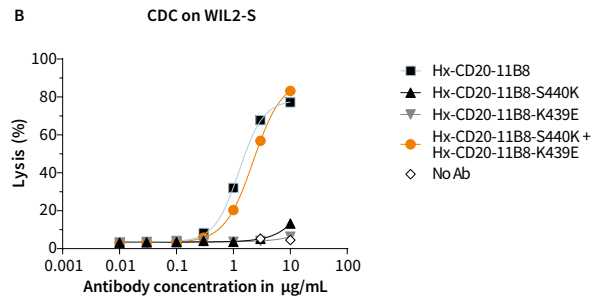
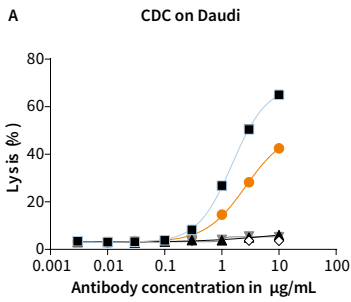
(A) Confocal fluorescence microscopy analysis to detect colocalization of cell-bound CD20 and CD37 mAbs. Raji cells were opsonized with hexamerization-enhanced A488-conjugated CD20 mAb 7D8-derived Hx-CD20-7D8 (image 1, green) and hexamerization-enhanced A594-conjugated CD37 mAb 37.3-derived Hx-CD37 (image 2, red), and incubated for 15 minutes at room temperature. Images were captured in PBS imaging medium at ambient temperature using a Zeiss AxioObserver LSM 700 microscope with Plan-Apochromat 63X/1.40 Oil DIC M27 objective lenses and acquired/processed using Zen software. Two excitation lasers were used at 488 and 555 nm. In the merged image, overlap of red and green produces orange or yellow. A representative example of two replicate experiments is shown. (B-C) FRET analysis to detect the molecular proximity of (B) WT type I CD20 mAb 7D8 (IgG1-CD20-7D8) or (C) WT type II CD20 mAb 11B8 (IgG1-CD20-11B8), WT CD37 mAb 37.3 (IgG1-CD37) or a combination thereof on the cell membrane of Daudi cells. (D-E) FRET analysis to detect the molecular proximity of hexamerization enhanced variants of (D) type I CD20 mAb 7D8-derived Hx-CD20-7D8 or (E) type II CD20 mAb 11B8-derived Hx-CD20-11B8, CD37 mAb 37.3-derived Hx-CD37 or a combination thereof on the cell membrane of Daudi cells. Daudi cells were opsonized with 10 µg/mL A555-conjugated- and 10 µg/mL A647-conjugated antibody variants for 15 minutes at 37 °C. FRET was calculated from MFI values as determined by flow cytometry. Data shown are mean and SD of six replicates collected from three independent experiments.

CD37 substantially increased FRET compared to each single mAb ( $P < 0.0001$ , Figure 4C), consistent with the enhanced CDC induction (Figure 2B). Combinations of Hx-CD20-7D8 or Hx-CD20-11B8 with Hx-CD37 further enhanced FRET compared to the FRET levels induced by the WT mAb combinations ( $P < 0.0001$ , Figure 4D-E). These results confirm that CD20 and CD37 IgG1 mAbs bind in close proximity on the cell membrane, which can be enhanced by introducing the E430G mutation.

##### **Hexamerization-enhanced CD20 and CD37 mAbs cooperate in CDC through Fc-mediated clustering in hetero-hexamers**

Both enhancing Fc-Fc interactions in the CD20 or CD37 mAbs and combining the two B-cell target mAbs resulted in enhanced mAb colocalization. Together with the dependency of CDC on the formation of hexameric IgG complexes on the cell surface<sup>15</sup>, this suggests that the CD20 and CD37 mAbs might not only form hexamers composed of mAbs bound to identical surface targets, but may cooperate by also forming mixed hexameric complexes of mAbs bound to either target, referred to here as hetero-hexamers. The contribution of Fc-Fc interactions between Hx-CD20-11B8 and Hx-CD37 to the CDC activity of the mAb combination was examined by the introduction of the complementary Fc-Fc interface mutations K439E and S440K. K439E and S440K suppress Fc-Fc interactions between antibody molecules containing the same mutation, whereas Fc-Fc interactions are restored in K439K and S440K antibody mixtures.<sup>15</sup> The capacity of Hx-CD20-11B8 and Hx-CD37 variants with K439E and S440K mutations to induce CDC was tested using Daudi and WIL2-S cells.

The CDC activity of Hx-CD20-11B8 was completely inhibited by introducing either the K439E or S440K Fc-Fc inhibiting mutation using Daudi and WIL2-S cells (Figure 5A-B). CDC activity was restored when Fc-Fc inhibition was



neutralized by mixing the two CD20 mAbs. Similar results were observed for Hx-CD37 on Daudi cells, while on WIL2-S cells, Hx-CD37 did not induce CDC, most likely due to low CD37 expression (Figure 5C-D). Combining Hx-CD20-11B8 and Hx-CD37 mAbs harboring the same Fc-Fc inhibiting mutation (K439E or S440K) strongly reduced CDC activity on Daudi and WIL2-S cells (Figure 5E-F). However, CDC of both cell lines was restored by mixing Hx-CD20-11B8 and Hx-CD37, each carrying one of the complementary mutations K439E or S440K. These data suggest that Hx-CD20-11B8 and Hx-CD37 can indeed form hetero-hexameric complexes, thereby cooperating to activate complement.

Next, the effect of the Fc-Fc interaction-inhibiting mutations on colocalization of Hx-CD20-11B8 and Hx-CD37 mAbs on the cell membrane of Daudi cells was evaluated using FRET analysis. mAb combinations with Hx-CD20-11B8 and Hx-CD37 variants, both harboring the same Fc-Fc inhibiting mutation (K439E or S440K) showed reduced FRET on Daudi cells (Figure 5G; Supplementary Figure 6). FRET levels were restored when Fc-Fc inhibition was neutralized by combining Hx-CD20-11B8 and Hx-CD37 mAbs, each having one of the complementary mutations K439E or S440K. Thus, donor- and acceptor-labeled Hx-CD20-11B8 and Hx-CD37 mAb variants come together in close proximity on the cell membrane of Daudi cells, which appears to be, at least in part, mediated by the Fc domain.

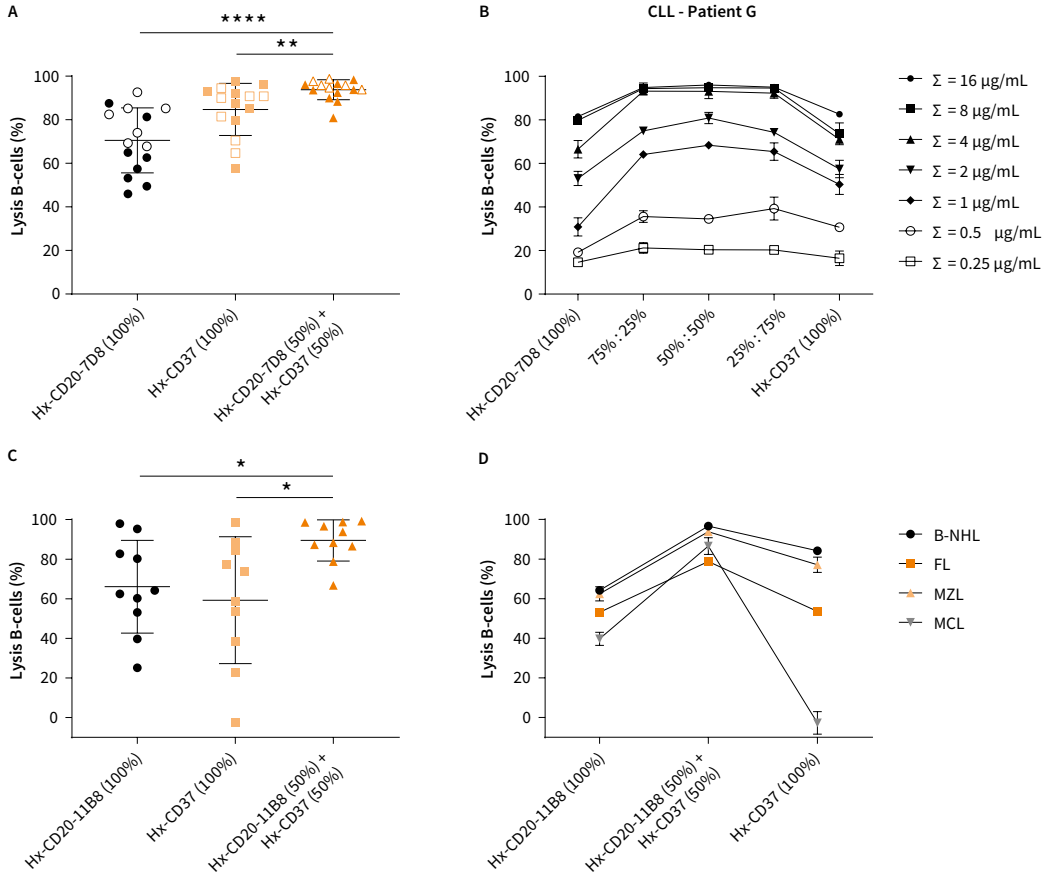
### **Combinations of hexamerization-enhanced CD20 and CD37 mAbs induce superior *ex vivo* CDC of tumor cells obtained from patients with B-cell malignancies**

We next examined the capacity of combinations of Hx-CD20 and Hx-CD37 mAbs to induce CDC *ex vivo* in tumor cells obtained from patients with B-cell malignancies. First, the CDC activity of Hx-CD20-7D8, Hx-CD37 or combinations was evaluated using tumor cells obtained from 15 patients diagnosed with CLL. Both Hx-CD20-7D8 and Hx-CD37 induced substantial CDC of CLL tumor cells from all 15 tested donors (Figure 6A), in accordance with Figure 1. Hx-CD37 was more effective in CDC than Hx-CD20-7D8, which may

#### **◀ Figure 5**

**Hexamerization-enhanced CD20 and CD37 mAbs cooperate in CDC through Fc-mediated clustering in hetero-hexamers.** The effect of introducing Fc-Fc inhibiting mutations S440K and K439E on the CDC induction of hexamerization-enhanced type II CD20 mAb 11B8-derived Hx-CD20-11B8 on Daudi cells (A) and WIL2-S cells (B), hexamerization-enhanced CD37 mAb 37.3-derived Hx-CD37 on Daudi (C) and WIL2-S cells (D) and the mAb combinations thereof on Daudi (E) and WIL2-S cells (F). Cells were opsonized with concentration series of Hx-CD20-11B8 and Hx-CD37 variants in the presence of 20% NHS. CDC induction is expressed as the percentage lysis determined by the fraction of PI-positive cells. Representative examples of two (WIL-2S) and three replicates (Daudi) are shown. (G) The effect of introducing Fc-Fc inhibiting mutations S440K and K439E on the molecular proximity of Hx-CD20-11B8 and Hx-CD37 variants on the cell membrane of Daudi cells. Daudi cells were incubated with 10 µg/mL A555-conjugated Hx-CD20-11B8 variants and 10 µg/mL A647-conjugated Hx-CD37 variants for 15 minutes at 37 °C. FRET was calculated from the MFI values as determined by flow cytometry. Data shown are mean and SD of six replicates collected from three independent experiments.

be explained by higher expression CD37 on CLL cells ( $P < 0.05$ , Supplementary Figure 3A-B). Importantly, significantly increased CDC levels were observed in 9 out of 15 tested CLL donors upon treatment with the combination of Hx-CD20-7D8 and Hx-CD37. Even at modest total concentrations of Hx-CD20-7D8 and Hx-CD37 ( $\Sigma 1.25 \mu\text{g}/\text{mL}$  for each mAb),  $>90\%$  CDC of B cells was induced in 12 out of the 15 tested CLL donors (Figure 6A). Enhanced CDC by the mAb combination was observed over a range of mAb concentrations and at different mAb ratios, and was more apparent at lower mAb concentrations as illustrated for one representative donor (Figure 6B). Next, we evaluated the cytotoxic capacity of Hx-CD20-11B8, Hx-CD37, and the combination thereof using tumor cells of 10 patients diagnosed with different B-cell lymphomas, including B-NHL (NOS), FL, MZL and MCL. While for the single agents a large variation in CDC efficacy was observed between the donors, the combination of Hx-CD20-11B8 and Hx-CD37 consistently showed enhanced CDC activity compared to the single mAbs (Figure 6C). Representative figures from each tested lymphoma subtype show that combinations of Hx-CD20-11B8 and Hx-CD37 at the tested 1:1 ratio may enhance CDC, even when CDC induced by the individual mAbs was low or absent (Figure 6D). Furthermore, analysis of CD20 and CD37 target expression levels on primary B cells from 24 CLL patients and 10 patients with different NHL subtypes illustrated a large diversity in target expression levels and ratios (Supplementary Figure 3A-C). These results suggest that combinations of Hx-CD20 and Hx-CD37 mAbs may generally increase the therapeutic potential of CDC-inducing mAbs in B-cell malignancies across different target expression levels and ratios.



### ▲ Figure 6

#### Combinations of hexamerization-enhanced CD20 and CD37 mAbs induce superior ex vivo CDC of tumor cells obtained from patients with B-cell malignancies.

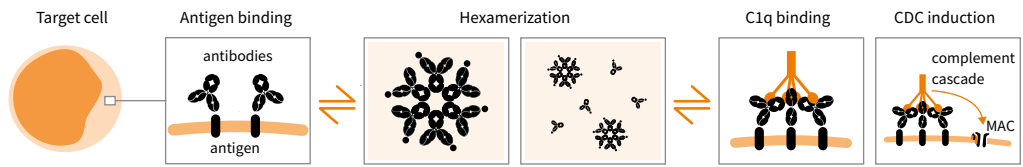
(A) B cells obtained from 15 patients diagnosed with CLL were opsonized with fixed concentrations of hexamerization-enhanced type I CD20 mAb 7D8-derived Hx-CD20-7D8 or hexamerization-enhanced CD37 mAb 37.3-derived Hx-CD37 (open symbols: 2.5  $\mu\text{g/mL}$ , closed symbols: 2  $\mu\text{g/mL}$ ; each presented as 100%), or 1:1 mixtures thereof (open symbols: 0.625  $\mu\text{g/mL}$  of each mAb, closed symbols: 0.5  $\mu\text{g/mL}$  of each mAb; each represented as 50%) in the presence of 50% NHS. CDC induction is presented as the percentage lysis determined by the fraction of TO-PRO-3 positive cells. (B) B cells of a representative CLL patient sample (patient G) were opsonized with different total mAb concentrations of Hx-CD20-7D8 or Hx-CD37 (single agents indicated as 100%) and combinations thereof at different antibody ratios (indicated as 75%:25%, 50%:50% and 25%:75%) in the presence of 50% NHS. CDC induction is presented as the percentage lysis determined by the fraction of TO-PRO-3 positive cells. Data shown are mean and SD of duplicate measurements. (C) B cells obtained from 10 patients diagnosed with different B-cell malignancies (B-NHL (NOS), FL, MZL and MCL) were opsonized with 10  $\mu\text{g/mL}$  of hexamerization-enhanced type II CD20 mAb 11B8-derived Hx-CD20-11B8 or Hx-CD37, and the combination thereof (5 + 5  $\mu\text{g/mL}$ ) in the presence of 20% NHS. CDC induction is presented as the percentage lysis determined by the fraction of 7-AAD positive B-lymphoma cells. (D) CDC assay with B-cell patient samples representative for B-NHL (NOS), FL, MZL and MCL as described in (C). Data shown are mean and SD of duplicate measurements.

## DISCUSSION

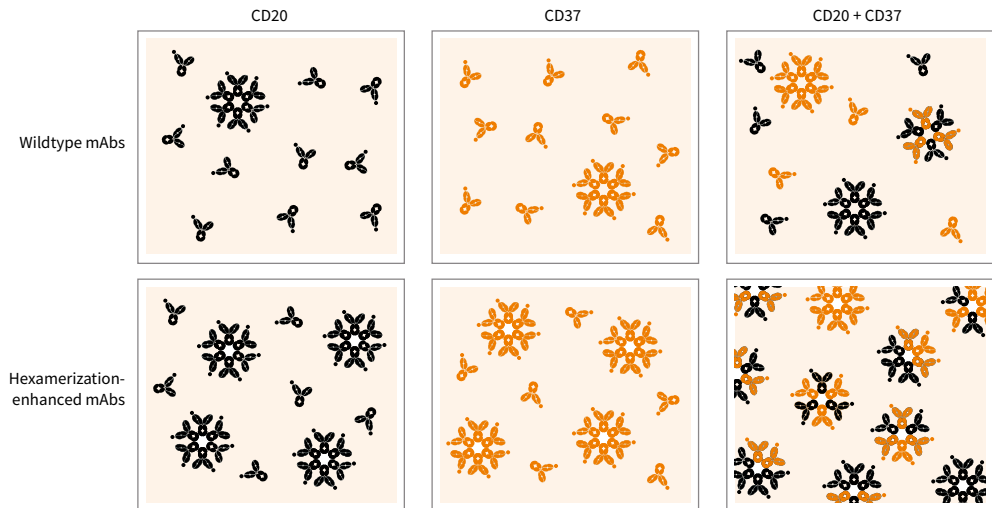
Improving therapeutic efficacy against (heterogeneous) tumors has been the focus of intense preclinical and clinical development. We previously showed that the therapeutic potential of IgG1 mAbs can be enhanced by introducing mutations that improve hexamerization by Fc-mediated clustering and thereby increase CDC activity.<sup>15,16</sup> In the present study, we introduced a Hx mutation, E430G, into CD20 and CD37 mAbs and observed an impressive increase in CDC activity in primary CLL samples. Moreover, combinations of CD20 and CD37 mAbs showed enhanced and synergistic CDC activity, including combinations of Hx-CD37 mAbs with the approved mAbs rituximab, ofatumumab and obinutuzumab. With several CD20 and CD37 mAbs approved or in clinical development, it is attractive to study the mechanism behind the cooperativity between mAbs targeting these two antigens.<sup>34,35</sup> It was recently reported that expression levels of CD20 and CD37 mRNA and protein are correlated on lymphoma B cells.<sup>36</sup> Here, using confocal microscopy and FRET analysis we show that CD20 and CD37 mAbs colocalize on surfaces of B cells and that enhancing Fc-Fc interactions increases mAb colocalization. The observed synergistic CDC activity of CD20 and CD37 mAbs was supported by increased C1q binding and increased CDC efficacy, as illustrated by enhanced CDC at relatively low C1q concentrations. Synergy in complement activation was most evident for CD37 mAbs in combination with type II CD20 mAbs, than with type I CD20 mAbs which are already effective at clustering as WT mAbs.

De Winde et al.,<sup>37</sup> recently suggested that the organization of the B-cell plasma membrane is shaped by dynamic protein-protein interactions and that this organization might be altered by targeted mAb therapies. It has previously been described that membrane proteins can cluster into lipid rafts or tetraspanin enriched microdomains (TEMs), enabling efficient signal transduction.<sup>38,39</sup> We hypothesized that the synergistic interactions in CDC between CD20 and CD37 mAbs could be driven by clustering of both target-bound mAbs into oligomeric complexes. By introducing Fc-Fc inhibiting mutations we were able to demonstrate that CD20 and CD37 mAbs do not only permit the formation of homo-hexamers consisting of mAbs bound to either single target separately, but also allow the formation of hetero-hexamers composed of alternating CD20 and CD37 mAbs, each bound to their own cognate target, explaining the synergistic effects. As proposed in Figure 7, other hetero-hexamer variants may occur, although the presence of such alternative variants remains to be demonstrated. We therefore propose a model for Fc-mediated clustering of synergistic mAb combinations on malignant B cells (Figure 7). Upon binding of mAbs targeting two different co-expressed antigens on the

**A General principle of hexamer formation**



**B Schematic representation of hexamer formation by CD20 and CD37 antibodies**



**▲ Figure 7**

**Model for Fc-mediated clustering of CD20 and CD37 mAbs in hetero-hexamers upon binding to the cell surface.**

(A) mAbs naturally cluster into hexameric complexes upon antibody binding to a cognate antigen on a target cell, thereby providing a docking site for C1q binding and CDC induction. (B) Upon binding of mAbs targeting two different co-expressed antigens on the plasma membrane that (are able to) colocalize, hetero-hexameric antibody complexes are formed consisting of both mAbs, providing a docking site for C1q binding and CDC induction. Introducing hexamerization-enhancing mutations can increase Fc-mediated clustering of mAbs, both into homo- and hetero-hexameric antibody complexes on the cell surface, thereby increasing the number of C1q docking sites and further potentiating CDC.

plasma membrane that (are able to) colocalize, hetero-hexameric complexes are formed, providing a docking site for C1q binding and CDC induction. Introducing hexamerization-enhancing mutations can increase Fc-mediated clustering of mAbs into both homo- and hetero-hexameric complexes, thereby increasing the number of hexamers and further potentiating CDC. Increasing the therapeutic potency of mAb combinations, driven by hetero-hexamerization, could be of clinical relevance as illustrated by a combination of Hx-CD20 and Hx-CD37 mAbs that showed strong CDC of tumor B cells obtained from patients with different B-cell malignancies. Hicks et al<sup>40</sup> recently reported that the antitumor activity of IMG529, a CD37-targeting antibody-drug conjugate in clinical development, was potentiated in combination with rituximab *in vivo*

in B-NHL xenograft models, which was associated with increased CD37 internalization rates. Other mechanisms of synergy between CD20 and CD37 have also been reported, such as upregulation of CD20 expression in Daudi cells after treatment with the radiolabeled anti-CD37 mAb  $^{177}\text{Lu}$ -lilotomab.<sup>41</sup>

The concept of antibody hetero-hexamer formation may hold relevance for a broader range of targets and effector mechanisms. An emerging therapeutic approach is the development of designer polyclonals, consisting of multiple mAbs in one product of which several are in clinical development, such as MM-151, targeting three epitopes on EGFR and Sym013, a mixture of six mAbs targeting all three HER family members (EGFR, HER2 and HER3).<sup>42,43</sup> One could speculate that enhancing Fc-mediated antibody clustering involving different co-expressing targets on hematologic or solid tumors may induce synergistic efficacy, providing a rationale for application in designer polyclonals. Whether effector mechanisms other than CDC, such as ADCC or ADCP are also enhanced by combinations of CD20 and CD37 mAbs remains to be elucidated. One may speculate that the engagement of two mAbs binding co-expressed targets allows for higher total antibody binding on the cell surface, allowing more efficient engagement of Fc $\gamma$ Rs on effector cells.

In the present work, we have demonstrated that synergy in CDC induced by combinations of CD20 and CD37 mAbs is likely driven by Fc-mediated clustering into hetero-hexameric antibody complexes on the cell surface. Enhancing hetero-hexamerization between mAb combinations using Fc engineering represents a powerful tool to increase the therapeutic efficacy of mAb combinations directed against hematologic tumor targets, as well as other tumor targets.



# REFERENCES

1. Deans JP, Li H, Polyak MJ. CD20-mediated apoptosis: signalling through lipid rafts. *Immunology* 2002; **107**(2): 176-82.
2. Gopal AK, Press OW. Clinical applications of anti-CD20 antibodies. *Transl Res* 1999; **134**(5): 445-50.
3. Leget GA, Czuczman MS. Use of rituximab, the new FDA-approved antibody. *Curr Opin Oncol* 1998; **10**(6): 548-51.
4. Beurskens FJ, Lindorfer MA, Farooqui M, et al. Exhaustion of cytotoxic effector systems may limit mAb-based immunotherapy in cancer patients. *J Immunol* 2012; **188**(7): 3532-41.
5. Taylor RP, Lindorfer MA. Analyses of CD20 Monoclonal Antibody-Mediated Tumor Cell Killing Mechanisms: Rational Design of Dosing Strategies. *Mol Pharmacol* 2014; **86**(5): 485-91.
6. Weiner GJ. Building better monoclonal antibody-based therapeutics. *Nat Rev Cancer* 2015; **15**(6): 361-70.
7. Wang X, Mathieu M, Brezski RJ. IgG Fc engineering to modulate antibody effector functions. *Protein Cell* 2018; **9**(1): 63-73.
8. Lazar GA, Dang W, Karki S, et al. Engineered antibody Fc variants with enhanced effector function. *PNAS* 2006; **103**(11): 4005-10.
9. Richards JO, Karki S, Lazar GA, Chen H, Dang W, Desjarlais JR. Optimization of antibody binding to Fc RIIa enhances macrophage phagocytosis of tumor cells. *Mol Cancer Ther* 2008; **7**(8): 2517-27.
10. Shields RL, Namenuk AK, Hong K, et al. High Resolution Mapping of the Binding Site on Human IgG1 for Fcγ1, Fcγ2, Fcγ3, and FcRn and Design of IgG1 Variants with Improved Binding to the Fcγ1. *J Biol Chem* 2000; **276**(9): 6591-604.
11. Stavenhagen JB, Gorlatov S, Tuailon N, et al. Fc Optimization of Therapeutic Antibodies Enhances Their Ability to Kill Tumor Cells In vitro and Controls Tumor Expansion In vivo via Low-Affinity Activating Fc Receptors. *Cancer Res* 2007; **67**(18): 8882-90.
12. Idusogie EE, Wong PY, Presta LG, et al. Engineered antibodies with increased activity to recruit complement. *J Immunol* 2001; **166**(4): 2571-5.
13. Natsume A, In M, Takamura H, et al. Engineered Antibodies of IgG1/IgG3 Mixed Isotype with Enhanced Cytotoxic Activities. *Cancer Res* 2008; **68**(10): 3863-72.
14. Melis JPM, Strumane K, Ruuls SR, Beurskens FJ, Schuurman J, Parren PWHI. Complement in therapy and disease: Regulating the complement system with antibody-based therapeutics. *Mol Immunol* 2015; **67**(2, Part A): 117-30.
15. Diebold CA, Beurskens FJ, de Jong RN, et al. Complement Is Activated by IgG Hexamers Assembled at the Cell Surface. *Science* 2014; **343**(6176): 1260.
16. de Jong RN, Beurskens FJ, Verploegen S, et al. A Novel Platform for the Potentiation of Therapeutic Antibodies Based on Antigen-Dependent Formation of IgG Hexamers at the Cell Surface. *PLoS Biol* 2016; **14**(1): e1002344.
17. Lindorfer MA, Cook EM, Tupitza JC, et al. Real-time analysis of the detailed sequence of cellular events in mAb-mediated complement-dependent cytotoxicity of B-cell lines and of chronic lymphocytic leukemia B-cells. *Mol Immunol* 2016; **70**: 13-23.
18. Teeling JL, French RR, Cragg MS, et al. Characterization of new human CD20 monoclonal antibodies with potent cytolytic activity against non-Hodgkin lymphomas. *Blood* 2004; **104**(6): 1793.
19. Dechant M, Weisner W, Berger S, et al. Complement-Dependent Tumor Cell Lysis Triggered by Combinations of Epidermal Growth Factor Receptor Antibodies. *Cancer Res* 2008; **68**(13): 4998.

20. Klausz K, Berger S, Lammerts van Bueren Jeroen J, et al. Complement-mediated tumor-specific cell lysis by antibody combinations targeting epidermal growth factor receptor (EGFR) and its variant III (EGFRvIII). *Cancer Sci* 2011; **102**(10): 1761-8.
21. Link MP, Bindl J, Meeker TC, et al. A unique antigen on mature B cells defined by a monoclonal antibody. *J Immunol* 1986; **137**(9): 3013.
22. Schwartz-Albiez R, Dörken B, Hofmann W, Moldenhauer G. The B cell-associated CD37 antigen (gp40-52). Structure and subcellular expression of an extensively glycosylated glycoprotein. *J Immunol* 1988; **140**(3): 905.
23. Deckert J, Park PU, Chicklas S, et al. A novel anti-CD37 antibody-drug conjugate with multiple anti-tumor mechanisms for the treatment of B-cell malignancies. *Blood* 2013; **122**(20): 3500.
24. Heider K-H, Kiefer K, Zenz T, et al. A novel Fc-engineered monoclonal antibody to CD37 with enhanced ADCC and high proapoptotic activity for treatment of B-cell malignancies. *Blood* 2011; **118**(15): 4159-68.
25. Pereira DS, Guevara CI, Jin L, et al. AGS67E, an Anti-CD37 Monomethyl Auristatin E Antibody-Drug Conjugate as a Potential Therapeutic for B/T-Cell Malignancies and AML: A New Role for CD37 in AML. *Mol Cancer Ther* 2015; **14**(7): 1650-60.
26. Repetto-Llamazares AHV, Larsen RH, Patzke S, et al. Targeted Cancer Therapy with a Novel Anti-CD37 Beta-Particle Emitting Radioimmunoconjugate for Treatment of Non-Hodgkin Lymphoma. *PLoS One* 2015; **10**(6): e0128816.
27. Zhao XB, Biswas S, Mone A, et al. Novel Anti-CD37 Small Modular Immunopharmaceutical (SMIP) Induces B-Cell-Specific, Caspase-Independent Apoptosis in Human CLL Cells. *Blood* 2004; **104**(11): 2515.
28. Burton DR, Pyati J, Koduri R, et al. Efficient neutralization of primary isolates of HIV-1 by a recombinant human monoclonal antibody. *Science* 1994; **266**(5187): 1024.
29. Deckert. J. CD37-binding molecules and immunoconjugates thereof. *WO 2011/112978A1* 2011.
30. Vink T, Oudshoorn-Dickmann M, Roza M, Reitsma J-J, de Jong RN. A simple, robust and highly efficient transient expression system for producing antibodies. *Methods* 2014; **65**(1): 5-10.
31. Cook EM, Lindorfer MA, van der Horst H, et al. Antibodies That Efficiently Form Hexamers upon Antigen Binding Can Induce Complement-Dependent Cytotoxicity under Complement-Limiting Conditions. *J Immunol* 2016; **197**(5): 1762-75.
32. Cragg MS, Morgan SM, Chan HTC, et al. Complement-mediated lysis by anti-CD20 mAb correlates with segregation into lipid rafts. *Blood* 2003; **101**(3): 1045.
33. Chou T-C. Theoretical Basis, Experimental Design, and Computerized Simulation of Synergism and Antagonism in Drug Combination Studies. *Pharmacol Rev* 2006; **58**(3): 621.
34. Beckwith KA, Byrd JC, Muthusamy N. Tetraspanins as therapeutic targets in hematological malignancy: a concise review. *Front Physiol* 2015; **6**: 91.
35. Teo EC-y, Chew Y, Phipps C. A review of monoclonal antibody therapies in lymphoma. *Crit Rev Oncol Hematol* 2016; **97**: 72-84.
36. Xu-Monette ZY, Li L, Byrd JC, et al. Assessment of CD37 B-cell antigen and cell of origin significantly improves risk prediction in diffuse large B-cell lymphoma. *Blood* 2016; **128**(26): 3083-100.
37. de Winde CM, Elfrink S, van Spriel AB. Novel Insights into Membrane Targeting of B Cell Lymphoma. *Trends Cancer* 2017; **3**(6): 442-53.
38. Hemler ME. Tetraspanin functions and associated microdomains. *Nat Rev Mol Cell Biol* 2005; **6**(10): 801-11.
39. Simons K, Sampaio JL. Membrane Organization and Lipid Rafts. *Cold Spring Harb Perspect Biol* 2011; **3**(10): a004697.
40. Hicks SW, Lai KC, Gavrilescu LC, et al. The Antitumor Activity of IMGNS529, a CD37-Targeting Antibody-Drug Conjugate, Is Potentiated by Rituximab in Non-Hodgkin Lymphoma Models. *Neoplasia* 2017; **19**(9): 661-71.

41. Repetto-Llamazares AHV, Malenge MM, O'Shea A, et al. Combination of (177) Lu-lilotomab with rituximab significantly improves the therapeutic outcome in preclinical models of non-Hodgkin's lymphoma. *Eur J Haematol* 2018; **101**(4): 522-31.
42. Dienstmann R, Patnaik A, Garcia-Carbonero R, et al. Safety and Activity of the First-in-Class Sym004 Anti-EGFR Antibody Mixture in Patients with Refractory Colorectal Cancer. *Cancer Discov* 2015; **5**(6): 598.
43. Jacobsen HJ, Poulsen TT, Dahlman A, et al. Pan-HER, an Antibody Mixture Simultaneously Targeting EGFR, HER2, and HER3, Effectively Overcomes Tumor Heterogeneity and Plasticity. *Clin Cancer Res* 2015; **21**(18): 4110.
44. Baig NA, Taylor RP, Lindorfer MA, et al. Complement dependent cytotoxicity (CDC) in chronic lymphocytic leukemia (CLL): Ofatumumab enhances alemtuzumab CDC and reveals cells resistant to activated complement. *Leuk Lymphoma* 2012; **53**(11): 2218-27.
45. Kennedy AD, Beum PV, Solga MD, et al. Rituximab Infusion Promotes Rapid Complement Depletion and Acute CD20 Loss in Chronic Lymphocytic Leukemia. *J Immunol* 2004; **172**(5): 3280.
46. Taylor RP, Wright EL, Pocanic F. Quantitative analyses of C3b capture and immune adherence of IgM antibody/dsDNA immune complexes. *J Immunol* 1989; **143**(11): 3626.
47. Manders E. M M, Verbeek F J, Aten J A. Measurement of co-localization of objects in dual-colour confocal images. *J Microsc* 1993; **169**(3): 375-82.
48. Schneider CA, Rasband WS, Eliceiri KW. NIH Image to ImageJ: 25 years of image analysis. *Nat Methods* 2012; **9**(7): 671-5.

# SUPPLEMENTARY METHODS AND MATERIALS

## Cells

CLL cells were purified from the blood of newly diagnosed CLL patients (University of Rochester), in accordance with standard protocols (University of Rochester Institutional Review Board).<sup>44</sup> Bone marrow mononuclear cells (BMNCs), peripheral blood mononuclear cells (PBMCs) and lymph node suspension cells from patients with B-cell non-Hodgkin lymphoma (B-NHL, not otherwise specified (NOS)), follicular lymphoma (FL), marginal zone lymphoma (MZL) and mantle cell lymphoma (MCL) were obtained from the Amsterdam University Medical Center (Amsterdam, The Netherlands) after written informed consent and stored using protocols approved by the Privacy Review Board of the Netherlands Cancer Registry in accordance with the declaration of Helsinki. BMNCs and PBMCs were isolated by density-gradient centrifugation (Ficoll-Paque PLUS, GE Healthcare) from bone marrow aspirates or peripheral blood samples of lymphoma patients. Lymph node suspension cells were obtained by mechanical dissociation held overnight at 37 °C and filtered using cell strainers. Cells were used in experiments directly or stored in liquid nitrogen until further use.

## Reagents

Fluorescein isothiocyanate (FITC) conjugated rabbit anti-human C1q (Dako) was used for flow cytometry experiments. C1q depleted serum and purified human C1q were obtained from Quidel. Mouse anti-human IgM antibody HB57 and mouse anti-human IgG1 mAb HB43 were used as described.<sup>45,46</sup> Pooled normal human serum (NHS; AB positive) was obtained from Sanquin (Amsterdam, The Netherlands). mAbs labeled with Alexa dyes (A488, A555, A594, A647) were reacted with N-hydroxysuccinimidyl-esters following manufacturer's instructions (Molecular Probes).

## Cell markers flow cytometry

Cell markers used to define cell populations from patients with B-cell lymphoma: CD45-KO (Beckman Coulter), CD19-PC7 (Beckman Coulter), CD3-V450 (BD), CD5-APC (BD), CD5-PE (Dako), CD10-APC-H7 (BD), CD10-PE (Dako), CD23-FITC (Biolegend), kappa-APC-H7 (BD), kappa-PE (Dako) and lambda-FITC (Emelca Bioscience). Within the CD45+ cell population, B cells were identified as CD3-CD19+ cells. Malignant cells were identified based on clonality by kappa/lambda staining (B-NHL (NOS), MZL). Tumor specific markers were used (when possible) depending on the lymphoma subtype: CD10+ (FL), CD5+CD23- (MCL).

### Expression analysis

Expression levels of cellular markers were determined using an indirect immunofluorescence assay (QIFIKIT<sup>®</sup>, Agilent Technologies) according to the manufacturer's instructions. Briefly, cells were labeled with primary mouse mAbs and incubated, in parallel with QIFIKIT<sup>®</sup> beads containing a defined number of mAb molecules, with FITC-labeled Polyclonal Goat Anti-Mouse Immunoglobulins F(ab')<sub>2</sub>. The number of antibody molecules per cell was determined by extrapolating the measured mean fluorescence intensity (MFI) to the calibration curve generated by plotting the MFI of the individual bead populations against the number of mAb molecules per bead.

### Förster Resonance Energy Transfer (FRET) analysis

500,000 Daudi cells/well were incubated with 10 µg/mL A555-conjugated donor mAbs and/or 10 µg/mL A647-conjugated acceptor mAbs in 10 mL of RPMI/0.2% BSA in 96-well round-bottom plates for 15 minutes at 37°C. Cells were washed twice, pelleted by centrifugation (3 minutes, 300xg) and resuspended in 200 µL PBST. Mean fluorescence intensities (MFI) were determined by flow cytometry (FACS Canto II) by recording 10,000 events at 585/42 nm (FL2, donor A488) and ≥670 nm (FL3), both excited at 488 nm, and at 660/20 nm (FL4, acceptor A647), excited at 635 nm. Unquenched donor fluorescence intensity was determined with cells incubated with A555-conjugated donor mAbs, and non-enhanced acceptor intensity was determined with cells incubated with A647-conjugated acceptor mAbs. Proximity-induced FRET was determined by measuring energy transfer between cells incubated with A555-conjugated donor and A647-conjugated acceptor mAbs. MFI values allowed calculation of FRET according to the following equation:

Energy transfer (ET) =  $FL3(D, A) - FL2(D, A) / a - FL4(D, A) / b$ , wherein  $a = FL2(D) / FL3(D)$ ,  $b = FL4(A) / FL3(A)$ , D is donor, A is acceptor and  $FL_n(D, A)$  = donor + acceptor.<sup>32</sup>

ET values obtained were normalized:

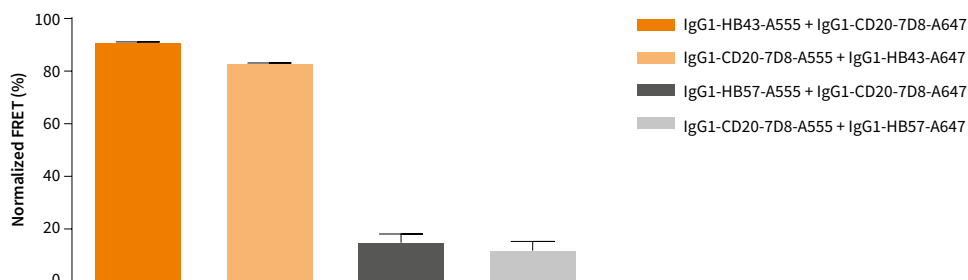
Normalized energy transfer (%) =  $100 * ET / FL3(D, A)$ .

### Synergy and colocalization analyses

Synergy between combinations of mAbs was determined using Loewe additivity-based combination index (CI) scores calculated by CompuSyn software (ComboSyn Inc., Paramus, NJ), whereby effects were categorized as additive (CI = 1), synergistic (CI < 1) or antagonistic (CI > 1).<sup>33</sup> In brief, synergistic lysis exceeds the level of one mAb plus the predicted fractional lysis induced by the other mAb on the remainder of the cell population.

mAb colocalization was quantified by calculating spatial overlap (Manders' coefficients) between images of cell-bound A488-labeled Hx-CD20-7D8 and cell-bound A594-labeled Hx-CD37 using the colocalization plugin in ImageJ.<sup>47,48</sup>

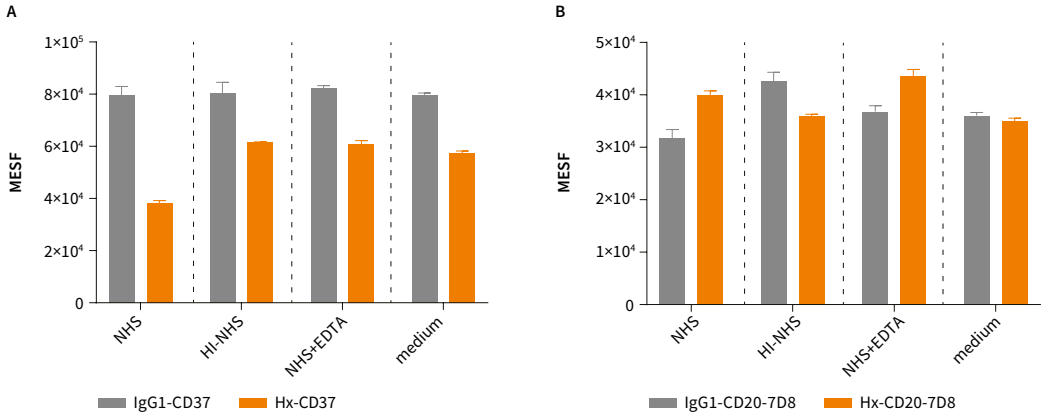
## SUPPLEMENTARY FIGURES AND TABLES



### ▲ Supplementary Figure 1

#### Evaluation of the dynamic range of fluorescence resonance energy transfer (FRET) detection determined by flow cytometry using control mAbs.

Daudi cells were incubated with 10  $\mu\text{g}/\text{mL}$  of A555- or A647-conjugated CD20 mAb 7D8 (IgG1-CD20-7D8) and washed, followed by 10  $\mu\text{g}/\text{mL}$  A555- or A647-conjugated mouse-anti-human IgG1 mAb HB43 (IgG1-HB43; positive control) or mouse-anti-human IgM mAb HB57 (IgG1-HB57; negative control) for 15 minutes at 37 °C. FRET was calculated from MFI values as determined by flow cytometry. Data shown are mean and SD of six replicates collected from three independent experiments. IgG1-HB43 was used as a positive control for proximity-induced FRET by virtue of its ability to directly bind, and thus colocalize with a human IgG1 mAb, such as the WT CD20 mAb 7D8 on the cell surface. As binding of A555- or A647-conjugated HB43 requires a cell surface-bound IgG1 mAb, unconjugated IgG1-CD20-7D8 was used for primary binding in the single stainings (calculating the unquenched donor and non-enhanced acceptor fluorescence intensities) and A555- or A647-conjugated IgG1-CD20-7D8 mAb was used for primary binding in the combination stainings (calculating energy transfer efficiency). Using the same setup, IgG1-HB57 was used as a negative control for proximity-induced FRET. HB57 is a murine mAb that binds membrane-bound human IgM (B-cell receptor) on Daudi cells, and was expected to poorly colocalize with the human antibody IgG1-CD20-7D8. Conjugated IgG1-CD20-7D8 and IgG1-HB43 efficiently colocalized with an energy transfer efficiency of 90%, while IgG1-CD20-7D8 and IgG1-HB57 poorly colocalized with ~10% energy transfer efficiency. These data validated the flow cytometry FRET analysis to assess antibody colocalization using A555- and A647-conjugated antibodies.

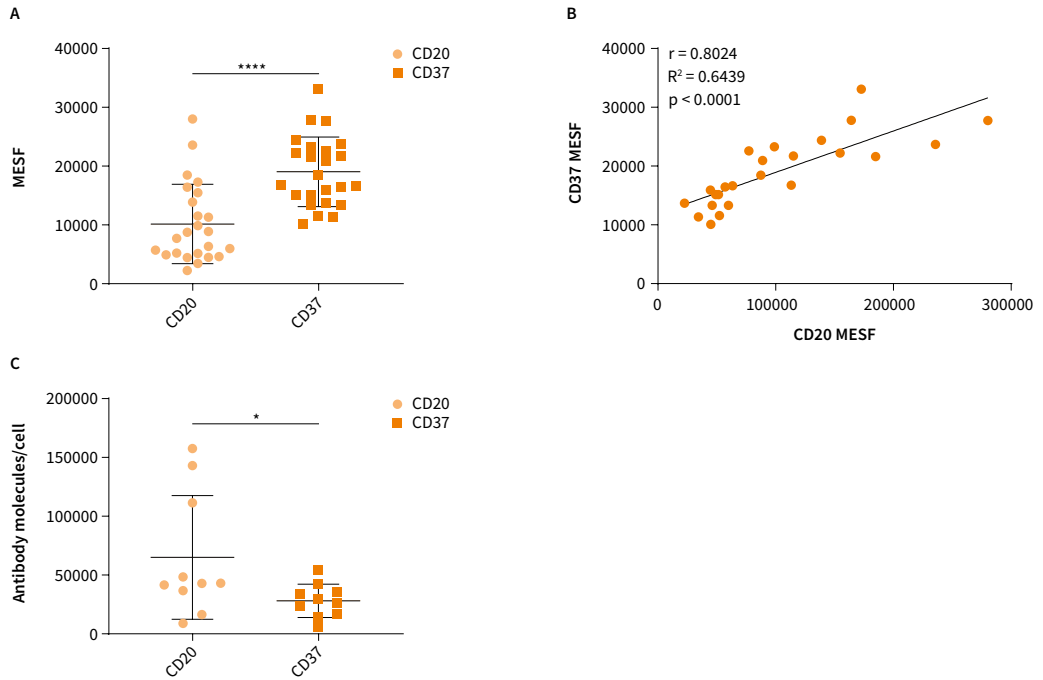


▲ **Supplementary Figure 2**

**Binding of CD20 and CD37 mAbs to tumor B cells obtained from a patient diagnosed with CLL (patient A).**

Antibody binding on primary CLL B cells was analyzed using 16 µg/mL WT CD37 mAb 37.3 (IgG1-CD37) and its hexamerization-enhanced variant Hx-CD37 (A) or WT CD20 mAb 7D8 (IgG1-CD20-7D8) and its hexamerization-enhanced variant Hx-CD20-7D8 (B) in the presence NHS, HI-NHS, NHS + EDTA or medium. Binding was detected using A488-conjugated mouse anti-human IgG1 Fc mAb HB43 and mean fluorescence intensities were converted to molecules of equivalent soluble fluorochrome (MESF) using calibrated beads (Spherotech). Representative examples of three replicate experiments are shown.

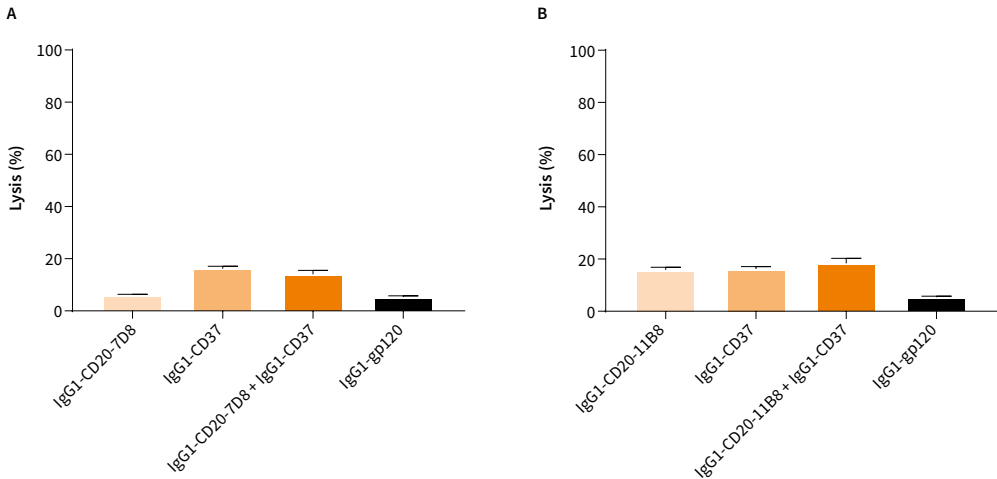




▲ **Supplementary Figure 3**

**CD20 and CD37 target expression levels on tumor B cells obtained from patients with B-cell malignancies.**

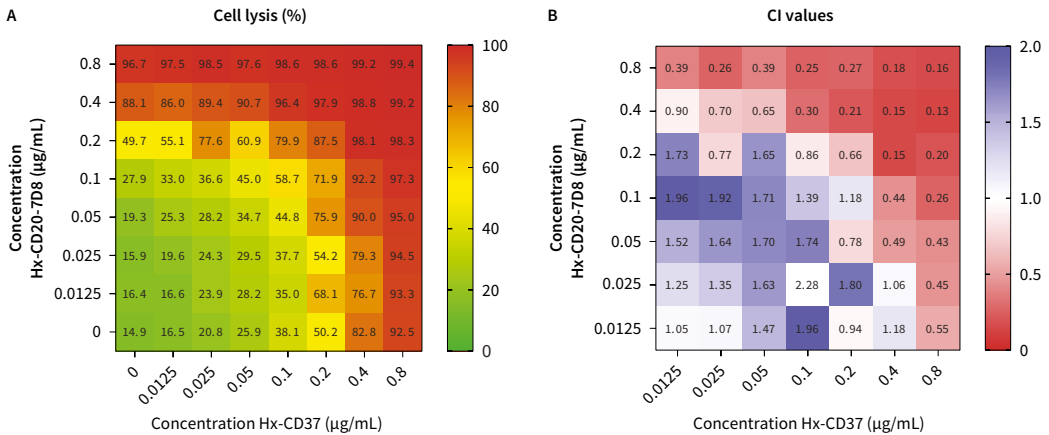
(A) CD20 and CD37 expression. Binding was detected using an A488-conjugated mouse anti-human IgG1 Fc mAb HB43 and mean fluorescence intensities were converted to molecules of equivalent soluble fluorochrome (MESF) using calibrated beads (Spherotech). (B) Correlation analysis of CD20 and CD37 expression levels on tumor B cells from 24 CLL patient samples described in (A). The Pearson's correlation coefficient ( $r$  and  $R^2$ ) was calculated using GraphPad Prism software. (C) CD20 and CD37 expression levels on tumor B cells of 2 B-NHL (NOS), 3 FL, 2 MZL and 3 MCL patient samples. Expression levels were determined using a human IgG calibrator kit (Agilent Technologies). The number of antibody molecules per cell was calculated from the antibody-binding capacity (mean fluorescence intensity) normalized to a calibration curve, according to the manufacturer's guidelines. Significant differences are indicated as \* $p < 0.05$  and \*\*\*\* $p < 0.0001$ .



**▲ Supplementary Figure 4**

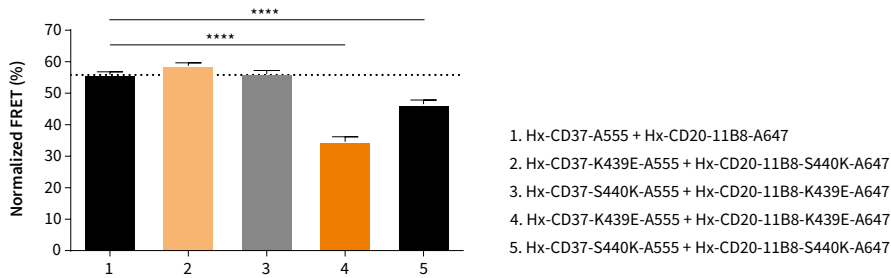
**Minimal cell lysis observed in assays with heat-inactivated serum indicates that cell killing is complement dependent.**

Daudi cells opsonized with 30 µg/mL WT type I CD20 mAb 7D8 (IgG1-CD20-7D8) (A) or WT type II CD20 mAb 11B8 (IgG1-CD20-11B8) (B), anti-CD37 mAb 37.3 (IgG1-CD37), or a combination thereof (15 + 15 µg/mL) for 45 minutes at 37°C in the presence of 20% heat-inactivated NHS. HIV gp120-specific mAb b12 (IgG1-gp120) was used as a negative control human mAb. Cell kill is expressed as the percentage lysis determined by the fraction of PI-positive cells. Representative examples of two replicates are shown.



**▲ Supplementary Figure 5**

(A) 8 x 8 CDC dose response matrix plot for the combination of hexamerization-enhanced CD37 mAb Hx-CD37 (0-0.8 µg/mL) with hexamerization-enhanced CD20 mAb Hx-CD20-7D8 (0-0.8 µg/mL) tested on Daudi cells and categorized as a color gradient from green (0% lysis) to yellow (50% lysis) to red (100% lysis). HIV gp120-specific mAb b12 (IgG1-gp120) was used as a negative control human mAb. (B) Loewe additivity-based Combination index (CI) values calculated by CompuSyn for the CDC dose response matrix as described in (A) and categorized as synergistic (<1, red), additive (1, white) and antagonistic (>1, blue). Representative examples of two replicate experiments are shown. CDC induction is expressed as the percentage lysis determined by the fraction of PI-positive cells.



### ▲ Supplementary Figure 6

**The effect of introducing Fc-Fc inhibiting mutations S440K and K439E on the molecular proximity of hexamerization-enhanced CD20 and CD37 mAbs on the cell membrane of Daudi cells.**

Daudi cells were incubated with 10 µg/mL A555-conjugated hexamerization-enhanced CD37 mAb 37.3 (Hx-CD37) variants and 10 µg/mL A647-conjugated hexamerization-enhanced CD20 mAb 11B8 (Hx-CD20-11B8) variants for 15 minutes at 37 °C. FRET was calculated from MFI values as determined by flow cytometry. Data shown are mean and SD of six replicates collected from three independent experiments.

Antibody Combination	CI values* at different effective doses (ED)			
	ED50	ED75	ED90	ED95
Hx-CD20-7D8 + Hx-CD37	0.96	0.66	0.47	0.37
Hx-CD20-11B8 + Hx-CD37	0.72	0.52	0.39	0.31

\* CI values can be categorized as synergistic (<1), additive (=1) and non-synergistic (>1).

### ▲ Supplementary Table 1

Average Loewe-additivity-based combination index (CI) values calculated by CompuSyn at different effective doses of a CDC dose-response matrix using combinations of hexamerization-enhanced CD20 mAb Hx-CD20-7D8 or Hx-CD20-11B8 with hexamerization-enhanced CD37 mAb Hx-CD37.



# 3

## DUOHEXABODY-CD37<sup>®</sup>, A NOVEL BIPARATOPIC CD37 ANTIBODY WITH ENHANCED FC-MEDIATED HEXAMERIZATION AS A POTENTIAL THERAPY FOR B-CELL MALIGNANCIES

Simone C. Oostindie,<sup>1,2</sup> Hilma J. van der Horst,<sup>3</sup> Laurens P. Kil,<sup>1</sup> Kristin Strumane,<sup>1</sup> Marije B. Overdijk,<sup>1</sup> Edward N. van den Brink,<sup>1</sup> Jeroen H. N. van den Brakel,<sup>1</sup> Hendrik J. Rademaker,<sup>1</sup> Berris van Kessel,<sup>1</sup> Juliette van den Noort,<sup>1</sup> Martine E. D. Chamuleau,<sup>3</sup> Tuna Mutis,<sup>3</sup> Margaret A. Lindorfer,<sup>4</sup> Ronald P. Taylor,<sup>4</sup> Janine Schuurman,<sup>1</sup> Paul W. H. I. Parren,<sup>1,2,5</sup> Frank J. Beurskens,<sup>1</sup> and Esther C. W. Breijl<sup>1†</sup>

Blood Cancer J. 2020 Apr 28;10(3):30.

- <sup>1</sup> Genmab, Utrecht, The Netherlands;
  - <sup>2</sup> Department of Immunohematology and Blood Transfusion, Leiden University Medical Center, Leiden, The Netherlands;
  - <sup>3</sup> Department of Hematology, Amsterdam University Medical Center, Amsterdam, The Netherlands;
  - <sup>4</sup> Department of Biochemistry and Molecular Genetics, University of Virginia School of Medicine, Charlottesville, Virginia, USA;
  - <sup>5</sup> Current affiliations: Department of Immunohematology and Blood Transfusion, Leiden University Medical Center, Leiden, The Netherlands and Lava Therapeutics, Utrecht, The Netherlands;
- † Corresponding author

**Corresponding author**

Esther C. W. Breij, Genmab, Uppsalalaan 15, 3584CT, Utrecht,  
The Netherlands; cell: +31623346799; e-mail: [ebj@genmab.com](mailto:ebj@genmab.com)

## ABSTRACT

Tetraspanin CD37 has recently received renewed interest as a therapeutic target for B-cell malignancies. Although complement-dependent cytotoxicity (CDC) is a powerful Fc-mediated effector function for killing hematological cancer cells, CD37-specific antibodies are generally poor inducers of CDC. To enhance CDC, the E430G mutation was introduced into humanized CD37 monoclonal IgG1 antibodies to drive more efficient IgG hexamer formation through intermolecular Fc-Fc interactions after cell surface antigen binding. DuoHexaBody-CD37, a bispecific CD37 antibody with the E430G hexamerization-enhancing mutation targeting two non-overlapping epitopes on CD37 (biparatopic), demonstrated potent and superior CDC activity compared to other CD37 antibody variants evaluated, in particular *ex vivo* in patient-derived chronic lymphocytic leukemia cells. The superior CDC potency was attributed to enhanced IgG hexamerization mediated by the E430G mutation in combination with dual epitope targeting. The mechanism of action of DuoHexaBody-CD37 was shown to be multifaceted, as it was additionally capable of inducing efficient antibody-dependent cellular cytotoxicity and antibody-dependent cellular phagocytosis *in vitro*. Finally, potent anti-tumor activity *in vivo* was observed in cell line- and patient-derived xenograft models from different B-cell malignancy subtypes. These encouraging preclinical results suggest that DuoHexaBody-CD37 (GEN3009) may serve as a potential therapeutic antibody for the treatment of human B-cell malignancies.

# INTRODUCTION

B-cell malignancies comprise a heterogeneous group of lymphoproliferative disorders including non-Hodgkin lymphomas (NHL) and chronic lymphocytic leukemia (CLL). In addition to chemotherapy and small molecule inhibitors, immunotherapy with anti-CD20 monoclonal antibodies (mAbs) such as rituximab, ofatumumab and obinutuzumab, has significantly improved the outlook for patients with B-NHL and CLL<sup>1-3</sup>. However, many patients eventually relapse and become resistant to treatment, creating an unmet need for alternative therapeutic strategies. In recent years, the tetraspanin plasma membrane protein CD37 has gained renewed interest as a promising therapeutic target for B-cell malignancies<sup>4-7</sup>. CD37 is selectively expressed on mature B cells and has limited or no expression on other hematopoietic cells such as T cells and NK cells, granulocytes, monocytes and dendritic cells<sup>8-10</sup>.

CD37 is involved in the spatial organization of the B-cell plasma membrane by forming tetraspanin-enriched micro domains (TEMs) through lateral associations with interaction partners, such as other tetraspanins or integrins<sup>11,12</sup>. CD37 is signaling-competent as it contains intracellular functional ITIM-like and ITAM-like motifs that play a role in pro-survival and pro-apoptotic signaling via the PI3K/AKT pathway. In addition, it controls IL-6 receptor signaling through interaction with SOCS3<sup>12,13</sup>.

In cancer, CD37 is highly expressed on malignant B cells in a variety of B-cell lymphomas and leukemias, including NHL and CLL<sup>14,15</sup>. To date, multiple CD37-targeting agents have shown preclinical or clinical efficacy<sup>5-7</sup>, including antibody drug conjugates<sup>16,17</sup>, a small modular immuno-pharmaceutical protein (SMIP)<sup>18</sup>, an antibody with enhanced antibody-dependent cellular cytotoxicity (ADCC) capacity<sup>19</sup>, a radiolabeled antibody<sup>20</sup> and chimeric antigen receptor (CAR) T cells<sup>21</sup>. The effector mechanisms of these agents include direct cytotoxicity mediated through conjugated cytotoxic or radioactive payloads, classical Fc $\gamma$ R-mediated effector functions such as ADCC, and T-cell mediated cytotoxicity. Interestingly, CD37 antibody-based therapeutics currently in (pre-)clinical development are poor inducers of complement-dependent cytotoxicity (CDC)<sup>5-7</sup>, another powerful Fc-mediated effector mechanism for killing hematological cancer cells<sup>22,23</sup>.

We have previously reported that activation of the classical complement pathway by IgG antibodies depends on IgG hexamer formation upon binding to membrane bound antigens. IgG hexamers, which form through intermolecular Fc-Fc interactions, provide an optimal docking site for hexavalent



C1q<sup>24-26</sup>. Activation of C1 triggers the complement cascade involving a series of proteolytic events leading to formation of membrane attack complexes that eventually kill target cells via disruption of their cell membrane. Introduction of a single point mutation, such as E430G, in the IgG Fc domain increases IgG hexamer formation and enhances CDC activity<sup>27,28</sup>. We combined this approach with the bispecific antibody technology DuoBody® to generate an obligate bispecific antibody for which potency was further increased compared to combinations of the parent molecules. Obligate bispecific antibodies represent a novel and most promising concept in current therapeutic antibody drug development<sup>29,30</sup>.

We hereby report the generation of a panel of CD37-targeting mAbs with an E430G hexamerization-enhancing mutation and characterized the preclinical mechanism of action and anti-tumor activity of the single mAbs, mAb combinations and CD37 biparatopic (bispecific) antibodies. It was demonstrated that CDC efficacy by single CD37-targeting mAbs was enhanced by combining two non-cross-blocking mAbs, which was most evident in the context of a biparatopic antibody variant, DuoHexaBody-CD37. DuoHexaBody-CD37 also induced potent FcγR-mediated effector functions, including ADCC and antibody-dependent cellular phagocytosis (ADCP). In addition, DuoHexaBody-CD37 showed significant anti-tumor efficacy *in vivo* in human cell line- and patient-derived xenograft models, indicating that DuoHexaBody-CD37 may serve as a promising novel therapeutic antibody for treatment of human B-cell malignancies.

# METHODS

## Antibodies

Anti-CD37 antibodies were generated through immunization (MAB Discovery GmbH, Germany) of rabbits with a mixture of HEK293F cells expressing human (sequence no. NP\_001765) or cynomolgus monkey (*Macaca fascicularis*, sequence no. XP\_005589942) CD37 or a mixture of Fc-fusion proteins containing the large extracellular loop of human or cynomolgus monkey CD37. CD37 antibodies were produced recombinantly as chimeric human IgG1s containing the hexamerization-enhancing mutation E430G (HexaBody<sup>®</sup> molecules<sup>27</sup>) and F405L or K409R mutations for bispecific antibody generation by controlled Fab-arm exchange (cFAE; DuoBody technology<sup>30,31</sup>) as appropriate. Humanized antibody sequences were generated using CDR-grafting in optimized human germ-line variable region sequences at Abzena (Cambridge, UK). The anti-HIV-1 gp120 mAb IgG1-b12 was used as a negative control antibody (IgG1-ctrl)<sup>32</sup>. Rituximab (MabThera<sup>®</sup>), ofatumumab (Arzerra<sup>®</sup>) and obinutuzumab (Gazyva<sup>®</sup>) were commercially obtained.

## Cell lines, patients, donors and reagents

Details on cell lines used in this study are summarized in Online Supplementary Methods. All primary patient cells were obtained after written and informed consent and stored using protocols approved by institutional review boards in accordance with the declaration of Helsinki (see Online Supplementary Methods). Blood samples and buffy coats from healthy human donors were obtained from the University Medical Center Utrecht (Utrecht, The Netherlands) and Sanquin (Amsterdam, The Netherlands), respectively. Pooled normal human serum (NHS; AB positive) was obtained from Sanquin. Details on antibodies/reagents used to define cell subsets within samples used for flow cytometry are provided in Online Supplementary Methods.

## Antibody binding assays

Antibody binding was assessed using target cells incubated with antibody for 30 minutes at 4°C. After washing, cells were incubated with R-Phycoerythrin (PE)-conjugated goat-anti-human IgG F(ab')<sub>2</sub> (Jackson ImmunoResearch Laboratories, West Grove, PA, USA) for 30 minutes at 4°C. Cells were washed and binding was analyzed by determining the geometric mean fluorescent intensity (gMFI) of the PE signal using flow cytometry.

For binding competition assays, target cells were incubated with primary unlabeled antibodies (final concentration 20 µg/mL) for 15 minutes at room temperature. Next, Alexa Fluor 488 (A488)-labelled antibodies (by reaction with

N-hydroxysuccinimidyl-esters following manufacturer's instructions [Molecular Probes, Eugene, OR, USA]) were added to cells at final concentration of 2  $\mu\text{g}/\text{mL}$ , followed by incubation for 15 minutes at room temperature. Cells were washed and gMFI of the A488 signal was determined by flow cytometry.

### **Alanine scanning**

A CD37 single residue alanine library was generated (GeneArt, Regensburg, Germany) in which all amino acid residues in the extracellular domains of human CD37 (UniProt P11049) were individually mutated to alanine, except for cysteines. The library was used to map amino acids in the extracellular loops of human CD37 involved in binding of mAbs Hx-CD37-010 and Hx-CD37-016 (details summarized in Online Supplementary Methods).

### **CDC assays**

CDC assays were performed as described using tumor cells incubated with antibody for 45 minutes at 37°C in the presence of NHS (20% final concentration) as a complement source<sup>33</sup>.

### **Expression analysis**

Expression levels of cellular markers were determined as described<sup>33</sup> using an indirect immunofluorescence assay (QIFIKIT<sup>®</sup>, Agilent, Santa Clara, CA, USA) according to the manufacturer's instructions.

### **ADCC and ADCP assays**

Activation of Fc $\gamma$ RIIIa- (H-131) and Fc $\gamma$ RIIIa-mediated (V-158) intracellular signaling was quantified using Luminescent Reporter Bioassays (Promega, Madison, WI, USA), according to the manufacturer's recommendations. Chromium-51 ( $\text{Cr}^{51}$ ) release ADCC assays were performed as described<sup>34</sup> and summarized in Online Supplementary Methods. ADCP assays were performed using tumor cells labeled with calcein AM (Life Technologies, Carlsbad, CA, USA) or pHRodo<sup>™</sup> Red AM Intracellular pH Indicator (ThermoFisher Scientific, Waltham, MA, USA) according to the manufacturer's instructions and opsonized with antibodies for 15 minutes at 37°C. Human monocyte-derived macrophages (h-MDM, isolation and culturing detailed in Online Supplementary methods) were added at effector to target (E:T) ratios of 2:1 or 1:1 and incubated for 4 hours at 37°C/5%CO<sub>2</sub>. During incubation, images were captured using an IncuCyte S3 Live Cell Analysis System with a 10x objective lense and acquired/processed using IncuCyte S3 software. Alternatively, tumor cells and h-MDM were stained for surface markers after incubation using fluorochrome-conjugated antibodies for 30 minutes at 4°C, fixed using 4% paraformaldehyde (ChemCruz, Dallas, TX, USA) and analyzed by flow cytometry. CD11b<sup>+</sup>/calcein AM<sup>+</sup>/CD19<sup>-</sup> cells were defined as h-MDM that phagocyto-

sed Daudi cells. CD11b<sup>-</sup>/calcein AM<sup>+</sup> cells were defined as non-phagocytosed Daudi cells remaining after co-culture, used to determine target cell depletion.

### **Whole blood assays**

Binding and cytotoxicity assays were performed with heparin- and hirudin-treated blood samples from healthy human donors, respectively. For cytotoxicity, blood samples were incubated with antibody for 4 hours at 37°C. Next, red blood cells were lysed and samples were stained for 30 minutes at 4°C with fluorochrome-labeled lineage-specific antibodies and TO-PRO-3 to characterize cell subsets and dead or dying cells respectively. For binding, red blood cells were first lysed and subsequently incubated with designated antibody mixtures. Binding was assessed by flow cytometry and expressed as the gMFI of AF488 fluorescence intensity for viable cell subsets. Depletion was determined as:

### **Animal studies**

Cell line-derived xenograft (CDX) and patient-derived xenograft (PDX) studies were conducted following protocols approved by institutional ethical committees, as provided in Online Supplementary Methods. *In vivo* pharmacokinetic analysis was performed as described<sup>27</sup>.

### **Data processing**

Flow cytometry data were analyzed using FlowJo V10 software. Graphs were plotted and analyzed using GraphPad Prism 8.0. Dose-response curves were generated using best-fit values of non-linear dose-response fits using log-transformed concentrations. All data shown are representative of at least two independent replicate experiments. Statistical differences in median animal tumor volumes were compared between treatment groups on the last day all groups were complete. In case of equal variance between groups (Bartlett's test) the parametric One Way ANOVA Uncorrected Fisher's LSD test (Daudi-Luc) was used. In case of unequal variance between groups (Bartlett's test) the non-parametric Mann-Whitney test (JVM-3, DOHH-2, NHL PDX) was used.

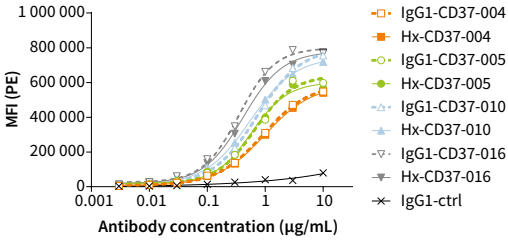
# RESULTS

## **Generation of CD37 mAbs and analysis of their binding characteristics**

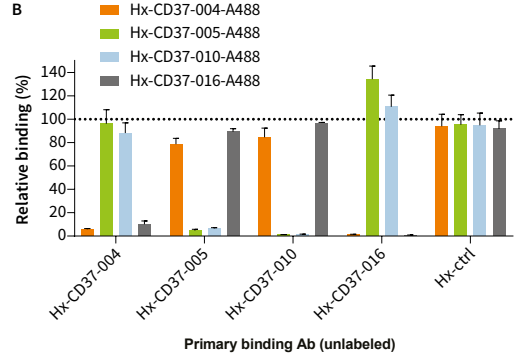
Rabbits were immunized with CD37 antigen to generate a diverse panel of mAbs recognizing human CD37. After humanization using CDR-grafting, antibodies were expressed in a human IgG1 backbone with and without the E430G hexamerization-enhancing mutation (Hx) and binding to CD37 on human tumor cells was assessed using Daudi cells. Four humanized CD37 mAbs were selected for further studies based on specific and efficient target binding ( $EC_{50} < 0.1 \mu\text{g/mL}$ ), CDR sequence diversity and cross-reactivity with human and cynomolgus monkey CD37. Hx-CD37-004, Hx-CD37-005, Hx-CD37-010 and Hx-CD37-016, and corresponding wild-type (WT) IgG1 variants showed dose-dependent binding to Daudi cells (Figure 1A) with  $EC_{50}$  values ranging from 0.42 - 0.92  $\mu\text{g/mL}$ . Comparable binding of WT anti-CD37 mAbs indicated that binding was not affected by the E430G mutation. We next performed cross-block binding experiments on Raji cells to examine cross-competition between the four humanized CD37 mAbs. Hx-CD37-004 competed with CD37-016 for binding, and Hx-CD37-005 competed with Hx-CD37-010 for binding to CD37 (Figure 1B). The mutually competing antibodies Hx-CD37-004 and Hx-CD37-016 were able to simultaneously bind to CD37 with one of the other mutually competing antibodies Hx-CD37-005 or Hx-CD37-010, thereby indicating that the four antibodies represent two different cross-blocking groups.

We selected one mAb candidate from each cross-blocking group, Hx-CD37-010 and Hx-CD37-016, and used alanine scanning analysis to map epitopes within the extracellular loops of human CD37. A library with alanine substitutions at all extracellular residues of human CD37, except for cysteines, was generated. Alanine mutants were expressed individually in HEK293F™ cells and binding of Hx-CD37-010 and Hx-CD37-016 was determined by flow cytometry. Loss of Hx-CD37-010 binding to human CD37 was observed with alanine substitutions at position Y182, D189, T191, I192, D194, K195, V196, I197 and P199, while for Hx-CD37-016, loss of antibody binding was observed with alanine substitutions at position E124, F162, Q163, V164, L165 and H175 (Figure 1C). These results showed that residues identified to be crucial for binding of Hx-CD37-010 are distinct from residues crucial for binding of Hx-CD37-016. Together, the binding analyses demonstrate that Hx-CD37-010 and Hx-CD37-016 bind different residues within the second extracellular domain (EC2) of human CD37 (Figure 1D).

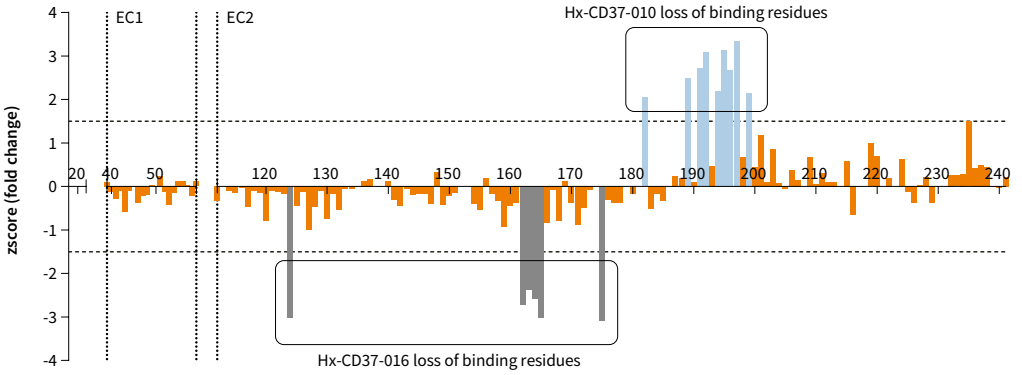
A



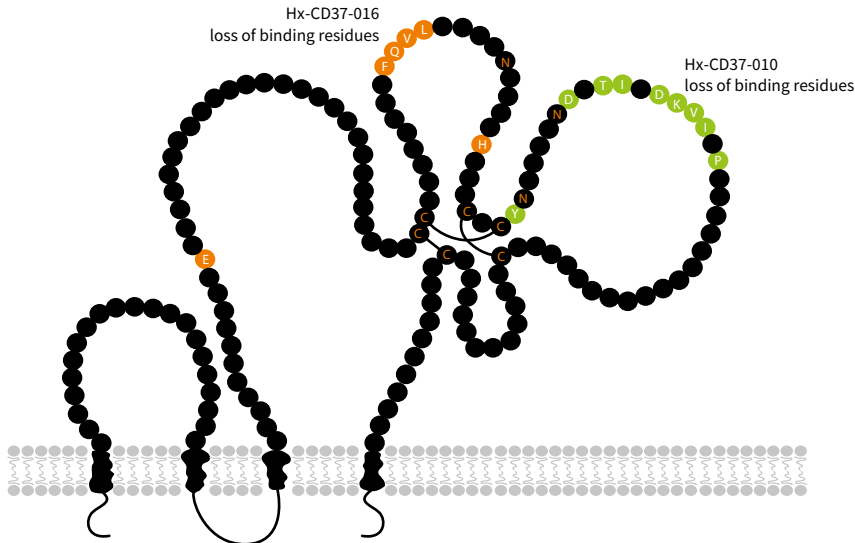
B



C



D. CD37



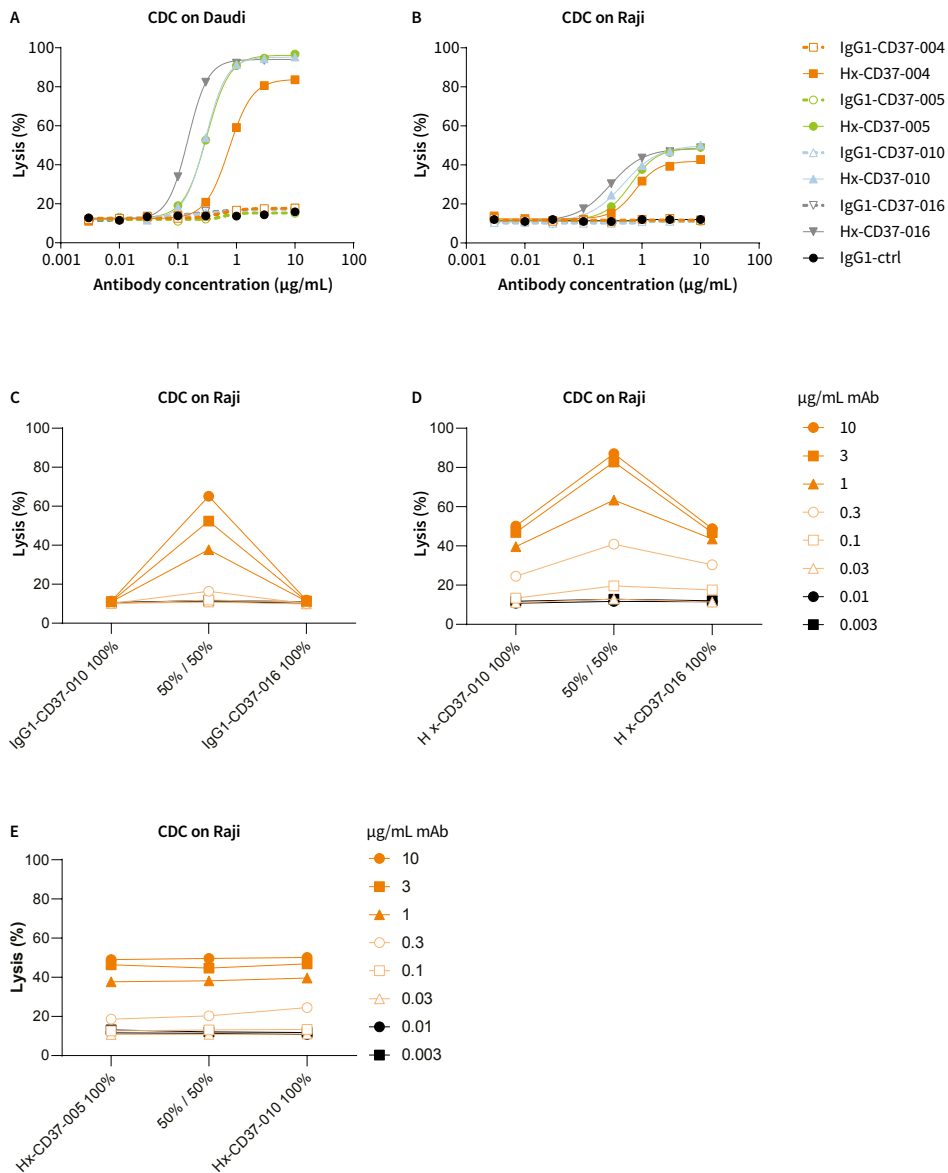
## CDC activity of CD37 mAbs is potentiated by enhanced hexamerization and dual epitope targeting

We previously reported that CDC by CD37 mAbs is potentiated by introducing the hexamerization-enhancing mutation E430G in the IgG Fc domain<sup>33</sup> and therefore investigated the potency of the novel CD37 mAbs to induce CDC *in vitro*. Whereas WT IgG1-CD37 antibodies were inactive, hexamerization-enhanced variants induced dose-dependent and potent CDC in Daudi cells ( $EC_{50}$  ranging from 0.15 - 0.75  $\mu\text{g}/\text{mL}$ ) (Figure 2A). In addition, introduction of the E430G mutation unlocked CDC activity of the CD37 mAbs in Raji cells ( $EC_{50}$  ranging from 0.29 - 0.77  $\mu\text{g}/\text{mL}$ ), which are expected to be less sensitive to CDC due to higher expression of complement regulatory protein CD59 (Figure 2B)<sup>35</sup>. An alternative way to enhance CDC is by dual epitope targeting using non-cross-blocking antibody combinations, as has been previously reported for a number of cell surface antigens, for example EGFR<sup>36</sup>. Also here, the WT IgG1-CD37 mAbs did not induce CDC as single agents, whereas combinations of non-cross-blocking WT IgG1-CD37-010 and IgG1-CD37-016 potentiated CDC to 65% maximum lysis in Raji cells (Figure 2C). Interestingly, while hexamerization-enhanced variants of these non-cross-blocking CD37 mAbs individually induced 50% maximum lysis in Raji cells, CDC-mediated lysis was strongly enhanced in the combination (87% maximum lysis) (Figure 2D), thereby clearly outperforming combinations of the WT non-cross-blocking CD37 mAbs. These results were confirmed with combinations of the other CD37-specific non-cross-blocking mAbs (data not shown). In contrast, combinations of Hx-CD37 mAbs that compete for CD37 binding did not show enhanced CDC activity compared to single antibodies, including the combination of Hx-CD37-005 and Hx-CD37-010 (Figure 2E) and the mixture of Hx-CD37-

### ◀ Figure 1

#### Binding characteristics of CD37 panel mAbs.

(A) Binding of WT (IgG1) and hexamerization-enhanced (Hx) antibody variants of the CD37 panel to Daudi cells. Antibody binding was assessed by flow cytometry and is expressed as the gMFI of the PE signal from a secondary IgG detection antibody. (B) Binding competition between Hx-CD37 panel antibodies was assessed on Raji cells by pre-incubating cells with 20  $\mu\text{g}/\text{mL}$  unlabeled Hx-CD37 panel antibodies (primary binding) followed by incubation with A488-labeled antibodies (2  $\mu\text{g}/\text{mL}$ ). Relative binding in presence of competing antibody was plotted (% relative binding =  $[\text{gMFI A488 in presence of competing antibody}]/[\text{gMFI A488 in absence of competing antibody}] * 100$ ). Data represents the mean and standard deviation (SD) of triplicate measurements. (C) Mapping of amino acids in the extracellular loops of human CD37 involved in binding of Hx-CD37-010 or Hx-CD37-016 as determined by alanine scanning. A z-score (fold change in binding compared to binding of a control antibody) for each mutant position was calculated and plotted. Z-scores  $< 0$  indicate loss of binding of Hx-CD37-016 in comparison to Hx-CD37-010 while z-scores  $> 0$  indicate loss of binding of Hx-CD37-010 in comparison to Hx-CD37-016. Amino acid residues where the z-score was higher than 1.5 (Hx-CD37-010) or lower than -1.5 (Hx-CD37-016), indicated by the horizontal dotted lines, were considered as 'loss of binding mutants'. The number above the x-axis refers to amino acid positions in full length human CD37. EC1 = small extracellular loop, EC2 = large extracellular loop of CD37, respectively. (D) Amino acid residues involved in Hx-CD37-010 (green) and Hx-CD37-016 (orange) binding to CD37 are depicted in a graphical representation based on UniProtKB P11049. The extracellular domain of CD37 contains six cysteines (Cys, C), which are indicated as an orange letter C; these form intramolecular disulphide bonds and contribute to the conformation of the tetraspanin. The asparagine residues (Asn, N) in the N-glycosylation site consensus sequence Asn-Xxx-Ser (NXS) are indicated as an orange letter N.



▲ **Figure 2**

**CDC activity of CD37 mAbs is potentiated by enhanced hexamerization and dual epitope targeting.**

(A-B) CDC in Daudi (A) and Raji (B) cells opsonized with WT (IgG1) or hexamerization-enhanced (Hx) variants of CD37 mAbs. (C-D) CDC in Raji cells opsonized with combinations of non-cross-blocking IgG1-CD37 (C) or Hx-CD37 (D) mAbs. (E) CDC in Raji cells opsonized with combinations of cross-blocking Hx-CD37 mAbs. The indicated antibody concentrations represent the total antibody concentration used. CDC induction was assessed in the presence of 20% NHS and expressed as the percentage lysis determined by the fraction of PI-positive cells.



004 and Hx-CD37-016 (data not shown). These results indicate that CDC activity of the CD37 mAbs is potentiated by enhanced hexamerization through the E430G mutation and by dual epitope targeting.

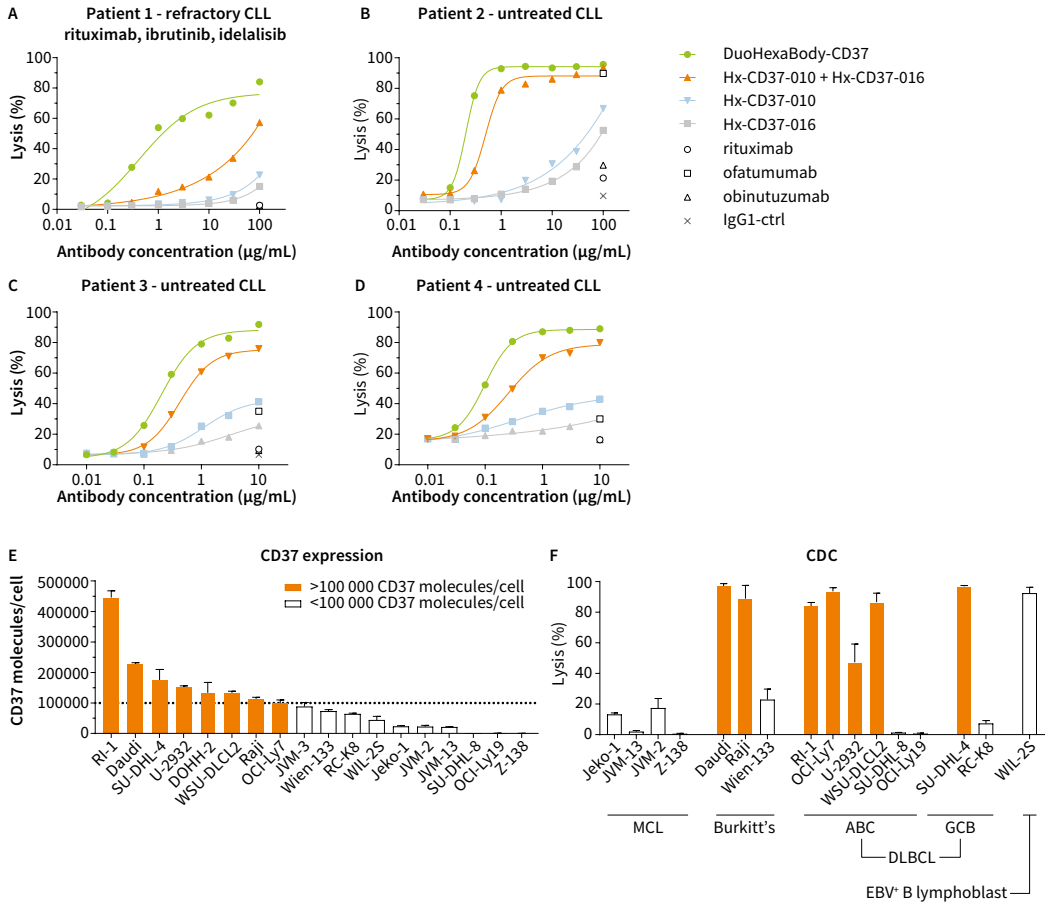
**A biparatopic hexamerization-enhanced CD37 antibody variant, DuoHexaBody-CD37, induces superior CDC activity in vitro and ex vivo**

We next explored the possibility of combining enhanced hexamerization with dual epitope targeting in a bispecific antibody. A biparatopic CD37 mAb variant, DuoHexaBody-CD37, was generated through controlled Fab-arm exchange between Hx-CD37-010 and Hx-CD37-016<sup>30,31</sup>. The CDC activity of DuoHexaBody-CD37 was compared to that of single mAbs and mAb combinations in samples from untreated CLL patients and a CLL patient relapsed/refractory to rituximab, ibrutinib and idelalisib. Strikingly, DuoHexaBody-CD37 induced superior CDC activity in all patient-derived CLL samples compared to either the single mAbs or the combination, which was most apparent in the refractory CLL sample (Figure 3A-D). Consistent with results in tumor cell lines, the mAb combination showed enhanced CDC compared to the single mAbs. Comparison of DuoHexaBody-CD37 with the approved CD20 antibodies rituximab, ofatumumab and obinutuzumab demonstrated superior CDC in all patient samples tested. None of the approved CD20 antibodies induced CDC in the refractory CLL sample (Figure 3A) while in untreated CLL samples, only ofatumumab induced CDC at concentrations of 10 mg/mL (Figure 3C-D) and 100 mg/mL (Figure 3B).

The capacity of DuoHexaBody-CD37 to induce CDC in malignant B-cells was further confirmed in CDC assays *in vitro* using 16 tumor cell lines with varying CD37 expression levels, derived from different B-cell lymphoma subtypes (Figure 3E). DuoHexaBody-CD37 induced potent CDC in 8 of the 16 cell lines tested, with generally higher levels of tumor cell lysis observed in cell lines with CD37 expression levels above 100 000 copies/cell (Figure 3E, F).

**DuoHexaBody-CD37 induces efficient ADCC and ADCP in vitro**

While the primary rationale behind the development of DuoHexaBody-CD37 was focused on maximizing its capacity to induce CDC, other Fc-mediated effector functions such as ADCC and ADCP, known to contribute to tumor cell kill, were also tested. The potential of DuoHexaBody-CD37 to induce ADCC and ADCP was first evaluated in FcγRIIIa (V-158) and FcγRIIa (H-131) reporter assays, respectively. When bound to Daudi target cells, DuoHexaBody-CD37 induced efficient, dose-dependent activation of FcγRIIIa and FcγRIIa signaling in transfected Jurkat effector T cells (Figure 4A, B). FcγRIIIa and FcγRIIa signaling was at least comparable to that induced by the CD20 antibody rituximab.



▲ **Figure 3**

**A biparatopic hexamerization-enhanced CD37 antibody variant, DuoHexaBody-CD37, induces superior CDC activity in vitro and ex vivo.**

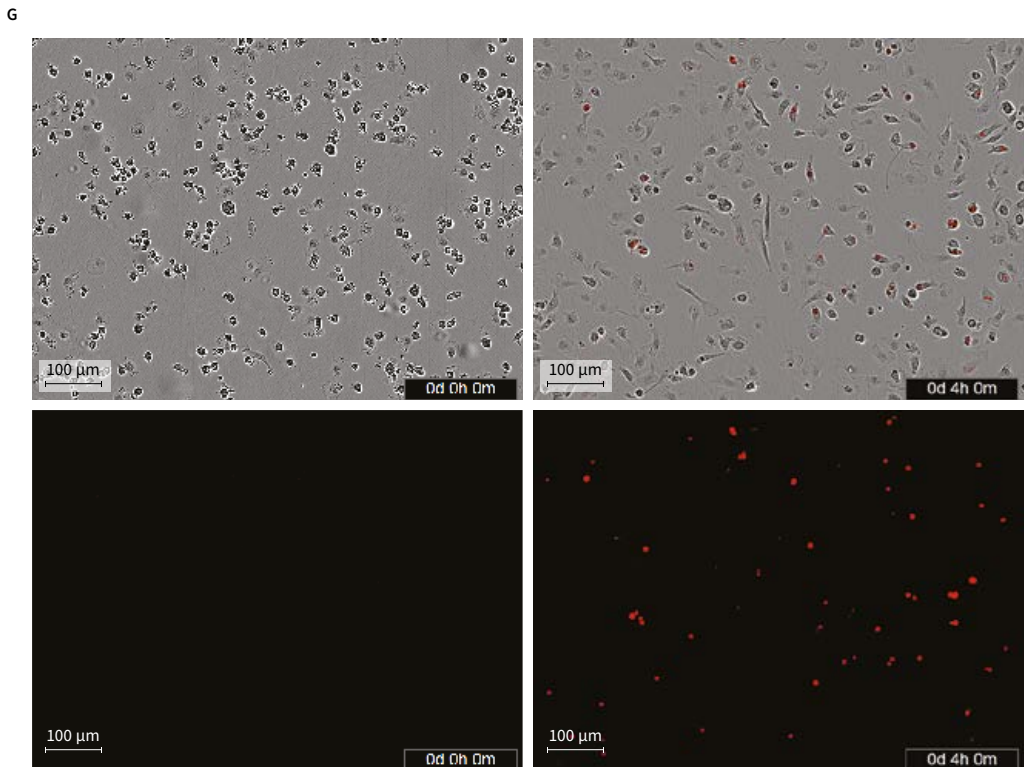
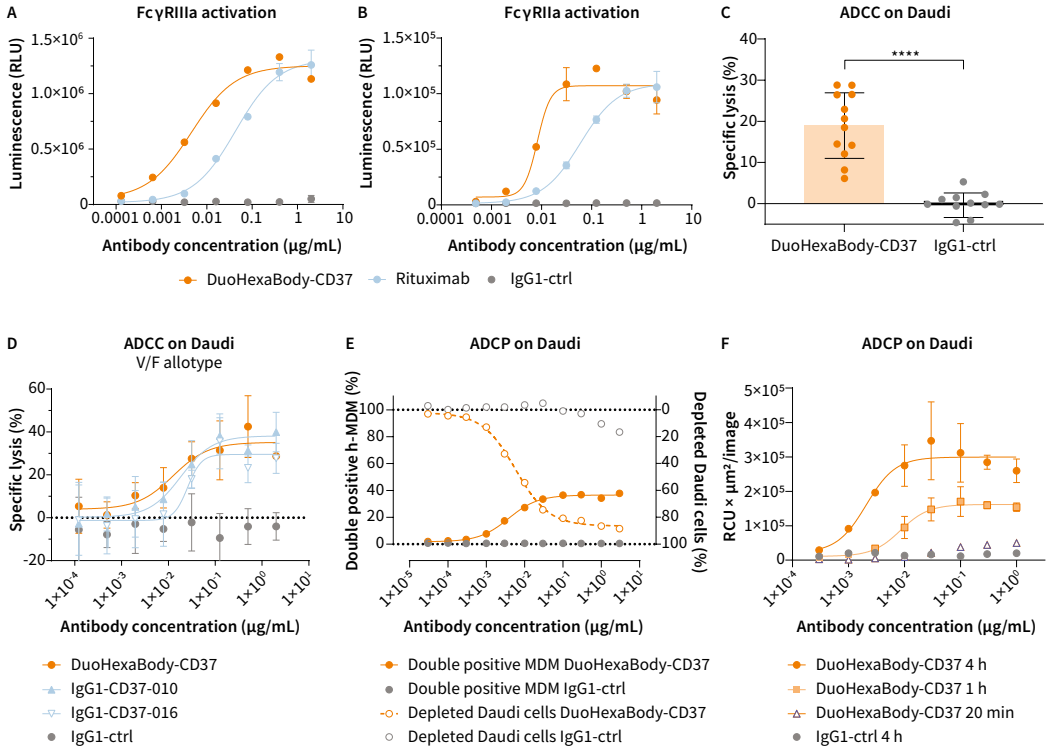
(A-D) PBMCs (A-B) or purified B-cells (C-D) from 4 chronic lymphocytic leukemia (CLL) patients were used to determine CDC induction by DuoHexaBody-CD37, and Hx-CD37 antibody variants (Hx-CD37-010 and Hx-CD37-016) alone or in combination (1:1 equimolar mixture). CDC induction was assessed in the presence of 20% NHS. The percentage lysis was determined by the fraction of PI-positive (A-B) or 7AAD-positive cells (C-D). (E) 17 B-lymphoma cell lines and the Epstein-Barr virus (EBV)-positive B-lymphoblastic cell line WIL-2S were evaluated for CD37 molecule expression on the cell surface using quantitative flow cytometry. The dotted line indicates 100,000 CD37 surface molecules/cell. (F) The capacity of 10  $\mu\text{g}/\text{mL}$  DuoHexaBody-CD37 to induce CDC in the presence of 20% NHS was tested in 16 cell lines also described in (E) and expressed as the percentage lysis determined by the fraction of PI-positive cells. The cell lines are grouped per B-lymphoma subtype: mantle cell lymphoma (MCL), Burkitt's lymphoma, diffuse large B-cell lymphoma (DLBCL) with activated B-cell (ABC) or germinal center B-cell (GCB) subtypes and an EBV-positive B-lymphoblastic cell line. Cell lines with >100,000 CD37 molecules per cell are indicated by orange bars, and those with <100,000 CD37 molecules per cell by white bars. Either four (E) or two (F) replicates were used per cell line (mean  $\pm$  SD).

ADCC induction by DuoHexaBody-CD37 was further evaluated in a  $^{51}\text{Cr}$  release assay using Daudi cells as target cells and human PBMCs from 12 healthy human donors as effector cells (E:T ratio 100:1). DuoHexaBody-CD37 induced efficient, dose-dependent ADCC of Daudi cells ( $\text{EC}_{50} = 9.9 \pm 10.0 \text{ ng/mL}$ ), which was comparable to the WT IgG1-CD37 mAbs without the E430G and F405L/K409R mutations (Figure 4C, D).

Next, ADCP was assessed in a flow cytometry-based assay using calcein AM-labeled Daudi target cells and h-MDM as effector cells. DuoHexaBody-CD37 induced efficient phagocytosis of calcein AM-labeled Daudi target cells by h-MDM, as illustrated by a dose-dependent increase in  $\text{CD11b}^+/\text{calcein AM}^+$  double positive h-MDM ( $\text{EC}_{50} = 13.5 \pm 13.1 \text{ ng/mL}$ ), resulting in almost complete depletion of Daudi target cells ( $\text{EC}_{50} = 5.8 \pm 2.3 \text{ ng/mL}$ ) (Figure 4E). DuoHexaBody-CD37-mediated ADCP was confirmed in an image-based assay using Daudi cells labeled with the pH-sensitive pHRodo dye that becomes increasingly fluorescent in the acidic lysosomal environment. Also here, DuoHexaBody-CD37 induced efficient engulfment and lysosomal degradation of Daudi cells by h-MDM (Figure 4F, G). Together, these data demonstrate that DuoHexaBody-CD37 induces efficient Fc $\gamma$ R-mediated immune effector functions to kill CD37-positive tumor cells.

#### **DuoHexaBody-CD37 depletes B cells, but not other leukocyte populations in human whole blood**

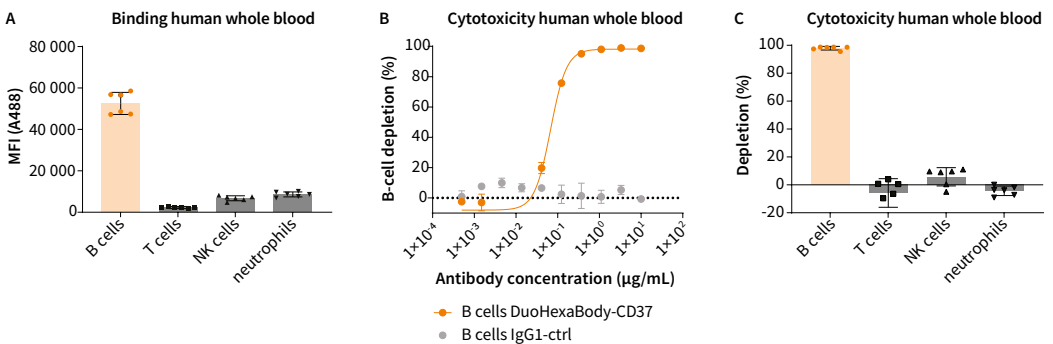
CD37 is reported to be highly expressed on mature B cells, with low expression levels on other leukocyte subsets<sup>8-10</sup>. Since non-malignant B-cell depletion may be used as a safety- and pharmacodynamic biomarker when exploring B-cell targeting therapies, the ability of DuoHexaBody-CD37 to bind and deplete B cells versus other leukocyte subsets was evaluated in whole blood derived from six healthy human donors. The blood was hirudin anticoagulated to preserve complement activity. DuoHexaBody-CD37 showed efficient binding to  $\text{CD19}^+$  B cells, while low binding was observed to T cells, NK cells and neutrophils for all six healthy human donors tested (Figure 5A). DuoHexaBody-CD37 showed potent depletion of the  $\text{CD19}^+$  B-cell population compared to the negative control, with  $98\% \pm 1.3\%$  depletion at  $10 \mu\text{g/mL}$  and an average  $\text{EC}_{50}$  of  $0.077 \pm 0.039 \mu\text{g/mL}$  (Figure 5B). For the T cells, NK cells and neutrophils that showed low DuoHexaBody-CD37 binding, no depletion was observed at saturating mAb concentrations of  $10 \mu\text{g/mL}$  (Figure 5C).



◀ **Figure 4**

**DuoHexaBody-CD37 induces efficient ADCC and ADCP *in vitro*.**

(A-B) FcγRIIIa (A) and FcγRIIa (B) crosslinking by DuoHexaBody-CD37 was analyzed in a bioluminescent Reporter Bioassay using Daudi target cells and engineered FcγRIIIa- or FcγRIIa-expressing Jurkat effector T cells that express luciferase upon FcγR crosslinking. Luciferase production is presented as relative luminescence units (RLU). Error bars represent the mean ± SD of duplicate measurements. (C) ADCC by 2 μg/mL DuoHexaBody-CD37 was evaluated in a classical <sup>51</sup>Cr release assay using Daudi target cells and PBMCs from 12 healthy human donors as a source of effector cells (E:T of 100:1). The percentage lysis was calculated relative to a Triton X-100 control (100% lysis) and no antibody control (0% lysis). \*\*\*\*P<0.00001, paired T-test with two-tailed 95% confidence intervals. (D) Dose-response ADCC (mean percentage lysis ± SD of 3 replicate samples) induced by DuoHexaBody-CD37, WT IgG1-CD37-010 and WT IgG1-CD37-016 shown for one representative responsive donor as described in (C). Error bars represent the mean ± SD of triplicate measurements. (E) ADCP induced by DuoHexaBody-CD37 using Daudi target cells and monocyte-derived h-MDM from healthy human donors as a source of effector cells. Calcein AM-labeled Daudi cells opsonized with DuoHexaBody-CD37 were incubated with CD11b<sup>+</sup> h-MDM at an E:T ratio of 2:1 and ADCP was analyzed by flow cytometry after a 4h co-culture. The amount of h-MDMs that phagocytosed Daudi cells is presented as % CD11b<sup>+</sup>/calcein AM<sup>+</sup>/CD19<sup>-</sup> double positive cells. CD19 was used to exclude macrophages with bound instead of phagocytosed tumor cells. The percentage CD11b<sup>+</sup>/calcein AM<sup>+</sup> cells was determined as an indicator of the amount of non-phagocytosed Daudi cells; presented here as a depleted cell fraction relative to a no antibody control sample. Data from one representative donor out of three is shown. (F) ADCP of pHRodo-labeled Daudi target cells by h-MDM induced by DuoHexaBody-CD37 over time at an E:T ratio of 1:1, shown for one out of three representative donors. Red fluorescence indicates phagocytosed Daudi target cells by h-MDM. ADCP was quantified by the total sum of the red fluorescent intensity in the image (RCUxμm<sup>2</sup>/image) and presented as the mean ± SD of duplicate measurements. (G) Phase contrast- and red fluorescent images of DuoHexaBody-CD37-opsonized (1 μg/mL) pHRodo-labeled Daudi target cells co-cultured with h-MDM effector cells at 0 hrs and 4 hrs incubation as described in (F).



▲ **Figure 5**

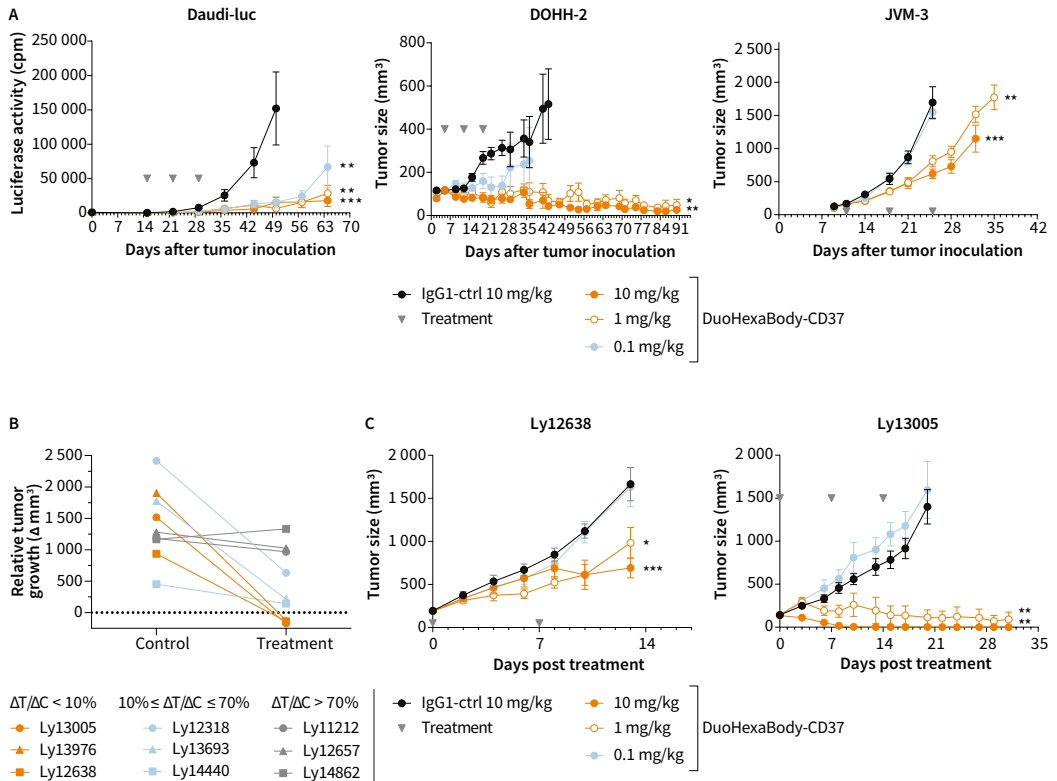
**DuoHexaBody-CD37 depletes B cells, but not other leukocyte populations in human whole blood.**

Binding to- and depletion of different leukocyte cell subsets in human whole blood by DuoHexaBody-CD37 was assessed by flow cytometry using six healthy donors. (A) Binding of A488-labeled DuoHexaBody-CD37 (30 μg/mL) is expressed as the gMFI ± SD of the A488 signal. (B-C) Cell depletion induced by a concentration series (B, one representative donor) or 10 μg/mL (C, six donors) DuoHexaBody-CD37 after a four hour incubation period presented as mean % depletion ± SD relative to a no antibody control sample. Leukocyte subsets were characterized as: B cells (CD19<sup>+</sup>), T cells (CD3<sup>+</sup>), NK cells (CD56<sup>+</sup>) and neutrophils (CD66<sup>+</sup>/CD16<sup>+</sup>).

### **DuoHexaBody-CD37 shows anti-tumor activity in vivo in xenograft models**

The anti-tumor activity of DuoHexaBody-CD37 *in vivo* was evaluated in CDX models obtained by intravenous or subcutaneous injection of B-cell lymphoma-derived Daudi-Luc and DOHH-2 cells and CLL-derived JVM-3 cells, that express moderate to high levels of CD37 (Figure 3E). First, we confirmed that DuoHexaBody-CD37 (which lacks cross-reactivity to murine CD37) has a normal clearance rate comparable to WT IgG1-ctrl in tumor-free mice, i.e. in the absence of target binding (data not shown). Next, SCID mice were injected with Daudi-luc, DOHH-2 or JVM-3 cells and treated with 0.1, 1, or 10 mg/kg DuoHexaBody-CD37 after tumors had established. Three weekly doses of DuoHexaBody-CD37 resulted in significantly reduced tumor growth in the Daudi-Luc model at all tested dose levels as compared to the IgG1-ctrl, and at 1 and 10 mg/kg in the JVM-3 and DOHH-2 models (Figure 6A).

The anti-tumor activity of DuoHexaBody-CD37 was also assessed in PDX models, which offer more reliable results for clinical outcomes because of their more conserved characteristics of the original tumor including heterogeneity, genetic and biological complexity and molecular diversity.<sup>37</sup> In a screening approach, we evaluated the anti-tumor efficacy induced by DuoHexaBody-CD37 using nine NHL PDX models in an experimental set up using a one mouse per group design. SCID mice were treated with two weekly doses of 5 mg/kg DuoHexaBody-CD37 or PBS after tumors had established, and the ratio between the relative tumor growth in the DuoHexaBody-CD37-treated mouse ( $\Delta T$ ) and the PBS control mouse ( $\Delta C$ ) was used to classify responders ( $\Delta T/\Delta C < 10\%$ ) versus non-responders ( $\Delta T/\Delta C > 70\%$ ) and intermediates ( $10\% \leq \Delta T/\Delta C \leq 70\%$ ). Three models were classified as responders, three as intermediates and three as non-responders (Figure 6B). From the three models that showed  $<10\%$  relative tumor growth (i.e. tumor stasis or tumor regression), two models achieved complete tumor regression and did not grow out during the complete observation period (~60 days). Although CD37 mRNA expression was confirmed for all PDX models, variability between models was limited and could not be associated with response (data not shown). Follow-up cohort studies in two responding PDX models (Ly12638 and Ly13005) confirmed potent, dose-dependent anti-tumor activity of DuoHexaBody-CD37 at doses as low as 1 mg/kg (Figure 6C). Collectively, these data indicate that DuoHexaBody-CD37 can mediate significant anti-tumor activity in both CDX and PDX *in vivo* models derived from different B-cell malignancy subtypes.



▲ **Figure 6**

**DuoHexaBody-CD37 shows anti-tumor activity in vivo in xenograft models.**

(A) The anti-tumor activity of DuoHexaBody-CD37 *in vivo* was evaluated in CDX models from Burkitt's lymphoma (Daudi-luc), CLL (JVM-3) and B-cell lymphoma (DOHH-2) cell lines using SCID mice. IgG1-ctrl is a non-binding negative control antibody. Grey arrows indicate antibody treatment (QWx3). Luciferase activity (mean  $\pm$  standard error of the mean [SEM]) as a measure of tumor burden, or average tumor size (mean  $\pm$  SEM) in mice treated with the indicated antibody dose is shown over time. (B) PDX clinical trial in which tumor fragments from 9 NHL patients were subcutaneously implanted in SCID mice, using a one mouse per group design. Mice were dosed with either two weekly doses (QWx2) of 5 mg/kg DuoHexaBody-CD37 or PBS as a negative control. The relative tumor growth is presented as the difference in tumor volume between day of first treatment and day of analysis (7-25 days after initiation of treatment) in the DuoHexaBody-CD37-treated mouse (treatment,  $\Delta T$ ) and the control mouse (control,  $\Delta C$ ). The ratio between the relative tumor growth in the treatment and control mouse, specifically  $\Delta T/\Delta C$ , was used to categorize models as responders ( $\Delta T/\Delta C < 10\%$ ), intermediates ( $10\% \leq \Delta T/\Delta C \leq 70\%$ ), or non-responders ( $\Delta T/\Delta C > 70\%$ ). (C) PDX dose response using two responding NHL models as described in (B) with indicated doses of DuoHexaBody-CD37 or IgG1-ctrl (n=8 mice/group). Average tumor size is shown  $\pm$  SEM. \* P<0.01, \*\* P<0.001, \*\*\* P<0.0001.

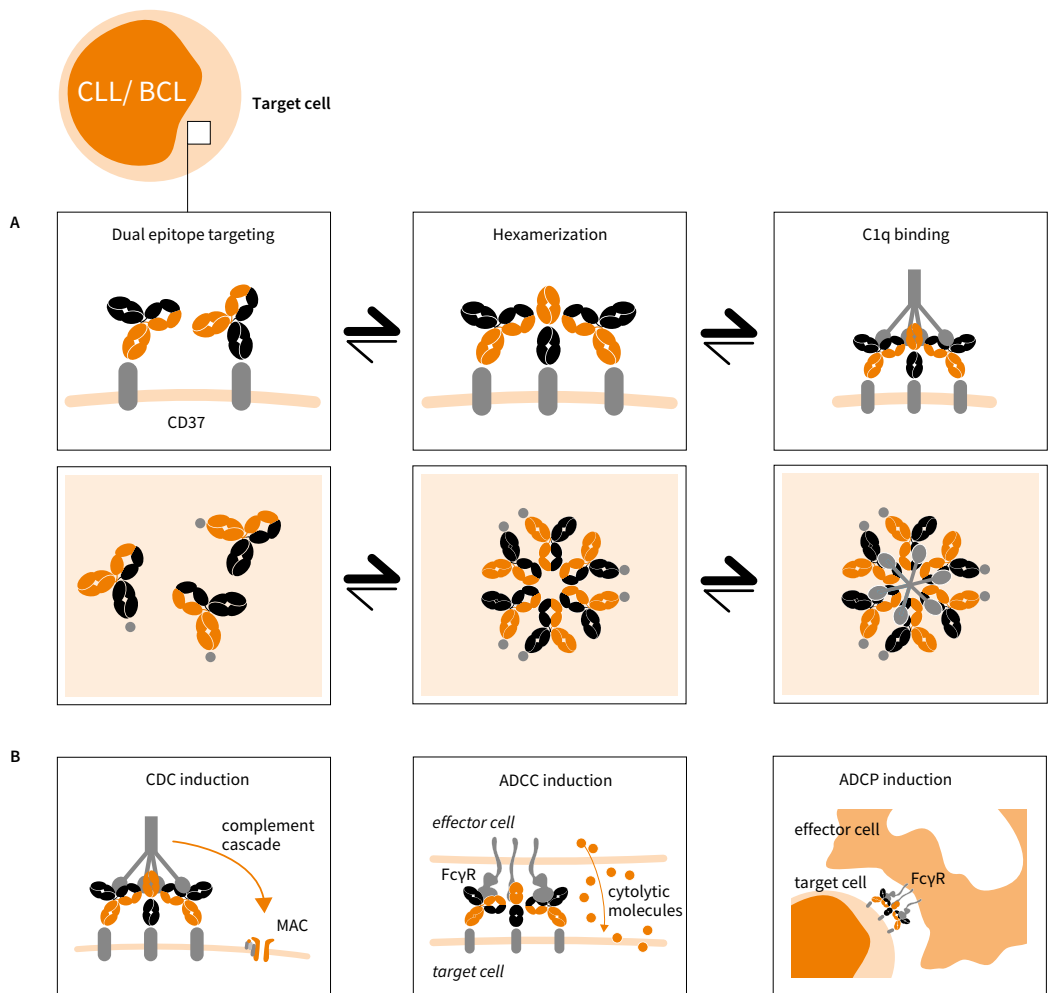
## DISCUSSION

The treatment landscape for B-cell malignancies has rapidly evolved since initial approval of the CD20-targeting mAbs. With resistance to CD20-targeted therapies arising, a number of alternative B-cell surface antigens have been evaluated for targeted mAb therapy including CD19, CD22, CD30, CD79b and CD37<sup>38</sup>. Similar to CD20, CD37 is highly expressed on tumor B cells across all major NHL and CLL subtypes. Although CD37 has long been recognized as a potential target for treatment of B-cell malignancies, it has recently received renewed interest with various agents currently in (pre)-clinical development. While multiple effector mechanisms have been reported for these agents, they are generally poor in inducing CDC<sup>5-7</sup>.

Here, we introduce DuoHexaBody-CD37, a novel CD37-targeted agent generated using an innovative approach that combines DuoBody and HexaBody<sup>®</sup> antibody platform technologies. DuoHexaBody-CD37 is a biparatopic bispecific IgG1 antibody with a hexamerization-enhancing mutation that induces strong anti-tumor activity in preclinical models *in vitro* and *in vivo* through potent CDC, ADCC and ADCP (Figure 7). DuoHexaBody-CD37 exhibits highly potent CDC activity *in vitro* and *ex vivo*, which was superior to the parental WT or hexamerization-enhanced CD37 mAbs and to the combinations thereof. DuoHexaBody-CD37 not only outperformed all other CD37 antibody variants evaluated in *ex vivo* CDC assays using primary CLL patient samples, but also outperformed approved CD20 mAbs rituximab, ofatumumab and obinutuzumab. We demonstrated that the superior CDC efficacy of DuoHexaBody-CD37 is caused by enhanced antibody hexamerization upon target binding and by dual epitope targeting inherent to binding two non-overlapping epitopes on CD37. Locally increasing the density of Fc-domains through dual epitope targeting can potentiate CDC<sup>36</sup> and may also favorably affect Fc-mediated antibody hexamerization, specifically in the context of the hexamerization-enhancing mutation. Consequently, the threshold for complement activation by DuoHexaBody-CD37 might be lower, which could result in enhanced anti-tumor efficacy in clinical settings. This could be of specific interest for patients who no longer respond to CD20 mAb treatment regimens, where antigen expression, cell surface antigen distribution or expression of complement inhibitors might be limiting factors<sup>22</sup>.

While DuoHexaBody-CD37 was shown to bind two non-overlapping epitopes on CD37, the fine mechanism of target binding, either bivalent or monovalent, and subsequent oligomerization into hexameric complexes remains to be elucidated. IgG oligomerization on target surfaces was recently reported to occur





▲ **Figure 7**

**Mechanism of action of DuoHexaBody-CD37.**

(A) The biological process of DuoHexaBody-CD37 binding to CD37 receptors on the cell surface and the formation of hexameric antibody complexes, thereby providing an optimal docking site for C1q, the hexavalent first component of the complement system. Fc-Fc-mediated clustering of CD37 antibodies into hexameric complexes on the cell surface can be enhanced through the introduction of an E430G hexamerization-enhancing mutation and by dual epitope targeting. (B) DuoHexaBody-CD37 was shown to induce kill in malignant B cells by inducing highly potent CDC and through FcγR-mediated effector functions such as ADCC and ADCP.

via Fc-Fc interaction-mediated recruitment of IgG molecules directly from solution, but also through lateral diffusion on the cell in case of preferentially monovalent binding IgG molecules<sup>25</sup>. CD37 is thought to be highly mobile due to its role in protein trafficking and organization in the plasma membrane and the formation of TEMs<sup>39</sup>. One could speculate that for DuoHexaBody-CD37 specifically, dual epitope targeting may optimize Fc-tail configuration in the process of IgG hexamerization, which may be augmented by lateral diffusion.

Besides inducing highly potent CDC, DuoHexaBody-CD37 was shown to efficiently engage with FcγRs in mediating ADCC and ADCP, indicating the mechanism of action of DuoHexaBody-CD37 is multifaceted. DuoHexaBody-CD37 compared favorably to rituximab in both FcγRIIIa and FcγRIIIa crosslinking, in cell line models that showed comparable levels of CD20 and CD37 expression. Importantly, DuoHexaBody-CD37 efficiently depleted peripheral blood B cells, but not other leukocyte populations from healthy human whole blood. Furthermore, in xenograft models *in vivo*, DuoHexaBody-CD37 induced significant inhibition of tumor growth in a CLL CDX model, 2 NHL CDX models and 6 out of 9 NHL PDX models. Notably, mice are not considered a suitable species to assess CDC-dependent tumor cell kill *in vivo*, suggesting FcγR-mediated effector functions may largely determine the observed anti-tumor activity.<sup>40</sup> Further studies are required to understand the contribution of individual effector mechanisms *in vivo*.

The current landscape of drug development in B-cell malignancies includes CD20-targeting antibodies such as ofatumumab and the glycoengineered obinutuzumab, and small molecule inhibitors targeting Bruton's tyrosine kinase, Bcl-2 and PI3K-δ such as ibrutinib, venetoclax and idelalisib, respectively<sup>3</sup>. These growing numbers of therapeutic agents might also provide opportunities for combination therapy with CD37-targeting antibodies. Combinations of DuoHexaBody-CD37 with anti-CD20 antibodies could be of particular interest, as we have previously shown enhanced CDC in CLL and B-NHL primary patient cells with combinations of CD20 and CD37 mAbs containing hexamerization-enhancing mutations<sup>33</sup>. Furthermore, CD37 has been reported to contain ITIM-like and ITAM-like regulatory motifs that regulate pro-survival and pro-apoptotic signaling processes via the PI3K/AKT pathway<sup>13</sup>. We speculate that combinations of DuoHexaBody-CD37 with pro-apoptotic PI3K-δ-inhibitors such as idelalisib may work synergistically, however the role of DuoHexaBody-CD37 in apoptotic signaling via CD37 remains to be elucidated.

In summary, we present here a novel therapeutic antibody that, for the first time, combines the proprietary DuoBody and HexaBody antibody platforms to create a biparatopic CD37 IgG1 antibody with enhanced Fc-mediated hexamerization upon target binding. The potent anti-tumor activity exhibited by DuoHexaBody-CD37 in preclinical B-cell malignancy models highlights its therapeutic potential. Preparations to evaluate the clinical safety and preliminary efficacy of DuoHexaBody-CD37 in a first-in-human clinical trial are currently ongoing.

# REFERENCES

1. Marshall MJE, Stopforth RJ, Cragg MS. Therapeutic Antibodies: What Have We Learnt from Targeting CD20 and Where Are We Going? *Front Immunol* 2017; **8**: 1245-.
2. Salles G, Barrett M, Foà R, et al. Rituximab in B-Cell Hematologic Malignancies: A Review of 20 Years of Clinical Experience. *Adv Ther* 2017; **34**(10): 2232-73.
3. Crisci S, Di Francia R, Mele S, et al. Overview of Targeted Drugs for Mature B-Cell Non-hodgkin Lymphomas. *Front Oncol* 2019; **9**: 443-.
4. Robak T. Emerging monoclonal antibodies and related agents for the treatment of chronic lymphocytic leukemia. *Future Oncol* 2013; **9**(1): 69-91.
5. Beckwith KA, Byrd JC, Muthusamy N. Tetraspanins as therapeutic targets in hematological malignancy: a concise review. *Front Physiol* 2015; **6**: 91.
6. Witkowska M, Smolewski P, Robak T. Investigational therapies targeting CD37 for the treatment of B-cell lymphoid malignancies. *Expert Opin Investig Drugs* 2018; **27**(2): 171-7.
7. Payandeh Z, Noori E, Khalesi B, Mard-Soltani M, Abdolalizadeh J, Khalili S. Anti-CD37 targeted immunotherapy of B-Cell malignancies. *Biotechnol Lett* 2018; **40**(11-12): 1459-66.
8. de Winde CM, Zuidscherwoude M, Vasaturo A, van der Schaaf A, Figdor CG, van Spriël AB. Multispectral imaging reveals the tissue distribution of tetraspanins in human lymphoid organs. *Histochem Cell Biol* 2015; **144**(2): 133-46.
9. Link MP, Bindl J, Meeker TC, et al. A unique antigen on mature B cells defined by a monoclonal antibody. *J Immunol* 1986; **137**(9): 3013-8.
10. Schwartz-Albiez R, Dorken B, Hofmann W, Moldenhauer G. The B cell-associated CD37 antigen (gp40-52). Structure and subcellular expression of an extensively glycosylated glycoprotein. *J Immunol* 1988; **140**(3): 905-14.
11. de Winde CM, Veenbergen S, Young KH, et al. Tetraspanin CD37 protects against the development of B cell lymphoma. *J Clin Invest* 2016; **126**(2): 653-66.
12. van Spriël AB, de Keijzer S, van der Schaaf A, et al. The tetraspanin CD37 orchestrates the alpha(4) beta(1) integrin-Akt signaling axis and supports long-lived plasma cell survival. *Sci Signal* 2012; **5**(250): ra82.
13. Lapalombella R, Yeh YY, Wang L, et al. Tetraspanin CD37 directly mediates transduction of survival and apoptotic signals. *Cancer Cell* 2012; **21**(5): 694-708.
14. Barrena S, Almeida J, Yunta M, et al. Aberrant expression of tetraspanin molecules in B-cell chronic lymphoproliferative disorders and its correlation with normal B-cell maturation. *Leukemia* 2005; **19**(8): 1376-83.
15. Moore K, Cooper SA, Jones DB. Use of the monoclonal antibody WR17, identifying the CD37 gp40-45 Kd antigen complex, in the diagnosis of B-lymphoid malignancy. *J Pathol* 1987; **152**(1): 13-21.
16. Deckert J, Sloss CM, Callaghan K, et al. IMG529, a Novel Antibody-Drug Conjugate (ADC) Targeting CD37 Shows Synergistic Activity with Rituximab in Non-Hodgkin Lymphoma (NHL) Models. *Blood* 2015; **126**(23): 1548.
17. Pereira DS, Guevara CI, Jin L, et al. AGS67E, an Anti-CD37 Monomethyl Auristatin E Antibody-Drug Conjugate as a Potential Therapeutic for B/T-Cell Malignancies and AML: A New Role for CD37 in AML. *Mol Cancer Ther* 2015; **14**(7): 1650-60.
18. Zhao X, Lapalombella R, Joshi T, et al. Targeting CD37-positive lymphoid malignancies with a novel engineered small modular immunopharmaceutical. *Blood* 2007; **110**(7): 2569-77.
19. Heider KH, Kiefer K, Zenz T, et al. A novel Fc-engineered monoclonal antibody to CD37 with enhanced ADCC and high proapoptotic activity for treatment of B-cell malignancies. *Blood* 2011; **118**(15): 4159-68.

20. Repetto-Llamazares AHV, Larsen RH, Patzke S, et al. Targeted Cancer Therapy with a Novel Anti-CD37 Beta-Particle Emitting Radioimmunoconjugate for Treatment of Non-Hodgkin Lymphoma. *PLoS One* 2015; **10**(6): e0128816-e.
21. Scarfò I, Ormhøj M, Frigault MJ, et al. Anti-CD37 chimeric antigen receptor T cells are active against B- and T-cell lymphomas. *Blood* 2018; **132**(14): 1495.
22. Melis JPM, Strumane K, Ruuls SR, Beurskens FJ, Schuurman J, Parren PWHI. Complement in therapy and disease: Regulating the complement system with antibody-based therapeutics. *Mol Immunol* 2015; **67**(2, Part A): 117-30.
23. Taylor RP, Lindorfer MA. The role of complement in mAb-based therapies of cancer. *Methods* 2014; **65**(1): 18-27.
24. Diebold CA, Beurskens FJ, de Jong RN, et al. Complement is activated by IgG hexamers assembled at the cell surface. *Science* 2014; **343**(6176): 1260-3.
25. Strasser J, de Jong RN, Beurskens FJ, et al. Unraveling the Macromolecular Pathways of IgG Oligomerization and Complement Activation on Antigenic Surfaces. *Nano Lett* 2019.
26. Ugurlar D, Howes SC, de Kreuk BJ, et al. Structures of C1-IgG1 provide insights into how danger pattern recognition activates complement. *Science* 2018; **359**(6377): 794-7.
27. de Jong RN, Beurskens FJ, Verploegen S, et al. A Novel Platform for the Potentiation of Therapeutic Antibodies Based on Antigen-Dependent Formation of IgG Hexamers at the Cell Surface. *PLoS Biol* 2016; **14**(1): e1002344.
28. Strasser J, de Jong RN, Beurskens FJ, et al. Unraveling the Macromolecular Pathways of IgG Oligomerization and Complement Activation on Antigenic Surfaces. *Nano Lett* 2019; **19**(7): 4787-96.
29. Labrijn AF, Janmaat ML, Reichert JM, Parren PWHI. Bispecific antibodies: a mechanistic review of the pipeline. *Nat Rev Drug Discov* 2019; **18**(8): 585-608.
30. Labrijn AF, Meesters JI, de Goeij BECG, et al. Efficient generation of stable bispecific IgG1 by controlled Fab-arm exchange. *Proc Natl Acad Sci U S A* 2013; **110**(13): 5145.
31. Labrijn AF, Meesters JI, Priem P, et al. Controlled Fab-arm exchange for the generation of stable bispecific IgG1. *Nat Protoc* 2014; **9**: 2450.
32. Burton DR, Pyati J, Koduri R, et al. Efficient neutralization of primary isolates of HIV-1 by a recombinant human monoclonal antibody. *Science* 1994; **266**(5187): 1024-7.
33. Oostindie SC, van der Horst HJ, Lindorfer MA, et al. CD20 and CD37 antibodies synergize to activate complement by Fc-mediated clustering. *Haematologica* 2019; **104**(9): 1841-52.
34. Overdijk MB, Verploegen S, van den Brakel JH, et al. Epidermal growth factor receptor (EGFR) antibody-induced antibody-dependent cellular cytotoxicity plays a prominent role in inhibiting tumorigenesis, even of tumor cells insensitive to EGFR signaling inhibition. *J Immunol* 2011; **187**(6): 3383-90.
35. Hu W, Ge X, You T, et al. Human CD59 inhibitor sensitizes rituximab-resistant lymphoma cells to complement-mediated cytotoxicity. *Cancer Res* 2011; **71**(6): 2298-307.
36. Dechant M, Weisner W, Berger S, et al. Complement-Dependent Tumor Cell Lysis Triggered by Combinations of Epidermal Growth Factor Receptor Antibodies. *Cancer Res* 2008; **68**(13): 4998.
37. Kopetz S, Lemos R, Powis G. The promise of patient-derived xenografts: the best laid plans of mice and men. *Clin Cancer Res* 2012; **18**(19): 5160-2.
38. Younes A, Ansell S, Fowler N, et al. The landscape of new drugs in lymphoma. *Nature reviews Clinical oncology* 2017; **14**(6): 335-46.
39. de Winde CM, Elfrink S, van Spriel AB. Novel Insights into Membrane Targeting of B Cell Lymphoma. *Trends in Cancer* 2017; **3**(6): 442-53.
40. Barth MJ, Mavis C, Czuczman MS, Hernandez-Ilizaliturri FJ. Ofatumumab Exhibits Enhanced In Vitro and In Vivo Activity Compared to Rituximab in Preclinical Models of Mantle Cell Lymphoma. *Clin Cancer Res* 2015; **21**(19): 4391-7.

# SUPPLEMENTARY METHODS

## Cells

The (origin of) cell lines used in this study are summarized in Supplementary Table 1. All cell lines were routinely tested for mycoplasma contamination and generally aliquoted and banked to allow in vitro assays to be performed from frozen cells instead of continuously cultured systems to ensure authenticity of the cell lines. Commercially available purified primary chronic lymphocytic leukemia (CLL) cells from newly diagnosed patients were obtained from All-Cells (Alameda, CA USA) and CLL peripheral blood mononuclear cells (PBMCs) were obtained from the Amsterdam University Medical Center (Amsterdam, The Netherlands) after written informed consent and stored using protocols approved by the Privacy Review Board of the Netherlands Cancer Registry in accordance with the declaration of Helsinki. PBMCs were isolated by density-gradient centrifugation (Ficoll-Paque PLUS, GE Healthcare, Chicago, IL, USA) from peripheral blood samples of lymphoma patients. Cells were used in experiments directly or stored in liquid nitrogen until further use.

## Antibodies

Details on antibodies used to define cell subsets within flow cytometry-based CDC assays with primary CLL patient samples, ADCP assays and human whole blood assays are described in Supplementary Table 2-5.

## Alanine scanning

A CD37 single residue alanine library (generated at GeneArt, Regensburg, Germany) was cloned into a pMAC expression vector and CD37 alanine mutants were expressed individually in FreeStyle HEK293F™ cells according to the manufacturer's instructions (Thermo Fischer Scientific, Waltham, MA, USA). Antibody binding was determined as described in main text using 3 µg/mL AF488-conjugated monovalent binding variants (one irrelevant binding arm) of Hx-CD37-010 (bslgG-CD37-010xctrl) and Hx-CD37-016 (bslgG-ctrlxCD37-016) and expressed as the gMFI of the ungated cell population. The two non-cross-blocking test antibodies served as control antibodies for each other. To correct for expression differences between the different CD37 mutants, data were normalized against the gMFI of the control antibody, using the following equation (wherein 'aa position' refers to the particular position of the alanine substitution in the extracellular loop of the human CD37 mutant):

$$\text{Normalized gMFI}_{\text{aa position}} = \text{Log}_{10} \left( \frac{\text{gMFI}_{\text{Test Ab}}}{\text{gMFI}_{\text{Control Ab}}} \right)$$

To express loss or of antibody binding, a z-score (fold change in binding compared to binding of a control antibody) was determined according to the following calculation:

$$\text{zscore (fold change)} = \frac{\text{normalizedgMFI}_{\text{aa position}} - \mu}{\sigma}$$

Where  $\mu$  and  $\sigma$  are the mean and SD of the normalized gMFI of all mutants. Z-scores  $< 0$  are caused by loss of binding of bslgG-ctrlxCD37-016 in comparison to bslgG-CD37-010xctrl while z-scores  $> 0$  are caused by loss of binding of bslgG-CD37-010xctrl in comparison to bslgG-ctrlxCD37-016. Amino acid residues where the z-score was higher than 1.5 (bsHx-CD37-010xctrl) or lower than  $-1.5$  (bsHx-ctrlxCD37-016), indicated by the horizontal dotted lines, were considered as ‘loss of binding mutants’.

### ADCC assays

Daudi target cells were labeled with 100  $\mu\text{Ci}$   $^{51}\text{Chromium}$  (Amersham Biosciences, Uppsala, Sweden) and incubated with antibody concentration series and PBMCs from healthy human donors (isolated from buffy coats) as effector cells at a 100:1 effector to target ratio for four hours at  $37^\circ\text{C}$ . After incubation, the supernatant was transferred to Microscint-40 solution and released  $^{51}\text{Chromium}$  was counted in a scintillation counter (PerkinElmer, Waltham, MA, USA). Maximal and spontaneous lysis were determined using target cells incubated with 5% Triton X-100 or medium without effector cells, respectively. Specific lysis was calculated as (wherein cpm is counts per minute):

$$\% \text{ specific lysis} = 100 * \frac{(\text{cpm sample} - \text{cpm spontaneous lysis})}{(\text{cpm maximal lysis} - \text{cpm spontaneous lysis})}$$

### Isolation of monocytes and culturing human monocyte-derived macrophages (h-MDM)

PBMCs were isolated from a buffy coat from healthy donors (Sanquin) through centrifugation using LeucoSep<sup>TM</sup>-tubes (Greiner Bio-One, Alphen aan den Rijn, Netherlands) containing Lymphocyte Separation Medium (Corning). Human CD14<sup>+</sup> monocytes were obtained from healthy donor PBMCs through positive isolation using CD14 MicroBeads (Miltenyi Biotec, Leiden, Netherlands) according to the manufacturer’s instructions. Monocytes were cultured in culture medium (CellGenix<sup>®</sup> GMP DC serum-free medium with 50 ng/mL M-CSF) in Nunc<sup>TM</sup> dishes with UpCell<sup>TM</sup> surface (Thermo Fisher Scientific) at  $37^\circ\text{C}/5\%-\text{CO}_2$  for 7-8 days to obtain human monocyte-derived macrophages (h-MDM). h-MDMs were characterized by flow cytometry for expression of myeloid- and macrophage-specific maturation markers (Supplementary Table 3).

### **Animal husbandry**

In house animal experiments were performed in compliance with the Dutch animal protection law (WoD) translated from the directives (2010/63/EU) and, if applicable, the Code of Practice “animal experiments for cancer research” (Inspection V&W, Zutphen, The Netherlands, 1999) and were approved by the Ethical Committee of Utrecht. Daudi-luc and DOHH-2 studies were performed with female C.B-17/IcrHan<sup>®</sup>Hsd-Prkdc<sup>scid</sup> mice, 7-8 weeks old, obtained from Envigo (Huntington, United Kingdom). Mice were housed in a barrier unit of the Central Laboratory Animal Research Facility (CLARF) of the Utrecht University (Netherlands) in sterile individually ventilated cages (IVC), 5 mice per cage, with sterile food and water provided ad libitum. Animals were housed and handled in accordance with good animal practice as defined by the Federation of European Laboratory Animal Science Associations (FELASA), in an Association for assessment and accreditation of laboratory animal care (AAALAC) and ISO 9001:2000 accredited animal facility (GDL, Utrecht, Netherlands).

JVM-3 studies were performed with CB17/ICR-Prkdc<sup>scid</sup>/IcrIcoCrl mice (Vital River Laboratories, Beijing, China) at Crown Bioscience, China. All studies were conducted following an approved Institutional Animal Care and Use Committee (IACUC) protocol. All experimental data management and reporting procedures were in strict accordance with applicable Crown Bioscience, Inc. Guidelines and Standard Operating Procedures.

NHL patient-derived xenograft (PDX) studies (Supplementary Table 6) were performed with CB-17SCID mice (Janvier labs, Le Genest-Saint-Isle, France) at EPO Experimental Pharmacology & Oncology Berlin-Buch GmbH, Germany. All animal experiments were performed in accordance with the Guidelines for the Welfare and Use of Animals in Cancer Research and of the German Animal Protection Law, and approved by the local responsible authorities, following standard operating procedures for optimal performance.

**Supplementary Table 1****The (origin of) cell lines used in this study**

Cell line	Origin	Company, cat. no.
Daudi	Burkitt's lymphoma	ATCC; CCL-213
DOHH-2	Diffuse large B-cell lymphoma	DSMZ; ACC-47
Jeko-1	Mantle cell lymphoma	DSMZ; ACC-553
JVM-2	Mantle cell lymphoma	DSMZ; ACC-12
JVM-13	Mantle cell lymphoma	ATCC; CRL-3003
OCI-Ly7	Diffuse large B-cell lymphoma	DSMZ; ACC-688
OCI-Ly19	Diffuse large B-cell lymphoma	DSMZ; ACC-528
Raji	Burkitt's lymphoma	ATCC; CCL-86
Ramos	Burkitt's lymphoma	ATCC; CRL-1596
RC-K8	Diffuse large B-cell lymphoma	DSMZ; ACC-561
RI-1	Diffuse large B-cell lymphoma	DSMZ; ACC 585
SU-DHL-4	Diffuse large B-cell lymphoma	ATCC; CRL-2957
SU-DHL-8	Diffuse large B-cell lymphoma	DSMZ; ACC-573
U-2932	Diffuse large B-cell lymphoma	DSMZ; ACC-633
Wien-133	Burkitt's lymphoma	BioAnaLab, Oxford, U.K
WIL2-S	EBV-positive B lymphoblastic cell line	ATCC; CRL-8885 <sup>0</sup>
WSU-DLCL2	Diffuse large B-cell lymphoma	DSMZ; ACC-575
Z-138	Mantle cell lymphoma	ATCC; CRL-3001

**Supplementary Table 2****Antibodies used for identification of cell subsets in primary patient sample CDC assays**

Target	Label	Target expression	Company	Cat. no
CD45	BV785	Leukocytes	BioLegend	304048
CD45	KO	Leukocytes	Beckman Coulter	B36294
CD19	PE	B cells	Beckman Coulter	A07769
CD19	PC7	B cells	Beckman Coulter	IM3628
CD3		T cells	BD	560365
CD5	APC	Expressed on most T cells and some B cell subsets, including some malignant B cells	BD	345783
CD5	PE	See CD5-APC	DAKO	R084201



### Supplementary Table 3

#### Antibodies used for h-MDM characterization

Target	Label	Target expression	Company	Clone	Cat. no
CD14	PE-Cy7	Maturation and lineage marker for monocytes/ macrophages	BD Pharmingen	M5E2	557742
CD11b	PE	General myeloid cell lineage and maturation marker	BD Pharmingen	ICRF44	555388
CD64	FITC	FcγRI (IgG1), expressed on mature antigen- presenting cells including macrophages	Biolegend	10.1	305006
CD80	APC	B7-1, expressed on activated antigen- presenting cells, including macrophages	Miltenyi	2D10	130-097-204
CD163	BV421	Macrophage sub lineage/maturity marker	Biolegend	GHI/61	333612
CD206	BV711	Mannose receptor, macrophage maturity/ sub lineage marker	Biolegend	15-2	321136
FVS	eFluor660	Staining of dead cells	BD Biosciences	NA	565694

### Supplementary Table 4

#### Antibodies used for identification of cell subsets in ADCP assays

Target	Label	Target expression	Company	Clone	Cat. no
CD11b	PE	h-MDM	BD Pharmingen	ICRF44	555388
CD19	BV711	Tumor B cells (Daudi)	Biolegend	SJ25C1	363026
FVS	eFluor660	Staining of dead cells	eBioscience	NA	65-0864-14

### Supplementary Table 5

#### Lineage-specific antibodies for identification of leukocyte subsets in human whole blood

Target	Label	Target expression	Company	Clone	Cat. no
CD19	BV711	B cells	Biolegend	H1B19	302245
CD3	eFluor450	T cells	e-Biosciences	OKT3	48-0037
CD56	PE-CF594	NK cells	BD	NCAM16.2	564849
CD16	BV785	Neutrophils	Biolegend	3G8	302046
CD66b	Pe-Cy7	Granulocytes	Biolegend	G10F5	305115

### Supplementary Table 6

#### Overview of NHL PDX models used in this study

Tumor model	Clinical type	Clinical status	Sample source	Cell-of-Origin (COO) classification
Ly11212	Triple hit DLBCL	Relapsed	Peripheral blood	GCB*
Ly12318	Double hit DLBCL	relapsed	Peripheral blood	ABC**
Ly12638	LBCL	untreated	Solid biopsy	GCB
Ly12657	pBCL	relapsed	Peripheral blood	intermediate/unclassified
Ly13005	DLBCL	untreated	Solid biopsy	ABC
Ly13693	DLBCL, EBV*** associated	untreated	Solid biopsy, retroperitoneal	GCB
Ly13976	DLBCL	untreated	Solid biopsy, LN	non GCB
Ly14440	DLBCL	relapsed	Solid biopsy, intraperitoneal	non GCB
Ly14862	Double hit DLBCL	untreated	Solid biopsy	non GCB

\* Germinal center B cell (GCB)

\*\* Activated B-cell (ABC)

\*\*\* Epstein-Barr virus

#### Cell line- and patient-derived xenograft studies

Samples sizes of animal models were chosen based on the specific tumor growth properties (homogeneous vs heterogeneous tumor growth) and the expected efficacy of the drug. Furthermore, our experience has taught us that especially outliers will influence the statistical power. Therefore, 10-20% more mice are added to the study design in models where heterogeneous tumor growth is expected, such that animals with the highest and/or the lowest tumor volumes can be excluded from the study at the moment of randomization.

The Daudi-Luc cell line-derived xenograft (CDX) study was performed with  $2.5 \times 10^6$  cells inoculated intravenously (IV) into 7-8 weeks old CB-17 SCID mice. Based on bioluminescence imaging on day 0 (obtained within 2 hours post injection of Daudi-luc cells), the animals were randomized into groups of 9 animals each. Animals which showed no signal in the lungs at this time point and/or a clear signal at the injection site (tail vein) were excluded from randomization. At days 14, 21 and 28 after tumor cell inoculation, mice were treated with antibody by intraperitoneal (IP) injection. At weekly intervals, tumor growth was assessed using bioluminescence imaging on a Photon Imager (Biospace Lab, Nesles-la-Vallée, France). Before imaging, mice were anaesthetized via isoflurane and synthetic D-luciferin (BioThema, Handen, Sweden) was injected IP at a dose of 125 mg/kg; M3 Vision software (Biospace Lab, Nesles-la-Vallée, France) was used for image analysis. The DOHH-2 and JVM-2 CDX studies were performed with  $1 \times 10^6$  and  $1 \times 10^7$  cells inoculated

subcutaneously (SC) into the flanks of 8-10 and 7-8 weeks old individual CB-17 SCID mice, respectively. Mice were randomized into groups (n=10) with equal tumor size distribution when tumors reached 100 and 200 mm<sup>3</sup> respectively, and treated IP (DOHH-2) or IV (JVM-3) with 3 weekly doses (QWx3) of antibody. Tumor volume was measured at least twice per week using caliper measurements and calculated as  $0.52 \times (\text{length}) \times (\text{width})^2$ . Animals were euthanized when tumors reached 1,500/2,000 mm<sup>3</sup>. During all CDX studies, heparinized blood samples were taken for determination of IgG levels in plasma. All CDX studies were performed using a blinded assessment of outcome measures.

NHL PDX models were performed with human tumor tissue implanted subcutaneously into the flanks of 6-7 weeks old CB17-SCID mice, and tumors were allowed to reach 100-250 mm<sup>3</sup>. Mice were randomized into groups (n=8) according to their tumor volume and treated IV with 2 weekly doses (QWx2) of antibody. Tumor volume was measured thrice weekly.

The PDX screening was performed as described above for regular PDX models, only using one mouse per group design. The relative tumor growth was defined as the ratio between the tumor growth in the DuoHex-aBody-CD37-treated mouse ( $\Delta T$ ) and the control mouse ( $\Delta C$ ), specifically  $\Delta T/\Delta C$ . Tumor growth was calculated as the difference in tumor volume between day of first treatment and day of analysis, ideally between 7 and 25 days after initiation of treatment. Models in which the control mouse tumor volume did not increase 2-fold after start treatment were excluded from analysis. Models were categorized according to the following criteria: responders =  $\Delta T/\Delta C < 10\%$ ; intermediates =  $10\% \leq \Delta T/\Delta C \leq 70\%$ ; non-responders =  $\Delta T/\Delta C > 70\%$ . All PDX studies were performed using a blinded assessment of outcome measures.



# 4

## POTENT PRECLINICAL EFFICACY OF DUOHEXABODY-CD37 IN B-CELL MALIGNANCIES

Hilma J. van der Horst<sup>1\*</sup>, Simone C. Oostindie<sup>2,3\*</sup>, Saskia. A. G. M. Cillessen<sup>4</sup>, Anne T. Gelderloos<sup>1</sup>, Marije B. Overdijk<sup>2</sup>, Inger. S. Nijhof<sup>1</sup>, Sonja Zweegman<sup>1</sup>, Martine E. D. Chamuleau<sup>1</sup>, Esther C. W. Breij<sup>2</sup>, Tuna Mutis<sup>1</sup>

Hemasphere. 2021 Jan;5(1):e504.

1 Department of Hematology, Cancer Center Amsterdam, Amsterdam UMC, VU Medical Center, Amsterdam, the Netherlands;

2 Genmab, Utrecht, the Netherlands;

3 Department of Immunohematology and Blood Transfusion, Leiden University Medical Center, the Netherlands;

4 Department of Clinical Pathology, Amsterdam UMC, Amsterdam, the Netherlands.

\* Both authors contributed equally to this study

**Correspondence**

Tuna Mutis (t.mutis@amsterdamumc.nl).

**Acknowledgements**

The authors thank Henk Lokhorst for his contribution in the early stage of the study.

## TO THE EDITOR,

Over the last decades, several surface antigens have been identified and validated for treatment of B-cell malignancies. CD20-targeting antibodies have emerged as an effective therapy for patients with B-cell malignancies and are now broadly used in clinical practice. Nonetheless, many patients develop resistance against CD20-targeting therapies, with little or no further treatment options.<sup>1</sup> Tetraspanin CD37 is expressed almost exclusively on hematopoietic cells with high expression on mature B-cells, including their malignant counterparts,<sup>2,3</sup> and is a well described and validated target for B-cell malignancies. A number of CD37 targeting agents are in (pre)clinical development, including antibody-drug conjugates (IMGN529 and AGS67E), an Fc-engineered antibody (BI836826), a homodimeric therapeutic protein (otlertuzumab/TRU-016), a radioimmunoconjugate (<sup>177</sup>Lu-lilotomab), and chimeric antigen receptor T-cells.<sup>4-6</sup> We recently reported on the development of DuoHexaBody-CD37, a novel biparatopic CD37-bispecific immunoglobulin G1 (IgG1) antibody with an E430G hexamerization-enhancing single point mutation in the Fc-domain.<sup>7</sup> In contrast to all other newly developed CD37 targeting agents, DuoHexaBody-CD37 mediates potent complement-dependent cytotoxicity (CDC), a powerful anti-tumor effector mechanism,<sup>8,9</sup> in addition to its Fc gamma receptor (FcγR)-mediated tumor cell kill mechanisms including antibody-dependent cellular cytotoxicity and cellular phagocytosis. DuoHexaBody-CD37 was designed based on recent discoveries that (1) initiation of CDC is dependent on Fc-mediated hexamer-formation of IgG1 antibodies after target engagement on the cell surface,<sup>10</sup> (2) antibody Fc-Fc interactions and hexamer formation can significantly be improved by introducing an E430G single point mutation in the Fc domain,<sup>10,11</sup> and (3) dual-epitope targeting of CD37 can potentiate or further enhance CDC.<sup>7</sup>

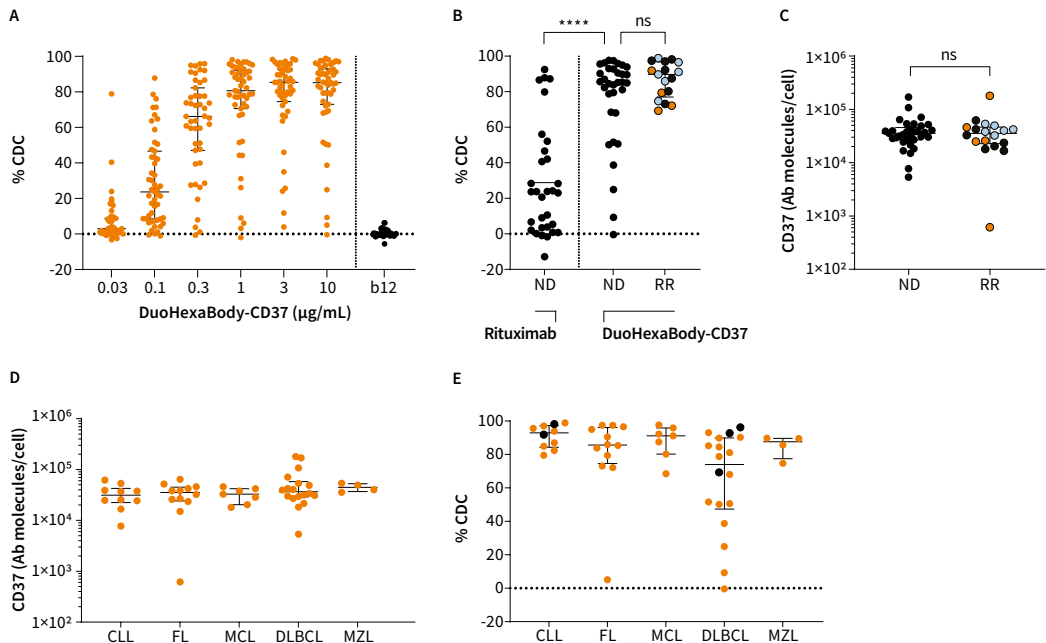
Here, we investigated the ex vivo therapeutic potential of DuoHexaBody-CD37 by evaluating its unique CDC-inducing capacity in primary tumor cell samples from a large cohort of newly diagnosed (ND) and relapsed/refractory (RR) patients with a broad range of B-cell malignancies, including chronic lymphocytic leukemia (CLL) and B-cell non-Hodgkin lymphoma, including diffuse large B-cell lymphoma (DLBCL), follicular lymphoma (FL), mantle cell lymphoma, and marginal zone lymphoma (Supplementary Material and Methods). DuoHexaBody-CD37 induced potent, dose-dependent CDC of malignant primary B-cells in 45-minute complement assays with a median maximal lysis of 86% (n = 51, range: 0%-99%) and a median half maximal effective concentration (EC<sub>50</sub>) of 0.10 µg/mL (range: 0.004-15.21 µg/mL) (Figure 1A). Strikingly, sensitivity of the patient samples to DuoHexaBodyCD37-induced

CDC was highly homogeneous. Only in 8 of 51 patient samples maximal lysis was lower than 60%, of which 3 samples demonstrated responses below 20% lysis. The CDC activity of DuoHexaBody-CD37 was comparable in samples from ND patients (n = 33; median maximal lysis of 85%; range CDC 0%-98%) and RR patients (n = 18; median maximal lysis of 89%; range CDC 5%-99%). Furthermore, DuoHexaBody-CD37 was significantly more potent than the CD20-targeting antibody rituximab in samples from ND patients, that is, CD20 antibody treatment naive patients (Figure 1B), even though CD37 expression was generally lower than expression of CD20 (Supplementary Figure 1).

Potent cytotoxicity was also observed in samples from patients who relapsed from (Figure 1B, blue symbols; n = 7) or were refractory to treatment regimens containing CD20- targeted antibodies (defined by progression of the disease within 6 months post treatment; Figure 1B, red symbols; n = 5), with the exception of one CD20-refractory FL patient. CD37 expression analysis (Figure 1C) revealed that this patient lacked CD37 expression on tumor B-cells. Since it has been reported that anti-CD20 therapy may induce CD20 antigen loss,<sup>12</sup> and CD20 colocalizes with CD37 on the cell surface,<sup>13</sup> we evaluated the possibility that CD37 expression levels were reduced on tumor B-cells derived from patients who had been exposed to anti-CD20. However, all anti-CD20-treated patient samples in our cohort showed high CD37 expression levels and no significant differences were observed in CD37 expression levels between samples from ND and RR patients (Figure 1C). In addition, CD37 was expressed homogeneously in all B-cell malignancy subtypes (Figure 1D), which is in alignment with several other reports<sup>2,6</sup> except for a recent study that suggested variable CD37 expression in DLBCL.<sup>14</sup> This study-related discrepancy could be due to differences in assay-dependent detection limits in our study (flow cytometry) versus the other (immunohistochemistry) study. DuoHexaBody-CD37 induced an effective and homogeneous CDC response in all samples from CLL (n = 10; median max lysis 93%; range, 80%-99%), mantle cell lymphoma (n = 7; 91%; 69%-98%) and marginal zone lymphoma (n=4; 88%; 75%-90%), and 11 of 12 FL patient samples (n=12; 86%; 5%-98%), while a more heterogeneous response was observed in DLBCL patient samples (n = 18; 74%; 0%-96%) (Figure 1E) (Kruskal-Wallis one-way analysis of variance (ANOVA), \*P = 0.0321). There were no differences in sensitivity between activated B-cell and germinal center B-cell subtypes of DLBCL (Supplementary Figure 2). Of note, also samples from ibrutinib-refractory CLL (n = 2) and double-hit DLBCL (n = 3) patients with poor prognosis were highly susceptible to DuoHexaBodyCD37-induced CDC (maximum lysis >60%) (Figure 1E).

Complement activation and CDC-mediated tumor cell lysis is not only dependent on antigen density but also on expression levels of complement regulatory proteins (CRPs) CD46 and CD55 that inhibit complement convertases, and



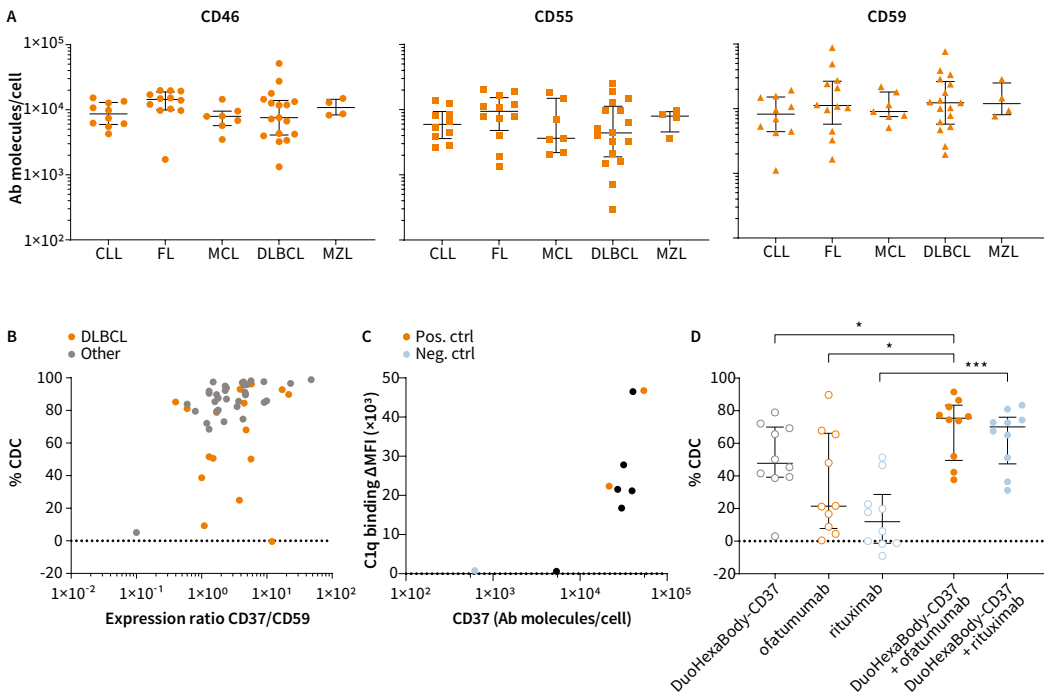


▲ **Figure 1**

**DuoHexaBody-CD37 induced potent CDC in samples obtained from ND and RR patients with various B-cell malignancies.**

(A) Dose-dependent CDC induced by DuoHexaBody-CD37 in tumor B-cells ( $n = 51$ ) derived from patients with various B-cell malignancy subtypes grouped together, in the presence of 20% NHS and in comparison to IgG1-ctrl (10  $\mu\text{g}/\text{mL}$ ). Levels of CDC-mediated tumor cell kill (% CDC) were determined by 7AAD-positive tumor cell staining, relative to a no antibody control sample. (B) Comparison of CDC activity of 10  $\mu\text{g}/\text{mL}$  DuoHexaBody-CD37 in samples from ND ( $n = 33$ ) and RR ( $n = 18$ ) patients (ns; Mann-Whitney U test), and comparison of rituximab (10  $\mu\text{g}/\text{mL}$ ) and DuoHexaBody-CD37 in ND patients (\*\*\*\* $P < 0.0001$ ; Wilcoxon matched-pairs signed rank test). RR patients include CD20 therapy-refractory patients ( $n = 5$ ; orange symbols), defined by progression of the disease within 6 months post therapy, and CD20 therapy-relapse patients ( $n = 6$ ; blue symbols). (C) CD37 expression levels (defined as the number of CD37 molecules on the cell surface, assessed by quantitative flow cytometry), on tumor B-cells in ND and RR patient samples (ns; Mann-Whitney U test). (D) Quantified CD37 expression levels (antibody molecules per cell) on tumor B-cells stratified according to B-cell malignancy subtype (ns, nonparametric Kruskal-Wallis test). All data are shown as the median and interquartile range. (E) CDC activity of DuoHexaBody-CD37 (10  $\mu\text{g}/\text{mL}$ ) stratified according to B-cell malignancy subtype, including CLL ( $n = 10$ ), FL ( $n = 12$ ), MCL ( $n = 7$ ), DLBCL ( $n = 18$ ), and MZL ( $n = 4$ ) (\* $P = 0.0321$ , nonparametric Kruskal-Wallis test with Dunn's multiple comparisons [n]). Black symbols indicate patient samples with poor prognosis: ibrutinib-refractory CLL ( $n = 2$ ) and double-hit DLBCL ( $n = 3$ ).

CD59 that inhibits the formation of the membrane attack complex.<sup>15</sup> Expression of CRPs was not associated with B-cell malignancy subtype (Figure 2A) or treatment status (Supplementary Figure 3). Furthermore, no correlation was observed between DuoHexaBody-CD37-induced CDC and expression of CD37 or CRPs (Supplementary Figure 4). A weak, but statistically significant correlation was observed between sensitivity to DuoHexaBody-CD37 and the ratio of CD37 and CD59 expression levels (Figure 2B). However, in DLBCL patient samples, differences in (the ratio of) CD37 and CD59 expression could not explain the heterogeneous response to DuoHexaBody-CD37 ex vivo (Figure 2B,



orange symbols). We therefore conclude that there is a limited impact of CRP expression on DuoHexaBody-CD37-mediated CDC. This was in contrast to rituximab-induced CDC, which already showed a strong correlation with CD20 expression but an even stronger correlation with the ratio of CD20 and CD55 (Supplementary Figure 5).

The first step of complement activation is the binding of C1q to membrane-bound antibodies that together with C1r and C1s forms the C1 complex, the first component of the classical complement pathway. Toward understanding the heterogeneity in CDC responses observed in DLBCL patient samples, we investigated the C1q binding capacity of membrane-bound DuoHexaBody-CD37 in DLBCL patient samples for which DuoHexaBody-CD37-mediated CDC levels were lower than 60% (N = 6). The C1q binding capacity in low CDC responders was comparable to that of 2 patient samples highly susceptible to DuoHexaBody-CD37-induced CDC (Figure 2C), indicating that the first step of complement activation is not impaired. Whether other steps in the complement activation pathway, such as membrane attack complex assembly and stability, or cell intrinsic mechanisms, play a role in resistance to CDC induction remains to be elucidated. Finally, we also evaluated whether combination with rituximab and/or ofatumumab could further enhance the CDC activity of DuoHexaBody-CD37, as we have previously reported enhanced CDC

◀ **Figure 2**

**Low sensitivity to DuoHexaBody-CD37-mediated CDC is not associated with expression of CD37 and CRPs and can be improved by combination with CD20 mAbs.**

(A) Quantified expression levels (antibody molecules per cell) of complement regulatory proteins CD46, CD55, and CD59 on tumor B-cells in specific B-cell malignancy subtypes; CLL (n = 10), FL (n = 12), MCL (n = 7), DLBCL (n = 18), and MZL (n = 4) (ns; nonparametric Kruskal-Wallis test). Data shown are CDC in individual patient samples, in addition to the median and interquartile range. (B) CDC activity of DuoHexaBody-CD37 (10 µg/mL) correlated with the ratio of CD37/CD59 expression levels for all B-cell malignancy subtypes grouped together, for DLBCL patient samples specifically and for B-cell malignancy subtypes other than DLBCL (Spearman's correlation  $r = 0.4423$ ,  $**P = 0.0013$ ;  $r = 0.2843$ ,  $P = 0.2678$ ; and  $r = 0.5158$ ,  $**P = 0.0025$ , respectively). Data are shown relative to a no antibody control sample. (C) Expression levels of CD37 (antibody molecules per cell) correlated with C1q binding ( $\Delta$ MFI) for six samples with low CDC response (CDC < 60%), one CD37-negative sample as negative control (blue symbol) and two high responding samples as positive control (orange symbol) (Spearman's correlation  $r = 0.7833$ ,  $*P = 0.0172$ ). (D) CDC induced by a combination of DuoHexaBody-CD37 and rituximab or ofatumumab (10 µg/mL + 10 µg/mL) versus single antibody (10 µg/mL) (n = 10) ( $*P < 0.05$ ,  $***P < 0.001$ ; Friedman test with Dunn's multiple comparisons test) relative to a no antibody control sample. All data are shown as the median and interquartile range.

in CLL and B-cell non-Hodgkin lymphoma primary patient cells with combinations of CD20 and CD37 antibodies.<sup>13</sup> Indeed, in 10 patient samples including samples with intermediate to low sensitivity to DuoHexaBody-CD37-mediated CDC (<80% CDC), the combination of DuoHexaBody-CD37 with rituximab and ofatumumab significantly enhanced the tumor cell kill in an additive manner (Figure 2D). In contrast to ofatumumab, rituximab as single antibody could generally not induce CDC in these samples and the CDC-effects of the combination with DuoHexaBody-CD37 are less striking.

In conclusion, this preclinical study indicates high therapeutic potential for DuoHexaBody-CD37 in a broad spectrum of B-cell malignancies either as single agent or in combination with CD20-targeting antibodies, and supports the recently initiated first-in-human clinical trial of DuoHexaBody-CD37 for patients with relapsed or refractory B-cell NHL (NCT04358458).

# REFERENCES

1. Salles G, Barrett M, Foà R, et al. Rituximab in B-Cell Hematologic Malignancies: A Review of 20 Years of Clinical Experience. *Adv Ther* 2017; **34**(10): 2232-73.
2. Deckert J, Park PU, Chicklas S, et al. A novel anti-CD37 antibody-drug conjugate with multiple anti-tumor mechanisms for the treatment of B-cell malignancies. *Blood* 2013; **122**(20): 3500-10.
3. Schwartz-Albiez R, Dörken B, Hofmann W, Moldenhauer G. The B cell-associated CD37 antigen (gp40-52). Structure and subcellular expression of an extensively glycosylated glycoprotein. *J Immunol* 1988; **140**(3): 905-14.
4. Köksal H, Dillard P, Josefsson SE, et al. Preclinical development of CD37CAR T-cell therapy for treatment of B-cell lymphoma. *Blood Adv* 2019; **3**(8): 1230-43.
5. Scarfò I, Ormhøj M, Frigault MJ, et al. Anti-CD37 chimeric antigen receptor T cells are active against B- and T-cell lymphomas. *Blood* 2018; **132**(14): 1495-506.
6. Witkowska M, Smolewski P, Robak T. Investigational therapies targeting CD37 for the treatment of B-cell lymphoid malignancies. *Expert Opin Investig Drugs* 2018; **27**(2): 171-7.
7. Oostindie SC, van der Horst HJ, Kil LP, et al. DuoHexaBody-CD37<sup>(®)</sup>, a novel biparatopic CD37 antibody with enhanced Fc-mediated hexamerization as a potential therapy for B-cell malignancies. *Blood Cancer J* 2020; **10**(3): 30.
8. de Weers M, Tai YT, van der Veer MS, et al. Daratumumab, a novel therapeutic human CD38 monoclonal antibody, induces killing of multiple myeloma and other hematological tumors. *J Immunol* 2011; **186**(3): 1840-8.
9. Di Gaetano N, Cittera E, Nota R, et al. Complement activation determines the therapeutic activity of rituximab in vivo. *J Immunol* 2003; **171**(3): 1581-7.
10. Diebold CA, Beurskens FJ, de Jong RN, et al. Complement is activated by IgG hexamers assembled at the cell surface. *Science* 2014; **343**(6176): 1260-3.
11. de Jong RN, Beurskens FJ, Verploegen S, et al. A Novel Platform for the Potentiation of Therapeutic Antibodies Based on Antigen-Dependent Formation of IgG Hexamers at the Cell Surface. *PLoS Biol* 2016; **14**(1): e1002344.
12. Kennedy AD, Beum PV, Solga MD, et al. Rituximab infusion promotes rapid complement depletion and acute CD20 loss in chronic lymphocytic leukemia. *J Immunol* 2004; **172**(5): 3280-8.
13. Oostindie SC, van der Horst HJ, Lindorfer MA, et al. CD20 and CD37 antibodies synergize to activate complement by Fc-mediated clustering. *Haematologica* 2019; **104**(9): 1841-52.
14. Xu-Monette ZY, Li L, Byrd JC, et al. Assessment of CD37 B-cell antigen and cell of origin significantly improves risk prediction in diffuse large B-cell lymphoma. *Blood* 2016; **128**(26): 3083-100.
15. Gorter A, Meri S. Immune evasion of tumor cells using membrane-bound complement regulatory proteins. *Immunol Today* 1999; **20**(12): 576-82.

# MATERIALS AND METHODS

## Therapeutic Antibodies

DuoHexaBody-CD37 and the negative control anti-HIV-1 gp120 antibody IgG1-b12 (mentioned in manuscript as IgG1-ctrl) were generated by Genmab (Utrecht, The Netherlands) as previously described.<sup>7</sup> Rituximab (MabThera<sup>®</sup>) and ofatumumab (Arzerra<sup>®</sup>) were obtained from Genmab.

## Patient samples

According to the Dutch Central Committee on Research involving Human Subjects (CCMO), this type of study does not require approval from an ethics committee. Primary patient samples were collected at Amsterdam University Medical Center, location VUmc, according to the *code of conduct for medical research*. Tissues from lymph node biopsies were mechanically disrupted, cultured overnight in a fully humidified incubator and the cells in suspension were collected and cryopreserved in liquid nitrogen until further use. For seven CLL samples and one MCL sample tumor cells were isolated from mononuclear cells of the bone marrow (BMNCs) or peripheral blood (PBMCs) by density-gradient centrifugation (Ficoll-Paque PLUS, Cytiva, MA, USA) according to manufacturer's instructions, and were either used directly or cryopreserved in liquid nitrogen until further use.

## Tumor-specific surface markers

B cells were identified using flow cytometry by gating for CD3<sup>+</sup>CD19<sup>+</sup> cells within the CD45<sup>+</sup> population and made up 20-80% of the total lymph node cell population. Malignant B cells were identified by kappa/lambda staining to screen for clonality and if possible also by the tumor-specific markers CD10<sup>+</sup> (FL and DLBCL), CD5<sup>+</sup> (CLL), CD5<sup>+</sup>CD23<sup>-</sup> (MCL). The following antibodies were used: CD45-KO and CD19-PC7 (Beckman Coulter, CA, USA), CD3-V450, CD5-APC, CD10-APC-H7 and kappa-APC-H7 (BD, NJ, USA), CD5-PE, CD10-PE and kappa-PE (DAKO, Agilent Technologies, CA, USA), CD23-FITC (BioLegend, CA, USA) and lambda-FITC (Emelca Bioscience, Clinge, Netherlands).

## Quantitated expression assays

Target cells were incubated with purified mouse anti-human IgG1 antibodies against CD37, CD46, CD55, CD59 and CD20 (BioLegend) and expression levels were quantified by flow cytometry using an indirect immunofluorescence assay (QIFIKIT<sup>®</sup>, Agilent Technologies) according to manufacturers protocol, followed by a staining for tumor specific cell surface markers.

### **Complement-dependent cytotoxicity assays**

Complement-dependent cytotoxicity assays were performed by incubation of single cell suspensions ( $1 \times 10^5$  cells/well) with serial dilutions (0.01-10  $\mu\text{g}/\text{mL}$ ) of DuoHexaBody-CD37 for 45 minutes at  $37^\circ\text{C}$  in the presence of 20% normal human serum (NHS; pooled from eight healthy donors) as a source of complement. Cells were analysed by flow cytometry and viability (%) and lysis (%) of malignant B cells was determined according to the following formulas:

$$\% \text{ viability} = 100 * \left( \frac{\% \text{ 7AAD} - \text{negative cells of test sample}}{\% \text{ 7AAD} - \text{negative cells of control sample}} \right)$$

$$\% \text{ lysis} = (100 - \% \text{ viability})$$

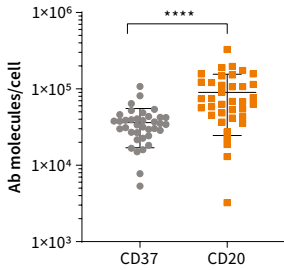
### **C1q binding assays**

Target cells were incubated with DuoHexaBody-CD37 (10  $\mu\text{g}/\text{mL}$ ) and purified human complement component C1q (2.5  $\mu\text{g}/\text{mL}$ ; Quidel, San Diego, CA) for 45 min at  $37^\circ\text{C}$ . After washing, purified C1q was labeled with a fluorescein isothiocyanate (FITC)-conjugated rabbit anti-human C1q antibody (Dako, Glostrup, Denmark). Binding was detected by flow cytometry and expressed as the median fluorescent intensity (MFI). MFI values of purified C1q labeled with FITC anti-human C1q were subtracted by MFI values of negative control (FITC-anti-human C1q only).

### **Statistical analysis**

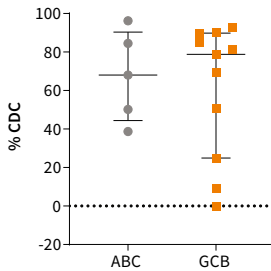
Flow cytometry data were analyzed using FACS DIVA software. Graphs were plotted using GraphPad Prism 8.2. for Windows. Statistical analysis was performed with the appropriate parametric or non-parametric test, as indicated in the figure legends. Two-sided  $P$  values  $< .05$  were considered statistically significant.

## SUPPLEMENTARY FIGURES



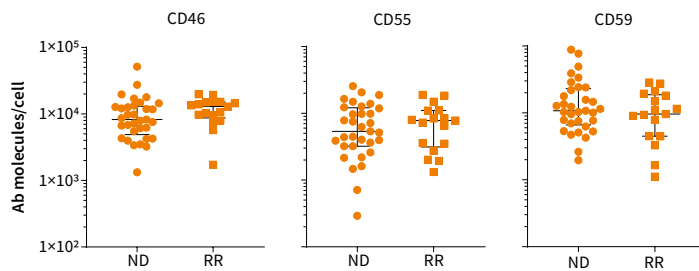
### ▲ Supplementary Figure 1

Expression levels (antibody molecules per cell) of CD37 and CD20 on tumor B cells in samples from ND patients (\*\*\*\* $P < 0.0001$ ; Wilcoxon matched-pairs signed rank test). Data are shown as the median and interquartile range.



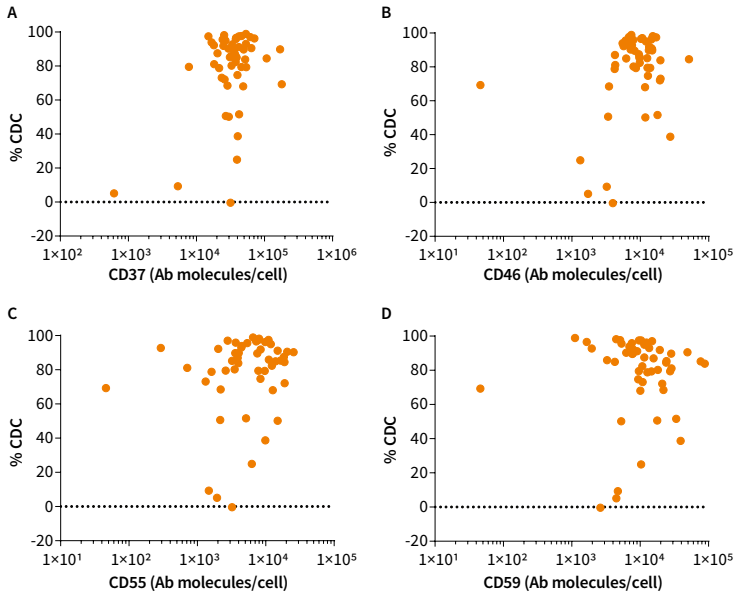
### ▲ Supplementary Figure 2

CDC activity of DuoHexaBody-CD37 (10  $\mu\text{g}/\text{mL}$ ) in DLBCL patient samples of ABC (n=5) and GCB subtype (n=11) (ns; Mann-Whitney U-test). Data are shown as the median and interquartile range.



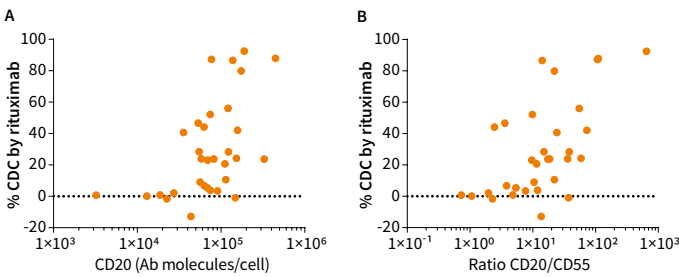
### ▲ Supplementary Figure 3

Expression levels (antibody molecules per cell) of complement regulatory proteins CD46, CD55 and CD59 on tumor B cells, according to treatment status; ND versus RR (ns; Mann-Whitney U test). Data are shown as the median and interquartile range.



▲ **Supplementary Figure 4**

CDC activity of DuoHexaBody-CD37 (10  $\mu\text{g}/\text{mL}$ ) correlated with quantified expression levels (antibody molecules per cell) of (A) CD37 and (B-D) complement regulatory proteins CD46, CD55 and CD59 (Spearman's correlation  $r = 0.1408$ ,  $P = 0.3243$ ;  $r = 0.1929$ ,  $P = 0.1751$ ;  $r = 0.1901$ ,  $P = 0.1814$ ;  $r = -0.2024$ ,  $P = 0.1542$ , respectively). Data are shown relative to a no antibody control sample.



▲ **Supplementary Figure 5**

CDC activity of rituximab (10  $\mu\text{g}/\text{mL}$ ) correlated with (A) quantified CD20 expression (antibody molecules per cell; Spearman's correlation  $r = 0.5488$ ,  $**p = 0.0011$ ) and (B) the ratio of expression levels of CD20 to complement regulatory protein CD55 (Spearman's correlation  $r = 0.5957$ ,  $***p = 0.0003$ ). Data are shown relative to a no antibody control sample.







# 5

## THERAPEUTIC IGG ANTIBODY COMBINATIONS ACTING AS BIO-LOGIC AND GATES

Simone C. Oostindie<sup>1,2</sup>, Frank J. Beurskens<sup>1</sup>, Gijs G. Zom<sup>1</sup>, Desiree Paulet<sup>1</sup>,  
Kusai Al-Tamimi<sup>1</sup>, Els van der Meijden<sup>1</sup>, Jennifer Scheick<sup>1</sup>, Janita J. Oosterhoff<sup>1</sup>,  
Julie Vignau<sup>1</sup>, Sandra Verploegen<sup>1</sup>, Janine Schuurman<sup>1</sup>, Rob N. de Jong<sup>1\*</sup>

Submitted for publication.

<sup>1</sup> Genmab, Uppsalalaan 15, 3584 CT Utrecht, The Netherlands

<sup>2</sup> Department of Immunology, Leiden University Medical Center, Leiden, The Netherlands

\* Corresponding author

**Correspondence**

Rob N. de Jong (rjo@genmab.com)

**Acknowledgements**

We thank Klara Besmüller and Tessa Wilpshaar for experimental support.

# ABSTRACT

The target space for therapeutic monoclonal antibodies is limited by expression in healthy tissues. We present a general approach to enhance functional selectivity by decoupling activity from individual antibody binding events. Immunoglobulin G (IgG)-mediated clustering of membrane receptors naturally occurs on cell surfaces to trigger complement- or cell-mediated effector functions, but can also be leveraged to initiate outside-in signaling. Here, we describe Fc-domain engineered IgG antibody pairs that act as Bio-Logic AND gates selectively activated after hetero-oligomerization. Pairwise IgG hetero-oligomerization and membrane receptor activation were stringently dependent on the presence of two targets co-expressed at the same cell surface. C1q recruitment integrated the binding signals encoded by two antibody components, translating into clustering-dependent activation of effector functions such as complement activity or target signaling. This 'HexElect<sup>®</sup>' technology may enable access to an untapped, combinatorial target space for the generation of antibody therapeutics that exhibit both selectivity and potency.

Monoclonal antibodies (mAbs) have reshaped drug development due to their highly targeted nature and their ability to activate specific immune effector molecules and cells. Superior effector functions have been engineered into mAbs to enhance therapeutic efficacy<sup>1</sup>. Complement- or cell-mediated effector functions can be triggered by antigen-dependent Immunoglobulin G (IgG) oligomerization into ordered hexameric complexes on the cell surface through non-covalent Fc-Fc interactions between neighboring antibodies<sup>2</sup>. These ordered hexamers provide natural high-avidity binding sites for complement complex C1, leading to activation of the classical complement pathway, or to receptor clustering and outside-in signaling<sup>3-6</sup>. IgG hexamerization and effector function activation can be enhanced by single amino acid point mutations in the Fc-domain, such as E430G, that promote interactions between Fc domains of cell-bound IgG<sup>2,7</sup>. Hexamerization-enhanced mutant antibody variants increased complement-dependent cytotoxicity (CDC) of B cells from patients with chronic lymphocytic leukemia (CLL) and were able to facilitate enhanced clustering and activation of members of the tumor necrosis factor receptor (TNFR) superfamily<sup>3,6,8</sup>.

The cell surface target space for therapeutic mAbs based on natural IgG backbones is largely limited to those targets that are highly selectively expressed on diseased cells. Hence, there may be advantages to therapeutic antibody technologies that enable the safe and effective targeting of antigens that currently cause undesirable toxicity on healthy cells, or insufficient potency on

diseased cells. We recently reported that mAbs targeting different membrane receptors can hetero-oligomerize into mixed hexameric complexes upon antigen binding, resulting in synergistic CDC of tumor B cells from various B-cell malignancies<sup>8</sup>. Here, we describe a general approach to create IgG antibody pairs that only induce pairwise activation of enhanced, hexamerization-dependent functions, if both antibodies have bound the same target cell. Decoupling functional activation from individual target binding enables these IgG antibody pairs to act as Boolean logic AND gates that integrate two antibody binding signals into a functional outcome only on cells or surfaces co-expressing both antibody targets.

# METHODS

## Antibodies

Rituximab (MabThera<sup>®</sup>) and obinutuzumab (Gazyvaro<sup>®</sup>) were obtained from the pharmacy (UMC Utrecht). All other antibodies were recombinantly produced at Genmab as described.<sup>3</sup> Mutations to enhance or inhibit Fc-Fc interactions and/or Fc-C1q binding interactions were introduced in expression vectors encoding the antibody heavy chain either using Quikchange technology (Agilent Technologies, Santa Clara, CA, USA) or via gene synthesis (ThermoFisher Scientific, Regensburg, Germany). Quality control of recombinantly produced antibodies was performed by different methods as described previously<sup>7</sup>: capillary electrophoresis sodium dodecyl sulfate (CE-SDS) on the Labchip GXII (Caliper Life Sciences/PerkinElmer Hopkinton) under reducing and non-reducing conditions (>90% intact IgG, >95% HC  $\beta$  LC under reducing conditions), Electrospray Ionization Time-of-Flight Mass Spectrometry (ESI-TOF MS) (Waters) or Orbitrap (Thermo Fisher Scientific), and High performance size-exclusion chromatography (HP-SEC) (aggregate level < 5%; Waters Alliance 2975 separation unit, Waters). The following IgG1 antibodies targeting human antigens were used: CD52 (P31358) mAb Campath<sup>37</sup>, CD20 (P11836) mAbs 11B8 and 7D8<sup>38-40</sup>, CD3 (P07766) mAb huCLB3/4<sup>41</sup>, CD37 (P11049) mAb IgG1-37.3<sup>42</sup>, DR5 (O14763) mAbs DR5-01 and DR5-05<sup>3</sup>. mAb IgG1-b12 targeting HIV-1 antigen gp120 (Q9IZE4) was used as a non-binding isotype control.<sup>43</sup>

## Cells and reagents

Daudi (human B-cell lymphoma), Raji (human B-cell lymphoma), Ramos (human B-cell lymphoma), COLO-205 (colorectal cancer) and BxPC-3 (pancreatic cancer) cell lines were obtained from the American Type Culture Collection (ATCC no. CCL-23, CCL-86, CRL-1596, CCL-222 and CRL-1687 respectively). The human B-lymphoma cell line U-698-M and the human B-precursor leukemia cell line REH were obtained from the Deutsche Sammlung von Mikroorganismen und Zellkulturen (cell line numbers ACC 22 and ACC 4 respectively; Braunschweig, Germany). Wien-133 cells (human Burkitt's lymphoma) were kindly provided by Dr. Geoff Hale (BioAnaLab Limited, Oxford, UK).

PBMCs derived from CLL patients were commercially obtained from Discovery Life Sciences (Huntsville, AL, USA). Buffy coats from healthy human donors and complement-competent, pooled normal human serum (NHS; AB positive) were obtained from Sanquin (Amsterdam, The Netherlands). Whole blood samples from healthy human volunteers were freshly obtained from the University Medical Center Utrecht (Netherlands). Purified C1q protein and C1

complex were obtained from Quidel (San Diego, CA, USA) and Complement Technology (Tyler, TX, USA) respectively.

### **Whole blood cytotoxicity**

Cytotoxicity assays were performed with healthy human donor blood samples that were hirudin anticoagulated or EDTA anticoagulated and recalcified using 5 mM CaCl<sub>2</sub> (Sigma Aldrich) for 30 minutes in the presence of 10 µg/mL hirudin (Genscript) to preserve complement activity. Briefly, whole blood was incubated with antibodies for 45 minutes or 18 hours at 37 °C 5% CO<sub>2</sub>. After 45 minutes incubation, samples were stained for 30 minutes at 4 °C with fluorochrome-labeled lineage-specific antibodies and fixable viability stain (FVS-BV510; BD) to characterize cell subsets and dead or dying cells, respectively. Next, red blood cells were lysed (lysis buffer: 10 mM KHCO<sub>3</sub>, 0.01 mM EDTA and 155 mM NH<sub>4</sub>Cl) and cells were fixed in 2% paraformaldehyde before measuring on a flow cytometer. After 18 hours incubation, red blood cells were lysed first and next samples were stained as described above, before measuring on an LSRFortessa (BD Biosciences, Franklin Lakes, NJ, USA) flow cytometer. Cell markers used to define cell populations were: CD45-PerCP (Biolegend, San Diego, CA, USA), CD66b-PE-Cy7 (Biolegend), CD3-eFluor450 (Waltham, MA, USA), CD4-APC-eFluor780 (eBioscience, San Diego, CA, USA) and CD19-BV711 (Biolegend). The gating strategy used to define cell populations is described in Supplementary Figure 7A. Cytotoxicity was calculated as the fraction (%) of cells remaining after treatment relative to a non-treated control sample (100%).

### **C1q binding**

Wien-133 cells were opsonized with antibody serial dilutions for 15 min at 37 °C. Subsequently, cells and antibodies were put on ice, purified human complement component C1q (2.5 µg/mL) was added and incubated for 45 min. After washing, C1q binding was detected using a Fluorescein isothiocyanate (FITC) conjugated rabbit anti-human C1q antibody (Dako, Glostrup, Denmark) and quantified as the FITC geometric mean fluorescent intensity (gMFI) determined on an iQue Screener flow cytometer (Sartorius, Göttingen, Germany).

### **CDC**

CDC assays were performed using tumor cells incubated with antibody concentration series or a fixed antibody concentration as indicated, for 45 minutes at 37 °C in the presence of normal human serum (NHS; 20% final concentration) as source of complement. Killing was calculated as the fraction of propidium iodide (PI)-positive cells (%) determined by an iQue Screener flow cytometer for B-tumor cell lines and as the fraction of TO-PRO-3-positive cells (%) determined by an LSRFortessa flow cytometer for CD19<sup>+</sup> CLL B cells.



### **FcγR binding**

Binding of antibody variants to the monomeric extracellular domain (ECD) of FcγRIIA (FCGR1AECDDHis) and to dimeric ECDs of FcγRIIA allotype 131H (diFCGR2AH-HisBAP), FcγRIIA allotype 131R (diFCGR2AR-HisBAP), FcγRIIIA allotype 158F (diFCGR3AF-HisBAP), and FcγRIIIA allotype 158V (diFCGR3AV-HisBAP) was tested in ELISA assays.<sup>44</sup> For binding to dimeric FcγR variants, 100 μL goat anti-human F(ab)<sub>2</sub> (1 μg/mL) was added per well for coating overnight at 4 °C. After washing the plates, non-specific binding was blocked for 1 hour at room temperature (RT) by adding 200 μL/well PBS/0.2% BSA. With washings in between incubations, plates were sequentially incubated with 100 μL of 20 μg/mL antibody variants in PBST with 0.2% BSA buffer for 1 hour at RT, 100 μL of the recombinant dimeric FcγR constructs (1 μg/mL) for 1 hour at RT, and 100 μL streptavidin-labelled Poly-HRP (1:10.000) for 30 minutes at RT. Development was performed for 10-30 minutes with 1 mg/mL ABTS (Roche, Mannheim, Germany). To stop the reactions, 100 μL/well of 2% oxalic acid was added. Absorbance was measured at 405 nm in a microplate reader (BioTek, Winooski, VT, USA). To detect binding to monomeric FcγRIa, plates were coated with monomeric his-tagged FCGR1A ECD and after antibody incubation, goat anti-human-kappaLC-HRP (1:5000) was used as detection antibody.

### **FcγR activation**

Activation of FcγRIIa- (allotype H-131) and FcγRIIIa-mediated (allotype V-158) intracellular signaling was quantified using Luminescent Reporter Bioassays (Promega, Madison, WI, USA), according to the manufacturer's recommendations.

### **ADCC**

ADCC was assessed using a DELFIA® EuTDA Cytotoxicity assay (PerkinElmer, Norwalk, CT, USA) according to the manufacturer's recommendations. Briefly, Wien-133 target cells were loaded with BATDA reagent, and 1E+04 cells were incubated with antibody serial dilutions and human healthy donor PBMCs (isolated from buffy coats through centrifugation using Leucosep™ tubes according to the manufacturer's instructions; Greiner Bio-one) as effector cells, at a 100:1 effector to target ratio, for 2 hours at 37 °C in a total volume of 160 μL. After incubation and centrifugation, 20 μL of supernatant was transferred to a 96 well plate, 200 μL Europium Solution was added, and the mixture was incubated for 15 min at RT while shaking. EuTDA release and time-resolved fluorescence was measured on an EnVision Multilabel Reader (PerkinElmer). Maximal and spontaneous release were determined using target cells incubated with 0.1% Triton X-100 or target cells in medium without effector cells, respectively. Specific release was calculated as:

$$\% \text{ specific release} = 100 * \frac{(\text{counts release sample} - \text{counts spontaneous release})}{(\text{counts maximal release} - \text{counts spontaneous release})}$$

### ADCP

ADCP assays were performed as described<sup>45</sup>. In short, human CD14<sup>+</sup> monocytes were obtained from healthy donor PBMCs (isolated from buffy coats through centrifugation using Leucosep™ tubes according to the manufacturer's instructions) through positive isolation using CD14 MicroBeads (Miltenyi Biotec, Leiden, Netherlands) according to the manufacturer's instructions. Monocytes were cultured in culture medium (CellGenix® GMP DC serum-free medium with 50 ng/ml M-CSF) in Nunc™ dishes with UpCell™ surface (Thermo Fisher Scientific) at 37 °C/5% CO<sub>2</sub> for 7-8 days to obtain human monocyte-derived macrophages (h-MDM). h-MDMs were characterized by flow cytometry for expression of myeloid- and macrophage-specific maturation markers (Supplementary Table 1). ADCP was determined using Raji cells labeled with calcein AM (Life Technologies, Carlsbad, CA, USA) according to the manufacturer's instructions and opsonized with antibodies for 15 minutes at 37°C. h-MDM were added at an effector to target (E:T) ratios of 2:1 and incubated for 4 hours at 37 °C/5% CO<sub>2</sub>. After incubation, tumor cells and h-MDM were stained for surface markers using fluorochrome-conjugated antibodies (Supplementary Table 2) for 30 minutes at 4 °C and analyzed on an LSR-Fortessa flow cytometer. The gating strategy used to define cell populations is described in Supplementary Figure 7B. ADCP was calculated as the fraction of CD11b<sup>+</sup>/calcein AM<sup>+</sup>/CD19<sup>-</sup> cells within the total hMDM (CD11b<sup>+</sup>) cell population.

### Target expression

Expression levels of cellular markers were determined using an indirect immunofluorescence assay (QIFIKIT®, Agilent Technologies, Santa Clara, CA, USA and Human IgG Calibrator kit, BioCytex, Marseille, France) according to the manufacturer's instructions.

### FRET

Proximity-induced FRET was determined by measuring energy transfer between cells incubated with A555-conjugated donor and A647-conjugated acceptor mAbs using flow cytometry as described.<sup>8,21</sup> Briefly, purified B cells (isolated from buffy coats using Dynal Dynabeads Untouched Human B cell isolation kit (Life Technologies) according to manufacturer instructions) were incubated with A555-conjugated donor mAbs and/or A647-conjugated acceptor mAbs in the presence or absence of purified human C1q (Quidel; 2.5 µg/

mL) or C1 (Complement Technology; 2.42 µg/mL). gMFI values were measured using an LSRFortessa flow cytometer by recording events at 585/42 nm (FL2, donor A488) and ≥670 nm (FL3), both excited at 488 nm, and at 660/20 nm (FL4, acceptor A647), excited at 635 nm. Unquenched donor fluorescence intensity was determined with cells incubated with A555-conjugated donor mAbs, and non-enhanced acceptor intensity was determined with cells incubated with A647-conjugated acceptor mAbs. Proximity-induced FRET was determined by measuring energy transfer between cells incubated with A555-conjugated donor and A647-conjugated acceptor mAbs. gMFI values allowed calculation of FRET according to the following equation:

$$\text{Energy transfer (ET)} = \text{FL3(D, A)} - \frac{\text{FL2(D, A)}}{(a)} - \frac{\text{FL4(D, A)}}{(b)}$$

Wherein a=FL2(D)/FL3(D), b=FL4(A)/FL3(A), D is donor, A is acceptor and FLn (D, A) = donor + acceptor.

ET values obtained were normalized:

$$\text{Normalized ET (\%)} = 100 * \frac{\text{ET}}{\text{FL3(D,A)}}$$

### **Viability assay**

Cell viability was determined using a CellTiter-Glo® luminescent cell viability assay, according to the supplier's protocol (Promega, Madison, WI, USA). Cells were seeded in white OptiPlates (PerkinElmer) and allowed to adhere overnight at 37 °C. The following day, antibody serial dilutions and purified human C1q (Complement Technology; 2.5 µg/mL) were added and incubated for 3 days at 37°C. 5 µM staurosporine treated cells and untreated cells were included as positive and negative controls of cell death induction, respectively. After incubation, Luciferin Solution Reagent was added and plates were incubated for 1.5 hours at 37°C. Luminescence was measured on an EnVision Multilabel Reader. The percentage of viable cells was calculated using the following formula:

$$\% \text{ viable cells} = 100 * \frac{\text{T-P}}{\text{V-P}}$$

Wherein T = luminescence of the test sample, P = luminescence of staurosporine control sample and V = luminescence of the medium control sample.

## Animals

Animal experiments were performed in compliance with the Dutch animal protection law (WoD) translated from the directives (2010/63/EU) and if applicable, the Code of Practice “animal experiments for cancer research” (Inspection V&W, Zutphen, The Netherlands, 1999) and were approved by the Dutch Central Committee for animal experiments and by the local Ethical committee. Animals were housed and handled in accordance with good animal practice as defined by the Federation of European Laboratory Animal Science Associations (FELASA), in an association for assessment and accreditation of laboratory animal care (AAALAC) and ISO 9001:2000 accredited animal facility (GDL, Utrecht, Netherlands).

## Pharmacokinetic analysis

Pharmacokinetic studies were performed using 11-12 weeks old female tumor-free C.B-17/IcrHan<sup>®</sup>Hsd-Prkdcscid mice (SCID, Envigo). Mice were injected intravenously (IV) with a single dose of 500 µg of each test reagent per mouse (n=3). Blood samples were drawn from the saphenous vein at 10 min, 4 h and 1, 2, 7, 14 and 21 days after antibody administration and collected into heparin-containing vials. Vials were centrifuged (10 min at 14.000 x g) to separate plasma from cells and plasma was stored at -20°C until further use. Total human IgG concentration in plasma samples was analyzed by ELISA. Plates were coated overnight at 4°C with 2 µg/mL of an in-house generated mouse-anti-human IgG2 recombinant Fab fragment in PBS and plasma human IgG was detected by a peroxidase-conjugated AffiniPure goat anti-human IgG Fcγ-specific antibody (Jackson, West Grace, PA, USA). Area under the curve (AUC) up to day 21 was determined using Graphpad Prism and clearance was calculated as  $(\text{Dose (mg.kg}^{-1}) * 1,000 / \text{AUC})$ .

## Data processing

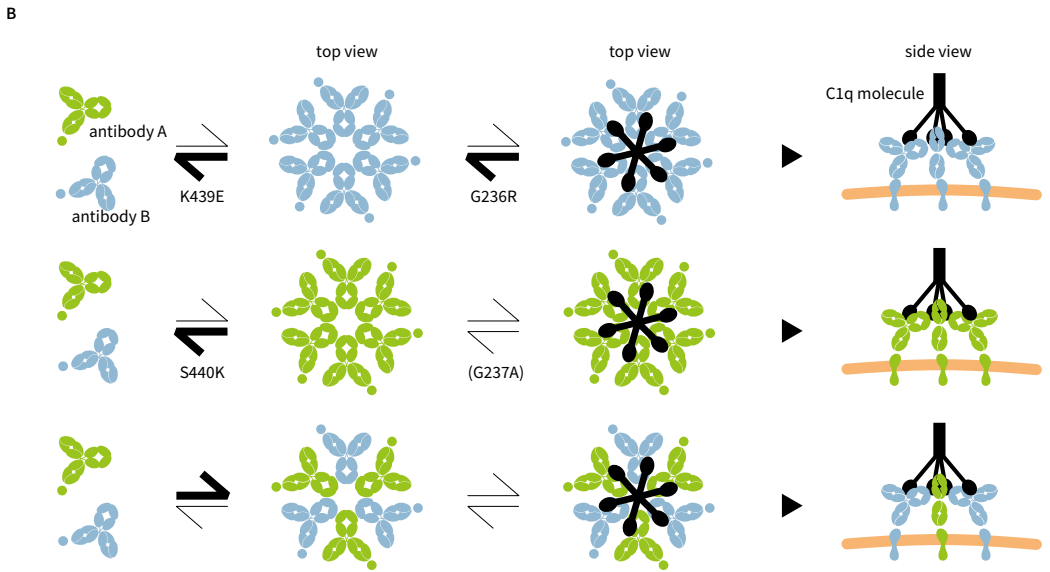
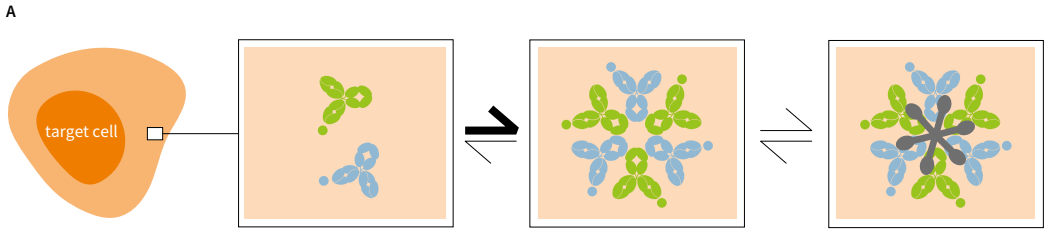
Flow cytometry data were analyzed using FlowJo V10 software. Graphs were plotted and analyzed using GraphPad Prism 8.0. Dose-response curves were generated using best-fit values of non-linear dose-response fits using log-transformed concentrations. All data shown are representative of at least three independent replicate experiments or three individual human donors tested. The mean area under the curve (AUC) ± standard deviation (SD) was determined for all available dose-response analyses and is summarized in Supplementary Table 3. Dose-response data from multiple experimental repeats were pooled, concentrations were log-transformed and the resulting AUC values were normalized relative to the positive control indicated (100%) and negative control non-binding antibody IgG1-b12 (0%). The datasets generated during and/or analyzed during the current study are available from the corresponding author on reasonable request.

# RESULTS

## **Combinations of CD52 and CD20 antibodies induce broad depletion of multiple hematological cell subsets**

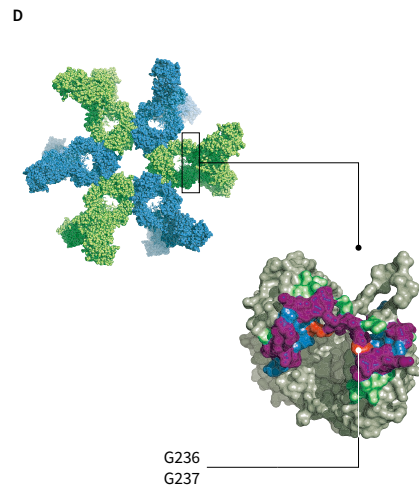
Previously, we showed that mutating amino acid positions Lys<sup>439</sup> and Ser<sup>440</sup> at the Fc-Fc interface into glutamate (K439E) and lysine (S440K), respectively, creates a pair of antibody mutants that show reduced self-oligomerization into homo-hexamers, but efficiently form hetero-hexamers in mixtures containing both mutants (Supplementary Figure 1)<sup>2,8</sup>. Here, we investigated if these mutations can be used to create antibody pairs targeting two different antigens that form hetero-hexameric complexes only when bound to the same target cell, enabling them to act as biologic equivalents of logic AND gates. These mutually dependent antibody pairs aim to activate effector functions only on cells expressing a combination of two targets A AND B, while preventing activation on cells expressing only target A or target B (Figure 1A-B).

To engineer antibody pairs that enable strictly mutually dependent activation, we chose a model system composed of antibodies targeting the abundantly expressed and well-characterized surface antigens CD52 and CD20. We generated hexamerization-enhanced (E430G) IgG1 antibodies that target CD52 (IgG1-Campath-E430G), expressed on various hematological cell subsets including T cells and B cells<sup>9</sup>, and CD20 (IgG1-11B8-E430G), primarily expressed on B cells<sup>10</sup>. A mixture of IgG1-Campath-E430G and IgG1-11B8-E430G efficiently killed Wien-133 lymphoma B cells and depleted both B cells and T cells in human whole blood (Figure 2A, Supplementary Figure 2A). We tested if introducing mutations K439E and S440K (IgG1-Campath-E430G-K439E and IgG1-11B8-E430G-S440K) could induce selective kill of B cells expressing both CD52 and CD20, while sparing T cells expressing only CD52. However, antibody combination IgG1-Campath-E430G-K439E and IgG1-11B8-E430G-S440K (Figure 2A) killed both B cells and T cells in human whole blood at antigen saturation, indicating residual effector function activation and non-selective cell depletion. When tested individually, in the presence of a non-binding control antibody (IgG1-b12) to keep IgG concentrations directly comparable, both single agents (Figure 2A) displayed substantial residual activity in whole blood. Analysis of individual antibody effector functions in B-lymphoma cell lines demonstrated that IgG1-Campath-E430G-K439E still induced residual complement activation (Figure 2B), while IgG1-Campath-K439E without the E430G mutation did not, indicating that selectivity was lost when Fc-Fc interactions were promoted (Supplementary Figure 2B). Furthermore, both single components IgG1-Campath-E430G-K439E and IgG1-11B8-E430G-S440K still activated FcγRIIIa- and FcγRIIIa-dependent signaling in



**C**

target A	target B	activity	
0	0	0	
1	0	0	
0	1	0	
1	1	1	



## ◀ Figure 1

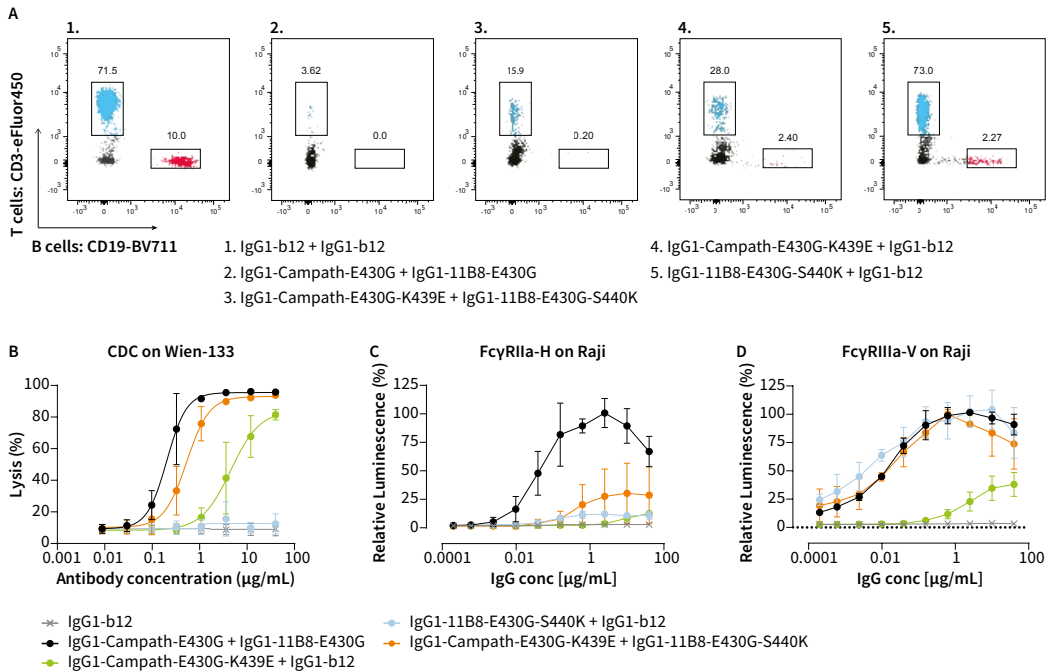
### Design of Fc-domain engineered IgG antibody pairs acting as Boolean logic AND gates.

(A) Schematic of antibody combinations that contain Fc domain modifications designed to induce hetero-hexamer formation only after cell surface target binding, aiming to recruit complement component C1q and induce effector function activation. (B) Mutually dependent antibody pairs may act as Bio-Logic AND gates by integrating two antibody-binding input signals into a functional output exclusively on cells or surfaces that co-express both antibody targets. (C) Summary of coupled biochemical equilibria illustrating how IgG1-hexamer-C1q avidity can be tuned using K439E/S440K and G236R/G237A mutations to favor hetero-hexamerization over homo-hexamerization. (D) Top left: overview of an IgG1 antibody hetero-hexamer based on the IgG1-b12 crystal structure (1HZH).<sup>46</sup> Bottom right: detailed view of an Fc hinge domain indicating amino acid positions involved in C1q- (green) and FcγR binding (blue). The largely shared C1q- and FcγR binding interface (purple) highlights preferred amino acid positions that differentially modulate C1q and FcγR binding (orange).

cell-based reporter assays (Figure 2C-D), suggesting that their activation was not strictly dependent on antibody hexamerization. Thus, this pair of antibody variants did not act in a strictly mutually dependent fashion, since the selective activation of effector functions by K439E and S440K mutant antibody pairs was compromised both by residual antibody clustering on single target cells, and by FcγR activity that was independent of antibody hexamerization.

### G236/G237 mutations can differentially modulate multiple IgG1 effector functions

To increase the selectivity of effector function activation by K439E and S440K mutant antibody pairs, we differentially modulated the binding to FcγR and C1q effector molecules (Figure 1C). IgG (hetero-) hexamer abundance and stability are the product of both Fc-Fc and Fc-C1q interactions<sup>2,5,11</sup> and the binding sites for C1q and FcγRs on the Fc domain of IgG1 show substantial overlap<sup>12-14</sup> (Figure 1D). We examined several amino acids at the shared IgG binding interface for C1q and FcγR that differentially modulated FcγR- and C1q binding affinity (data not shown). Mutations G236R and G237A were selected to simultaneously maximize the therapeutic index between individual and mutually dependent C1q recruitment, and to suppress or eliminate FcγR-mediated effector functions such as antibody dependent cellular cytotoxicity (ADCC) and antibody dependent cellular phagocytosis (ADCP) (Supplementary Figure 3, Figure 1C-D). Hexamerization-independent FcγR binding and activation was strongly suppressed by introducing G236R in IgG1-Campath-E430G-K439E (IgG1-Campath-RGE) and G237A in IgG1-11B8-E430G-S440K (IgG1-11B8-AGK), both for the two single agents as well as in the mixture of both components (Figure 3A, Supplementary Figure 4). In a functional assay setup, no ADCC could be detected using either of the single antibody components or the antibody combination (Figure 3B). By contrast, low level ADCP activity was still detectable, which may be attributed to residual binding to FcγRI and FcγRIIa by IgG1-11B8-AGK (Figure 3C). Importantly, tuning of the C1q binding affinity using G236R eliminated the single agent CDC activity of IgG1-Campath-RGE on Wien-133 tumor B cells, while mixed IgG1-Campath-RGE and IgG1-11B8-AGK recovered highly potent CDC activity (Figure 3D), indicating



▲ **Figure 2**

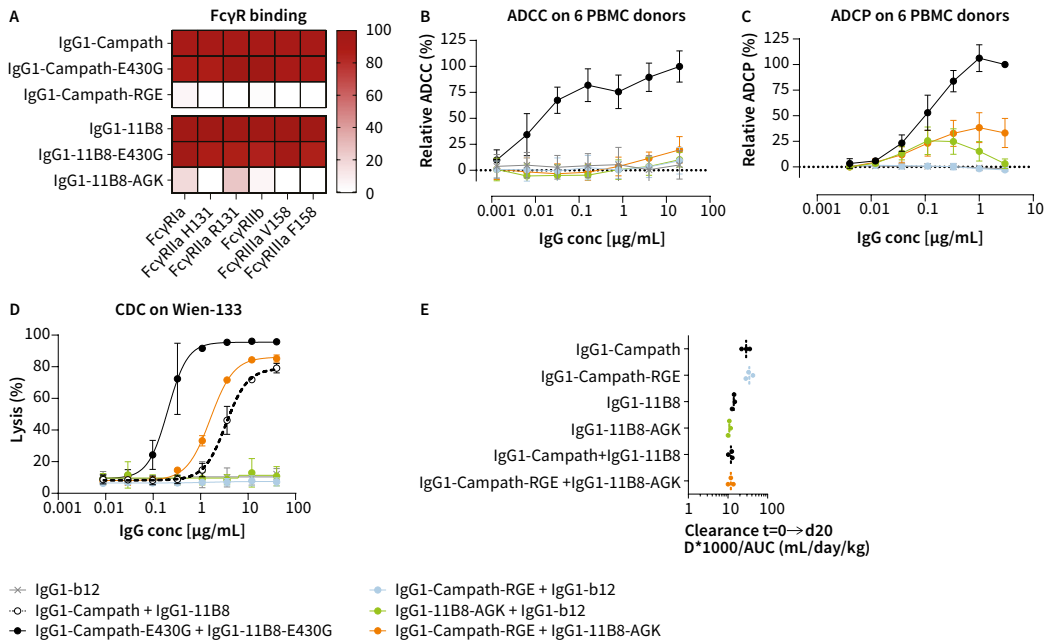
**Non-selective depletion of hematological cell subsets by CD52 and CD20 antibody combinations.**

(A) B- and T-cell cytotoxicity was assessed in healthy human whole blood incubated with non-binding control antibody IgG1-b12 or equimolar mixtures (final concentration 10 µg/mL total IgG) of anti-CD52 mAb IgG1-Campath and anti-CD20 mAb IgG1-11B8 antibody variants for 18 hours at 37 °C and analyzed by flow cytometry. The fraction (%) of B- or T cells remaining within the lymphocyte population (CD66b<sup>+</sup>) from one representative donor (out of 5 tested donors) is shown. (B) CDC of Wien-133 cells in dose-response titrations of IgG1-Campath and IgG1-11B8 antibody variants. Mean and standard deviation (SD) from three experimental repeats are shown. (C-D) Dose-dependent activation of FcγRIIIa- (C) and FcγRIIIa-mediated (D) intracellular signaling by IgG1-Campath and IgG1-11B8 antibody variants was quantified by a luminescent reporter bioassay using Raji target cells and Jurkat T-effector cells expressing FcγRIIIa H131 (C) or FcγRIIIa V158 (D). Luminescence values were normalized to the value for 10 µg/mL IgG1-11B8-E430G + IgG1-b12 prior to pooling, and are presented as the percentage relative luminescence. Mean and SD from three experimental repeats are shown. (B-D) Statistical analysis of area under the curve (AUC) values is described in Supplementary Table 3.

that complement activation was strictly mutually dependent. Non-equimolar target expression, as well as the asymmetric C1q binding affinity imposed by mutations G236R and G237A, restricted C1q binding by mixed IgG1-Campath-RGE and IgG1-11B8-AGK components to levels comparable to that of the wild-type IgG1-Campath and IgG1-11B8 combination (Supplementary Figure 5).

We also investigated if the selected mutations affected the pharmacokinetic profile of IgG1-Campath and IgG1-11B8 antibodies by analyzing the clearance rate in tumor free C.B-17 SCID mice in the absence of target binding. Both single IgG1-Campath-RGE and IgG1-11B8-AGK antibody components showed clearance rates comparable to those of wild-type IgG1-Campath and IgG1-11B8, respectively. Mixed IgG1-Campath-RGE and IgG1-11B8-AGK components





▲ **Figure 3**

**Clustering-dependent effector function activation by differential modulation of effector binding through G236/G237 mutations.**

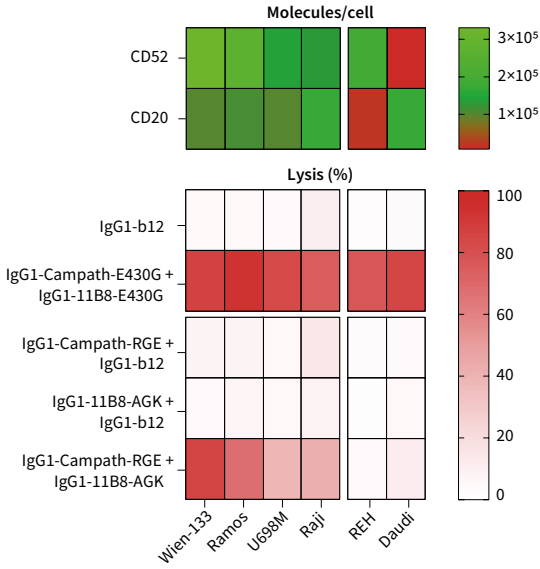
(A) Binding of 20 μg/mL IgG1-Campath and IgG1-11B8 antibody variants to FcγRs (ELISA). Data were normalized to IgG1-b12 (0% binding) and wild-type IgG1-Campath or IgG1-11B8 (100% binding) and presented as the mean of three independent experiments. (B) ADCC or (C) ADCP by IgG1-Campath and IgG1-11B8 antibody variants using (B) Wien-133 target cells and PBMC effector cells (E:T 1:100), or (C) Calcein AM-labeled Raji target cells and CD11b<sup>+</sup> h-MDM effector cells (E:T 2:1). Data were normalized to IgG1-b12 (0% ADCC/ADCP) and a mixture of IgG1-Campath-E430G and IgG1-11B8-E430G (100% ADCC/ADCP). Mean and SD of six donors are shown. (D) CDC of Wien-133 cells by IgG1-Campath and IgG1-11B8 antibody variants. Mean and SD from three experimental repeats are shown. (B-D) Statistical analysis of AUC values is described in Supplementary Table 3. (E) PK analysis of IgG1-Campath and IgG1-11B8 antibody variants in SCID mice (three mice per group). Clearance of a single antibody dose (500 μg) was monitored for three weeks and is expressed as Dose (D)\*1,000/AUC. Statistical comparison between groups is described in Supplementary Table 4.

displayed a clearance rate similar to that of a mixture of wild type IgG1-Campath and IgG1-11B8 (Figure 3E).

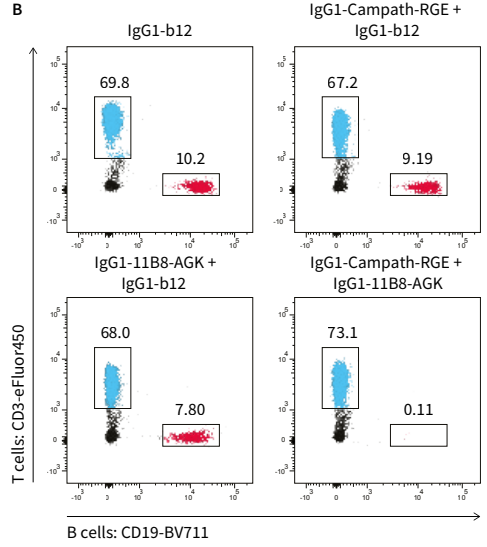
**A mutually dependent antibody combination induces selective depletion of healthy and tumor B cells co-expressing CD52 and CD20**

To assess whether cytotoxicity of the IgG1-Campath-RGE and IgG1-11B8-AGK antibody combination is restricted to cells co-expressing CD52 and CD20, we analyzed the CDC activity of individual and mixed antibody components on six tumor B-cell lines with variable CD52 and CD20 target expression levels. All six cell lines were sensitive to CDC by a combination of the independently hexamerizing antibodies IgG1-Campath-E430G and IgG1-11B8-E430G. Tested as single components, neither IgG1-Campath-RGE, nor IgG1-11B8-AGK induced

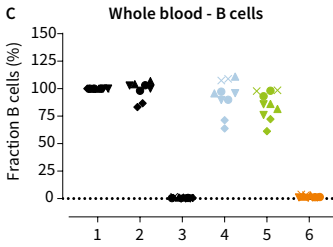
A



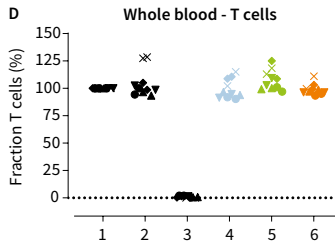
B



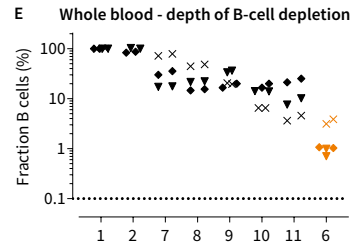
C



D



E

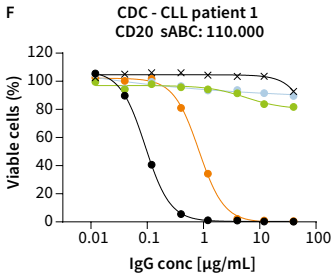


1. No Ab
2. IgG1-b12
3. IgG1-Campath-E430G + IgG1-11B8-E430G
4. IgG1-CD52-Campath-RGE + IgG1-b12
5. IgG1-11B8-AGK + IgG1-b12
6. IgG1-Campath-RGE + IgG1-11B8-AGK

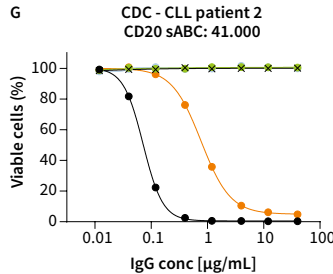
7. Rituximab + IgG1-b12
8. Obinutuzumab + IgG1-b12
9. IgG1-11B8 + IgG1-b12
10. IgG1-11B8-E430G + IgG1-b12
11. IgG1-7D8 + IgG1-b12

- Donor 1
- ▲ Donor 2
- ▼ Donor 3
- ◆ Donor 4
- × Donor 5

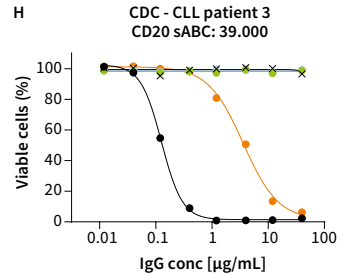
F



G



H



- × IgG1-b12
- IgG1-Campath-E430G + IgG1-11B8-E430G
- ▲ IgG1-Campath-RGE + IgG1-b12
- ◆ IgG1-11B8-AGK + IgG1-b12
- × IgG1-Campath-RGE + IgG1-11B8-AGK

#### ◀ Figure 4

##### **Mutually dependent CD52 and CD20 antibody combinations induced selective depletion of healthy- and tumor B cells.**

(A) CDC (lower panel) induced by IgG1-Campath and IgG1-11B8 antibody variants (40 µg/mL final concentration) in different B-tumor cell lines expressing various levels of CD52 and CD20 quantified by the number of antibody molecules bound per cell (top panel). Data shown are mean values of at least three independent experiments. (B-E) Cytotoxicity induced by IgG1-Campath and IgG1-11B8 antibody variants (10 µg/mL final concentration) incubated for 18 hours in healthy human whole blood, as analyzed by flow cytometry. (B) The fraction (%) of B or T cells remaining within the lymphocyte population (CD66b<sup>+</sup>) is shown for one representative donor. (C-D) Summary of cytotoxicity results relative to a non-treated (no antibody) control sample for five donors containing variable levels of B and T cells. (E) B-cell depletion induced by mutually dependent IgG1-Campath and IgG1-11B8 antibody combinations compared to that of different existing CD20 antibody molecules, shown for three donors relative to a non-treated (no antibody) control sample. (F) Dose response CDC in PBMCs derived from three CLL patients opsonized with serial dilutions of IgG1-Campath and IgG1-11B8 mutant antibody variants and ranked according to CD20 expression levels. sABC, specific antibody binding capacity.

CDC on any of the cell lines tested (Figure 4A). In contrast, the combination of IgG1-Campath-RGE and IgG1-11B8-AGK induced mutually dependent CDC on CD52/CD20 double positive cell lines only, in which the maximal lysis was dependent on the relative expression of both targets.

To test selectivity for double positive cells within a heterogeneous cell mixture, we evaluated B- and T-cell depletion by the CD52- and CD20- mutually dependent antibody combination in human whole blood. Indeed, a combination of IgG1-Campath-RGE and IgG1-11B8-AGK induced selective depletion of CD19<sup>+</sup> B cells, expressing both CD52 and CD20, in human whole blood derived from five healthy donors, while the CD3<sup>+</sup> T-cell population, expressing CD52 only, remained unaffected (Figure 4B-D). Single components IgG1-Campath-RGE or IgG1-11B8-AGK did not show any depletion of B or T cells, demonstrating that cytotoxicity was dependent on binding of both components to antigens co-expressed on the same target cell. Remarkably, as compared to CD20 antibody molecules known to deplete B cells in human whole blood<sup>15-17</sup>, the mutually dependent IgG1-Campath-RGE and IgG1-11B8-AGK antibody combination induced superior, or at least comparable depletion of B cells in human whole blood derived from three healthy donors (Figure 4E). Together, these results demonstrate highly efficient and selective CDC-driven depletion of B cells in whole blood.

Finally, the potency of the mutually dependent CD52 and CD20 antibody combination was tested in B cells derived from peripheral blood mononuclear cells (PBMCs) of CLL patients *ex vivo*. The IgG1-Campath-RGE and IgG1-11B8-AGK antibody combination induced potent and almost complete lysis of B cells derived from three different CLL patients (Figure 4F), in contrast to the individual antibody components. Collectively, these findings confirmed potent, selective and mutually dependent functional activation by the IgG1-Campath-RGE and IgG1-11B8-AGK antibody combination.

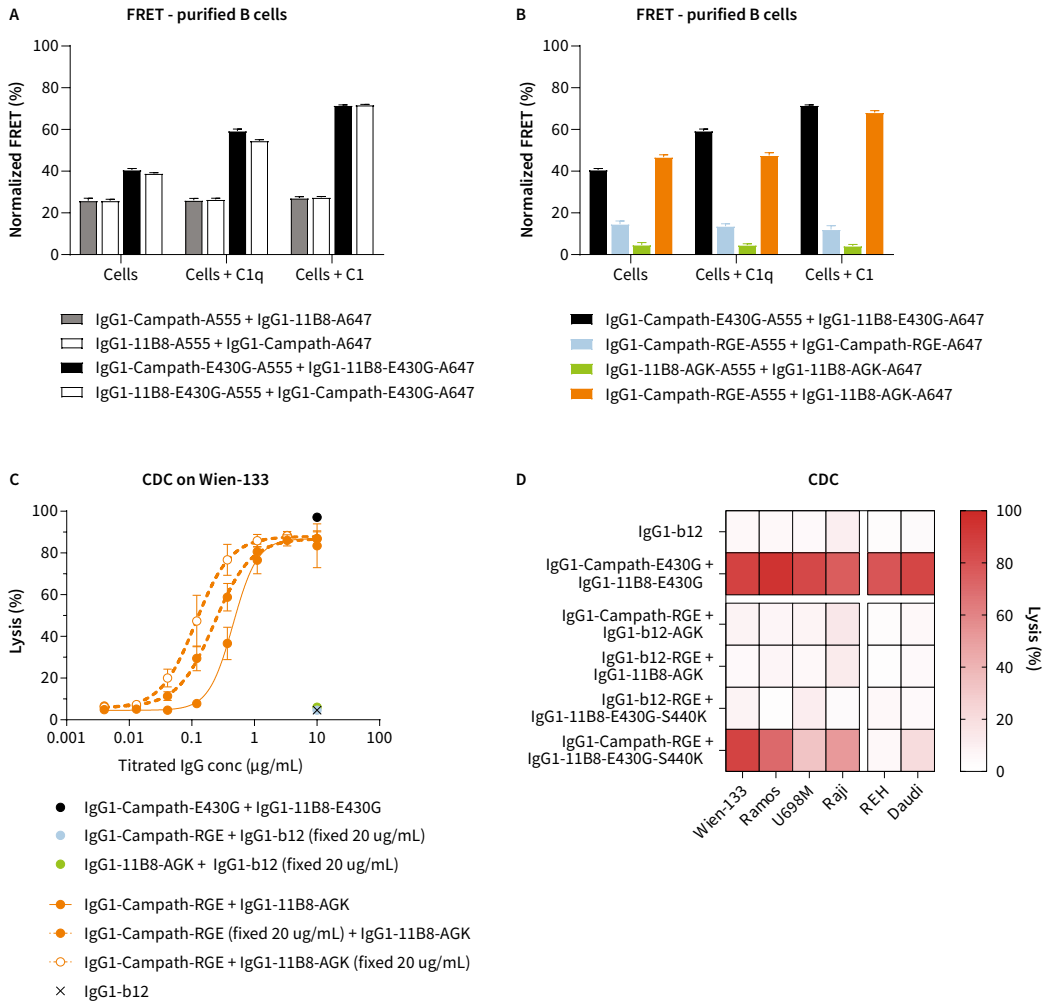
### **Mutually dependent antibody combinations form hetero-hexameric complexes on co-expressing cells**

Antibodies targeting CD37 and CD20 were shown to co-localize and form hetero-hexameric complexes on co-expressing cell surfaces.<sup>8</sup> Here, we used fluorescence resonance energy transfer (FRET) analysis to test the molecular proximity of antibody combinations targeting CD52 and CD20. Purified human B cells from healthy donors were opsonized with fluorescently labeled CD52 and CD20 antibody variants added either individually or in combinations. While wild-type CD52 and CD20 antibody combinations elicited limited proximity-induced FRET, introduction of hexamerization-enhancing mutation E430G increased FRET intensity (Figure 5A). Intriguingly, adding purified C1q or C1 enhanced FRET induction by combinations of CD52 and CD20 antibodies only if they contained mutation E430G, suggesting that Fc-Fc interactions and C1q or C1 recruitment cooperatively promoted CD52 and CD20 antibody co-localization. The mutually dependent CD52 and CD20 antibody combination IgG1-Campath-RGE and IgG1-11B8-AGK induced FRET levels similar to those of a combination of CD52 and CD20 antibodies containing an E430G mutation, whereas FRET was substantially reduced for either single antibody component (Figure 5B). Thus, hetero-hexamer formation and proximity-induced FRET by mutually dependent antibody combinations was dependent on binding of both components to the same target cell.

We next evaluated how mixing mutually dependent CD52 and CD20 antibody components at non-equimolar concentrations affected CDC potency. At saturating concentrations of either IgG1-Campath-RGE or IgG1-11B8-AGK, a titration of the second antibody component recovered essentially identical CDC activity compared to an equimolar mixture of the antibody combination, indicating that specificity and potency was preserved for a range of different mixture compositions (Figure 5C).

We also examined whether non-binding antibodies could be recruited from solution by cell surface-bound antibodies if both contain complementary mutations. Mixing either IgG1-Campath-RGE or IgG1-11B8-AGK with non-binding antibodies containing Fc domains with complementary mutations (IgG1-b12-AGK and IgG1-b12-RGE respectively) did not result in detectable CDC activity in a panel of six tumor B-cell lines (Figure 5D). This indicates that antigen binding-independent recruitment did not meaningfully contribute to tumor cell kill induced by mutually dependent antibody combinations.

For tumor targeting applications, it could be beneficial to permit ADCC activity selectively for a tumor-specific antibody component, when used in combination with a component that targets a more broadly expressed antigen. We therefore analyzed the impact of preserving FcγR binding in antibody compo-



### ▲ Figure 5

#### Cell surface co-localization by mutually dependent CD52 and CD20 antibody combinations

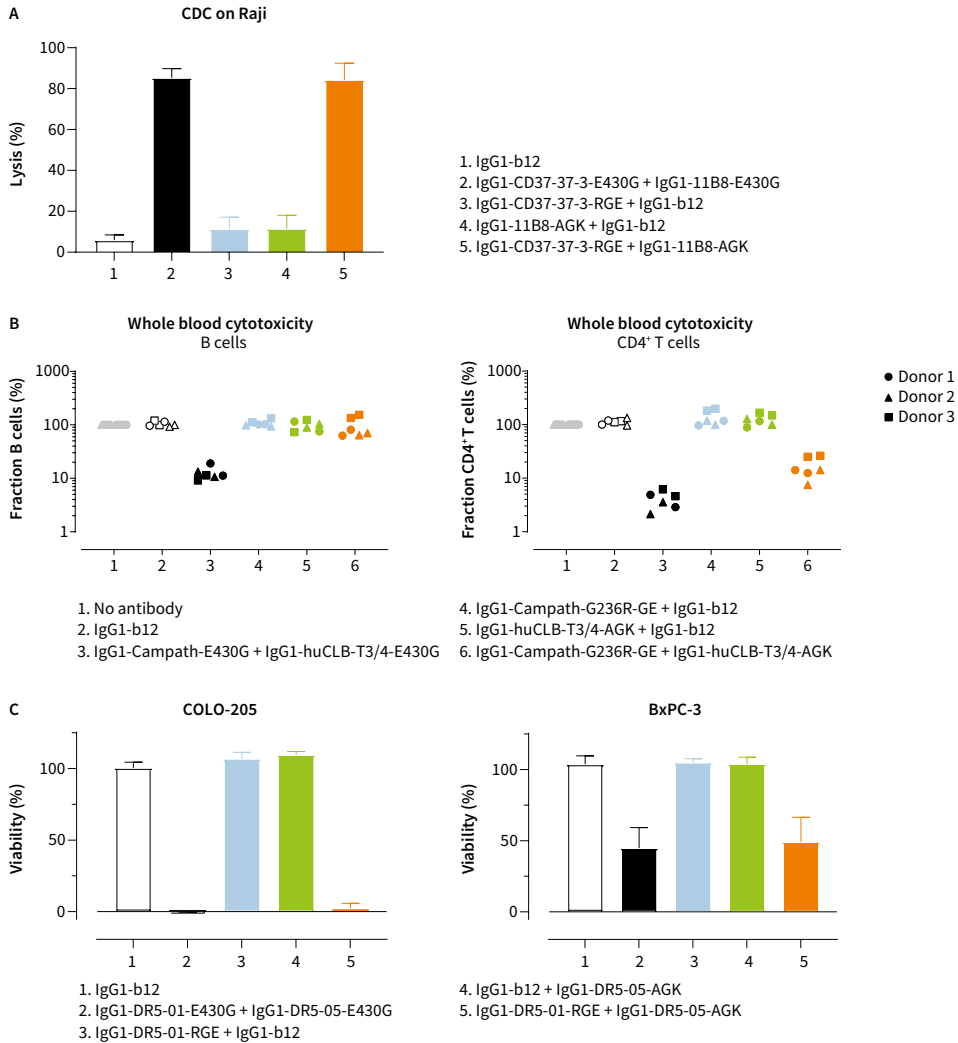
(A-B) FRET analysis to detect the molecular proximity of (A) wild-type and E430G mutant IgG1-Campath or IgG1-11B8 antibody combinations or (B) IgG1-Campath and IgG1-11B8 mutually dependent antibody combinations. Purified healthy donor B cells were opsonized with 10  $\mu\text{g}/\text{mL}$  A555-conjugated- and 10  $\mu\text{g}/\text{mL}$  A647-conjugated antibody variants in the presence or absence of purified human C1q (2.5  $\mu\text{g}/\text{mL}$ ) or C1 (2.42  $\mu\text{g}/\text{mL}$ ) and FRET was calculated from normalized MFI values as determined by flow cytometry. Data shown are mean and SD of four replicates collected from two independent experiments. (C) Dose response CDC on Wien-133 cells opsonized with non-equimolar mixtures of mutually dependent IgG1-Campath and IgG1-11B8 antibody combinations. Titrated antibodies were mixed with antibodies at a fixed (10  $\mu\text{g}/\text{mL}$ ) concentration. Mean and SD from three experimental repeats are shown. See Supplementary Table 3 for statistical analysis of AUC values. (D) CDC induced by IgG1-Campath and IgG1-11B8 antibody variants (40  $\mu\text{g}/\text{mL}$  final concentration) in different B-tumor cell lines. Data shown are mean values of at least three independent experiments.

nant IgG1-11B8-E430G-S440K (Figure 2B-D) on the CDC activity after mixing with IgG1-Campath-RGE (Figure 5D). This functionally asymmetric antibody combination retained selective activation of CDC only on CD52/CD20 double positive cell lines, while recruiting more C1q than the FcγR-suppressed antibody combination (Supplementary Figure 5). These results indicate that the effector functions of such combinations can be adapted to the target expression profiles and product design specifications.

### **Mutually dependent antibody combinations can target distinct cellular subsets distinguished by different antigen combinations**

Potential applications of mutually dependent antibody combinations composed of one antibody with RGE mutations and one antibody with AGK mutations were further explored for different target combinations. A combination of antibodies targeting CD37 (IgG1-CD37.3-RGE) and CD20 (IgG1-11B8-AGK) induced potent and mutually dependent CDC on a CD37 and CD20 double-positive tumor cell line (Figure 6A). We next investigated whether, in addition to B-cells, also other cellular subsets could be selectively targeted using antibody combinations. We therefore tested if T cells could be selectively depleted in human whole blood using an antibody combination targeting CD52 (IgG1-Campath-RGE) and CD3 (IgG1-huCLB3/4-AGK), which are co-expressed on T cells. Indeed, the antibody combination targeting CD52 and CD3 induced selective depletion of CD4<sup>+</sup> T cells expressing both CD52 and CD3, while sparing CD52-only expressing B cells in human whole blood derived from four healthy donors (Figure 6B). T-cell depletion was strictly mutually dependent, as neither of the single antibody components induced any T- or B-cell depletion.

We thus far showed that mutually dependent antibody combinations could regulate hexamerization-dependent complement activation. Hexamerization-enhanced antibodies targeting TNFR superfamily members such as death receptor 5 (DR5) and OX40, which are activated via higher order receptor clustering, were also reported to enhance agonistic signaling and tumor cell death (Supplementary Figure 6)<sup>3,6</sup>. Hence, we evaluated whether an antibody combination targeting non-overlapping epitopes on DR5 (IgG1-DR5-01-RGE and IgG1-DR5-05-AGK) could achieve agonistic activation. Indeed, while both single antibody components were silent, the antibody combination targeting DR5 showed potent induction of apoptosis in COLO-205 and Bx-PC3 solid tumor cell lines (Figure 6C). In contrast, dual epitope targeting by the two WT antibodies showed limited to no efficacy (Supplementary Figure 6). Collectively, these results illustrate that mutually dependent antibody combinations can be designed to target different cell surface antigen combinations, and to elicit potent complement activation or agonistic activation of target signaling<sup>3</sup>.



▲ **Figure 6**

**Mutually dependent antibody combinations are applicable to different cell surface antigen combinations.**

(A) CDC on Raji cells opsonized with 40  $\mu\text{g}/\text{mL}$  anti-CD37 mAb IgG1-37.3 and IgG1-11B8 antibody variants. Mean and SD from three independent experiments are shown. See Supplementary Table 3 for statistical analysis of AUC values. (B) Cytotoxicity induced by anti-CD3 mAb IgG1-huCLB-T3/4 and IgG1-Campath antibody variants (10  $\mu\text{g}/\text{mL}$  final concentration) incubated for 45 minutes in healthy human whole blood, as analyzed by flow cytometry. The fraction (%) of B cells and CD4<sup>+</sup> T cells remaining within the lymphocyte population (CD66b<sup>+</sup>) is shown for three individual donors relative to a non-treated (no antibody) control sample. (C) COLO-205 and BxPC-3 cells were incubated with anti-DR5 IgG1-DR5-01 and IgG1-DR5-05 antibody variants (final concentration 20  $\mu\text{g}/\text{mL}$ ) in the presence of 2.5  $\mu\text{g}/\text{mL}$  purified human C1q and cell viability (%) was measured after 72 hours. Mean  $\pm$  SD of data from three independent experiments are shown. See Supplementary Table 3 for statistical analysis of AUC values.

## DISCUSSION

Activation of antibody-mediated effector functions to eliminate pathogens or destroy tumor cells primarily requires avid antibody binding to cognate antigens on the target cell. Potent effector activity by antibody-based therapies however, may lead to undesired on- or off-target toxicity<sup>18</sup>. Here, we describe an AND-gated approach to decouple effector function activation by antibody combinations from individual antibody binding events. Both antibodies may target different membrane receptors and bind various cellular subtypes individually, but specific point mutation combinations modulate Fc-Fc, C1q and Fc gamma receptor (FcγR) interactions to make IgG hetero-oligomerization and functional activation stringently dependent on the presence of both antibody components<sup>2,7,8,19</sup>. This AND-gated approach was generalizable to different effector mechanisms, including complement activation and agonistic signaling, and to multiple target combinations present on both hematologic and solid tumor cells. Asymmetric silencing of FcγR-mediated effector functions in antibody combinations was possible, enabling design variations that mitigate or leverage on-target toxicity depending on target expression profiles. In some assays, the G237A mutation appeared to only partially suppress FcγR binding and ADCP activity consistent with recent findings<sup>20</sup>, which may limit its application when targeting some broadly and highly expressed antigens, although full selectivity was preserved in whole blood assays in the presence of PBMC populations.

Potential therapeutic applications of mutually dependent antibody combinations requires targets that co-localize and/or allow for antibody hetero-hexamization after target binding. This process may be affected by target-specific restraints other than abundance, such as antigen size, density, mobility, epitope-membrane distance, surface distribution, and the compatibility of epitopes with antibody hetero-hexamer formation<sup>10,21-25</sup>. The challenge of identifying target and epitope combinations that recover maximal potency seems reminiscent of the challenges inherent to covalent bispecific antibody design<sup>26</sup>. Nevertheless, an AND-gated approach could considerably broaden the therapeutic combinatorial target space and thereby simultaneously enhance the therapeutic index. For example, highly potent but “toxic” activity of antibodies directed towards broadly expressed, non-tumor-specific targets could be made dependent on the presence of antibodies directed against disease-specific targets. Herein, we consistently observed that mutually dependent antibody pairs retained maximal potency at doses exceeding target saturation, while avoiding the potency loss referred to as the hook or pro-zone effect, caused by the self-competition observed for covalent bispecific



designs<sup>27</sup>. This is explained by the strict dependence of antibody hexamerization and C1q binding on prior cell surface antigen binding, while monomeric antibodies in solution are incapable of C1q binding. Appropriate dosing might theoretically represent another challenge in the design of mutually dependent antibody combinations, as both components in the mixture might show different pharmacokinetics. Experiments with a wide range of non-equimolar antibody concentrations retained consistent potency, suggesting that non-equimolar mixtures could provide an option to address differences in clearance rates of the two components.

Artificial logic gates, inspired by electronic engineering, have been applied in synthetic biology to control biological processes<sup>28-30</sup>. In human disease, Boolean logic gates are increasingly examined for their potential to enhance therapeutic selectivity, in particular for improving the specificity of natural, or chimeric antigen receptor (CAR), T-cell recruitment<sup>31-35</sup>. In another approach, Boolean logic was applied to create auto-inhibited or capped AND-gated antibodies that rely on a second, exogenous factor to activate binding<sup>36</sup>. The AND-gated approach we describe here solely decouples antibody binding from effector function activation to achieve selectivity and is therefore not dependent on the environmental presence of secondary molecules such as enzymes or proteases. The mutually dependent antibody combinations described herein are minimally engineered, displayed regular pharmacokinetic properties, and preserved regular manufacturability and developability characteristics. We therefore expect this approach to be broadly applicable to IgG Fc-domain based therapeutics, and generalizable to multiple applications, including direct cell killing, agonistic activation, and potentially other more complex Boolean logic gates. Furthermore, the methodology described herein is readily applicable to combinatorial, high throughput screening of large antibody panels for drug discovery. As for any therapeutic, potential novel drug candidates based on AND-gated IgG backbones will require careful assessment of efficacy, safety, and different manufacturing and dosing strategies.

In summary, we present an approach to generate mutually dependent antibody combinations (HexElect) that only allow for pairwise hetero-hexamerization and effector function activation after binding to two targets co-expressed at the same cell surface. This decoupling of effector function activation from individual antibody binding events provides a unique opportunity to enhance selectivity while maintaining potency, and may allow for the creation of a next generation of differentiated antibody therapeutics.

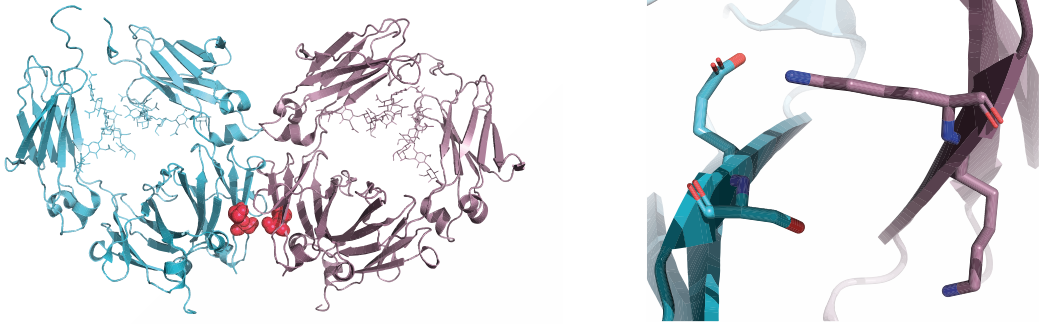
# REFERENCES

1. Wang X, Mathieu M, Brezski RJ. IgG Fc engineering to modulate antibody effector functions. *Protein Cell* 2018; **9**(1): 63-73.
2. Diebold CA, Beurskens FJ, de Jong RN, et al. Complement is activated by IgG hexamers assembled at the cell surface. *Science* 2014; **343**(6176): 1260-3.
3. Overdijk MB, Strumane K, Beurskens FJ, et al. Dual epitope targeting and enhanced hexamerization by DR5 antibodies as a novel approach to induce potent anti-tumor activity through DR5 agonism. *Mol Cancer Ther* 2020: molcanther.0044.2020.
4. Strasser J, de Jong RN, Beurskens FJ, et al. Unraveling the Macromolecular Pathways of IgG Oligomerization and Complement Activation on Antigenic Surfaces. *Nano lett* 2019; **19**(7): 4787-96.
5. Ugurlar D, Howes SC, de Kreuk BJ, et al. Structures of C1-IgG1 provide insights into how danger pattern recognition activates complement. *Science* 2018; **359**(6377): 794-7.
6. Zhang D, Goldberg MV, Chiu ML. Fc Engineering Approaches to Enhance the Agonism and Effector Functions of an Anti-OX40 Antibody. *J Biol Chem* 2016; **291**(53): 27134-46.
7. de Jong RN, Beurskens FJ, Verploegen S, et al. A Novel Platform for the Potentiation of Therapeutic Antibodies Based on Antigen-Dependent Formation of IgG Hexamers at the Cell Surface. *PLOS Biol* 2016; **14**(1): e1002344.
8. Oostindie SC, van der Horst HJ, Lindorfer MA, et al. CD20 and CD37 antibodies synergize to activate complement by Fc-mediated clustering. *Haematologica* 2019.
9. Rao SP, Sancho J, Campos-Rivera J, et al. Human Peripheral Blood Mononuclear Cells Exhibit Heterogeneous CD52 Expression Levels and Show Differential Sensitivity to Alemtuzumab Mediated Cytolysis. *PLoS One* 2012; **7**(6): e39416.
10. Teeling JL, Mackus WJ, Wiegman LJ, et al. The biological activity of human CD20 monoclonal antibodies is linked to unique epitopes on CD20. *J Immunol* 2006; **177**(1): 362-71.
11. Wang G, de Jong RN, van den Bremer ET, et al. Molecular Basis of Assembly and Activation of Complement Component C1 in Complex with Immunoglobulin G1 and Antigen. *Mol Cell* 2016; **63**(1): 135-45.
12. Idusogie EE, Presta LG, Gazzano-Santoro H, et al. Mapping of the C1q binding site on rituxan, a chimeric antibody with a human IgG1 Fc. *J Immunol* 2000; **164**(8): 4178-84.
13. Morgan A, Jones ND, Nesbitt AM, Chaplin L, Bodmer MW, Emtage JS. The N-terminal end of the CH2 domain of chimeric human IgG1 anti-HLA-DR is necessary for C1q, Fc gamma RI and Fc gamma RIII binding. *Immunology* 1995; **86**(2): 319-24.
14. Shields RL, Namenuk AK, Hong K, et al. High resolution mapping of the binding site on human IgG1 for Fc gamma RI, Fc gamma RII, Fc gamma RIII, and FcRn and design of IgG1 variants with improved binding to the Fc gamma R. *J Biol Chem* 2001; **276**(9): 6591-604.
15. Bologna L, Gotti E, Manganini M, et al. Mechanism of Action of Type II, Glycoengineered, Anti-CD20 Monoclonal Antibody GA101 in B-Chronic Lymphocytic Leukemia Whole Blood Assays in Comparison with Rituximab and Alemtuzumab. *J Immunol* 2011; **186**(6): 3762.
16. van Meerten T, Rozemuller H, Hol S, et al. HuMab-7D8, a monoclonal antibody directed against the membrane-proximal small loop epitope of CD20 can effectively eliminate CD20 low expressing tumor cells that resist rituximab-mediated lysis. *Haematologica* 2010; **95**(12): 2063-71.
17. Bologna L, Gotti E, Da Roit F, et al. Ofatumumab Is More Efficient than Rituximab in Lysing B Chronic Lymphocytic Leukemia Cells in Whole Blood and in Combination with Chemotherapy. *J Immunol* 2013; **190**(1): 231.

18. Alinari L, Lapalombella R, Andritsos L, Baiocchi RA, Lin TS, Byrd JC. Alemtuzumab (Campath-1H) in the treatment of chronic lymphocytic leukemia. *Oncogene* 2007; **26**(25): 3644-53.
19. Hezareh M, Hessel AJ, Jensen RC, van de Winkel JG, Parren PW. Effector function activities of a panel of mutants of a broadly neutralizing antibody against human immunodeficiency virus type 1. *J Virol* 2001; **75**(24): 12161-8.
20. Brinkhaus M, Douwes RGJ, Bentlage AEH, et al. Glycine 236 in the Lower Hinge Region of Human IgG1 Differentiates FcγR from Complement Effector Function. *J Immunol* 2020.
21. Cragg MS, Morgan SM, Chan HT, et al. Complement-mediated lysis by anti-CD20 mAb correlates with segregation into lipid rafts. *Blood* 2003; **101**(3): 1045-52.
22. Hughes-Jones NC, Gorick BD, Howard JC, Feinstein A. Antibody density on rat red cells determines the rate of activation of the complement component C1. *Eur J Immunol* 1985; **15**(10): 976-80.
23. Parce JW, Kelley D, Heinzelmann K. Measurement of antibody-dependent binding, proteolysis, and turnover of C1s on liposomal antigens localizes the fluidity-dependent step in C1 activation. *Biochim Biophys Acta* 1983; **736**(1): 92-8.
24. Rougé L, Chiang N, Steffek M, et al. Structure of CD20 in complex with the therapeutic monoclonal antibody rituximab. *Science* 2020: eaaz9356.
25. Xia MQ, Hale G, Waldmann H. Efficient complement-mediated lysis of cells containing the CAMPATH-1 (CDw52) antigen. *Mol Immunol* 1993; **30**(12): 1089-96.
26. Labrijn AF, Janmaat ML, Reichert JM, Parren P. Bispecific antibodies: a mechanistic review of the pipeline. *Nat Rev Drug Discov* 2019; **18**(8): 585-608.
27. Mazor Y, Yang C, Borrok MJ, et al. Enhancement of Immune Effector Functions by Modulating IgG's Intrinsic Affinity for Target Antigen. *PLoS One* 2016; **11**(6): e0157788-e.
28. Hasty J, McMillen D, Collins JJ. Engineered gene circuits. *Nature* 2002; **420**(6912): 224-30.
29. Lu TK, Khalil AS, Collins JJ. Next-generation synthetic gene networks. *Nat Biotechnol* 2009; **27**(12): 1139-50.
30. Chen Z, Kibler RD, Hunt A, et al. De novo design of protein logic gates. *Science* 2020; **368**(6486): 78.
31. Lajoie MJ, Boyken SE, Salter AI, et al. Designed protein logic to target cells with precise combinations of surface antigens. *Science* 2020; **369**(6511): 1637.
32. Minogue E, Millar D, Chuan Y, et al. Redirecting T-Cells Against AML in a Multidimensional Targeting Space Using T-Cell Engaging Antibody Circuits (TEAC). *Blood* 2019; **134**(Supplement\_1): 2653-.
33. Morsut L, Roybal Kole T, Xiong X, et al. Engineering Customized Cell Sensing and Response Behaviors Using Synthetic Notch Receptors. *Cell* 2016; **164**(4): 780-91.
34. Roybal Kole T, Rupp Levi J, Morsut L, et al. Precision Tumor Recognition by T Cells With Combinatorial Antigen-Sensing Circuits. *Cell* 2016; **164**(4): 770-9.
35. Banaszek A, Bumm TGP, Nowotny B, et al. On-target restoration of a split T cell-engaging antibody for precision immunotherapy. *Nat Commun* 2019; **10**(1): 5387.
36. Gunnoo SB, Finney HM, Baker TS, Lawson AD, Anthony DC, Davis BG. Creation of a gated antibody as a conditionally functional synthetic protein. *Nat Commun* 2014; **5**(1): 4388.
37. Crowe JS, Hall VS, Smith MA, Cooper HJ, Tite JP. Humanized monoclonal antibody CAMPATH-1H: myeloma cell expression of genomic constructs, nucleotide sequence of cDNA constructs and comparison of effector mechanisms of myeloma and Chinese hamster ovary cell-derived material. *Clin Exp Immunol* 1992; **87**(1): 105-10.
38. Teeling JL, French RR, Cragg MS, et al. Characterization of new human CD20 monoclonal antibodies with potent cytolytic activity against non-Hodgkin lymphomas. *Blood* 2004; **104**(6): 1793-800.

39. Maloney DG, Liles TM, Czerwinski DK, et al. Phase I clinical trial using escalating single-dose infusion of chimeric anti-CD20 monoclonal antibody (IDEC-C2B8) in patients with recurrent B-cell lymphoma. *Blood* 1994; **84**(8): 2457-66.
40. Mossner E, Brunker P, Moser S, et al. Increasing the efficacy of CD20 antibody therapy through the engineering of a new type II anti-CD20 antibody with enhanced direct and immune effector cell-mediated B-cell cytotoxicity. *Blood* 2010; **115**(22): 4393-402.
41. Parren PW, Geerts ME, Boeije LC, Aarden LA. Induction of T-cell proliferation by recombinant mouse and chimeric mouse/human anti-CD3 monoclonal antibodies. *Res Immunol* 1991; **142**(9): 749-63.
42. Deckert. J. CD37-binding molecules and immunoconjugates thereof. *WO 2011/112978A1* 2011.
43. Burton DR, Pyati J, Koduri R, et al. Efficient neutralization of primary isolates of HIV-1 by a recombinant human monoclonal antibody. *Science* 1994; **266**(5187): 1024-7.
44. Wines BD, Vandervan HA, Esparon SE, Kristensen AB, Kent SJ, Hogarth PM. Dimeric FcγR Ectodomains as Probes of the Fc Receptor Function of Anti-Influenza Virus IgG. *J Immunol* 2016; **197**(4): 1507-16.
45. Oostindie SC, van der Horst HJ, Kil LP, et al. DuoHexaBody-CD37<sup>®</sup>, a novel biparatopic CD37 antibody with enhanced Fc-mediated hexamerization as a potential therapy for B-cell malignancies. *Blood Cancer J* 2020; **10**(3): 30.
46. Saphire EO, Parren PW, Pantophlet R, et al. Crystal structure of a neutralizing human IGG against HIV-1: a template for vaccine design. *Science* 2001; **293**(5532): 1155-9.

## SUPPLEMENTARY FIGURES AND TABLES

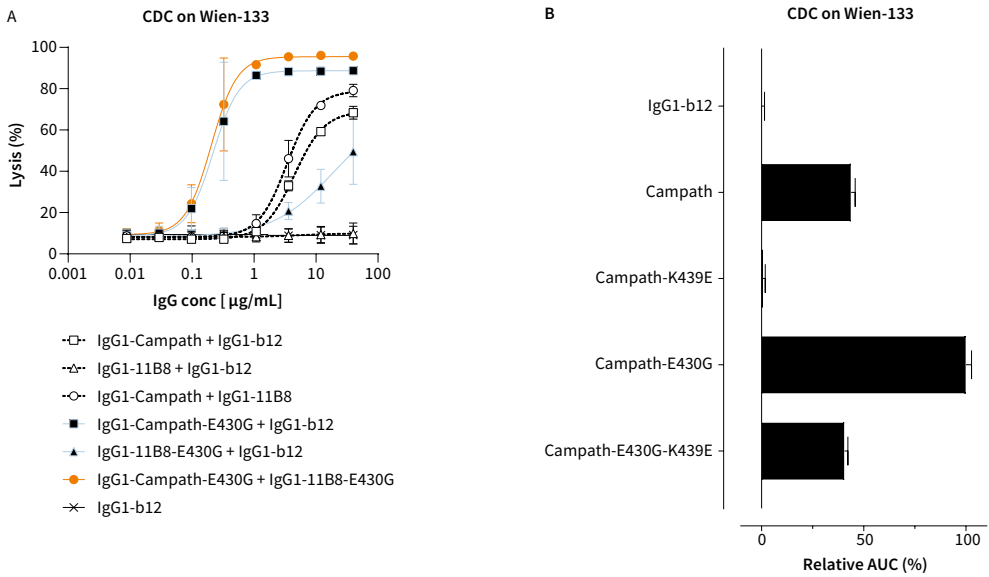


### ▲ Supplementary Figure 1

#### Fc-Fc interaction interface model.

Left: Ribbon diagram of two Fc segments with residues (Lys<sup>439</sup> and Ser<sup>440</sup>) critical for Fc-Fc interactions indicated in pink.

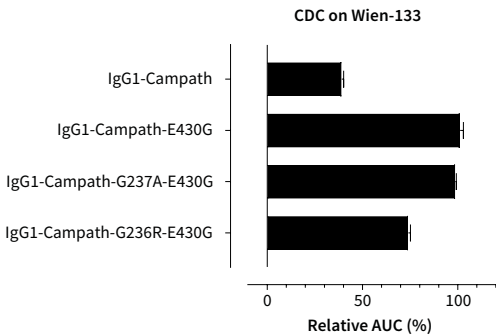
Right: modeled interactions of a K439E (Lys<sup>439</sup> → Glu) mutant facing the S440K (Ser<sup>440</sup> → Lys) mutant on the complementary Fc segment of a neighboring antibody. Figure adapted from Diebold et al. Science 343:1260-1263 (2014).



**▲ Supplementary Figure 2**

**Complement-mediated cytotoxicity on Wien-133 cells opsonized with different IgG1-Campath and IgG1-11B8 antibody variants.**

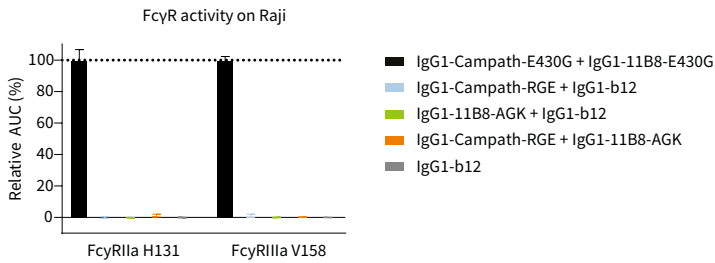
(A) CDC by wild-type and hexamerization-enhanced variants of CD52 and CD20 antibodies. Mean and standard deviation (SD) from three experimental repeats are shown. (B) Residual CDC by Fc-Fc interface mutant CD52 antibody variants. CDC was assessed on Wien-133 cells opsonized with a concentration series of different IgG1-Campath antibody variants. Data was averaged over three experiments, normalized to IgG1-b12 (0 % lysis) and IgG1-Campath-E430G (100% lysis), and is presented as the area under the curve (AUC). (A-B) See Supplementary Table 3 for statistical analysis of AUC values.



**▲ Supplementary Figure 3**

**Complement activation by C1q- and FcγR-binding mutant CD52 antibody variants.**

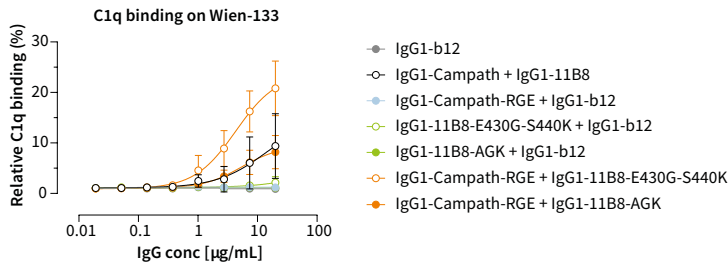
CDC was assessed using Wien-133 cells opsonized with a concentration series of different IgG1-Campath antibody variants. Data was averaged over three experiments, normalized to IgG1-b12 (0 % lysis) and IgG1-Campath-E430G (100% lysis), and is presented as the area under the curve (AUC). See Supplementary Table 3 for statistical analysis of AUC values.



▲ **Supplementary Figure 4**

**Activation of FcγRIIa- and FcγRIIIa-mediated intracellular signaling by IgG1-Campath and IgG1-11B8 mutant antibody variants.**

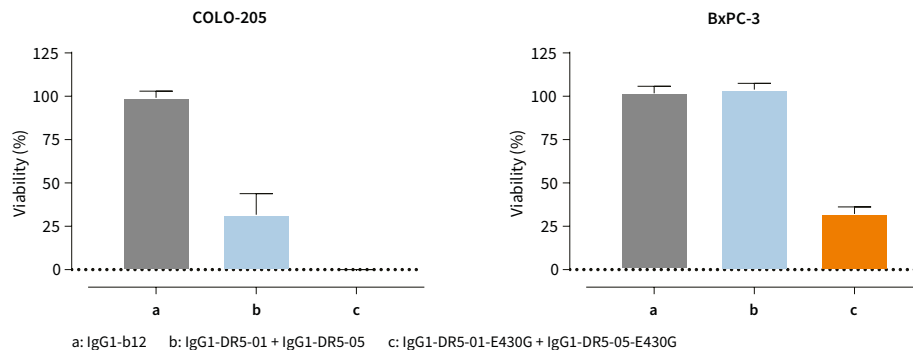
Activation of FcγR-mediated signaling was assessed in a Luminescent Reporter Bioassay using Raji target cells and Jurkat T-effector cells. Luminescence values were normalized to the value of 10 μg/mL IgG1-11B8-E430G + IgG1-b12 prior to pooling. Area under the curve (AUC) values were averaged over three experiments, normalized to IgG1-b12 (0% activation) and a mixture of IgG1-11B8-E430G and IgG1-Campath-E430G (100% activation). See Supplementary Table 3 for statistical analysis of AUC values.



▲ **Supplementary Figure 5**

**C1q binding by IgG1-Campath and IgG1-11B8 mutant antibody variants.**

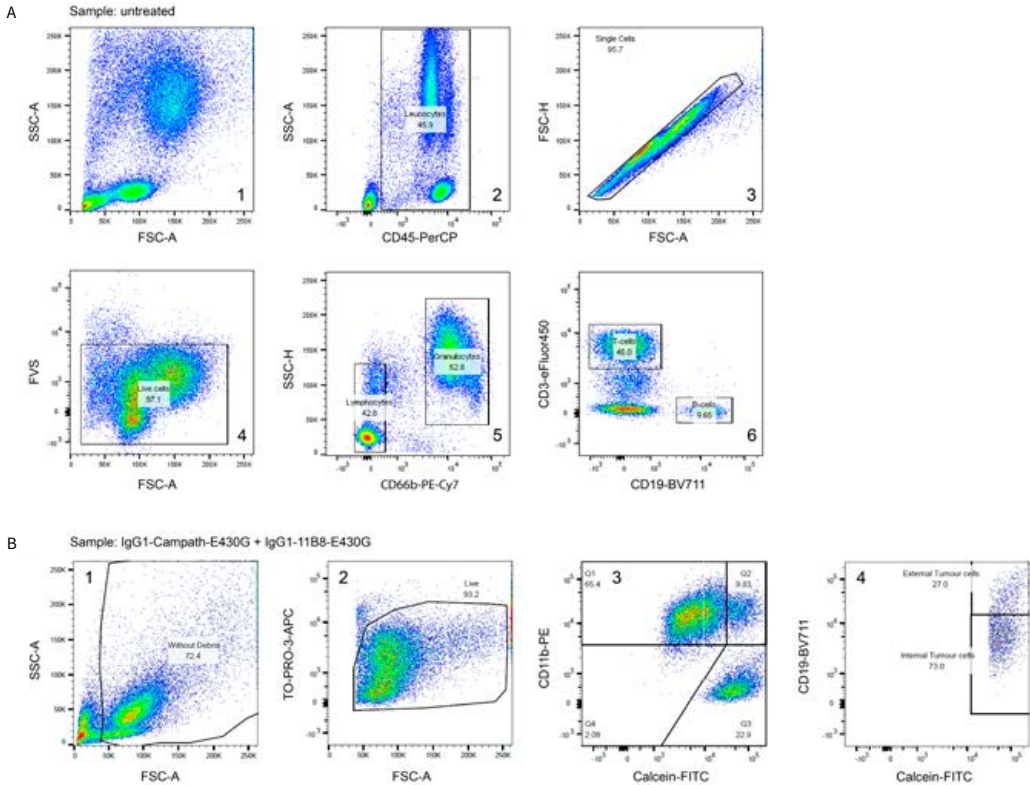
C1q binding to Wien-133 cells opsonized with a concentration series of IgG1-Campath and IgG1-11B8 mutant antibody variants. Data were normalized to IgG1-b12 (0% C1q binding) and a mixture of IgG1-11B8-E430G and IgG1-Campath-E430G (100% C1q binding). Mean and standard deviation (SD) from three independent experiments are shown. See Supplementary Table 3 for statistical analysis of AUC values.



▲ **Supplementary Figure 6**

**Agonistic activity by wild-type and hexamerization-enhanced IgG1-DR5 antibody variants.**

COLO-205 and BxPC-3 cells were incubated with wild-type and hexamerization-enhanced (E430G) anti-DR5 IgG1-DR5-01 and IgG1-DR5-05 antibody variants (final concentration 20 μg/mL) in the presence of 2.5 μg/mL purified human C1q and cell viability (%) was measured after 72 hours. Mean ± SD of data from three independent experiments are shown. See Supplementary Table 3 for statistical analysis of AUC values.



▲ **Supplementary Figure 7**

**Flow cytometry gating strategy used to define cell populations by flow cytometry.**

(A) Example of whole blood cytotoxicity flow cytometry gating strategy, as illustrated for a negative control sample (untreated cells) derived from a healthy human donor. (1) Cells were identified based on forward scatter (FSC) vs. side scatter (SSC). (2) Leukocytes were selected by CD45<sup>+</sup> staining. (3) Doublets were excluded by FSC-A vs. FSC-H. (4) Dead cells were excluded by TO-PRO-3 staining. (5) Lymphocytes and granulocytes were separated based on CD66b staining. (6) B- and T cells within the lymphocyte (CD66b<sup>-</sup>) cell population were identified as CD19<sup>+</sup> and CD3<sup>+</sup>/(CD4<sup>+</sup>, data not shown), respectively. Cytotoxicity was calculated as the fraction (%) of cells remaining after treatment relative to a non-treated control sample (100%). (B) Example of ADCP flow cytometry gating strategy, as illustrated for a positive control sample (IgG1-Campath-E430G + IgG1-11B8-E430G) with Raji target cells and human monocyte-derived macrophage (h-MDM) effector cells. (1) Cells were identified based on forward scatter (FSC) vs. side scatter (SSC). (2) Dead cells were excluded by fixable viability stain (FVS). (3) Raji target cells and h-MDM effector cells were separated by calcein AM and CD11b staining respectively. (4) CD19 was used as a marker to exclude external (non-phagocytosed) Raji target cells. CD11b<sup>+</sup>/calcein AM<sup>+</sup>/CD19<sup>-</sup> cells were identified as h-MDM that phagocytosed Daudi cells. ADCP was calculated as the fraction of CD11b<sup>+</sup>/calcein AM<sup>+</sup>/CD19<sup>-</sup> cells within the total h-MDM (CD11b<sup>+</sup>) cell population.



**Supplementary Table 1****Antibodies used for h-MDM characterization**

<b>Target</b>	<b>Label</b>	<b>Target expression</b>	<b>Company</b>	<b>Clone</b>	<b>Cat. No.</b>
<b>CD14</b>	PE-Cy7	Maturation and lineage marker for monocytes/macrophages	BD Pharmingen	M5E2	557742
<b>CD11b</b>	PE	General myeloid cell lineage and maturation marker	BD Pharmingen	ICRF44	555388
<b>CD64</b>	FITC	FcγRI (IgG1), expressed on mature antigen-presenting cells including macrophages	Biolegend	10.1	305006
<b>CD80</b>	APC	B7-1, expressed on activated antigen-presenting cells, including macrophages	Miltenyi	2D10	130-097-204
<b>CD163</b>	BV421	Macrophage sub lineage/maturity marker	Biolegend	GHI/61	333612
<b>CD206</b>	BV711	Mannose receptor, macrophage maturity/sub lineage marker	Biolegend	15-2	321136
<b>FVS</b>	eFluor660	Staining of dead cells	BD Biosciences		565694

**Supplementary Table 2****Antibodies used for identification of cell subsets in ADCP assays**

<b>Target</b>	<b>Label</b>	<b>Target expression</b>	<b>Company</b>	<b>Clone</b>	<b>Cat. No.</b>
<b>CD11b</b>	PE	h-MDM	BD Pharmingen	ICRF44	555388
<b>CD19</b>	BV711	Tumor B cells (Daudi)	Biolegend	SJ25C1	363026
<b>TO-PRO-3</b>	APC	Staining of dead cells	Molecular Probes		T3605

**Supplementary Table 3**

Area under the curve statistics as determined for multiple dose-response analyses

Fig. Sub	Item <sup>1</sup>	Antibody component 1	Antibody component 2	Assay	Cells	N <sup>2</sup>	Mean rel. AUC (%) <sup>3</sup>	SD	95% CI of diff. to PC <sup>4</sup>	Adjusted P-value <sup>5</sup>	95% CI of diff. to NC <sup>6</sup>	Adjusted P-value <sup>7</sup>
2	b	PC	IgG1-Campath-E430G	CDC	Wien-133	3	100.0	4.63			-107.0 to -92.98	<0.0001
2	b	TI	IgG1-Campath-E430G-K439E	CDC	Wien-133	3	34.85	5.13	57.22 to 73.09	<0.0001	-41.87 to -27.82	<0.0001
2	b	TI	IgG1-11B8-E430G-S440K	CDC	Wien-133	3	2.54	2.75	89.53 to 105.4	<0.0001	-9.566 to 4.483	0.7404
2	b	TI	IgG1-Campath-E430G-K439E	CDC	Wien-133	3	79.85	4.05	12.22 to 28.08	<0.0001	-86.88 to -72.83	<0.0001
2	b	NC	IgG1-b12	CDC	Wien-133	6	0.00	1.87	93.13 to 106.9	<0.0001		
2	c	PC	IgG1-Campath-E430G	FcyRIIIa H131 activity	Raji	3	99.99	6.71			-110.3 to -89.67	<0.0001
2	c	TI	IgG1-Campath-E430G-K439E	FcyRIIIa H131 activity	Raji	3	2.46	0.48	87.21 to 107.8	<0.0001	-12.78 to 7.856	0.8932
2	c	TI	IgG1-11B8-E430G-S440K	FcyRIIIa H131 activity	Raji	3	9.01	0.98	80.66 to 101.3	<0.0001	-19.33 to 1.302	0.0904
2	c	TI	IgG1-Campath-E430G-K439E	FcyRIIIa H131 activity	Raji	2	19.87	7.01	69.80 to 90.44	<0.0001	-30.19 to -9.555	0.0008
2	c	NC	IgG1-b12	FcyRIIIa H131 activity	Raji	3	0.00	0.30	89.67 to 110.3	<0.0001		
2	d	PC	IgG1-Campath-E430G	FcyRIIIa V158 activity	Raji	3	99.99	2.33			-107.7 to -92.29	<0.0001
2	d	TI	IgG1-Campath-E430G-K439E	FcyRIIIa V158 activity	Raji	3	14.13	2.00	75.50 to 96.22	<0.0001	-21.84 to -6.428	0.0014
2	d	TI	IgG1-11B8-E430G-S440K	FcyRIIIa V158 activity	Raji	3	110.50	5.14	-20.87 to -0.1465	0.0468	-118.2 to -102.8	<0.0001
2	d	TI	IgG1-Campath-E430G-K439E	FcyRIIIa V158 activity	Raji	2	94.10	4.45	-2.721 to 14.51	0.2079	-102.7 to -85.49	<0.0001
2	d	NC	IgG1-b12	FcyRIIIa V158 activity	Raji	3	0.00	0.17	92.29 to 107.7	<0.0001		
3	b	PC	IgG1-Campath-E430G	ADCC	Wien-133	6	100.0	18.03			-117.9 to -82.06	<0.0001

Fig. Sub	Item <sup>1</sup>	Antibody component 1	Antibody component 2	Assay	Cells	N <sup>2</sup>	Mean rel. AUC (%) <sup>3</sup>	SD	95% CI of diff. to PC <sup>4</sup>	Adjusted P-value <sup>5</sup>	95% CI of diff. to NC <sup>6</sup>	Adjusted P-value <sup>7</sup>
3	b	TI	IgG1-Campath-RGE	ADCC	Wien-133	6	-2.90	5.40	84.95 to 120.8	<0.0001	-15.05 to 20.84	0.9910
3	b	TI	IgG1-11B8-AGK	ADCC	Wien-133	6	-3.44	5.31	85.50 to 121.4	<0.0001	-14.50 to 21.39	0.9805
3	b	TI	IgG1-Campath-RGE	ADCC	Wien-133	6	1.72	5.21	80.33 to 116.2	<0.0001	-19.67 to 16.22	0.9987
3	b	NC	IgG1-b12	ADCC	Wien-133	6	0.00	5.37	82.06 to 117.9	<0.0001		
3	c	PC	IgG1-Campath-E430G	ADCP	Raji	6	100.0	5.59			-106.5 to -93.54	<0.0001
3	c	TI	IgG1-Campath-RGE	ADCP	Raji	6	0.17	1.51	93.37 to 106.3	<0.0001	-6.628 to 6.291	>0.9999
3	c	TI	IgG1-11B8-AGK	ADCP	Raji	6	25.79	4.84	67.75 to 80.67	<0.0001	-32.25 to -19.33	<0.0001
3	c	TI	IgG1-Campath-RGE	ADCP	Raji	6	39.16	5.83	54.38 to 67.30	<0.0001	-45.62 to -32.70	<0.0001
3	c	NC	IgG1-b12	ADCP	Raji	6	0.00	1.05	93.54 to 106.5	<0.0001		
3	d	PC	IgG1-Campath	CDC	Wien-133	3	100.0	5.76			-113.7 to -86.29	<0.0001
3	d	TI	IgG1-Campath-E430G	CDC	Wien-133	3	276.92	12.83	-192.4 to -161.5	<0.0001	-290.6 to -263.2	<0.0001
3	d	TI	IgG1-Campath-RGE	CDC	Wien-133	3	-12.51	2.78	97.04 to 128.0	<0.0001	-1.207 to 26.22	0.0808
3	d	TI	IgG1-11B8-AGK	CDC	Wien-133	3	3.86	7.82	80.68 to 111.6	<0.0001	-17.57 to 9.857	0.9091
3	d	TI	IgG1-Campath-RGE	CDC	Wien-133	3	146.83	3.01	-62.29 to -31.36	<0.0001	-160.5 to -133.1	<0.0001
3	d	NC	IgG1-b12	CDC	Wien-133	6	0.00	5.17	86.61 to 113.4	<0.0001		
5	c	PC	Tit IgG1-Campath-RGE	CDC	Wien-133	3	100.0	2.91			ND	ND
5	c	TI	Tit IgG1-Campath-RGE	CDC	Wien-133	3	141.7	4.24	-50.01 to -33.39	<0.0001	ND	ND
5	c	TI	20 µg/mL IgG1-Campath-RGE	CDC	Wien-133	3	122.00	3.38	-30.31 to -13.70	0.0005	ND	ND
6	a	PC	IgG1-37.3-E430G	CDC	Raji	3	100.0	3.69			-107.1 to -92.91	<0.0001
6	a	TI	IgG1-37.3-RGE	CDC	Raji	3	7.33	1.70	85.58 to 99.77	<0.0001	-14.42 to -0.2342	0.0428
6	a	TI	IgG1-11B8-AGK	CDC	Raji	3	4.26	1.60	88.65 to 102.8	<0.0001	-11.35 to 2.839	0.3028
6	a	TI	IgG1-37.3-RGE	CDC	Raji	3	62.18	4.97	30.73 to 44.92	<0.0001	-69.27 to -55.08	<0.0001
6	a	NC	IgG1-b12	CDC	Raji	3	0.00	1.18	92.91 to 107.1	<0.0001		
6	c	PC	IgG1-DR5-01-E430G	Apoptosis	COLO-205	3	100.0	2.38			-107.2 to -92.75	<0.0001
6	c	TI	IgG1-DR5-01-RGE	Apoptosis	COLO-205	3	10.57	2.94	82.18 to 96.67	<0.0001	-17.82 to -3.325	0.0059

Fig.	Sub	Item <sup>1</sup>	Antibody component 1	Antibody component 2	Assay	Cells	N <sup>2</sup>	Mean rel. AUC (%) <sup>3</sup>	SD	95% CI of diff. to PC <sup>4</sup>	Adjusted P-value <sup>5</sup>	95% CI of diff. to NC <sup>6</sup>	Adjusted P-value <sup>7</sup>
6	c	TI	IgG1-DR5-05-AGK	IgG1-b12	Apoptosis	COLO-205	3	6.19	2.50	86.56 to 101.1	<0.0001	-13.44 to 1.056	0.0990
6	c	TI	IgG1-DR5-01-RGE	IgG1-DR5-05-AGK	Apoptosis	COLO-205	3	86.02	4.87	6.733 to 21.23	0.0008	-93.27 to -78.77	<0.0001
6	c	NC	IgG1-b12	IgG1-b12	Apoptosis	COLO-205	3	0.00	1.70	92.75 to 107.2	<0.0001		
6	c	PC	IgG1-DR5-01-E430G	IgG1-DR5-05-E430G	Apoptosis	BxPC-3	3	100.0	8.60			-113.1 to -86.91	<0.0001
6	c	TI	IgG1-DR5-01-RGE	IgG1-b12	Apoptosis	BxPC-3	3	2.21	3.73	84.71 to 110.9	<0.0001	-15.29 to 10.88	0.9647
6	c	TI	IgG1-DR5-05-AGK	IgG1-b12	Apoptosis	BxPC-3	3	-10.72	2.66	97.63 to 123.8	<0.0001	-2.369 to 23.80	0.1164
6	c	TI	IgG1-DR5-01-RGE	IgG1-DR5-05-AGK	Apoptosis	BxPC-3	3	80.08	7.11	6.831 to 33.00	0.0045	-93.17 to -67.00	<0.0001
6	c	NC	IgG1-b12	IgG1-b12	Apoptosis	BxPC-3	3	0.00	2.88	86.91 to 113.1	<0.0001		
S2	a	PC	IgG1-Campath-E430G	IgG1-11B8-E430G	CDC	Wien-133	3	100.0	4.63			-105.5 to -94.52	<0.0001
S2	a	TI	IgG1-Campath-E430G	IgG1-b12	CDC	Wien-133	3	90.58	5.76	2.705 to 16.13	0.0039	-97.30 to -83.87	<0.0001
S2	a	TI	IgG1-11B8-E430G	IgG1-b12	CDC	Wien-133	3	15.03	2.90	78.26 to 91.68	<0.0001	-21.74 to -8.319	<0.0001
S2	a	TI	IgG1-Campath	IgG1-b12	CDC	Wien-133	3	25.79	0.81	67.50 to 80.92	<0.0001	-32.50 to -19.08	<0.0001
S2	a	TI	IgG1-11B8	IgG1-b12	CDC	Wien-133	3	-1.41	1.44	94.70 to 108.1	<0.0001	-5.299 to 8.124	0.9839
S2	a	TI	IgG1-Campath	IgG1-11B8	CDC	Wien-133	3	36.11	2.08	57.18 to 70.60	<0.0001	-42.82 to -29.40	<0.0001
S2	a	NC	IgG1-b12	IgG1-b12	CDC	Wien-133		0.00	1.87	94.52 to 105.5	<0.0001		
S2	b	PC	IgG1-Campath-E430G	x	CDC	Wien-133	3	100.0	2.77			-105.1 to -94.89	<0.0001
S2	b	TI	IgG1-Campath-E430G-K439E	x	CDC	Wien-133	3	40.63	1.59	55.19 to 63.54	<0.0001	-44.81 to -36.46	<0.0001
S2	b	TI	IgG1-Campath	x	CDC	Wien-133	3	43.84	2.01	51.05 to 61.27	<0.0001	-48.95 to -38.73	<0.0001
S2	b	TI	IgG1-Campath-K439E	x	CDC	Wien-133	3	0.76	1.03	94.13 to 104.3	<0.0001	-5.872 to 4.348	0.9722
S2	b	NC	IgG1-b12	x	CDC	Wien-133	3	0.00	1.45	94.89 to 105.1	<0.0001		
S3	PC		IgG1-Campath-E430G	x	CDC	Wien-133	3	100.0	1.22			ND	ND
S3	TI		IgG1-Campath	x	CDC	Wien-133	3	39.06	1.02	59.43 to 64.92	<0.0001	ND	ND
S3	TI		IgG1-Campath-G237A-E430G	x	CDC	Wien-133	3	74.06	1.08	-0.2705 to 5.211	0.0763	ND	ND
S3	TI		IgG1-Campath-G236R-E430G	x	CDC	Wien-133	3	98.76	0.47	24.43 to 29.92	<0.0001	ND	ND
S4	PC		IgG1-Campath-E430G	IgG1-11B8-E430G	FcyRIIa H131 activity	Raji	3	99.99	6.71			-107.2 to -92.81	<0.0001

Fig. Sub	Item <sup>1</sup>	Antibody component 1	Antibody component 2	Assay	Cells	N <sup>2</sup>	Mean rel. AUC (%) <sup>3</sup>	SD	95% CI of diff. to PC <sup>4</sup>	Adjusted P-value <sup>5</sup>	95% CI of diff. to NC <sup>6</sup>	Adjusted P-value <sup>7</sup>
S4	TI	IgG1-Campath-RGE	IgG1-b12	FcyRIIIa HI131 activity	Raji	3	0.01	0.58	92.80 to 107.2	<0.0001	-7.188 to 7.173	>0.9999
S4	TI	IgG1-11B8-AGK	IgG1-b12	FcyRIIIa HI131 activity	Raji	3	-0.27	0.33	93.08 to 107.4	<0.0001	-6.917 to 7.445	0.9999
S4	TI	IgG1-Campath-RGE	IgG1-11B8-AGK	FcyRIIIa HI131 activity	Raji	3	1.20	0.82	91.61 to 106.0	<0.0001	-8.386 to 5.976	0.9652
S4	NC	IgG1-b12	IgG1-b12	FcyRIIIa HI131 activity	Raji	3	0.00	0.30	92.81 to 107.2	<0.0001		
S4	PC	IgG1-Campath-E430G	IgG1-11B8-E430G	FcyRIIIa V158 activity	Raji	3	99.99	2.33			-102.7 to -97.30	<0.0001
S4	TI	IgG1-Campath-RGE	IgG1-b12	FcyRIIIa V158 activity	Raji	3	1.03	0.98	96.27 to 101.7	<0.0001	-3.726 to 1.659	0.6487
S4	TI	IgG1-11B8-AGK	IgG1-b12	FcyRIIIa V158 activity	Raji	3	0.01	0.24	97.29 to 102.7	<0.0001	-2.701 to 2.683	>0.9999
S4	TI	IgG1-Campath-RGE	IgG1-11B8-AGK	FcyRIIIa V158 activity	Raji	3	0.17	0.16	97.13 to 102.5	<0.0001	-2.863 to 2.521	0.9990
S4	NC	IgG1-b12	IgG1-b12	FcyRIIIa V158 activity	Raji	3	0.00	0.17	97.30 to 102.7	<0.0001		
S5 <sup>8</sup>	PC	IgG1-Campath	IgG1-11B8	C1q binding	Wien-133	6	100.0	41.07			-10.43 to -0.7746	0.0132
S5	TI	IgG1-Campath-E430G	IgG1-11B8-E430G	C1q binding	Wien-133	6	1859	87.50	-108.2 to -88.82	<0.0001	-114.4 to -93.85	<0.0001
S5	TI	IgG1-Campath-RGE	IgG1-b12	C1q binding	Wien-133	6	8.93	5.36	0.2520 to 9.948	0.0202	-1.092 to 0.09230	0.0629
S5	TI	IgG1-11B8-E430G-S440K	IgG1-b12	C1q binding	Wien-133	6	16.07	5.36	-0.1480 to 9.548	0.0284	-1.492 to -0.3077	0.0016
S5	TI	IgG1-11B8-AGK	IgG1-b12	C1q binding	Wien-133	6	5.36	3.57	0.4746 to 10.13	0.0168	-0.7511 to 0.1511	0.1945
S5	TI	IgG1-Campath-RGE	IgG1-11B8-E430G-S440K	C1q binding	Wien-133	6	287.5	39.29	-15.58 to -5.424	<0.0001	-20.72 to -11.48	<0.0001
S5	TI	IgG1-Campath-RGE	IgG1-11B8-AGK	C1q binding	Wien-133	6	92.86	19.64	-4.160 to 4.960	>0.9999	-7.537 to -2.863	0.0007
S5	NC	IgG1-b12	IgG1-b12	C1q binding	Wien-133	6	0.00	3.57	0.7746 to 10.43	0.0132		
S6	PC	IgG1-DR5-01-E430G	IgG1-DR5-05-E430G	Apoptosis	BxPC-3	3	100.0	1.10			-105.5 to -94.46	<0.0001

Fig. Sub	Item <sup>1</sup>	Antibody component 1	Antibody component 2	Assay	Cells	N <sup>2</sup>	Mean rel. AUC (%) <sup>3</sup>	SD	95% CI of diff. to PC <sup>4</sup>	Adjusted P-value <sup>5</sup>	95% CI of diff. to NC <sup>6</sup>	Adjusted P-value <sup>7</sup>
S6	TI	IgG1-DR5-01	IgG1-DR5-05	Apoptosis	BxPC-3	3	55.13	3.64	39.33 to 50.41	<0.0001	-60.67 to -49.59	<0.0001
S6	NC	IgG1-b12	IgG1-b12	Apoptosis	BxPC-3	3	0.00	1.55	94.46 to 105.5	<0.0001		
S6	PC	IgG1-DR5-01-E430G	IgG1-DR5-05-E430G	Apoptosis	COLO-205	3	100.0	4.67			-111.6 to -88.39	<0.0001
S6	TI	IgG1-DR5-01	IgG1-DR5-05	Apoptosis	COLO-205	3	5.51	4.91	82.88 to 106.1	<0.0001	-17.12 to 6.105	0.3561
S6	NC	IgG1-b12	IgG1-b12	Apoptosis	COLO-205	3	0.00	5.31	88.39 to 111.6	<0.0001		

1 Items: positive control (PC), negative control (NC) or test item (TI) used in comparisons.

2 Number of independent experimental repeats, performed on separate days, using independently prepared antibody mixtures.

3 Dose-response data from multiple experimental repeats were pooled, concentrations were log-transformed and the resulting AUC values were normalized relative to the positive control indicated in grey (100%) and negative control non-binding antibody IgG1-b12 (0%).

4 95% confidence interval of the difference between measured value (test item) and value measured for positive control antibody or antibody mixture.

5 Adjusted p-value of one-way ANOVA analysis of difference between test item and positive control using Dunnett's multiple comparisons test. Analyses were performed using GraphPad Prism release 8.4.1.

6 95% confidence interval of the difference between test item and negative control values.

7 Adjusted P-value calculated as described \*5, here for the difference between test item and negative control values. ND: not determined.

8 Dunnett's T3 multiple comparisons test was used to address the different standard deviations between groups.

**Supplementary Table 4**

**Statistical analysis of Pharmacokinetics data**

Fig.	Sub	Item <sup>1</sup>	Antibody component 1	Antibody component 2	Assay	Cells	N <sup>2</sup>	Clearance rate <sup>3</sup>	SD	95% CI of diff. to PC <sup>3</sup>	Adjusted P-value <sup>4</sup>
3	e	PC	IgG1-Campath	-	PK	N/A	3	28.8	6.7		
3	e	TI	IgG1-Campath-RGE	-	PK	N/A	3	34.6	7.3	-16.99 to 5.393	0.5862
3	e	PC	IgG1-11B8	-	PK	N/A	3	14	1.1		
3	e	TI	IgG1-11B8-AGK	-	PK	N/A	3	10.8	0.9	-14.39 to 7.993	0.9513
3	e	PC	IgG1-Campath	IgG1-11B8	PK	N/A	3	11.9	1.5		
3	e	TI	IgG1-Campath-RGE	IgG1-11B8-AGK	PK	N/A	3	11.8	1.9	-11.09 to 11.29	>0.9999

1 Items: positive control (PC) or test item (TI) used in comparisons.

2 Number of mice.

3 Clearance of a single antibody dose (500 µg) was monitored for three weeks and is expressed as Dose (D)\*1000/area under the curve (ml/day/kg).

4 95% confidence interval of the difference between measured value (test item) and value measured for positive control antibody or antibody mixture.

5 Adjusted p-value of one-way ANOVA analysis of difference between test items and positive controls using Tukey's multiple comparisons test.





# 6

## AVIDITY IN ANTIBODY EFFECTOR FUNCTIONS AND BIOTHERAPEUTIC DRUG DESIGN

Simone C. Oostindie<sup>1,2</sup>, Greg A. Lazar<sup>3</sup>, Janine Schuurman<sup>1</sup> and Paul W.H.I. Parren<sup>2,4,\*</sup>

Submitted for publication.

1 Genmab, Utrecht, Netherlands

2 Department of Immunology, Leiden University Medical Center, Leiden, Netherlands

3 Department of Antibody Engineering, Genentech, Inc., South San Francisco, California, USA

4 Lava Therapeutics, Utrecht, Netherlands

\* Corresponding author

**Correspondence**

Paul W.H.I. Parren (p.parren@lavatherapeutics.com)

## ABSTRACT

Antibodies, the cardinal effector molecules of the immune system, are being leveraged to enormous success as biotherapeutic drugs. Adaptive immune responses consist of epitope-diverse polyclonal antibody mixtures that are capable of neutralizing their targets via binding interference and by mediating humoral and cellular effector functions. A mechanistic theme fundamental to virtually all aspects of antibody biology, including binding strength, clonal selection and downstream effects, is the utilization of avidity to drive and tune responses beyond a physiological threshold. This principle also underlies the mechanisms of action of many successful antibody drug regimens, and forms an important design principle for the engineering of enhanced and novel properties in next generation biotherapeutics with leapfrog potential. Here we describe the conglomerate of avidity interactions as a central trigger for overall efficacy of functional responses both in natural antibody biology and their therapeutic application. Within this framework, we comprehensively review therapeutic antibody mechanisms of action, with particular emphasis on engineered optimizations and platforms. We describe how affinity- and avidity- tuning of engineered immunoglobulin architectures are enabling a new wave of differentiated antibody drugs with tailored properties and novel functions, marshalling the promise of an ever-more optimal fit for treating a wide variety of diseases.

# INTRODUCTION

Antibodies are critical components in the humoral adaptive immune response against disease-causing molecules, viruses and cells by flagging them for destruction. Upon exposure to foreign antigen, the immune system mounts a genetically diverse polyclonal response comprising antibodies that recognize multiple (non-)overlapping antigenic epitopes. While these initial antibodies have low binding affinities, activated antibody-producing B cells undergo a conserved affinity maturation process through somatic hyper mutation and clonal selection, thereby successively generating antibodies with greater affinities<sup>1-3</sup>. Target neutralization and elimination is subsequently triggered via multiple tightly regulated processes including protein- and cellular-mediated effector functions.

The development of the hybridoma technology by Köhler and Milstein enabled the stable generation of monoclonal antibodies of defined specificity, hallmarking a new era of antibody-based drug discovery<sup>4</sup>. Owing to their superb specificity, modular and highly adaptable architecture, favorable pharmacokinetic properties and standardizable drug development, antibodies have since grown into an established and exceptionally versatile class of therapeutic agents for treating a wide spectrum of human diseases. The ascendance and impact of antibody-based therapeutics is evidenced by over 100 granted marketing approvals in Europe and US to date, and more than 600 antibody-based therapeutics at various stages of clinical development<sup>5,6</sup>. Building on this success there is a continued search for next-generation antibody-based therapeutics, fueled by progressive mechanistic insights in both correlates of efficacy as well as emerging limitations of contemporary targeted therapies such as disease heterogeneity, plasticity and refractoriness. Indeed, the rise of diverse innovative antibody formats including bi- and multispecifics, tailored Fc-mediated effector functions, diverse isotypes and fragments, and payload delivery of small molecules or bioactive fusion proteins is steering the antibody landscape towards more tailored drug design<sup>7-11</sup>. Emerging developments in immune-oncology furthermore are demonstrating the revolutionary potential of therapeutic antibodies to transmogrify patients' immune systems and achieve long-term protection against disease. Understanding the multidimensional design principles to generate antibody therapeutics that optimally fit the intended target biology and effectively achieve the envisioned mechanistic objectives remain one of the key challenges in drug discovery.

While many factors contribute to the success of antibody-based treatment, central to their pharmacologic mechanism are the interactions with their targets, and more specifically the affinity and avidity of binding interactions<sup>7,12</sup>. Avidity, defined herein as the accumulated binding strength of multiple affinities derived from individual non-covalent interactions, is fundamental to virtually all aspects of antibody biology. The neutralization of soluble proteins such as toxins or cytokines based on single binding interactions display a limited potency ceiling, which may be surpassed by orders of magnitude in antibody combinations<sup>13,14</sup>. Furthermore, it is generally understood that singular antibody-antigen binding interactions alone are insufficient to achieve successful neutralization or effector function activity for eliminating pathogens or diseased cells<sup>15-18</sup>. Considerable evidence suggests that antibody-based effector functions are triggered by multivalent target binding and clustering of IgG molecules on the cell surface<sup>18-22</sup>. Avidity-driven surface clustering of IgG molecules can be interpreted to serve as a threshold for effector function activation, by providing an “avid docking surface” for the subsequent binding and activation of immune effector molecules. In this review, we describe recent advances in understanding the contribution of avidity interactions to both natural- and therapeutic antibody-based mechanisms of action. The unifying thread is the fundamental role of avidity in determining the quality or “impact” of antibody functional responses. Special emphasis is placed on engineering strategies and platforms that utilize avidity tuning to boost therapeutic activity, including classical effector functions as well as novel engineered mechanisms of action. Within this conceptual framework we also discuss current translational efforts regarding avidity-based antibody concepts in the clinic and provide future perspectives that we believe will aid the development of the next wave of differentiated biotherapeutics that may leapfrog contemporary approaches.

# THE ROLE OF AVIDITY IN ANTIBODY BIOLOGY

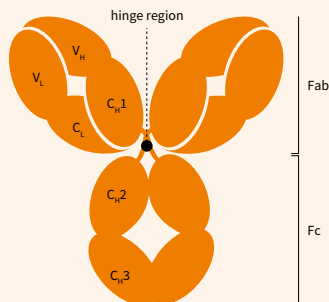
## Antibody functional responses

Antibody or immunoglobulin (Ig) function is characterized by three distinct regions of the Ig molecule (Box 1): a fragment antigen-binding (Fab) region defining target specificity and affinity, a fragment crystallizable (Fc) region that interacts with immune effector molecules, and a hinge region linking the Fab and Fc. The iconic Y-shaped IgG structure solved in 1963 provided a first view of the bivalency of the molecule and functional implications for multivalency<sup>23,24</sup>. Two Fab fragments are connected to the Fc by a hinge region, which flexibly links interactions with antigen effector molecules. The strength of a single binding interaction between an antibody Fab fragment and antigen is defined by the term *affinity*. In biology, functional interactions are often not only dependent on affinity, but also on *avidity*. Avidity is defined as the increase in binding strength that results from multivalent interactions, which for antibodies may occur upon binding to antigens on the surface of cells or pathogens, interaction with effector molecules, or cooperation in polyclonal responses<sup>25</sup>.

The importance of affinity and avidity to antibody-antigen recognition in both natural immunity and therapeutic application has long been recognized<sup>12,25,26</sup>. The primary mechanism by which antibodies combat infection is through binding and direct neutralization of a target on a pathogen. Antibody Fab arms bind specific pathogen structures or antigens, thereby preventing interactions with host cell receptors and blocking their functionality such as viral entry into a cell. Already in 1937, Burnet and colleagues recognized that a single antibody binding event was likely insufficient to inactivate viruses and argued that neutralization occurs through multivalent antibody binding to a significant proportion of viral epitopes<sup>27</sup>. It is this polyclonal immune complexation, rather than single molecular binding events, that is the central trigger for downstream humoral and cellular responses. Importantly, antibodies are not merely antigen binding molecules, as their Fc domain allows for interactions with multiple immune effector molecules present in human plasma or expressed on immune cells. Classical antibody Fc-mediated effector mechanisms such as complement-dependent cytotoxicity (CDC), antibody-dependent cellular cytotoxicity (ADCC) and antibody-dependent cellular phagocytosis (ADCP) are key mechanisms for the elimination of pathogens or diseased cells such as infected or cancerous cells. As with immune complexation, a single binding interaction between antibody and antigen is generally not sufficient to induce an effective Fc-mediated cellular response. Altogether,

## Human immunoglobulin architecture.

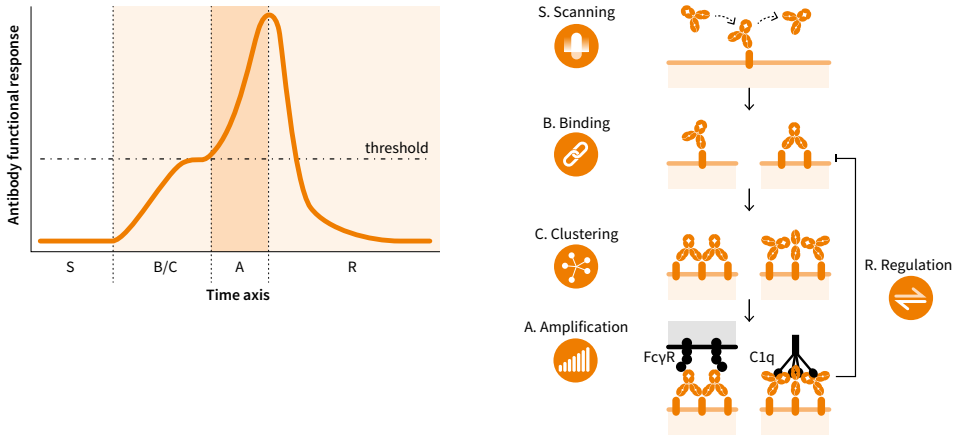
Human immunoglobulins (Igs) consist of three distinct regions including an antigen-binding fragment (Fab) region that binds antigen, a crystallizable fragment (Fc) region that interacts with immune effector molecules and a hinge region that links the Fab to the Fc and defines conformational flexibility. A monomeric Ig molecule is Y-shaped and usually composed of four distinct protein chains including two identical heavy- and light chains (HC and LC). The HC is comprised of three or four generic constant domains ( $C_H$ ), depending on the antibody isotype, while the LC contains a single constant domain ( $C_L$ ). The constant domains together form the Fc-, hinge- and base of the Fab region. The Fab region comprises the variable domains which determine antigen binding specificity and affinity. Disulfide bonds shape the overall quaternary structure of the molecule, by linking the two HC in the hinge region as well as the HC and LC in the Fab region. In humans, variations in the HC constant domain during an immune response generates five different isotypes; IgM, IgD, IgG, IgA and IgE. IgG and IgA can be further subdivided into subclasses 1-4 and 1-2 respectively. Whilst IgG, IgD and IgE exist as monomers, IgA and IgM may contain an additional polypeptide J-chain that allows the formation of dimers and pentamers respectively. A small fraction of IgM antibodies exist as hexamers in which the J-chain protein is exchanged by an extra monomer subunit. IgA may further contain a secretory component that provides protection against proteolytic degradation. The  $C_H$  domains of IgG interact with the neonatal Fc receptor (FcRn) which protects from catabolism and thereby substantially increases IgG plasma half-life. Ig isotypes and subclasses can further be distinguished by variation in the hinge length, the number and location of disulfide bridges and *N*- or *O*-linked glycosylation within the HC. The hinge region serves not only as a connector but also modulates to effector function potency. The hinge region therefore represents a third functional domain; indeed modification of the hinge length and flexibility has allowed for fine tuning of IgG effector activity<sup>157</sup>. Together, changes in antibody valency, hinge length and flexibility and glycosylation status can influence avidity interactions and overall functional response kinetics.



through high avidity binding interactions via both Fab and Fc and with the hinge in a modulatory role, antibodies constitute a remarkably sensitive adaptor system that enables rapid initiation and amplification of different effector mechanisms in combatting human disease.

In our view, response kinetics and thresholds governing antibody function can be described in terms that are generally observed in many biological systems that integrate input, output and feedback (Figure 1). We distinguish five distinct activation phases that include a scanning, binding, clustering, amplification and regulation phase. Antibody binding to antigen is a reversible process that follows the law of mass action and is highly dependent on the affinity of antibody for its target. Association and dissociation constants determine the on- and off-rate of binding kinetics at equilibrium (S – scanning phase). Thus, antibody-antigen complex formation is favored when the on-rate is faster than the off-rate (B – binding phase). Subsequently, tethering of multiple Fab arms to antigens on the cell surface enhances the overall strength or avidity of binding (C – clustering phase). The overall avidity sum of these interactions is defined by the intrinsic affinity, valency, flexibility and structural arrangement of proteins in the complex. Antibody-antigen clustering consequently provides an avid docking surface for Fc-mediated binding and clustering of immune effector molecules, thereby triggering potent activation of the functional response (A – amplification phase). However, conditions to reach the threshold before response amplification may vary per effector mechanism. For instance, different types of effector mechanisms might require different antibody concentrations to reach the maximal effect as they operate at distinct target occupancy ratios (Figure 2A)<sup>28</sup>. Similarly, other parameters such as antigen expression and distribution, the presence of systemic effector elements or different Ig subclasses and expression of inhibitory receptors can all impact the overall avidity of antibody interactions and consequent amplification of a functional response (Figure 2B)<sup>29,30</sup>. We propose that all these parameters combine into one overall “impact factor”, illustrated by  $D_i$ , which can be used to describe the quality of an antibody functional response. Finally, negative feedback occurs when the output of a system acts to reduce or dampen the response amplification (R – regulation phase; Figure 1). After amplification of the antibody functional response, regulation can be induced by target-related outputs such as elimination of target cells, target density dropping below the amplification threshold or regulatory molecules expressed on the target cell or recruited from plasma. Similarly, systemic regulation can occur when there is a shortage of effector molecules or cells, or by interfering Ig subclasses<sup>31-33</sup>. Although not the focus of this review, insufficient regulation may conversely cause an antibody functional response to become pathogenic through excessive and/or constitutive activation.

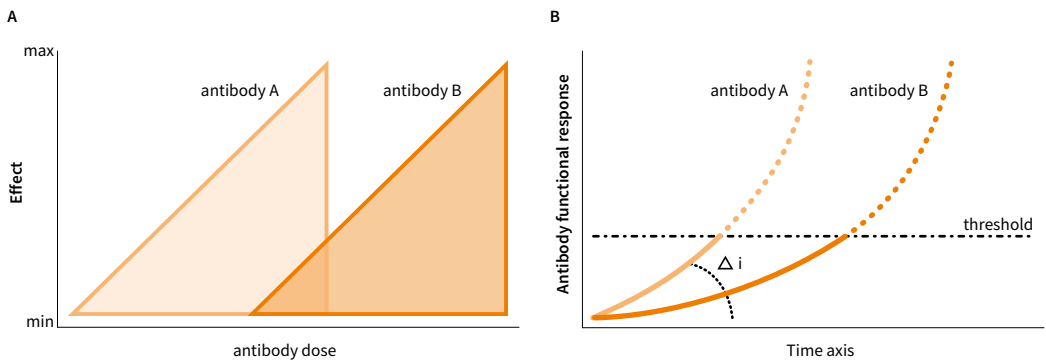




▲ **Figure 1**

**Response kinetics governing antibody function.**

The kinetics of antibody functional response activation are distinguished by five different phases integrating common biological mechanisms of input, output and feedback. **(S)** Scanning phase: association and dissociation constants determine the on- and off-rate of antibody binding kinetics at equilibrium. **(B)** Binding phase: monovalent or bivalent antibody-antigen complex formation is favored when the on-rate is faster than the off-rate. **(C)** Clustering phase: tethering of multiple Fab arms to antigens on the cell surface enhances the overall binding avidity. **(A)** Amplification phase: antibody-antigen clustering provides an avid docking surface for Fc-mediated binding of soluble or cell-bound immune effector molecules, thereby surpassing a threshold and triggering potent activation of the functional response. **(R)** Regulation phase: antibody functional response amplification may be regulated or dampened by for example elimination of target cells, target density dropping below the amplification threshold or regulatory molecules either expressed on the target cell or recruited from plasma.



▲ **Figure 2**

**Factors impacting antibody functional response activation**

**(A)** Schematic representation of dose-effect relationships for antibodies with different effector mechanisms. Antibody A may require different antibody concentrations to reach the maximal effect compared to antibody B, as both operate at distinct target occupancy ratios. **(B)** Schematic representation of how conditions to reach the threshold before antibody functional response amplification may vary per effector mechanism. Such varying conditions may be defined by different parameters including; (1) antibody dose (A), affinity and valency, (2) antigen expression and distribution, (3) type and presence of systemic effector elements and (4) presence of regulatory molecules expressed on the target cell or recruited from plasma. All these parameters combine into one overall “impact factor”, illustrated by  $\Delta i$ , which could be used to describe the quality of an antibody functional response. Note that the example is not intended to imply that antibody B is necessarily ‘worse’ than antibody A. Depending on the intended use, it may be required to tune a functional response, e.g. to retain activity against target cells while minimizing activity against normal cells expressing the target antigen.

The quality and impact of antibody functional responses is therefore dependent on multidimensional effects anchored in avidity-based interactions between antibodies, antigens and effector molecules. How these interactions orchestrate both natural, autoimmune and therapeutic antibody mechanisms of action is detailed and discussed in the following subsections of this review. Furthermore, we discuss how avidity tuning may serve as a basic engineering principle for optimizing the  $\Delta i$  and thereby the functional response of antibody-based therapeutics.

### **The humoral adaptive immune response**

The humoral adaptive immune response does not consist of a single species of antibody, but instead comprises a complex polyclonal mixture of multiple antibodies directed towards diverse immunogenic epitopes that change and accumulate over time. The huge potential and versatility of this response is illustrated by the projection that humans may produce a quintillion ( $10^{15}$ ) different antibodies<sup>34</sup>. The role of avidity in humoral immunity is already evident early in the initiation of the immune response, both in the context of triggering antibody production by B cells as well as in their maturation. Upon entry of foreign antigens into lymphoid tissues, naïve B-cells present in lymph node follicles are activated through antigen binding to their B-cell receptors (BCRs, Box 2). BCRs expressed on mature B cells are integral membrane Ig molecules that are activated following antigen-induced aggregation (Figure 1, binding/clustering phase, Figure 3A)<sup>35</sup>. Furthermore, while several different models have been proposed for BCR activation, considerable evidence suggests that BCRs display activation-dependent localization into membrane micro domains, likely facilitating higher order BCR clustering and signal transduction<sup>36,37</sup>. Upon activation, some IgM<sup>+</sup> B cells become plasma cells in which IgM expression through alternative RNA processing switches from being primarily membrane-associated to being abundantly secreted (Box 2)<sup>38</sup>. Secreted IgM antibodies are predominantly pentameric molecules (hexameric molecules comprise <5% of serum IgM<sup>39,40</sup>) that, despite binding with characteristically low intrinsic affinity ( $K_a$   $10^4$ – $10^6$  [mol/L]<sup>-1</sup>), are able to avidly engage immunogens due to their 10 identical epitope binding sites and high conformational flexibility<sup>41</sup>. As discussed further in a later section, IgM antibodies are especially effective in protection against microbes with highly expressed, closely spaced surface epitopes, a consequence in part of efficient avidity-based interactions between IgM and the complement system. Other activated IgM<sup>+</sup> B cells undergo rapid proliferation aided by additional stimuli provided by T cells, thereby triggering the activation-induced deaminase (AID) enzyme that mediates somatic hypermutation (SHM)<sup>42</sup>. B-cell clones producing higher affinity BCRs are consequently favored in a Darwinian competition for antigens and T-cell help that drive B-cell clonal selection and affinity maturation, resulting in an increase in intrinsic affinity up to  $10^{10}$  [mol/L]<sup>-1</sup><sup>43,44</sup>. Addition-

## Human immunoglobulin functional properties

### B-cell receptor

Each of the Ig (sub)classes may be expressed in monomeric form with an integral membrane domain to form the B-cell receptor (BCR) on a B cell's surface.

Expression of membrane versus secreted form is regulated by alternative RNA processing. Secreted Ig is identical in sequence to the BCR except for the absence of the transmembrane region and potential post-translational modifications or quaternary structures as discussed below.

*IgM*: Secretory IgM largely exists as pentamers linked together by disulfide bonds and a polypeptide J-chain, while a small fraction exists as a covalent IgM hexamer in absence of J-chain. Owing to their structural and functional differences, pentameric and hexameric IgM might be viewed as distinct IgM subclasses<sup>64</sup>. Studies have shown that both pentameric and hexameric IgM adopt a hexagonal platform conformation supporting high avidity binding interactions with C1q and efficient complement activation<sup>178,179</sup>.

### IgG

IgG is most abundant in human serum and accounts for about 10-20% of plasma protein. The four different subclasses in order of decreasing abundance are named IgG1, IgG2, IgG3 and IgG4. Each subclass contains a unique profile with respect to antigen-, complement- and FcγR binding. Structural determinants in the middle or “core” hinge region in particular can influence antibody function. For example, modification of glycan N297 impacts FcγR binding, while increasing hinge length and flexibility enhances binding to antigen and immune complex formation as well as binding to complement component C1q<sup>95,157,180</sup>. The flexibility of the Fab arms impacts the relative binding of subclasses to FcγRs and C1q and is ranked as: IgG3 > IgG1 > IgG4 > IgG2.

### IgD

IgD is primarily expressed as a transmembrane antigen receptor on naïve mature B cells. IgD possesses a long hinge region with high flexibility and is thereby capable of acquiring a T-shaped structure. This structural flexibility was suggested to potentially contribute to the regulation of B-cell responsiveness to different types of antigens due to preferential binding of IgD to multimeric rather than monomeric antigens<sup>181,182</sup>. Secreted IgD weakly interacts with complement or FcδRs, but binds basophils, mast cells, monocytes and dendritic cells in an FcδR-independent manner, thereby contributing to mucosal homeostasis through the production of antimicrobial peptides and inflammatory cytokines.

## IgA

IgA has two subclasses, IgA1 and IgA2, which are distinguished by a heavily glycosylated T-shaped hinge and a more rigid Y-shaped hinge respectively. IgA exists in monomeric- and dimeric (monomers linked by a polypeptide J-chain and a secretory component) form. Monomeric IgA is abundantly present in serum, while dimeric IgA (secretory IgA) is mainly found in secretions lining the mucosal surfaces. IgA immune complexes efficiently interact with FcαRI on myeloid cells including neutrophils and macrophages<sup>183</sup>.

## IgE

IgE is the least abundant and fastest clearing (half-life <1 day versus ~3 weeks for IgG) isotype in human plasma. While IgE does not activate complement, it potently binds to the high-affinity FcεRI on mast cells. IgE glycosylation is essential for IgE-FcεRI interactions and this requirement is primarily attributed to one of seven N-linked glycan sites (N394)<sup>184</sup>. IgE can remain bound to FcεRI for weeks to months, thereby contributing to a long tissue half-life<sup>185</sup>.

ally, AID facilitates class- or isotype switching from IgM to IgG1-4, IgA1-2 or IgE that results in changes in the antibody Fc domain and associated effector function properties such as complement fixation and Fc receptor (FcR) binding. Through these processes, the adaptive immune system generates a highly diverse pool of antibodies capable of effectively recognizing and eliminating antigens and associated pathogens or diseased cells. Conversely, as typical in any biological system, B-cell activation is subject to physiological control mechanisms via Fc-mediated antibody feedback. Secreted antibodies inhibit B-cell activation by forming antibody-antigen immune complexes that, in the context of interaction with membrane Ig (through antigen), co-engage the inhibitory FcγRIIb (through the antibody's Fc). Simultaneous ligation of both the BCR and FcγRIIb results in inhibition of BCR complex signaling through phosphatases associated with the cytoplasmic tail of FcγRIIb (Figure 1, regulation phase)<sup>35,45,46</sup>. Overall, the BCR diversification that is triggered by antigen exposure is highly conserved over 200 million years of evolution, which despite mechanistic differences in the generation of repertoire diversity (e.g. through combinatorial rearrangements versus gene conversion) follows similar principles in all vertebrates, illustrating the crucial role of affinity and avidity-based antibody interactions in adaptive immunity<sup>1,47,48</sup>.

### **Antibody-mediated effector functions**

An antibody-mediated immune response is a culmination of effector functions mediated through both the Fab- and the Fc domain. How antigen binding by the Fab domain translates into Fc-mediated activation of effector functions has been an active area of research for many years. In addition to Fab-me-

diated neutralization of pathogen-host interactions, the Fc domain recruits serum complement component C1q and binds FcRs on innate immune cells to induce cytotoxicity, phagocytosis, and immune cell activation including cytokine release. While the processes of antigen binding by the Fab domain and effector function activation by the Fc domain have long been thought to act independently, multiple studies have challenged this view, and an optimal configuration of immune complexes likely exists for different types of effector functions. The antigen:antibody ratio greatly influences immune complex size, where antibody shortage or excess can reduce FcR-mediated effector potency due to suboptimal clustering or self-competition, also referred to as a hook or prozone effect<sup>49</sup>. In addition to the associative cooperativity observed in effector function activation by IgGs, there is also accumulating evidence for allosteric or intramolecular cooperativity<sup>30</sup>. For example, the optimal immune complex stoichiometry required for complement activation may be facilitated by IgG Fc-Fc interactions and stabilized by the associated Fab domains<sup>50,51</sup>. Fab and Fc function may even be considered interdependent, as efficient effector function activation requires clustering of cell-bound IgGs through both Fab-Fab and Fc-Fc interactions, thereby forming optimal docking sites for recruitment of C1q and crosslinking of FcRs on innate immune cells. Thus, knowledge of how antibody structure impacts function is crucial for understanding different antibody-mediated effector mechanisms, as further discussed individually in the following subsections.

### Neutralization

Fab domain-mediated neutralization is the simplest form of pathogen, toxin or self-antigen inactivation. Binding of the Fab domain to specific pathogenic structures prevents interactions with host cells, thereby blocking toxin activity or viral entry into the cell (Figure 3B). While the role of avidity in antibody-mediated neutralization of toxins and viruses has long been recognized, its crucial importance is exemplified by human immunodeficiency virus type 1 (HIV-1) that escapes neutralizing antibodies not only by its rapid mutation rate and shielding of conserved epitopes on the spike trimer, but also by impeding bivalent high avidity antibody binding. In contrast to antibodies targeting viruses such as influenza and respiratory syncytial virus (RSV), which are able to bind viral surface bivalently and thereby take advantage of avidity effects<sup>52,53</sup>, antibodies against HIV-1 envelope glycoproteins are thought to predominantly bind the viral surface monovalently<sup>54-56</sup>. Several studies suggest that HIV-1 evades bivalent high avidity antibody binding through its low spike density on the virion surface combined with an unfavorable distribution of epitopes on the spike trimer, thereby limiting both inter- and intra-spike crosslinking<sup>57</sup>. Often, high avidity antibody binding alone is not enough to confer sufficient toxin or pathogen neutralization and instead requires the Fc domain to augment neutralization of toxin activity or pathogen entry through

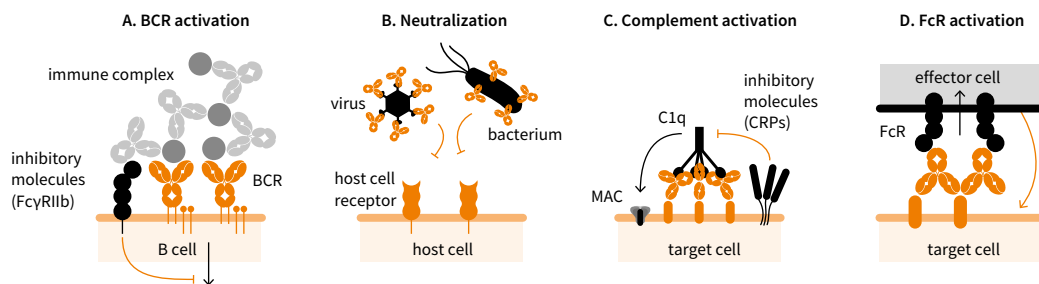
recruitment of complement or binding of FcγRs on immune cells (Figure 1, amplification phase). In the case of HIV-1, the neutralizing capacity of HIV-targeting broadly neutralizing antibodies was compromised upon administration of Fc domain variants that had decreased affinity for FcRs<sup>58,59</sup>. In autoimmune disease, the avidity of autoantibodies against self-antigens impacts on their pathogenicity, such as for example shown by the induction of symptoms of Myasthenia gravis in monkeys treated with bivalent IgG1 antibodies but not monovalent IgG4 antibodies against acetylcholine receptor<sup>60</sup>.

One of the most striking illustrations of the selective pressure of repeating microbial epitopes is the VH domain-swapped dimer formed by the anti-HIV-1 antibody 2G12, which enables multivalent interactions with conserved carbohydrate clusters on the HIV-1 envelope glycoprotein subunit gp120<sup>61</sup>. While the germline precursor to this antibody adopts a conventional (non-swapped) structure, a minimum of five somatic mutations permitted a significant fraction of domain exchange<sup>62</sup>, suggesting this unique structural rearrangement may be more generally accessible to antibodies. The plot thickened further upon subsequent discovery that domain swap was not limited to intramolecular IgG, but also promoted an intermolecular IgG dimer composed of four Fabs and two Fcs that provided >50-fold neutralization potency compared with monomeric 2G12<sup>63</sup>. This work demonstrates not only the important role that avidity plays for microbial epitope neutralization, but also illustrates how nature truly is the unrivalled antibody engineer, able to couple the extensive immune repertoire with modular immunoglobulin architecture to bring creative avid solutions to the fight against infectious agents.

### Complement activation

The complement system is a potent innate immune defense mechanism composed of an amplifiable enzymatic cascade that kills pathogens and attracts immune effector cells. Complement is activated through three distinct pathways; the classical-, lectin- and alternative pathway, which depend on binding of C1q, mannan-binding lectin or spontaneously activated complement to pathogenic surfaces respectively. All pathways ultimately converge in the generation of C3 and C5 convertases that cooperate in the production of opsonins, anaphylatoxins, chemoattractants and the formation of the membrane attack complex (MAC) that breaches the target cell membrane to kill the cell<sup>64</sup>.

The classical pathway is triggered upon binding of C1q to the Fc region of cell-bound IgG or IgM antibodies. C1q consists of six collagen-like triple-helical stalks connected to a globular headpiece that closely resembles the shape of a bunch of tulips<sup>65</sup>. The binding affinity of monomeric IgG Fc for C1q is weak ( $K_d \sim 10^4$  M) resulting in highly transient interactions (Figure 1 – scanning phase). Consequently, functional C1q binding and activation requires an



▲ **Figure 3**

### Avidity in antibody biology

(A) B-cell receptor (BCR) activation and FcγRIIb inhibition following antigen-induced aggregation during clonal selection. (B) Fab domain-mediated neutralization of pathogen structures to prevent interactions with host cells and blocking pathogen entry into the cell. (C) Complement activation initiated by IgGs that assemble into ordered hexameric structures through non-covalent Fc-Fc interactions. Ordered IgG Fc domains serve as an optimal docking structure for C1q binding, which trigger a series of proteolytic events leading to lysis of the cell via formation of the membrane attack complex (MAC). Complement activation is regulated by membrane-bound complement regulatory proteins (CRPs). (D) FcR-mediated (innate and adaptive) immune effector function activation through multimerization of cell-bound IgG. Activation of FcRs may induce a number of antibody-dependent cellular effector functions including ADCC and ADCP.

increase in apparent binding affinity ( $K_d \sim 10^8$  M) through multivalent antibody interactions<sup>66</sup> IgM antibodies naturally exist in multimerized form, either organized into a pentameric (>95%) or hexameric arrangement (<5%), thereby providing them with a superior ability to interact with C1q to activate complement<sup>39,40,67</sup>. Diebolder et al. reported that IgGs assemble into ordered hexameric structures after target engagement on the cell surface through non-covalent interactions between neighboring IgG Fc domains (Figure 1 – binding/clustering phase)<sup>19</sup>. These ordered IgG Fc domains form an optimal docking structure, effectively serving as a danger signal for C1q binding, enabling subsequent C1 activation and amplification of the complement cascade (Figure 1 – amplification phase, Figure 3C). The high amplification potential of the complement system is counterbalanced by strong regulation through numerous soluble (e.g. C1 inhibitor, C4bp, factors I and H) and cell surface expressed proteins, (e.g. CD46, CD55 and CD59; Figure 1 – regulation phase)<sup>68</sup>. Compelling evidence for the requirement of higher order IgG oligomers for optimal complement activation was provided by mass-spectrometry-, cryo-EM tomography- and mutational studies. These studies demonstrated that IgG monomers, dimers and trimers do not significantly contribute to CDC and illustrated the requirement of at least four C1q binding sites to achieve sufficient CDC potency<sup>17,50,51</sup>. Additional studies focusing on the dynamics and kinetics of IgG-C1q interactions showed that at high antigen density, oligomerization may occur through IgG recruitment from solution to predominantly bivalently-attached IgGs that then serve as nucleation sites. However at low antigen density or high IgG concentrations, predominantly monovalently-bound IgGs have been reported to additionally be capable of oligomerization via lateral

diffusion<sup>51</sup>. Interestingly, functionally monovalent antibodies (e.g. bispecific antibodies comprising only a single Fab arm for a target cell), were shown to induce CDC more potently, potentially due to a superior ability to form hexamers and engage C1<sup>17,19,51,69</sup>.

As discussed earlier, an ideal immune complex stoichiometry likely exists for efficient activation and amplification of Fc-mediated effector functions such as the complement cascade. Apart from optimal Ig oligomerization, a number of additional factors can influence triggering of complement activity. For example, there are several structural prerequisites that affect Ig Fc-Fc interactions and optimal placement of the hexameric C1q docking platform relative to the cell surface, including antigen-dependent constraints such as size, distribution, epitope geometry and orientation. These antigen- and epitope-dependent constraints are perhaps most evidently exemplified by recent studies that solve the enigma of the existence of two functional types of antibodies against the well-known therapeutic target CD20 in B-cell malignancies and inflammatory diseases. Type I CD20 antibodies are known to induce CD20 translocation into lipid rafts and kill via complement and ADCC, whereas type II's do not cluster CD20 and instead mediate cell killing via apoptosis and ADCC<sup>70,71</sup>. In these studies, the authors used structural and thermodynamic analyses to illustrate that CD20 forms a dimer that provides two binding sites for type I CD20 antibodies such as rituximab and ofatumumab, thereby facilitating efficient antibody clustering and complement activation. By contrast, each antigen binding site (i.e. Fab arm) of the type II CD20 antibody obinutuzumab can only bind a single CD20 dimer, thereby precluding higher order avidity interactions<sup>21,72</sup>. In another study, combinations of IgG antibodies simultaneously targeting CD20 and CD37 antigens were shown to induce synergistic CDC of tumor B cells by forming mixed hetero-hexameric complexes on the cell surface, while the individual antibodies were unable to activate complement<sup>73</sup>. This cooperativity between antibodies targeting two different antigens is likely caused by an optimal (re)distribution of antigen targets on the cell surface, thereby enabling colocalization and co-clustering. Additionally, antibody-dependent structural constraints such as hinge length and glycan heterogeneity also influence Ig oligomerization and complement activation<sup>74-77</sup>. These structural elements also account for the differences in complement activation observed between IgG subclasses (Box 2). Similarly, the presence of different IgG subclasses (e.g. certain IgG4 forms that are functionally monovalent<sup>60</sup>) and other classes like IgA and IgE could potentially dampen or regulate IgG-mediated complement activation, resulting from differences in flexibility, conformation, valency and steric interference with Fc-Fc interactions required for efficient oligomerization<sup>60,78-81</sup>. Thus, efficient activation and amplification of the complement system is dependent on a complex interplay between both Ig Fab- and Fc-mediated avidity interactions (Figure 1).



### FcR-mediated cellular effector functions

The Fc domain of antibodies can interact with different FcRs expressed on various immune cells to mediate effector functions such as ADCC and ADCP. IgG binds to FcγRs (Box 2), which are broadly classified as either activating or inhibitory, depending on whether their intracellular signaling domain contains an immunoreceptor tyrosine activating motif (ITAM) or immunoreceptor tyrosine inhibitory motif (ITIM) respectively. Activating FcγRs in humans include FcγRI (CD64), FcγRIIa (CD32a) and FcγRIIIa (CD16a), in addition to the less well characterized FcγRIIc (CD16c). By contrast, FcγRIIb (CD32b) represents the sole inhibitory FcγR, regulating the function of activating FcγRs, as well as serving as the main scavenging receptor in the liver, thereby further controlling antibody production by B lymphocytes. Finally FcγRIIIb (CD16b) uniquely contains no intracellular signaling domain and is instead glycosylphosphatidylinositol (GPI)-anchored to the membrane. FcγRs are differentially expressed on lymphoid- and myeloid-derived effector cells, although the receptor distribution is unique to each cell type<sup>82</sup>. FcγRIIIa is expressed on monocytes/macrophages and natural killer (NK) cells, and is the main receptor for mediating ADCC, promoting release of cytotoxic granules and pro-apoptotic signaling molecules after engaging IgG-opsonized target cells. Phagocytes such as macrophages and dendritic cells (DCs) express a combination of different FcγRs including FcγRI, FcγRIIa, FcγRIIIa and FcγRIIb that mediate not only ADCP for innate destruction of IgG-opsonized target cells, but can also promote cross-presentation to T cells to mediate adaptive cellular immunity for a vaccinal effect<sup>83-85</sup>. Studies have shown that FcγRIIa and in particular the balance of signals between activating FcγRIIa and inhibitory FcγRIIb are important determinants of the ability of antibody:antigen immune complexes to activate monocytes and DCs<sup>83,86-88</sup>. While the link between FcγRs and cellular immunity has historically been indirect through antigen presentation by cells, in a recent twist it was demonstrated that FcγRIIa is capable of directly promoting activation of CD4+ T cells by IgG immune complexes<sup>89</sup>.

FcγRs are bound by the different human IgG isotypes with varying affinities. Only FcγRI can bind monomeric IgG with high, nM range, affinity. All other FcγRs exhibit low, μM affinities for monomeric IgG, and as a consequence monomeric binding is transient under physiological conditions (Figure 1 – scanning phase)<sup>90</sup>. In the extreme, low affinity FcγRs including FcγRIIa and FcγRIIIa only interact with multimerized IgG on opsonized cells or multimeric IgG immune complexes under physiological conditions, thereby preventing inappropriate effector cell activation in the absence of a pathogenic trigger. Multimerization of cell-bound IgG strengthens FcγR binding interactions, thereby generating sufficient avidity (Figure 1 – binding/clustering phase) to trigger receptor signaling through phosphorylation of ITAM domains

(Figure 1 – amplification phase), which in turn leads to elimination of target cells via ADCC or ADCP and other immune cellular effects (Figure 3D).

Besides IgG binding to Fc $\gamma$ R<sub>s</sub>, other Ig subclasses bind to corresponding FcR<sub>s</sub> including Fc $\alpha$ RI (IgA), Fc $\epsilon$ RI (IgE), Fc $\mu$ R (IgM) and IgD (Ig $\delta$ R) and Fc $\alpha/\mu$ R (IgA/IgM). IgA plays a key role in mucosal areas by regulating the tolerance to- and protection from exposure to antigens, food and (commensal) microorganisms, while IgE is well known for its role in allergic reactions through binding the high affinity to Fc $\epsilon$ RI expressed on mast cells (Box 2)<sup>91,92</sup>. IgA immune complexes avidly bind Ig $\alpha$ RI expressed on myeloid cells including neutrophils, eosinophils, monocytes and macrophages. IgA antibodies have been reported to recruit neutrophils by crosslinking Fc $\alpha$ R1 and tumor cells in the context of a bispecific molecule and additionally induced efficient neutrophil-mediated killing of various tumor cell types via ADCC or ADCP<sup>92-94</sup>.

A multitude of factors influence the overall avidity and degree of antibody-FcR crosslinking, including antibody and FcR binding affinity, location of the antigenic epitope, and cell surface rigidity<sup>22</sup>. Several studies have demonstrated that different Fc $\gamma$ R allotype variants display a wide range of binding affinities for different IgG subclasses, which may impact Fc $\gamma$ R crosslinking and activation<sup>90,95</sup>. More recently, Mazor et al., showed that at saturating concentrations, high affinity antibody variants targeting EGFR and HER2 elicited a weaker ADCC response compared to low affinity antibody variants<sup>49</sup>. The observed difference was attributed to increased cell surface opsonization by low affinity antibodies, which display faster off rates and are thus expected to predominantly engage their target via monovalent binding interactions, leading to a higher local density of Fc domains. In contrast, high affinity antibodies were hypothesized to engage target bivalently, thereby occupying more antigen sites and consequently displaying lower local Fc domain densities. We additionally suggest that monovalent (low affinity) binding interactions may allow greater mobility and flexibility in crosslinking Fc $\gamma$ R<sub>s</sub>. One could also hypothesize that high affinity interactions and a slow off-rate may thwart the assembly of antibodies into higher order avidity structures. This view is supported by the earlier mentioned studies demonstrating that while bivalent (high affinity) binding can lead to stagnation, monovalent binding can trigger association and enhanced complement activation via lateral diffusion across cell surfaces<sup>51,96</sup>. In a related study, phagocytosis of emulsion droplets was shown to be more efficient at lower IgG concentrations compared to solid particles<sup>97</sup>. The authors speculated that lateral diffusion of IgGs attached to the surface observed in emulsion droplets was otherwise prevented in solid particles displaying higher cell surface rigidity. Altogether these examples illustrate the interplay between affinity and avidity interactions in tuning of antibody effector biology for responsiveness to infectious immune complexes.<sup>90</sup>

# AVIDITY ENGINEERING OF ANTIBODY THERAPEUTICS

Antibodies have become widely established as therapies for numerous diseases, including cancer, infectious diseases, inflammatory diseases and autoimmunity<sup>16</sup>. The challenges of designing differentiating therapeutics, next to disease heterogeneity, therapy resistance and escape have shifted therapeutic antibody development from canonical IgG antibodies towards formats with novel functionalities, increased potency and breadth. The search for approaches to enhance antibody function is not surprising considering the limitations imposed by monospecificity. Indeed, the single-agent use of monoclonal antibodies for therapy seems contradictory in light of the avidity-tuned polyclonal nature of antibody responses generated during natural immune responses.

## The avidity engineering toolbox

A broad spectrum of novel antibody engineering strategies and format concepts are emerging that enhance or tune avidity to boost ‘classical’ effector functions and enable novel therapeutic mechanisms. Some approaches may be biologically relevant optimizations (e.g. effector function enhancement), while others design elements for *de novo* yet non-native mechanisms of action (e.g. effector cell redirection or receptor agonism).

We describe an ‘avidity engineering toolbox’, and discuss the impact of different strategies on the different phases of antibody functional response activation as defined in Figure 1. Strategies include (i) multi-targeting approaches directed towards multiple epitopes, (ii) multi-targeting approaches directed to multiple surface receptors expressed on the same- or on different target cells, (iii) increasing antibody valency and (iv) optimizing binding towards complement or FcγRs. Many of these approaches have advanced into clinical development, and as of March 2021, the commercial clinical pipeline included 26 programs leveraging avidity to increase antibody function (Table 1). This overview table excludes clinical programs investigating obligate or combinatorial bispecific antibodies for which we refer to a recent review by Labrijn et al<sup>10</sup>. In the subsections below we highlight some of these key engineering strategies exploiting avidity to boost antibody functional responses.

## Multispecific targeting

In recent years, a growing number of antibody format technologies were introduced that enable increased antibody binding by targeting more than one epitope or target. While the initial design goal may be focused on improv-

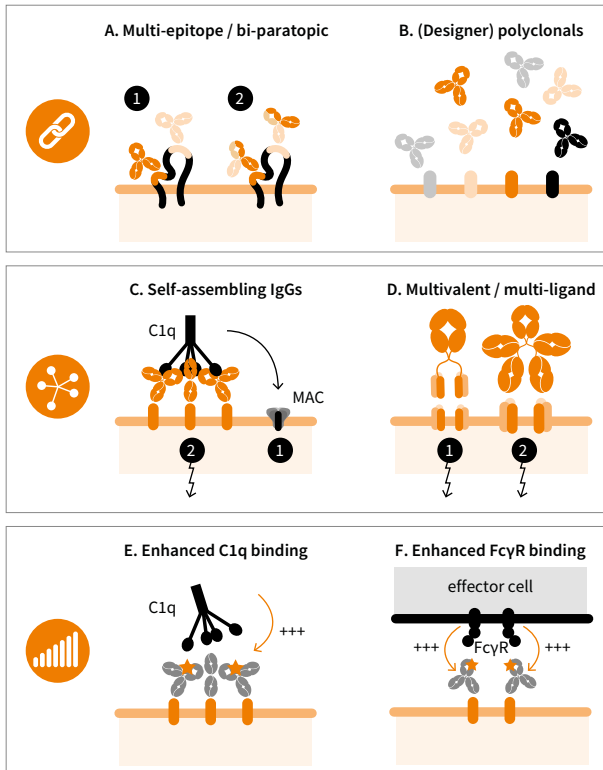
ing tissue selectivity through targeting multiple disease-related targets or signaling pathways, multi-targeting concepts may simultaneously benefit from enhanced functional activity by already promoting avidity interactions in early phases of antibody functional response activation. Multi-targeting concepts include combinations of two or more antibody molecules with different defined specificities; e.g. antibody mixtures or designer polyclonals, and antibody architectures and formats combining two or more specificities in a single antibody molecule; e.g. bispecifics or multispecifics.

### Targeting multiple epitopes

Multi-targeting antibody technologies that come closest to mimicking high avidity interactions of natural polyclonal antibodies are those directed towards non-overlapping epitopes on the same target (Figure 4A). Such technologies often build on increasing target occupancy and local Fc domain density to enhance antibody clustering and overall functional activity, while some may even potentiate additional novel effector functions (Figure 1, binding/clustering phase). For example, while complement activity by monoclonal antibodies has rarely been shown in solid tumor models, complement activation was reportedly triggered by combining two antibodies targeting non-overlapping epitopes on EGFR<sup>98,99</sup>. Similarly, biparatopic bispecific heavy chain antibody constructs targeting non-overlapping epitopes on CD38 were reported to potently enhance CDC activity in multiple myeloma and Burkitt's lymphoma cell lines<sup>100</sup>. Potentiation of CDC was additionally reported for simultaneously targeting non-overlapping epitopes on a number of other cell surface targets including CD37, HLA, Factor H-binding protein and folate receptor<sup>101-104</sup>. Targeting multiple non-overlapping epitopes may overcome complement defense mechanisms through increased binding and crosslinking of the same target, thereby exploiting the natural capacity of antibodies to form hexameric complexes and induce CDC.

Targeting non-overlapping epitopes using multi-specific antibody technologies is being explored in viral diseases to reduce resistance and lower the risk of viral escape. Trispecific antibody formats combining binding domains of broadly neutralizing antibodies (bNAbs) directed against different functional HIV-1 epitopes on the envelope spike exhibited higher neutralization potency and breadth compared to (combinations of) the parental bNAbs both in vitro and in vivo<sup>105,106</sup>.

Formats that enhance antibody binding by targeting multiple non-overlapping epitopes on a single antigen represent the largest group of clinical programs leveraging avidity tuning (Table 1). Such formats range from mixtures of two or more non-competing antibodies to bi- or multi-specific antibody architectures combining different epitope binding specificities in a single molecule. A num-



◀ **Figure 4**

**Antibody avidity engineering strategies**

(A) Enhancing antibody binding; (1) dual epitope targeting, (2) biparatopic bispecific targeting. (B) Enhancing antibody binding; (designer) polyclonals. (C) Enhancing antibody (-mediated) clustering; (1) self-assembling IgGs inducing complement activation or (2) self-assembling IgGs inducing cell surface receptor clustering and agonism. (D) Enhancing antibody-mediated clustering; (1) Hera-ligand technology or (2) multivalent antibody architectures inducing TNFRSF receptor clustering and agonism. (E-F) Enhancing antibody functional response amplification; increasing C1q- (E) and FcγR (F) binding affinity.

ber of clinical programs are investigating the efficacy of therapeutics targeting multiple epitopes on one of the EGFR family members that are overexpressed in many solid tumor indications<sup>107-109</sup>. There are substantial clinical data illustrating that patients who initially respond to EGFR-specific antibodies eventually become resistant. Targeting multiple receptor epitopes may overcome resistance, as was demonstrated by a proof of principle study with the anti-EGFR antibody cocktail Sym004 showing clinical activity in a metastatic colorectal cancer (mCRC) patient with acquired, EGFR mutation-mediated resistance to cetuximab<sup>110</sup>. Similarly, multi-epitope-targeting antibody formats also hold promise for treating patients with highly variant RNA viruses, who are likely to culminate escape variants after treatment with a single mAb. Indeed, a dual-epitope-targeting antibody cocktail is currently in phase III clinical development for severe acute respiratory syndrome coronavirus 2 (SARS-CoV-2) and has recently received an emergency use authorization from the United States Food and Drug Administration<sup>111-113</sup>. *In vitro* studies with this antibody cocktail prevented the selection of escape mutants in cultures growing a pseudo virus expressing the SARS-COV-2 spike, in contrast to pseudo virus grown in the presence of the individual antibodies<sup>114</sup>. In addition to dual-epitope targeting, multi-epitope targeting is also being explored in a phase I clinical trial

in the form of a triparatopic antibody containing binding domains from three broadly neutralizing antibodies (bnAbs; VRC01-LS, PGDM1400 and 10E8v4) directed towards the HIV-1 envelope spike<sup>106</sup>. Furthermore, a cocktail of three non-competing IgG1 antibodies (atoltivimab, maftivimab and odesivimab) was recently approved for treatment of Zaire ebolavirus (ZEBOV)<sup>115</sup>.

#### Targeting multiple cell surface receptors

Antibody cocktails targeting two or more cell surface receptors represent an archetypical example of avidity engineering through enhanced binding (Figure 4B). While such cocktails generate increased target occupancy, they may simultaneously benefit from additional avidity effects through enhanced antibody clustering (Figure 1, binding/clustering phase). We recently described a mixture of two antibodies targeting CD20 and CD37 antigens on tumor B cells that co-engaged in hetero-hexameric complexes, thereby potentiating complement activity<sup>61</sup>. Likewise, Jacobsen and colleagues reported on a mixture of six antibodies which, in synergistic pairs, target each of the HER family members EGFR, HER2 and HER3<sup>116</sup>. This PAN-HER mixture (Sym013) was shown to down modulate all three targets and overcome acquired resistance due to compensatory receptor upregulation in HER family-expressing tumors.

Other approaches to target multiple cell surface receptors include combining multiple binding specificities into a single molecule in the form of bi- or multi-specifics which, either *in-cis* or *in-trans*, bridge different receptors on the same cell or on different cell types respectively. The strength of bi- or multispecifics lies within their capacity to activate novel or 'designed' effector functions that could not otherwise be achieved by antibody mixtures, which are also referred to as 'obligate' mechanisms of action in the case of bispecifics<sup>10</sup>. Furthermore, their therapeutic index may be increased through localized tethering of receptors, thereby restricting therapeutic activity to preferred cells or tissues and limiting on- and off-target toxicity<sup>117</sup>. The most widely studied 'obligate' bispecific antibodies are those focusing on redirecting the cytotoxic activity of T cells or other effector cell types to eliminate tumor cells<sup>118</sup>. These bispecific antibodies are composed of effector cell-binding domain(s) physically linked to tumor cell-binding domain(s) and represent an inherent example of avidity tuning, as effector cells are brought in close contact with tumor cells. Such *in-trans* binding antibody concepts increase avidity interactions already in early phases of antibody functional response activation through enhanced binding and recruitment of effector cells and enhanced clustering via formation of the immunological synapse, while simultaneously boosting functional response amplification by effector-cell mediated killing of the target cell (Figure 1, binding/clustering/amplification phase). T-cell redirection has proven particularly useful in mediating sufficient avidity when targeting low-den-

sity cell surface receptors. In a clever use of avidity to improve therapeutic index, engineering two low affinity anti-Her2 Fab arms into an anti-HER2/CD3 bispecific enabled selective targeting of HER2-overexpressing tumor cells with high potency while sparing cells that express low HER2 found in normal tissue<sup>119</sup>.

An interesting example of how *in-cis* bridging can unlock obligate mechanisms of action is represented by amivantamab (Table 1), a bispecific antibody targeting EGFR and MET. Crosslinking of MET using bivalent antibodies causes undesirable tumor cell activation, which can be circumvented by combining a single (non-crosslinking) MET-binding arm with an EGFR-binding arm in a bispecific configuration that blocks both MET and EGFR signaling<sup>120</sup>. This example is also noteworthy in terms of avidity tuning, as it illustrates the importance of understanding both antibody- and target biology in the design of effective antibody-based therapeutics.

The targeting of multiple receptors surprisingly can also be achieved in a single binding domain. Lameris et al. recently described a single-domain antibody (VHH) 1D12 targeting the glycolipid-presenting major histocompatibility complex (MHC) class I-like molecule CD1d that can simultaneously interact with CD1d and the type I natural killer T (NKT) cell receptor. Cross-linking by VHH 1D12 stabilizes this interaction and induces anti-tumor activity by type I NKT cell through intrinsic bispecificity while retaining the T-cell receptor's (TCR) specificity for presented antigen<sup>121</sup>. VHH 1D12 is linked to a VHH targeting the Vg9Vd2 TCR in LAVA-051, which through its unique trispecific properties recruits both type I NKT cells and Vg9Vd2 T cells for tumor cells killing. LAVA-051 is a next-gen T-cell engager in development for the treatment of hematological cancers including CLL, MM and AML (Table 1).

Combined *cis*- and *trans*-bridging of receptors can also be achieved by engineering additional antibody fragments onto a classical bispecific antibody format, thereby creating tri- or multi-specific antibodies that enable simultaneous targeting of multiple cell types and same-cell receptors<sup>122,123</sup>. For instance, Shivange and colleagues recently reported on the generation of a Bispecific-Anchored Cytotoxicity-Activator (BaCa) antibody that simultaneously targets DR5 and folate receptor-1 (FOLR-1) both expressed on ovarian cancer cells. This Baca antibody was reported to bind FOLR-1 and crosslink DR5 both *in-cis* and *in-trans*, by which FOLR-1 served as tumor-specific anchor and primary clustering point for agonist DR5 signaling<sup>124</sup>.

## Enhancing / optimizing valency

Over the past few years multiple engineering strategies have focused on enhancing antibody clustering to improve antibody function (Figure 1, clustering phase). Such engineering strategies are often aimed at increasing antibody valency by transferring IgG variable regions to IgM-like formats or through multiplication of (parts of) Fab or Fc domains in (non-) IgG-like structures or fragments. Several studies reported on the design of antibody architectures containing multiple Fc domains to enhance Fc $\gamma$ R crosslinking and ADCC<sup>125-128</sup>. In a more recent study, Miller and colleagues adapted the tetramerization domain of p53 and fused it to different antigen binding domains to create octavalent monospecific and bispecific (Quads) antibody variants with increased functional activity<sup>129</sup>. Alternatively, CDC by IgG1 antibodies can be enhanced through the covalent association of up to six IgG1 monomers using the  $\mu$ -tailpiece of IgM, thereby generating IgM-like structures that efficiently bind and activate complement<sup>130</sup>. In contrast to pre-assembled antibody multimers, the ability of IgGs to self-assemble into ordered oligomers on antigenic surfaces via Fc-Fc interactions may be exploited in therapeutic applications, with notion that the use of IgG antibodies with standard architecture would simplify design and development. De Jong and colleagues were first to report on a novel HexaBody<sup>®</sup> technology platform that uses specific single-point mutations in the Fc domain to enhance self-assembly of IgG molecules into hexameric complexes after target binding on a cell surface (Figure 4C)<sup>131</sup>. In a mutational screening approach, they identified two Fc residues, E345 and E430 which, when substituted with any other amino acid, enhanced IgG hexamer formation and complement activation for a wide range of cell surface targets. Furthermore, by systematically depleting individual complement components, Taylor et al, elegantly showed that antibodies containing such hexamer-enhancing mutations required a reduced presence of MAC-forming complement components to promote CDC<sup>132</sup>. Thus, cell surface oligomerization of hexamer-enhanced antibodies is likely to be highly efficient, resulting in a lower complement activation threshold compared to regular IgGs.

Besides improving antagonistic antibody function, enhancement of antibody clustering may also have novel applications in amplifying ‘designed’ antibody functions such as agonistic receptor signaling. Some receptors, including those with multimeric cognate ligands or those that interact at cell-cell synapses, require higher order clustering before activation of downstream signaling. The most widely studied receptors of this class are members of the Tumor Necrosis Factor Receptor Super Family (TNFRSF), which are of growing interest to drug developers owing to their important function in regulating cell survival and inflammatory signaling. Regular binding of agonistic immunomodulatory antibodies targeting these receptors is generally not sufficient to engage higher order TNFRSF clustering and activation. Many require additional extrinsic



crosslinking via FcγRs, in particular FcγRIIb, on immune effector cells<sup>133-135</sup>. Pioneering work by Ashkenazi, Presta, and colleagues demonstrated that engineered tandem Fab repeats can enhance the forward signaling activity of antibodies targeting DR5 and CD20<sup>136</sup>. Alternatively, introducing hexamer-enhancing mutations in antibodies targeting TNFRSF members also proved an effective strategy to enhance agonistic signaling and tumor cell death. Recently, Overdijk et al. described the generation of a novel antibody mixture of two non-competing DR5-targeting (TRAIL-R2) antibodies containing an E430G hexamer-enhancing mutation that improves DR5 agonistic signaling and tumor cell death independent of FcγR crosslinking in a wide range of tumor types<sup>137</sup>. Intermolecular Fc-Fc interactions between noncompeting hexamer-enhanced DR5 IgG molecules were shown to be essential for DR5 agonistic activity and binding of complement component C1q reportedly contributed to the potency observed *in vitro* and *in vivo*, potentially resulting from increased clustering after C1 binding (Figure 1, clustering phase).

Besides targeting TNFRSF members such as TRAIL on tumor cells, immune effector cells also express TNFRSF activating receptors including OX40, CD27, CD40, 4-1BB and GITR. Much effort has been directed towards the use of their respective ligands or agonist antibodies to stimulate T-cell proliferation and cytotoxic activity. Enhanced hexamerization using an E435R Fc mutation was reported to increase the agonistic activity of OX40-targeting antibodies<sup>138,139</sup>. Alternative approaches to enhance TNFR activation independent of FcγR crosslinking include Fc fusions with six (hexavalent) ligand receptor binding domains, IgM class switching, covalently trimerized fusion proteins and tetravalent bi-epitopic targeting concepts (Figure 4D)<sup>140-143</sup>. The hexavalent receptor agonist (HERA) technology for example, makes use of single chain trimeric TNFR ligand binding domains fused to a silenced IgG1-derived Fc domain to enhance clustering of CD40, GITR and CD27 and boost antigen-specific T-cell responses<sup>144-146</sup>. Likewise, combined multivalent and multi-epitopic engagement of DR5 and OX40 using various tetravalent bi-epitopic antibody formats was shown to induce agonistic signaling without the need for extrinsic crosslinking<sup>143</sup>.

While more complex and challenging than IgGs with respect to production, glycosylation, and pharmacokinetics, naturally multivalent immunoglobulin isotypes such as IgM and IgA are being clinically translated, with a steady increase in engineering for their optimization<sup>41,147,148</sup>. In a unique ocular application, Agard and colleagues leveraged not only the multivalent nature of IgM to effectively agonize Tie2, but also capitalized on its large size to reduce vitreal clearance<sup>149</sup>.

Avidity-engineered formats are advancing clinically particularly in the context of antibody-mediated targeting of TNFRSF members (Table 1). Previous efforts to develop TNFRSF-targeting antibodies have yielded limited clinical success, partly due to lack of efficacy due possibly to insufficient (FcγR-mediated) crosslinking, and in some cases due to adverse events or toxicity<sup>150,151</sup>. Interest has revived upon development of antibody formats with increased valency that allow for superior TNFR crosslinking and signaling independent of Fc interactions. At present, four valency-increased antibodies targeting TNFRSF members have entered early-stage clinical trials, including a pentameric IgM-based antibody construct targeting DR5 (IGM-8444), and tetravalent (INBRX-109) or hexavalent (INBRX-106, ABBV-621) formats containing multiple (ligand) binding domains fused to an Fc domain targeting DR5, TRAIL and OX40 respectively. Moreover, at present, two clinical programs leverage avidity through a combination of enhanced binding and clustering, both in the context of antibodies targeting two non-overlapping epitopes that contain an Fc domain mutation driving self-assembly of IgGs in hexameric complexes. Combining dual epitope targeting with enhanced hexamerization is being explored as an antibody mixture targeting DR5 on solid tumors (GEN1029) and as a bispecific (biparatopic) molecule targeting CD37 in hematologic malignancies (GEN3009)<sup>102,137</sup>.

### **Optimizing binding to Fc effector receptors**

Canonical therapeutic antibodies rely on their Fc domain to effectively initiate immune effector functions (Figure 1, amplification phase). Therefore, much effort has been made to engineer the Fc domain and enhance binding affinity towards immune effector molecules and cells. As the various IgG subclasses differ in their complement activating potency (IgG3 > IgG1 >> IgG2 ≈ IgG4), reshuffling of segments from different IgG subclasses has been a common engineering strategy for optimization<sup>152-155</sup>. In human IgG1, multiple amino acid residues were identified to be critical for binding of C1q including D270, K322, P329 and P331 in the second heavy chain constant domain (C<sub>H</sub>2)<sup>156</sup>. Several groups have enhanced C1q binding affinity and CDC by mutating amino acid positions in the Fc region (Figure 4E)<sup>156-160</sup>. Other positions in the IgG Fc region differentially affect FcγR binding and can likewise be modified to enhance ADCC or ADCP activity (Figure 4F)<sup>88,161,162</sup>. For example, S239D/I332E amino acid substitutions in the Fc domain of antibodies targeting EGFR, CD52 and CD20 were shown to enhance FcγRIIIa/FcγRIIb affinity and increase ADCC and ADCP activity<sup>161</sup>. Another successful engineering approach for enhancing antibody effector function is glycoengineering of the Fc region for reduced fucose content, which selectively improves binding to FcγRIIIa. Enhancement of FcγR binding interactions may not only improve classical FcγR-mediated effector functions, but can also be employed to increase the agonistic activity of immunomodulatory antibodies. For instance, FcγR affinity enhancement

using S267E/L328F or E233D/G237D/H268D/P271G/A330R Fc mutations was reported to increase the anti-tumor activity of DR5 and OX40 TNFRSF members<sup>133,139,163-165</sup>. Additionally, isoelectric point engineering or selective enhancement to FcγRIIb in pH-dependent antibodies, which bind to antigen at neutral pH in plasma and dissociate at acidic pH in endosomes, was also reported to improve soluble antigen clearance from circulation<sup>166,167</sup>.

At present, seven active clinical programs apply Fc engineering to boost (amplify) FcγR-mediated effector functions (Table 1). A combination of two Fc domain single point mutations (S239D/I332E) enhances ADCC and ADCP functional activity of antibodies targeting the envelope spike on HIV-1 and CD19 on B tumor cells, of which the latter (tafasitamab) was recently approved for treatment of relapsed/refractory diffuse large B-cell lymphoma (DLBCL) in combination with lenalidomide. Recently margetuximab, an anti-HER2 antibody Fc engineered with the variant L235V/F243L/R292P/Y300L/P396L, was approved for HER2+ breast cancer<sup>168,169</sup>. Glycoengineering for effector function enhancement has met broad clinical success, with three approved antibodies with reduced Fc fucose content (mogamulizumab)<sup>170,171</sup>, obinutuzumab<sup>172</sup>, benralizumab<sup>173,174</sup> and one under regulatory review (amivantamab)<sup>120,175</sup>.

As described above, FcγRs not only mediate cytotoxic and phagocytic effector functions, but can also play a role in activation of DCs by antibody:antigen immune complexes to mediate adaptive cellular immunity for a vaccinal effect. Recently, Ravetch and colleagues have demonstrated that antibodies Fc engineered for selective enhancement to FcγRIIa<sup>88</sup> can increase DC maturation and induce protective CD8<sup>+</sup> T cell anti-viral response<sup>176</sup>.

## CONCLUSIONS AND FUTURE PERSPECTIVES

Antibody function relies on complex interactions between antibodies and their target, as well as their ability to associate with effector molecules and cells of the immune system. There is considerable evidence demonstrating the crucial role of avidity in natural antibody biology, from antibody affinity maturation early in the immune response, to effector function activation after target engagement. Antibody effector mechanisms including CDC, ADCC and ADCP all require a certain level of ordered clustering prior to activation either via self-assembling Ig Fc domains or crosslinking of FcRs on immune effector cells. Although the threshold by which antibody avidity interactions translate in an effective functional response may vary per effector mechanism, antibody clustering may be viewed as the checkpoint before response amplification and thus in large part determines the efficacy or impact of functional response (Figure 1). Understanding the key determinants that shape antibody functional response kinetics, including avidity interactions and response regulators, is therefore crucial in the design of novel and ‘impactful’ antibody-based therapeutics. In that light, we take lessons from the natural polyclonal antibody response, which is highly efficient at establishing avidity interactions through the generation of antibodies with different affinities, valencies and binding specificities. Upon repeat exposure, somatic mutation and selection, such responses mature to high affinity responses which are more oligoclonal in nature while retaining multi-epitope targeting as a principal feature. In essence, the historical single-agent use of monoclonal antibodies for therapy seems contradictory to antibody function as established in natural biology. In traditional drug development, single agent safety and activity is required for a drug to be registered. Drug combinations are typically sought thereafter, often using empirical approaches. This process however, is in conflict with the biologic function of immunity, in which the body matures a polyclonal immune response that is combinatorial from the start. Awareness on this paradox has steadily grown as antibody-based therapeutics have evolved from classical, non-modified monoclonal antibodies towards more complex antibody architectures and formats in an effort to enhance functional activity.



Novel formats are emerging that leverage antibody avidity interactions to boost classical as well as novel or ‘designed’ effector functions. Many of these formats feature some of the strengths offered by polyclonals including increased affinity, valency or binding specificities, either as antibody cocktails or encompassed within a single antibody molecule. Using this concept, distinct avidity engineering approaches may be combined for incremental avidity

effects. Thus for example, multi-epitope or multi-valent formats may be combined with (self-) assembling technologies that may be further enhanced by effector molecules (Figure 4 and see Table 1 for examples). We believe that multi-agent approaches are a major part of the future of antibody therapy, either in the form of bi- or multispecifics with obligate functions or designer polyclonals. The ever-growing list of investigational therapeutic antibodies entering or undergoing clinical development argues for greater effort towards rational design of oligoclonal antibody cocktails. For example, with five programmed cell death protein 1 (PD-1) antibodies approved for clinical use and over ten in clinical development, combination trials with multiple existing antibodies targeting non-overlapping epitopes on PD-1 may offer advantages over (yet another) single-agent approach<sup>177</sup>. Notably, forward-looking antibody discovery approaches that perform unbiased screening of antibody libraries in their final format will be critical to identification of the most optimal multispecific candidates or antibody combinations. Collectively, recent novel insights into antibody effector biology together with current antibody design efforts that extend our capabilities beyond the classic monoclonal antibody format are paving the way for novel transformative biotherapeutics that positively impact patient lives.

**Table 1**















**Avidity-based therapeutic antibody concepts in the clinic and engineering platforms that optimize them**

Data available as of 1 March 2021. ADC, antibody-drug conjugate; ADCC, antibody-dependent cellular cytotoxicity; ADCP, antibody-dependent cellular phagocytosis; AML, acute myeloid leukemia; bnAb, broadly neutralizing antibody; BLA, Biologics License Application; B-NHL, B-cell non-Hodgkin lymphoma; CCR4, C-C Motif Chemokine Receptor 4; CD, cluster of differentiation; CLL, chronic lymphocytic leukemia; CODV-Ig, cross-over dual variable Ig-like protein; COVID-19, coronavirus disease 2019; CRIB, charge repulsion induced bispecificity; DLBCL, diffuse large B-cell lymphoma; DR5, death receptor 5; EGFR, epidermal growth factor receptor; Fc, fragment crystallizable; FL, follicular lymphoma; HER2, human epidermal growth factor receptor 2; HIV-1, human immunodeficiency virus 1; IL, interleukin; mCRC, metastatic colorectal cancer; MET, tyrosine-protein kinase Met; MM, multiple myeloma; MPER, membrane-proximal external region; NKT, natural killer T cell; OX40, tumor necrosis factor receptor superfamily member 4; NSCLC, non-small cell lung cancer; SARS-CoV-2, severe acute respiratory syndrome coronavirus 2; sdAb, single-domain antibody; TCR, T-cell receptor; TNFRSF, tumor necrosis factor receptor super family; TRAIL, TNF-related apoptosis-inducing ligand; VHH, single-domain antibodies; ZEBOV, Zaire ebolavirus. Engineering data provided in the fourth column were obtained from public documents (scientific literature, abstracts, posters and patent publications).

Antibody name(s) (Company)	Target	Optimizing <sup>1</sup>	Format (Technology platform)	Indication (Selected)	Development status (Selected trials)
<b>Targeting multiple epitopes</b>					
Sym015 (Symphogen)	cMET	 	Mixture of two IgG1 antibodies binding non-overlapping epitopes on the SEMA-a domain of MET	Solid tumors (NSCLC)	Phase IIa (NCT02648724)
REGN5093 (Regeneron)	cMET	 	Biparatopic bispecific IgG1 antibody targeting two non-overlapping epitopes on MET (Veloci-Bi® bispecific technology)	Solid tumors (NSCLC)	Phase I/II (NCT04077099)
Sym004 (Symphogen)	EGFR	 	Mixture of two IgG1 antibodies (futuximab, modotuximab) binding non-overlapping epitopes on EGFR	Solid tumors (mCRC)	Phase III ready (NCT02083653)
KN026 (Alphamab)	HER2	 	Biparatopic bispecific IgG1 antibody targeting two non-overlapping epitopes on HER2 (CRIB technology)	Solid tumors (breast and gastric cancer)	Phase I (NCT03619681 and NCT03847168)
MBS301 (Beijing Mabworks Biotech)	HER2	 	Afucosylated biparatopic bispecific IgG1 antibody targeting two non-overlapping epitopes on HER2 (knobs-into-holes bispecific technology)	Solid tumors (HER2*)	Phase I (NCT03842085)
Zanidatamab, ZW25 (Zymeworks)	HER2	 	Biparatopic bispecific IgG1 antibody targeting two non-overlapping epitopes on HER2 (Azymetric™ bispecific technology)	Solid tumors (HER2*)	Phase II (NCT04466891, NCT03929666 and NCT04224272)










 Binding  Clustering  Amplification

1 See Figure 1 for additional information about different phases (binding, clustering and amplification) of antibody functional response activation.

Antibody name(s) (Company)	Target	Optimizing <sup>1</sup>	Format (Technology platform)	Indication (Selected)	Development status (Selected trials)
ZW49 (Zymeworks)	HER2	 	Biparotopic bispecific IgG1 antibody targeting two non-overlapping epitopes on HER2 (Asymmetric bispecific technology) conjugated to auristatin (Zymelink™ ADC technology)	Solid tumors (HER2 <sup>+</sup> )	Phase I (NCT03821233)
Casirivimab, imdevimab, REGN-COV2 (Regeneron)	SARS-CoV-2 spike	 	Mixture of two human IgG1 antibodies binding non-overlapping epitopes on the SARS-CoV-2 viral spike	COVID-19	Emergency approval, Phase III (NCT04452318 and NCT04381936)
ADM03820 (Ology Bioservices)	SARS-CoV-2 spike	 	Mixture of two human IgG1 antibodies binding non-overlapping epitopes on the SARS-CoV-2 viral spike	COVID-19	Phase I (NCT04592549)
SAR441236 (Sanofi)	HIV-1 envelope	 	Triparotopic IgG1 bnAb (derived from VRC01-LS, PGDM1400 and 10E8v4) targeting the CD4bs, gp41 MPER and V1/V2 glycan-directed binding sites on HIV-1 (CODV-Ig technology)	HIV-1	Phase I (NCT03705169)
Inmazeb, REGN-EB3 (Regeneron)	ZEBOV glycoprotein	 	A mixture of three IgG1 antibodies (atoltivimab, maftivimab and odesivimab) that each bind to different, non-overlapping epitopes on the Zaire ebolavirus glycoprotein	ZEBOV	Approved
<b>Targeting multiple cell surface receptors</b>					
LAVA-051 (Lava Therapeutics)	CD1d, Vd2 TCR	  	CD1d bispecific gamma-delta T-cell engager: VHH targeting CD1d that simultaneously binds CD1d and the type I NKT TCR, thereby stabilizing this interaction through intrinsic bispecificity linked to a VHH targeting Vg9Vd2 TCR	Hematologic malignancies (CLL, MM, AML)	Phase I (pending)
<b>Enhancing / optimizing valency</b>					
IGM-8444 (IgM Biosciences)	DR5		Pentameric IgM antibody with 10 binding sites specific for DR5	Solid tumors	Phase I (NCT04553692)

 Binding  Clustering  Amplification








1 See Figure 1 for additional information about different phases (binding, clustering and amplification) of antibody functional response activation.

Antibody name(s) (Company)	Target	Optimizing <sup>1</sup>	Format (Technology platform)	Indication (Selected)	Development status (Selected trials)
INBRX-109 (INHIBRX)	DR5		Four single domain antibodies (tetravalent) fused to an Fc domain (sdAb technology – binding units derived from heavy chain only antibodies)	Solid tumors	Phase I (NCT03715933)
INBRX-106 (INHIBRX)	OX40		Six single domain antibodies (hexavalent) fused to an Fc domain (sdAb technology – binding units derived from heavy chain only antibodies)	Solid tumors	Phase I (NCT04198766)
ABBV-621, APG350, HERA-TRAIL (Abbvie, Apogenix)	TRAIL		Hexavalent TNFRSF agonist comprising a fusion protein composed of three receptor binding domains in a single chain arrangement, linked to a silenced human IgG1 Fc-domain (HERA-ligand technology)	Solid tumors, hematologic malignancies	Phase I (NCT03082209)
GL-2045 (Gliknik)	C1q		Recombinant human IgG1-based Fc multimer; fusion of the complete IgG1 hinge-CH2-CH3 coding region to the IgG2 hinge region (Stradomer technology™)	Autoimmune diseases	Phase I (NCT03275740)
<b>Targeting multiple epitopes &amp; enhancing / optimizing valency</b>					
GEN3009, DuoHexaBody- CD37 (Genmab, AbbVie)	CD37	 	Biparatopic bispecific IgG1 antibody targeting two non-overlapping epitopes on CD37 containing an E430G hexamerization-enhancing Fc mutation ((DuoHexaBody® technology)	Hematologic malignancies (B-NHL, CLL)	Phase I (NCT04358458)
GEN1029; HexaBody DR5/ DR5 (Genmab)	DR5	 	Mixture of two IgG1 antibodies targeting non-overlapping epitopes on DR5, both containing an E430G hexamerization-enhancing Fc mutation (HexaBody® technology)	Solid tumors	Phase I (NCT03576131)
<b>Optimizing binding to Fc effector receptors</b>					
Monjuvi, tafasitamab-cxix (MorphoSys/ Incyte)	CD19		IgG1 antibody containing S239D/I332E Fc mutations for enhanced ADCC and ADCP (high cytotoxicity XmAb® Fc domain technology)	Hematologic malignancies (DLBCL)	Approved

 Binding    Clustering    Amplification

1 See Figure 1 for additional information about different phases (binding, clustering and amplification) of antibody functional response activation.



Antibody name(s) (Company)	Target	Optimizing <sup>1</sup>	Format (Technology platform)	Indication (Selected)	Development status (Selected trials)
Elipovimab, GS-9722 (Gilead Sciences)	HIV-1 envelope		IgG1 bnAb (derived from PGT121) containing S239D/I332E and M428L/N434S Fc mutations for lower immunogenicity, improved PK, enhanced ADCC and ADCP (high cytotoxicity XmAb & Xtend™ Fc domain technology)	HIV-1	GS-US-420-3902 Adisinsight entry (not listed in clinicaltrials.gov)
Margenza, margetuximab (Macrogenics)	HER2		IgG1 antibody containing L235V/F243L/R292P/Y300L/P396L Fc mutations for enhanced ADCC	Solid tumors (HER2 <sup>+</sup> breast cancer)	Approved
Poteligeo, Mogamulizumab (Kyowa Hakko Kirin)	CCR4		IgG1 antibody containing reduced fucose in the Fc region for enhanced ADCC (Potelligent® Technology)	Adult T-cell leukemia or lymphoma	Approved
Gazyva, obinutuzumab (Roche)	CD20		IgG1 antibody containing reduced fucose in the Fc region for enhanced ADCC (GlycoMab® Technology)	Hematologic malignancies (CLL, FL)	Approved
Fasenra, benralizumab (Astra Zeneca, Kyoa Hakko Kirin)	IL-5Ra		IgG1 antibody containing reduced fucose in the Fc region for enhanced ADCC (Potelligent Technology)	Asthma	Approved
<b>Targeting multiple cell surface receptors &amp; optimizing binding to Fc effector receptors</b>					
Amivantamab (Janssen/JNJ)	HER2, cMET	 	IgG1 bispecific antibody containing reduced fucose in the Fc region for enhanced ADCC (DuoBody® technology)	Solid tumors (Metastatic NSCLC with EGFR exon 20 insertion mutations)	BLA

 Binding    Clustering    Amplification

1 See Figure 1 for additional information about different phases (binding, clustering and amplification) of antibody functional response activation.

# REFERENCES

1. Eisen HN. Affinity Enhancement of Antibodies: How Low-Affinity Antibodies Produced Early in Immune Responses Are Followed by High-Affinity Antibodies Later and in Memory B-Cell Responses. *Cancer Immunol Res* 2014; **2**(5): 381.
2. Rajewsky K. Clonal selection and learning in the antibody system. *Nature* 1996; **381**(6585): 751-8.
3. Tonegawa S. Somatic generation of antibody diversity. *Nature* 1983; **302**(5909): 575-81.
4. Kohler G, Milstein C. Continuous cultures of fused cells secreting antibody of predefined specificity. *Nature* 1975; **256**(5517): 495-7.
5. Kaplon H, Reichert JM. Antibodies to watch in 2021. *mAbs* 2021; **13**(1): 1860476.
6. <https://www.antibodysociety.org/resources/approved-antibodies/>.
7. Chiu ML, Goulet DR, Teplyakov A, Gilliland GL. Antibody Structure and Function: The Basis for Engineering Therapeutics. *Antibodies* 2019; **8**(4): 55.
8. Goulet DR, Atkins WM. Considerations for the Design of Antibody-Based Therapeutics. *J Pharm Sci* 2020; **109**(1): 74-103.
9. Wang Y, Yang S. Multispecific drugs: the fourth wave of biopharmaceutical innovation. *Signal Transduct Target Ther* 2020; **5**(1): 86.
10. Labrijn AF, Janmaat ML, Reichert JM, Parren P. Bispecific antibodies: a mechanistic review of the pipeline. *Nat Rev Drug Discov* 2019; **18**(8): 585-608.
11. Schuurman J, Parren PW. Editorial overview: Special section: New concepts in antibody therapeutics: What's in store for antibody therapy? *Curr Opin Immunol* 2016; **40**: vii-xiii.
12. Rudnick SI, Adams GP. Affinity and avidity in antibody-based tumor targeting. *Cancer Biother Radiopharm* 2009; **24**(2): 155-61.
13. Marks JD. Deciphering antibody properties that lead to potent botulinum neurotoxin neutralization. *Mov Disord* 2004; **19 Suppl 8**: S101-8.
14. Wang XZ, Coljee VW, Maynard JA. Back to the future: recombinant polyclonal antibody therapeutics. *Curr Opin Chem Eng* 2013; **2**(4): 405-15.
15. Parren PW, Burton DR. The antiviral activity of antibodies in vitro and in vivo. *Adv Immunol* 2001; **77**: 195-262.
16. Carter PJ, Lazar GA. Next generation antibody drugs: pursuit of the 'high-hanging fruit'. *Nat Rev Drug Discov* 2018; **17**(3): 197-223.
17. Ugurlar D, Howes SC, de Kreuk B-J, et al. Structures of C1-IgG1 provide insights into how danger pattern recognition activates complement. *Science* 2018; **359**(6377): 794-7.
18. Sondermann P, Szymkowski DE. Harnessing Fc receptor biology in the design of therapeutic antibodies. *Curr Opin Immunol* 2016; **40**: 78-87.
19. Diebolder CA, Beurskens FJ, de Jong RN, et al. Complement Is Activated by IgG Hexamers Assembled at the Cell Surface. *Science* 2014; **343**(6176): 1260-3.
20. Hiramoto E, Tsutsumi A, Suzuki R, et al. The IgM pentamer is an asymmetric pentagon with an open groove that binds the AIM protein. *Sci Adv* 2018; **4**(10): eaau1199.
21. Rougé L, Chiang N, Steffek M, et al. Structure of CD20 in complex with the therapeutic monoclonal antibody rituximab. *Science* 2020; **367**(6483): 1224-30.
22. Patel KR, Roberts JT, Barb AW. Multiple Variables at the Leukocyte Cell Surface Impact Fc  $\gamma$  Receptor-Dependent Mechanisms. *Front Immunol* 2019; **10**(223).
23. Fleischman JB, Porter RR, Press EM. The arrangement of the peptide chains in gamma-gobulin. *Biochem J* 1963; **88**(2): 220-8.

24. Porter RR. The hydrolysis of rabbit  $\gamma$ -globulin and antibodies with crystalline papain. *Biochem J* 1959; **73**: 119-26.
25. Karush F. Multivalent binding and functional affinity. *Contemp Top Mol Immunol* 1976; **5**: 217-28.
26. Vorup-Jensen T. On the roles of polyvalent binding in immune recognition: Perspectives in the nanoscience of immunology and the immune response to nanomedicines. *Adv Drug Deliv Rev* 2012; **64**(15): 1759-81.
27. Burnet FM, Keogh EV, Lush D. The Immunological Reactions of the Filterable Viruses. *Aust J Exp Biol Med Sci* 1937; **15**(Pt. 3): 227-368.
28. Bleeker WK, Lammerts van Bueren JJ, van Ojik HH, et al. Dual mode of action of a human anti-epidermal growth factor receptor monoclonal antibody for cancer therapy. *J Immunol* 2004; **173**(7): 4699-707.
29. Rhoden JJ, Dyas GL, Wroblewski VJ. A Modeling and Experimental Investigation of the Effects of Antigen Density, Binding Affinity, and Antigen Expression Ratio on Bispecific Antibody Binding to Cell Surface Targets. *J Biol Chem* 2016; **291**(21): 11337-47.
30. Yang D, Kroe-Barrett R, Singh S, Roberts CJ, Laue TM. IgG cooperativity – Is there allostery? Implications for antibody functions and therapeutic antibody development. *mAbs* 2017; **9**(8): 1231-52.
31. Beurskens FJ, Lindorfer MA, Farooqui M, et al. Exhaustion of cytotoxic effector systems may limit monoclonal antibody-based immunotherapy in cancer patients. *J Immunol* 2012; **188**(7): 3532-41.
32. Lilienthal G-M, Rahmüller J, Petry J, Bartsch YC, Leliavski A, Ehlers M. Potential of Murine IgG1 and Human IgG4 to Inhibit the Classical Complement and Fc $\gamma$  Receptor Activation Pathways. *Front Immunol* 2018; **9**(958).
33. Prodjinotho UF, Hoerauf A, Adjobimey T. IgG4 antibodies from patients with asymptomatic bancroftian filariasis inhibit the binding of IgG1 and IgG2 to C1q in a Fc-Fc-dependent mechanism. *Parasitol Res* 2019; **118**(10): 2957-68.
34. Briney B, Inderbitzin A, Joyce C, Burton DR. Commonality despite exceptional diversity in the baseline human antibody repertoire. *Nature* 2019; **566**(7744): 393-7.
35. Dal Porto JM, Gauld SB, Merrell KT, Mills D, Pugh-Bernard AE, Cambier J. B cell antigen receptor signaling 101. *Mol Immunol* 2004; **41**(6-7): 599-613.
36. Feng Y, Wang Y, Zhang S, Haneef K, Liu W. Structural and immunogenomic insights into B-cell receptor activation. *J Genet Genomics* 2020; **47**(1): 27-35.
37. Treanor B. B-cell receptor: from resting state to activate. *Immunology* 2012; **136**(1): 21-7.
38. Peterson ML. Mechanisms controlling production of membrane and secreted immunoglobulin during B cell development. *Immunol Res* 2007; **37**(1): 33-46.
39. Cattaneo A, Neuberger MS. Polymeric immunoglobulin M is secreted by transfectants of non-lymphoid cells in the absence of immunoglobulin J chain. *EMBO J* 1987; **6**(9): 2753-8.
40. Hughey CT, Brewer JW, Colosia AD, Rosse WF, Corley RB. Production of IgM Hexamers by Normal and Autoimmune B Cells: Implications for the Physiologic Role of Hexameric IgM. *J Immunol* 1998; **161**(8): 4091.
41. Keyt BA, Baliga R, Sinclair AM, Carroll SF, Peterson MS. Structure, Function, and Therapeutic Use of IgM Antibodies. *Antibodies* 2020; **9**(4).
42. Noia JMD, Neuberger MS. Molecular Mechanisms of Antibody Somatic Hypermutation. *Annu Rev Biochem* 2007; **76**(1): 1-22.
43. Batista FD, Neuberger MS. Affinity dependence of the B cell response to antigen: a threshold, a ceiling, and the importance of off-rate. *Immunity* 1998; **8**(6): 751-9.
44. Foote J, Eisen HN. Kinetic and affinity limits on antibodies produced during immune responses. *Proc Natl Acad Sci U S A* 1995; **92**(5): 1254-6.
45. Daëron M. Fc receptors as adaptive immunoreceptors. *Curr Top Microbiol Immunol* 2014; **382**: 131-64.

46. Nimmerjahn F, Ravetch JV. FcγRs in health and disease. *Curr Top Microbiol Immunol* 2011; **350**: 105-25.
47. Maizels N. Immunoglobulin gene diversification. *Annu Rev Genet* 2005; **39**: 23-46.
48. Arakawa H, Buerstedde JM. Immunoglobulin gene conversion: insights from bursal B cells and the DT40 cell line. *Dev Dyn* 2004; **229**(3): 458-64.
49. Mazor Y, Yang C, Borrok MJ, et al. Enhancement of Immune Effector Functions by Modulating IgG's Intrinsic Affinity for Target Antigen. *PLoS One* 2016; **11**(6): e0157788-e.
50. Wang, de Jong, van den Bremer, et al. Molecular Basis of Assembly and Activation of Complement Component C1 in Complex with Immunoglobulin G1 and Antigen. *Mol Cell* 2016; **63**(1): 135-45.
51. Strasser J, de Jong RN, Beurskens FJ, et al. Unraveling the Macromolecular Pathways of IgG Oligomerization and Complement Activation on Antigenic Surfaces. *Nano Lett* 2019; **19**(7): 4787-96.
52. Schofield DJ, Stephenson JR, Dimmock NJ. Variations in the neutralizing and haemagglutination-inhibiting activities of five influenza A virus-specific IgGs and their antibody fragments. *J Gen Virol* 1997; **78**(10): 2431-9.
53. Wu H, Pfarr DS, Tang Y, et al. Ultra-potent Antibodies Against Respiratory Syncytial Virus: Effects of Binding Kinetics and Binding Valence on Viral Neutralization. *J Mol Biol* 2005; **350**(1): 126-44.
54. Klein JS, Gnanaprasam PN, Galimidi RP, Foglesong CP, West AP, Jr., Bjorkman PJ. Examination of the contributions of size and avidity to the neutralization mechanisms of the anti-HIV antibodies b12 and 4E10. *Proc Natl Acad Sci U S A* 2009; **106**(18): 7385-90.
55. Ofek G, Tang M, Sambor A, et al. Structure and mechanistic analysis of the anti-human immunodeficiency virus type 1 antibody 2F5 in complex with its gp41 epitope. *J Virol* 2004; **78**(19): 10724-37.
56. Zhang MY, Xiao X, Sidorov IA, et al. Identification and characterization of a new cross-reactive human immunodeficiency virus type 1-neutralizing human monoclonal antibody. *J Virol* 2004; **78**(17): 9233-42.
57. Klein JS, Bjorkman PJ. Few and Far Between: How HIV May Be Evading Antibody Avidity. *PLOS Pathog* 2010; **6**(5): e1000908.
58. Bournazos S, Klein F, Pietzsch J, Seaman MS, Nussenzweig MC, Ravetch JV. Broadly neutralizing anti-HIV-1 antibodies require Fc effector functions for in vivo activity. *Cell* 2014; **158**(6): 1243-53.
59. Hessel AJ, Hangartner L, Hunter M, et al. Fc receptor but not complement binding is important in antibody protection against HIV. *Nature* 2007; **449**(7158): 101-4.
60. van der Neut Kofschoten M, Schuurman J, Losen M, et al. Anti-Inflammatory Activity of Human IgG4 Antibodies by Dynamic Fab Arm Exchange. *Science* 2007; **317**(5844): 1554.
61. Calarese DA, Scanlan CN, Zwick MB, et al. Antibody domain exchange is an immunological solution to carbohydrate cluster recognition. *Science* 2003; **300**(5628): 2065-71.
62. Huber M, Le KM, Doores KJ, et al. Very few substitutions in a germ line antibody are required to initiate significant domain exchange. *J Virol* 2010; **84**(20): 10700-7.
63. Wu Y, West AP, Jr., Kim HJ, Thornton ME, Ward AB, Bjorkman PJ. Structural basis for enhanced HIV-1 neutralization by a dimeric immunoglobulin G form of the glycan-recognizing antibody 2G12. *Cell Rep* 2013; **5**(5): 1443-55.
64. Melis JP, Strumane K, Ruuls SR, Beurskens FJ, Schuurman J, Parren PW. Complement in therapy and disease: Regulating the complement system with antibody-based therapeutics. *Mol Immunol* 2015; **67**(2 Pt A): 117-30.
65. Reid KBM, Porter RR. Subunit composition and structure of subcomponent C1q of the first component of human complement. *Biochem J* 1976; **155**(1): 19-23.

66. Burton DR. Antibody: the flexible adaptor molecule. *Trends Biochem Sci* 1990; **15**(2): 64-9.
67. Collins C, Tsui FWL, Shulman MJ. Differential activation of human and guinea pig complement by pentameric and hexameric IgM. *Eur J Immunol* 2002; **32**(6): 1802-10.
68. Meyer S, Leusen JHW, Boross P. Regulation of complement and modulation of its activity in monoclonal antibody therapy of cancer. *mAbs* 2014; **6**(5): 1133-44.
69. Strasser J, de Jong RN, Beurskens FJ, et al. Weak Fragment Crystallizable (Fc) Domain Interactions Drive the Dynamic Assembly of IgG Oligomers upon Antigen Recognition. *ACS Nano* 2020; **14**(3): 2739-50.
70. Alduaij W, Ivanov A, Honeychurch J, et al. Novel type II anti-CD20 monoclonal antibody (GA101) evokes homotypic adhesion and actin-dependent, lysosome-mediated cell death in B-cell malignancies. *Blood* 2011; **117**(17): 4519-29.
71. Beers SA, Chan CH, French RR, Cragg MS, Glennie MJ. CD20 as a Target for Therapeutic Type I and II Monoclonal Antibodies. *Semin Hematol* 2010; **47**(2): 107-14.
72. Kumar A, Planchais C, Fronzes R, Mouquet H, Reyes N. Binding mechanisms of therapeutic antibodies to human CD20. *Science* 2020; **369**(6505): 793.
73. Oostindie SC, van der Horst HJ, Lindorfer MA, et al. CD20 and CD37 antibodies synergize to activate complement by Fc-mediated clustering. *Haematologica* 2019; **104**(9): 1841-52.
74. Dangl JL, Wensel TG, Morrison SL, Stryer L, Herzenberg LA, Oi VT. Segmental flexibility and complement fixation of genetically engineered chimeric human, rabbit and mouse antibodies. *EMBO J* 1988; **7**(7): 1989-94.
75. Tan LK, Shopes RJ, Oi VT, Morrison SL. Influence of the hinge region on complement activation, C1q binding, and segmental flexibility in chimeric human immunoglobulins. *Proc Natl Acad Sci U S A* 1990; **87**(1): 162-6.
76. Coloma MJ, Trinh KR, Wims LA, Morrison SL. The hinge as a spacer contributes to covalent assembly and is required for function of IgG. *J Immunol* 1997; **158**(2): 733.
77. Raju TS. Terminal sugars of Fc glycans influence antibody effector functions of IgGs. *Curr Opin Immunol* 2008; **20**(4): 471-8.
78. Kerr MA. The structure and function of human IgA. *Biochem J* 1990; **271**(2): 285-96.
79. Dechant M, Valerius T. IgA antibodies for cancer therapy. *Crit Rev Oncol Hematol* 2001; **39**(1): 69-77.
80. Labrijn AF, Aalberse RC, Schuurman J. When binding is enough: nonactivating antibody formats. *Curr Opin Immunol* 2008; **20**(4): 479-85.
81. Davies AM, Jefferis R, Sutton BJ. Crystal structure of deglycosylated human IgG4-Fc. *Mol Immunol* 2014; **62**(1): 46-53.
82. Bruhns P, Jönsson F. Mouse and human FcR effector functions. *Immunol Rev* 2015; **268**(1): 25-51.
83. Dhodapkar KM, Dhodapkar MV. Recruiting dendritic cells to improve antibody therapy of cancer. *Proc Natl Acad Sci U S A* 2005; **102**(18): 6243.
84. Dhodapkar MV, Geller MD, Chang DH, et al. A Reversible Defect in Natural Killer T Cell Function Characterizes the Progression of Premalignant to Malignant Multiple Myeloma. *J Exp Med* 2003; **197**(12): 1667-76.
85. Groh V, Li YQ, Cioca D, et al. Efficient cross-priming of tumor antigen-specific T cells by dendritic cells sensitized with diverse anti-MICA opsonized tumor cells. *Proc Natl Acad Sci U S A* 2005; **102**(18): 6461.
86. Boruchov AM, Heller G, Veri MC, Bonvini E, Ravetch JV, Young JW. Activating and inhibitory IgG Fc receptors on human DCs mediate opposing functions. *J Clin Invest* 2005; **115**(10): 2914-23.
87. DiLillo DJ, Ravetch JV. Differential Fc-Receptor Engagement Drives an Anti-tumor Vaccinal Effect. *Cell* 2015; **161**(5): 1035-45.

88. Richards JO, Karki S, Lazar GA, Chen H, Dang W, Desjarlais JR. Optimization of antibody binding to FcγRIIIa enhances macrophage phagocytosis of tumor cells. *Mol Cancer Ther* 2008; **7**(8): 2517.
89. Holgado MP, Sananez I, Raiden S, Geffner JR, Arruvito L. CD32 Ligation Promotes the Activation of CD4+ T Cells. *Front Immunol* 2018; **9**(2814).
90. Bruhns P, Iannascoli B, England P, et al. Specificity and affinity of human Fcγ receptors and their polymorphic variants for human IgG subclasses. *Blood* 2009; **113**(16): 3716-25.
91. Sutton BJ, Davies AM, Bax HJ, Karagiannis SN. IgE Antibodies: From Structure to Function and Clinical Translation. *Antibodies* 2019; **8**(1): 19.
92. Breedveld A, van Egmond M. IgA and FcαRI: Pathological Roles and Therapeutic Opportunities. *Front Immunol* 2019; **10**: 553-.
93. Heemskerck N, van Egmond M. Monoclonal antibody-mediated killing of tumour cells by neutrophils. *Eur J Clin Invest* 2018; **48 Suppl 2**(Suppl Suppl 2): e12962.
94. van Egmond M, Bakema JE. Neutrophils as effector cells for antibody-based immunotherapy of cancer. *Semin Cancer Biol* 2013; **23**(3): 190-9.
95. Vidarsson G, Dekkers G, Rispens T. IgG subclasses and allotypes: from structure to effector functions. *Front Immunol* 2014; **5**: 520-.
96. Preiner J, Kodera N, Tang J, et al. IgGs are made for walking on bacterial and viral surfaces. *Nat Commun* 2014; **5**(1): 4394.
97. Ben M'Barek K, Molino D, Quignard S, et al. Phagocytosis of immunoglobulin-coated emulsion droplets. *Biomaterials* 2015; **51**: 270-7.
98. Dechant M, Weisner W, Berger S, et al. Complement-Dependent Tumor Cell Lysis Triggered by Combinations of Epidermal Growth Factor Receptor Antibodies. *Cancer Res* 2008; **68**(13): 4998-5003.
99. Klausz K, Berger S, Lammerts van Bueren JJ, et al. Complement-mediated tumor-specific cell lysis by antibody combinations targeting epidermal growth factor receptor (EGFR) and its variant III (EGFRvIII). *Cancer Sci* 2011; **102**(10): 1761-8.
100. Schütze K, Petry K, Hambach J, et al. CD38-Specific Biparatopic Heavy Chain Antibodies Display Potent Complement-Dependent Cytotoxicity Against Multiple Myeloma Cells. *Front Immunol* 2018; **9**: 2553.
101. Macor P, Mezzanzanica D, Cossetti C, et al. Complement Activated by Chimeric Anti-Folate Receptor Antibodies Is an Efficient Effector System to Control Ovarian Carcinoma. *Cancer Res* 2006; **66**(7): 3876-83.
102. Oostindie SC, van der Horst HJ, Kil LP, et al. DuoHexaBody-CD37®, a novel biparatopic CD37 antibody with enhanced Fc-mediated hexamerization as a potential therapy for B-cell malignancies. *Blood Cancer J* 2020; **10**(3): 30.
103. Peschiera Ilaria, Giuliani Maria, Giusti Fabiola, et al. Structural basis for cooperativity of human monoclonal antibodies to meningococcal factor H-binding protein. *Commun Biol* 2019; **2**(1): 241-.
104. Rijkers M, Schmidt D, Lu N, et al. Anti-HLA antibodies with complementary and synergistic interaction geometries promote classical complement activation on platelets. *Haematologica* 2019; **104**(2): 403-16.
105. Steinhardt JJ, Guenaga J, Turner HL, et al. Rational design of a trispecific antibody targeting the HIV-1 Env with elevated anti-viral activity. *Nature commun* 2018; **9**(1): 877-.
106. Xu L, Pegu A, Rao E, et al. Trispecific broadly neutralizing HIV antibodies mediate potent SHIV protection in macaques. *Science* 2017; **358**(6359): 85-90.
107. Huang S, Li F, Liu H, et al. Structural and functional characterization of MBS301, an afucosylated bispecific anti-HER2 antibody. *mAbs* 2018; **10**(6): 864-75.

108. Koefoed K, Steinaa L, S oderberg JN, et al. Rational identification of an optimal antibody mixture for targeting the epidermal growth factor receptor. *mAbs* 2011; **3**(6): 584-95.
109. Wei H, Cai H, Jin Y, et al. Structural basis of a novel heterodimeric Fc for bispecific antibody production. *Oncotarget* 2017; **8**(31): 51037-49.
110. S anchez-Mart ın FJ, Bellosillo B, Gelabert-Baldrich M, et al. The First-in-class Anti-EGFR Antibody Mixture Sym004 Overcomes Cetuximab Resistance Mediated by EGFR Extracellular Domain Mutations in Colorectal Cancer. *Clin Cancer Res* 2016; **22**(13): 3260-7.
111. Baum A, Ajithdoss D, Copin R, et al. REGN-COV2 antibodies prevent and treat SARS-CoV-2 infection in rhesus macaques and hamsters. *Science* 2020: eabe2402.
112. Hansen J, Baum A, Pascal KE, et al. Studies in humanized mice and convalescent humans yield a SARS-CoV-2 antibody cocktail. *Science* 2020; **369**(6506): 1010.
113. Cohen MS. Monoclonal Antibodies to Disrupt Progression of Early Covid-19 Infection. *N Engl J Med* 2021; **384**(3): 289-91.
114. Baum A, Fulton BO, Wloga E, et al. Antibody cocktail to SARS-CoV-2 spike protein prevents rapid mutational escape seen with individual antibodies. *Science* 2020; **369**(6506): 1014.
115. Mulangu S, Dodd LE, Davey RT, et al. A Randomized, Controlled Trial of Ebola Virus Disease Therapeutics. *N Engl J Med* 2019; **381**(24): 2293-303.
116. Jacobsen HJ, Poulsen TT, Dahlman A, et al. Pan-HER, an Antibody Mixture Simultaneously Targeting EGFR, HER2, and HER3, Effectively Overcomes Tumor Heterogeneity and Plasticity. *Clin Cancer Res* 2015; **21**(18): 4110-22.
117. Deshaies RJ. Multispecific drugs herald a new era of biopharmaceutical innovation. *Nature* 2020; **580**(7803): 329-38.
118. Clynes RA, Desjarlais JR. Redirected T Cell Cytotoxicity in Cancer Therapy. *Annu Rev Med* 2019; **70**(1): 437-50.
119. Slaga D, Ellerman D, Lombana TN, et al. Avidity-based binding to HER2 results in selective killing of HER2-overexpressing cells by anti-HER2/CD3. *Sci Transl Med* 2018; **10**(463): eaat5775.
120. Grugan KD, Dorn K, Jarantow SW, et al. Fc-mediated activity of EGFR x c-Met bispecific antibody JNJ-61186372 enhanced killing of lung cancer cells. *mAbs* 2017; **9**(1): 114-26.
121. Lameris R, Shahine A, Pellicci DG, et al. A single-domain bispecific antibody targeting CD1d and the NKT T-cell receptor induces a potent antitumor response. *Nat Cancer* 2020; **1**(11): 1054-65.
122. K ugler M, Stein C, Kellner C, et al. A recombinant trispecific single-chain Fv derivative directed against CD123 and CD33 mediates effective elimination of acute myeloid leukaemia cells by dual targeting. *Br J Haematol* 2010; **150**(5): 574-86.
123. Wu L, Seung E, Xu L, et al. Trispecific antibodies enhance the therapeutic efficacy of tumor-directed T cells through T cell receptor co-stimulation. *Nature Cancer* 2020; **1**(1): 86-98.
124. Shivange, Urbanek, Przanowski, et al. A Single-Agent Dual-Specificity Targeting of FOLR1 and DR5 as an Effective Strategy for Ovarian Cancer. *Cancer Cell* 2018; **34**(2): 331-45.e11.
125. Goulet DR, Zwolak A, Williams JA, Chiu ML, Atkins WM. Design and characterization of novel dual Fc antibody with enhanced avidity for Fc receptors. *Proteins* 2019.
126. Jain A, Poonia B, So EC, et al. Tumour antigen targeted monoclonal antibodies incorporating a novel multimerisation domain significantly enhance antibody dependent cellular cytotoxicity against colon cancer. *Eur J Cancer* 2013; **49**(15): 3344-52.
127. Rowley Tania, Peters Shirley, Aylott Mike, et al. Engineered hexavalent Fc proteins with enhanced Fc-gamma receptor avidity provide insights into immune-complex interactions. *Proc Natl Acad Sci U S A* 2018; **1**(1): 146-.

128. Zhang X, Olsen HS, Chen S, et al. Anti-CD20 Antibody with Multimerized Fc Domains: A Novel Strategy To Deplete B Cells and Augment Treatment of Autoimmune Disease. *J Immunol* 2016; **196**(3): 1165-76.
129. Miller A, Carr S, Rabbitts T, Ali H. Multimeric antibodies with increased valency surpassing functional affinity and potency thresholds using novel formats. *mAbs* 2020; **12**(1): 1752529.
130. Smith RI, Coloma MJ, Morrison SL. Addition of a mu-tailpiece to IgG results in polymeric antibodies with enhanced effector functions including complement-mediated cytotoxicity by IgG4. *J Immunol* 1995; **154**(5): 2226-36.
131. de Jong RN, Beurskens FJ, Verploegen S, et al. A Novel Platform for the Potentiation of Therapeutic Antibodies Based on Antigen-Dependent Formation of IgG Hexamers at the Cell Surface. *PLoS Biol* 2016; **14**(1): e1002344.
132. Cook EM, Lindorfer MA, van der Horst H, et al. Antibodies That Efficiently Form Hexamers upon Antigen Binding Can Induce Complement-Dependent Cytotoxicity under Complement-Limiting Conditions. *J Immunol* 2016; **197**(5): 1762-75.
133. Li F, Ravetch JV. Apoptotic and antitumor activity of death receptor antibodies require inhibitory Fcγ receptor engagement. *Proc Natl Acad Sci U S A* 2012; **109**(27): 10966-71.
134. White AL, Chan HT, Roghanian A, et al. Interaction with FcγRIIB is critical for the agonistic activity of anti-CD40 monoclonal antibody. *J Immunol* 2011; **187**(4): 1754-63.
135. Wilson NS, Yang B, Yang A, et al. An Fcγ receptor-dependent mechanism drives antibody-mediated target-receptor signaling in cancer cells. *Cancer Cell* 2011; **19**(1): 101-13.
136. Miller K, Meng G, Liu J, et al. Design, Construction, and In Vitro Analyses of Multivalent Antibodies. *J Immunol* 2003; **170**(9): 4854-61.
137. Overdijk MB, Strumane K, Beurskens FJ, et al. Dual Epitope Targeting and Enhanced Hexamerization by DR5 Antibodies as a Novel Approach to Induce Potent Antitumor Activity Through DR5 Agonism. *Mol Cancer Ther* 2020; **19**(10): 2126.
138. Zhang D, Armstrong AA, Tam SH, et al. Functional optimization of agonistic antibodies to OX40 receptor with novel Fc mutations to promote antibody multimerization. *mAbs* 2017; **9**(7): 1129-42.
139. Zhang D, Goldberg MV, Chiu ML. Fc Engineering Approaches to Enhance the Agonism and Effector Functions of an Anti-OX40 Antibody. *J Biol Chem* 2016; **291**(53): 27134-46.
140. Gieffers C, Kluge M, Merz C, et al. APG350 induces superior clustering of TRAIL receptors and shows therapeutic antitumor efficacy independent of cross-linking via Fcγ receptors. *Mol Cancer Ther* 2013; **12**(12): 2735-47.
141. Liu H, Su D, Zhang J, et al. Improvement of Pharmacokinetic Profile of TRAIL via Trimer-Tag Enhances its Antitumor Activity in vivo. *Sci Rep* 2017; **7**(1): 8953.
142. Piao X, Ozawa T, Hamana H, et al. TRAIL-receptor 1 IgM antibodies strongly induce apoptosis in human cancer cells in vitro and in vivo. *Oncoimmunology* 2016; **5**(5): e1131380.
143. Yang Y, Yeh SH, Madireddi S, et al. Tetravalent biepitopic targeting enables intrinsic antibody agonism of tumor necrosis factor receptor superfamily members. *mAbs* 2019; **11**(6): 996-1011.
144. Merz C, Sykora J, Marschall V, et al. The Hexavalent CD40 Agonist HERA-CD40L Induces T-Cell-mediated Antitumor Immune Response Through Activation of Antigen-presenting Cells. *J Immunother* 2018; **41**(9): 385-98.
145. Richards DM, Marschall V, Billian-Frey K, et al. HERA-GITRL activates T cells and promotes anti-tumor efficacy independent of FcγR-binding functionality. *J Immunother Cancer* 2019; **7**(1): 191-.
146. Thiemann M, Richards DM, Heinonen K, et al. A Single-Chain-Based Hexavalent CD27 Agonist Enhances T Cell Activation and Induces Anti-Tumor Immunity. *Front Oncol* 2018; **8**: 387.



147. Leusen JH. IgA as therapeutic antibody. *Mol Immunol* 2015; **68**(1): 35-9.
148. van Tetering G, Evers M, Chan C, Stip M, Leusen J. Fc Engineering Strategies to Advance IgA Antibodies as Therapeutic Agents. *Antibodies* 2020; **9**(4).
149. Chen Y, Paluch M, Zorn JA, et al. Targeted IgMs agonize ocular targets with extended vitreal exposure. *mAbs* 2020; **12**(1): 1818436.
150. de Miguel D, Lemke J, Anel A, Walczak H, Martinez-Lostao L. Onto better TRAILs for cancer treatment. *Cell Death Differ* 2016; **23**(5): 733-47.
151. von Karstedt S, Montinaro A, Walczak H. Exploring the TRAILs less travelled: TRAIL in cancer biology and therapy. *Nat Rev Cancer* 2017; **17**(6): 352-66.
152. Natsume A, In M, Takamura H, et al. Engineered antibodies of IgG1/IgG3 mixed isotype with enhanced cytotoxic activities. *Cancer Res* 2008; **68**(10): 3863-72.
153. Natsume A, Shimizu-Yokoyama Y, Satoh M, Shitara K, Niwa R. Engineered anti-CD20 antibodies with enhanced complement-activating capacity mediate potent anti-lymphoma activity. *Cancer Sci* 2009; **100**(12): 2411-8.
154. Sensel MG, Kane LM, Morrison SL. Amino acid differences in the N-terminus of C(H)2 influence the relative abilities of IgG2 and IgG3 to activate complement. *Mol Immunol* 1997; **34**(14): 1019-29.
155. Xu Y, Oomen R, Klein MH. Residue at position 331 in the IgG1 and IgG4 CH2 domains contributes to their differential ability to bind and activate complement. *J Biol Chem* 1994; **269**(5): 3469-74.
156. Idusogie EE, Presta LG, Gazzano-Santoro H, et al. Mapping of the C1q binding site on rituxan, a chimeric antibody with a human IgG1 Fc. *J Immunol* 2000; **164**(8): 4178-84.
157. Dall'Acqua WF, Cook KE, Damschroder MM, Woods RM, Wu H. Modulation of the Effector Functions of a Human IgG1 through Engineering of Its Hinge Region. *J Immunol* 2006; **177**(2): 1129.
158. Idusogie EE, Wong PY, Presta LG, et al. Engineered antibodies with increased activity to recruit complement. *J Immunol* 2001; **166**(4): 2571-5.
159. Michaelsen TE, Sandlie I, Bratlie DB, Sandin RH, Ihle O. Structural difference in the complement activation site of human IgG1 and IgG3. *Scand J Immunol* 2009; **70**(6): 553-64.
160. Moore GL, Chen H, Karki S, Lazar GA. Engineered Fc variant antibodies with enhanced ability to recruit complement and mediate effector functions. *mAbs* 2010; **2**(2): 181-9.
161. Lazar GA, Dang W, Karki S, et al. Engineered antibody Fc variants with enhanced effector function. *Proc Natl Acad Sci U S A* 2006; **103**(11): 4005-10.
162. Shields RL, Namenuk AK, Hong K, et al. High resolution mapping of the binding site on human IgG1 for Fc gamma RI, Fc gamma RII, Fc gamma RIII, and FcRn and design of IgG1 variants with improved binding to the Fc gamma R. *J Biol Chem* 2001; **276**(9): 6591-604.
163. Chu SY, Vostiar I, Karki S, et al. Inhibition of B cell receptor-mediated activation of primary human B cells by coengagement of CD19 and FcγRIIb with Fc-engineered antibodies. *Mol Immunol* 2008; **45**(15): 3926-33.
164. Mimoto F, Igawa T, Kuramochi T, et al. Novel asymmetrically engineered antibody Fc variant with superior FcγR binding affinity and specificity compared with afucosylated Fc variant. *mAbs* 2013; **5**(2): 229-36.
165. Mimoto F, Katada H, Kadono S, et al. Engineered antibody Fc variant with selectively enhanced FcγRIIb binding over both FcγRIIa(R131) and FcγRIIa(H131). *Protein Eng Des Sel* 2013; **26**(10): 589-98.
166. Iwayanagi Y, Igawa T, Maeda A, et al. Inhibitory FcγRIIb-Mediated Soluble Antigen Clearance from Plasma by a pH-Dependent Antigen-Binding Antibody and Its Enhancement by Fc Engineering. *J Immunol* 2015; **195**(7): 3198-205.

167. Sampei Z, Haraya K, Tachibana T, et al. Antibody engineering to generate SKY59, a long-acting anti-C5 recycling antibody. *PLoS One* 2018; **13**(12): e0209509.
168. Nordstrom JL, Gorlatov S, Zhang W, et al. Anti-tumor activity and toxicokinetics analysis of MGAH22, an anti-HER2 monoclonal antibody with enhanced Fcγ receptor binding properties. *Breast Cancer Res* 2011; **13**(6): R123.
169. Rugo HS, Im SA, Cardoso F, et al. Efficacy of Margetuximab vs Trastuzumab in Patients With Pretreated ERBB2-Positive Advanced Breast Cancer: A Phase 3 Randomized Clinical Trial. *JAMA Oncol* 2021.
170. Niwa R, Shoji-Hosaka E, Sakurada M, et al. Defucosylated chimeric anti-CC chemokine receptor 4 IgG1 with enhanced antibody-dependent cellular cytotoxicity shows potent therapeutic activity to T-cell leukemia and lymphoma. *Cancer Res* 2004; **64**(6): 2127-33.
171. Ollila TA, Sahin I, Olszewski AJ. Mogamulizumab: a new tool for management of cutaneous T-cell lymphoma. *Onco Targets Ther* 2019; **12**: 1085-94.
172. Tobinai K, Klein C, Oya N, Fingerle-Rowson G. A Review of Obinutuzumab (GA101), a Novel Type II Anti-CD20 Monoclonal Antibody, for the Treatment of Patients with B-Cell Malignancies. *Adv Ther* 2017; **34**(2): 324-56.
173. Ghazi A, Trikha A, Calhoun WJ. Benralizumab--a humanized mAb to IL-5Ra with enhanced antibody-dependent cell-mediated cytotoxicity--a novel approach for the treatment of asthma. *Expert Opin Biol Ther* 2012; **12**(1): 113-8.
174. Kolbeck R, Kozhich A, Koike M, et al. MEDI-563, a humanized anti-IL-5 receptor alpha mAb with enhanced antibody-dependent cell-mediated cytotoxicity function. *J Allergy Clin Immunol* 2010; **125**(6): 1344-53.e2.
175. Vijayaraghavan S, Lipfert L, Chevalier K, et al. Amivantamab (JNJ-61186372), an Fc Enhanced EGFR/cMet Bispecific Antibody, Induces Receptor Downmodulation and Antitumor Activity by Monocyte/Macrophage Trophocytosis. *Mol Cancer Ther* 2020; **19**(10): 2044-56.
176. Bournazos S, Corti D, Virgin HW, Ravetch JV. Fc-optimized antibodies elicit CD8 immunity to viral respiratory infection. *Nature* 2020; **588**(7838): 485-90.
177. Guo L, Wei R, Lin Y, Kwok HF. Clinical and Recent Patents Applications of PD-1/PD-L1 Targeting Immunotherapy in Cancer Treatment-Current Progress, Strategy, and Future Perspective. *Front Immunol* 2020; **11**: 1508-.
178. Müller R, Gräwert MA, Kern T, et al. High-resolution structures of the IgM Fc domains reveal principles of its hexamer formation. *Proc Natl Acad Sci U S A* 2013; **110**(25): 10183.
179. Sharp TH, Boyle AL, Diebolder CA, Kros A, Koster AJ, Gros P. Insights into IgM-mediated complement activation based on in situ structures of IgM-C1-C4b. *Proc Natl Acad Sci U S A* 2019; **116**(24): 11900.
180. Redpath S, Michaelsen TE, Sandie I, Clark MR. The influence of the hinge region length in binding of human IgG to human Fcγ receptors. *Hum Immunol* 1998; **59**(11): 720-7.
181. Hobeika E, Maity PC, Jumaa H. Control of B Cell Responsiveness by Isotype and Structural Elements of the Antigen Receptor. *Trends Immunol* 2016; **37**(5): 310-20.
182. Übelhart R, Hug E, Bach MP, et al. Responsiveness of B cells is regulated by the hinge region of IgD. *Nat Immunol* 2015; **16**(5): 534-43.
183. Breedveld A, van Egmond M. IgA and FcαRI: Pathological Roles and Therapeutic Opportunities. *Front Immunol* 2019; **10**(553).
184. Shade KT, Platzer B, Washburn N, et al. A single glycan on IgE is indispensable for initiation of anaphylaxis. *J Exp Med* 2015; **212**(4): 457-67.
185. Kubo S, Nakayama T, Matsuoka K, Yonekawa H, Karasuyama H. Long term maintenance of IgE-mediated memory in mast cells in the absence of detectable serum IgE. *J Immunol* 2003; **170**(2): 775-80.





## GENERAL DISCUSSION

Antibodies represent a class of therapeutic agents that revolutionized the development of ‘targeted therapies’ against disease. In contrast to most small molecule drugs, which often are more prone to off-target adverse effects, antibodies are highly target-specific and capable of efficiently interacting with the host immune system. Owing to their modular and highly adaptable architecture, relatively predictable developability and favorable pharmacokinetics, they are also highly suitable for engineering into formats with novel functionalities, improved drug safety or increased potency. Nevertheless, optimally designing and tuning effector functions towards a desired outcome and ‘improving on nature’ by mimicking the full potential of antibody functional activity as observed in natural immunity is not straightforward. Understanding the key determinants that govern efficient effector function activation is thereby crucial in the design of novel and more efficacious antibody-based therapies. One of the factors central to efficient effector function activation is the accumulated strength, or ‘avidity’ of binding interactions between antibodies and their target (**Chapter 6**). The aim of this thesis was to explore the role of antibody avidity interactions, and more specifically the importance of ‘ordered clustering’, in antibody mechanisms of action and to apply the knowledge obtained in designing novel and improved antibody-based therapeutics.

### **Enhancing therapeutic antibody function: (hetero-) hexamerization**

Antibody-mediated activation of the classical complement pathway represents a powerful effector mechanism that triggers killing of the target cell via complement-dependent cytotoxicity (CDC). Moreover, intermediates in the complement cascade can act as anaphylatoxins with potent chemoattractant properties, and opsonins that recruit and activate immune effector cells<sup>1</sup>. Complement is activated through binding of C1q to antigen-bound IgM or IgG antibodies. High avidity binding of C1q to IgG molecules requires oligomerization of neighboring IgG Fc regions into ordered hexameric arrangements via specific non-covalent Fc-Fc interactions<sup>2</sup>. Many monoclonal IgG antibodies are insufficiently capable of

hexamerization and CDC induction, which relates to multiple factors *inter alia* including target biology, target density, epitope specificity and overcoming target cell complement protection and resistance. It is now demonstrated that monoclonal antibodies (mAbs) targeting two different cell surface antigens may cooperate in complement activation through the formation of hetero-hexamers (**Chapter 2**). In addition to CD20, CD37 is abundantly expressed on malignant B cells and membrane-bound CD20 and CD37 antibodies were shown to colocalize by forming mixed hexameric complexes and synergize in CDC activity. Previously, it was demonstrated that antibody hexamer formation and complement activation could be increased by introducing specific point mutations, such as E430G and E345K, in the Fc domain<sup>3</sup>. These mutant antibody variants potentiated or enhanced CDC of tumor cells expressing a range of different target antigens including CD20, CD38, CD52 and EGFR. Likewise, while wild-type (WT) IgG mAbs targeting CD37 are poor inducers of CDC, introduction of the E430G hexamerization-enhancing mutation substantially potentiated CDC of malignant B cells (**Chapter 2 & 3**). In addition, we showed that the E430G mutation further increased antibody colocalization, hetero-hexamers and complement activation by combinations of CD20 and CD37 mAbs (**Chapter 2**). These results may have clinical relevance for combination therapies, as enhancing antibody Fc-Fc interactions to bring different cell surface receptors in close proximity could potentially broaden the combinatorial therapeutic target space. In this respect, understanding antibody structural characteristics in combination with target receptor biology and distribution are key in the development of effective antibody combination therapies. How different antibody formats may impact function is discussed in the next paragraphs.

### **Enhancing therapeutic antibody function: the impact of different Fc formats**

In cancer, complement activation has been demonstrated to contribute to the tumor cell kill mediated by therapeutic antibodies targeting various cell surface receptors expressed on hematologic tumor cells including CD20, CD38 and CD52<sup>4-6</sup>. Different CD20-targeting antibodies have been developed for treatment of B-cell malignancies including rituximab, ofatumumab and obinutuzumab, all of which vary in their capacity to activate complement. CD20 antibodies are generally classified as type I or type II, each type exhibiting distinct binding and functional characteristics<sup>7</sup>. Type I CD20 antibodies including rituximab and ofatumumab bind CD20 dimers in a 2:2 stoichiometry (2 Fabs per CD20 dimer)<sup>8,9</sup>. This antibody binding orientation may lead to rapid CD20 concatenation and antibody hexamerization, thereby facilitating efficient complement activation<sup>10</sup>. The next-generation CD20 antibody ofatumumab activates complement more effectively than rituximab by binding a CD20 epitope located closer to the cell membrane, thereby allowing more efficient C1q binding and complement deposition<sup>11</sup>. By contrast, the type II CD20 antibody

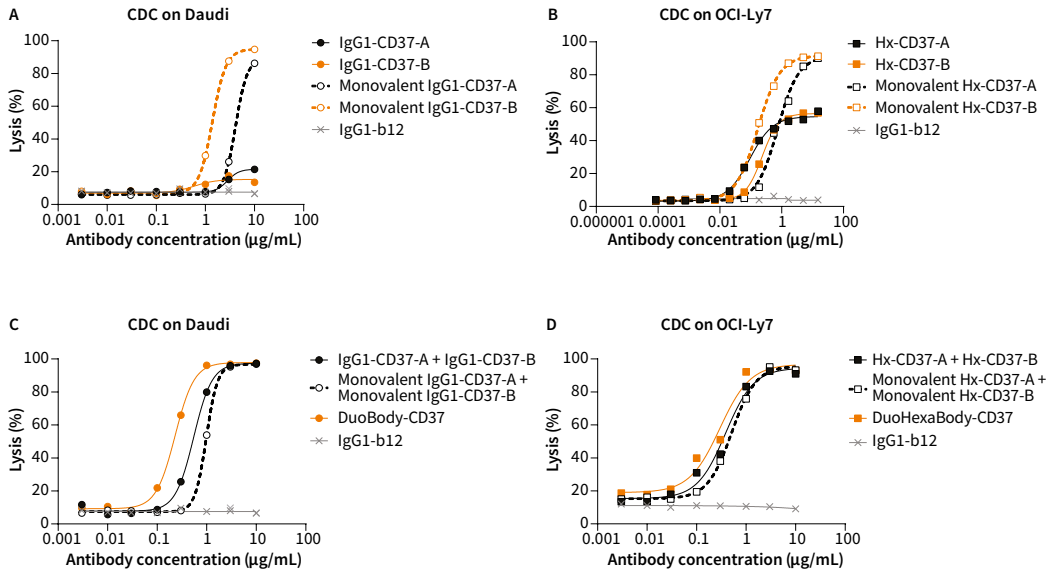
obinutuzumab only weakly activates complement, presumably due to binding CD20 in a 2:1 stoichiometry (1 Fab per dimer) that results in steric hindrance between Fabs and a decreased ability to form hexameric complexes<sup>8,9</sup>.

Targeting of alternative B-cell antigens has also been explored, including the tetraspanin plasma membrane protein CD37. Like CD20, CD37 is mainly expressed on mature B cells and B cell-derived malignancies and represents an attractive target for novel antibody therapies<sup>12-15</sup>. While to date, multiple CD37-targeting antibodies have been described, none of these reported potent activation of the complement cascade<sup>16</sup>. Based on our previous observation that CDC by CD37 antibodies could be potentiated by enhanced antibody clustering via a single point mutation E430G in the IgG Fc domain (**Chapter 2**), I sought to investigate the therapeutic potential of this antibody technology platform. In **Chapter 3**, the generation and characterization of a panel of CD37 antibodies containing an E430G mutation in the Fc domain is described. The mutation was added in an effort to optimize CD37 antibodies to engage in multiple effector mechanisms, specifically potent CDC. During lead candidate selection, multiple CD37 antibody clones exhibiting potent CDC activity were identified, some of which were able to bind CD37 simultaneously despite the relatively small extracellular domain (151 amino acids). Efficient CDC induction depends on locally increasing the density of IgG Fc domains, thereby facilitating enhanced Fc-Fc interactions and efficient antibody hexamerization. In that respect, increasing CD37 target binding by combining non-crossblocking CD37 antibodies, either as antibody mixtures or in a biparatopic (bispecific) configuration, appeared a promising approach to further enhance CDC. Therefore as a next step, single CD37 antibodies, combinations of non-crossblocking CD37 antibodies and biparatopic (bispecific) CD37 antibody variants were systematically evaluated for their CDC-inducing capacity. Surprisingly, the biparatopic (bispecific) CD37 antibody variant, Duo-HexaBody-CD37, outperformed all other antibody variants evaluated both *in vitro* and *ex vivo*. This superior CDC activity was attributed to a combination of dual epitope targeting and enhanced antibody hexamerization in the context of the E430G Fc mutation.

The superior CDC efficacy of the biparatopic (bispecific) CD37 antibody compared to a combination of two non-crossblocking antibodies, especially in relapsed/refractory primary chronic lymphocytic leukemia (CLL) patient samples, raised questions about the binding mechanism of the bispecific and whether hexamer formation could be favored in certain binding configurations. Cryo-electron tomography illustrated that the optimal docking platform for C1q consists of six monovalently-bound antibodies arranged into a hexameric complex through Fc-Fc interactions<sup>2</sup>. I therefore hypothesized a preferred role for monovalent antibody binding in antibody hexamer formation and

tested different WT or hexamerization-enhanced (Hx) functionally monovalent CD37 antibody variants (one CD37-binding Fab-arm and one non-binding IgG-b12 Fab-arm in a bispecific configuration) and combinations thereof in CDC assays. Interestingly, functionally monovalent variants of both WT (IgG1-) and HexaBody (Hx-) CD37 antibodies showed enhanced CDC activity compared to their bivalent counterparts (Figure 1 A-B), suggesting that monovalent binding enables more efficient Fc-Fc-mediated hexamerization and CDC. Potentiated CDC activity has previously been reported for functionally monovalent bispecific antibody variants targeting EGFR on solid tumor cells<sup>2</sup>. In experiments comparing combinations of IgG1- or Hx-CD37 antibodies targeting non-overlapping epitopes, either bivalent or functionally monovalent, CDC potency was highly comparable (Figure 1 C-D). Minor differences in EC50 values between functionally monovalent mixtures versus bivalent antibody mixtures are most likely caused by the availability of CD37 binding arms. Furthermore, IgG1 and Hx biparatopic (bispecific) antibody variants (bsAb-CD37 and DuoHexaBody-CD37 respectively) showed at least comparable or increased CDC activity compared to the respective bivalent or monovalent binding CD37 antibody combinations. Overall, monovalent rather than bivalent antibody binding appears to contribute to enhanced CDC potency, both in the context of IgG1- and Hx-CD37 antibody variants. In case of bivalent CD37 antibody combinations targeting non-overlapping CD37 epitopes, I cannot exclude that these also drive monovalent binding. Strasser et al. recently reported that bivalent-binding antibodies might sterically suppress Fc-Fc interactions occurring through lateral diffusion across cell surfaces<sup>17</sup>. In IgG1- or Hx-CD37 antibody combinations targeting non-overlapping CD37 epitopes, binding competition may also sterically suppress bivalent antibody binding and conversely promote monovalent antibody binding and lateral diffusion. Here, the interplay between antibody affinity and multiple levels of avidity interactions are key determinants of the functional outcome (**Chapter 6**). Antibodies with higher affinities (i.e. bivalent) have slower off rates, which promote avidity interactions through multivalent antibody binding, but may thwart the assembly into higher order avidity structures. Conversely, lower affinity (i.e. monovalent) antibodies have faster off rates that may preclude multivalent binding interactions. They can however, promote higher order avidity structures through efficient Fc-Fc interactions, resulting in the formation hexameric complexes that provide sufficient avidity for subsequent C1q binding. Similarly, mimicking polyclonal antibody binding through multi epitope targeting may add an additional level of complexity to avidity interactions and the resulting functional response. Thus, optimally balancing multiple levels of antibody avidity including 1) binding or first order avidity (monovalent versus bivalent interactions), 2) higher order avidity (functional interactions with effector molecules) and 3) cooperative avidity (result of polyclonal binding on





▲ **Figure 1**

**Effect of monovalent binding, enhanced hexamerization and dual epitope targeting on the CDC activity of CD37 antibodies.**

CD37-A and CD37-B represent different humanized CD37 antibody clones (010 and 016 respectively) binding non-overlapping epitopes on CD37. Functionally monovalent variants of both WT IgG1 and Hx-CD37 antibodies were generated through controlled Fab-arm exchange with a non-binding IgG1-ctrl arm (IgG1-b12). IgG1-b12 served as a non-binding control antibody. Daudi and OCI-Ly7 cells express a mean of 227.832 and 99.654 CD37 copies/cell respectively. (A) Comparing CDC activity between bivalent wild-type (WT) IgG1-CD37 and functionally monovalent IgG1-CD37 antibody variants on Daudi cells. (B) Comparing CDC activity between bivalent hexamerization-enhanced (Hx)-CD37 and functionally monovalent Hx-CD37 antibody variants on OCI-Ly7 cells. (C) Comparing CDC activity among combinations of bivalent WT IgG1-CD37 antibodies, combinations of functionally monovalent WT IgG1-CD37 antibodies and biparatopic (bispecific) WT IgG1-CD37 antibodies (BsAb-CD37) expressed on Daudi cells. (D) Comparing CDC activity among combinations of bivalent Hx-CD37 antibodies, combinations of functionally monovalent Hx-CD37 antibodies and biparatopic (bispecific) Hx-CD37 antibodies (DuoHexaBody-CD37) expressed on OCI-Ly7 cells. Data shown are representative of three repeat experiments.

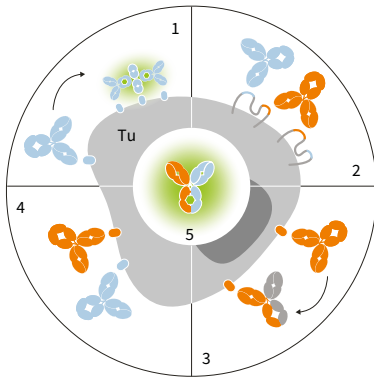
functional interactions), is crucial in understanding antibody mechanisms of action and designing more effective antibody therapeutics.

In conclusion, the superior CDC activity observed for DuoHexaBody-CD37 may be driven by efficient hexamerization facilitated by monovalent binding of the Fab arms to distinct CD37 epitopes (i.e. two antibody molecules monovalently-bound to one CD37 antigen), which is further enhanced through the E430G mutation. Monovalent antibody binding potentially driving IgG oligomerization and effector function activation, by optimally balancing affinity and avidity interactions, is an important observation with wider implications for antibody-based drug discovery.

The unique CDC-inducing capacity and ex vivo therapeutic potential of DuoHexaBody-CD37 was further evaluated in **Chapter 4**, in which potent complement-mediated tumor cell kill was observed in primary CLL and B cell non-Hodgkin's lymphoma patient samples irrespective of the patients' relapse status, prior treatments or malignancy subtype. Additionally, and consistent with observations in **Chapter 2**, combining DuoHexaBody-CD37 with rituximab or ofatumumab significantly enhanced tumor cell kill in patient samples with intermediate to low sensitivity to DuoHexaBody-CD37-mediated CDC. Notably, CD37 and CD20 expression levels substantially differed in experiments performed using tumor cell lines (**Chapter 2** and **Chapter 3**) versus experiments performed using primary patient cells (**Chapter 4**). In cell lines, DuoHexaBody-CD37-mediated CDC was generally most potent at CD37 expression levels above 100,000 molecules/cell. By contrast, the CD37 expression threshold for DuoHexaBody-CD37-mediated CDC was substantially lower in primary patient cells that expressed a median of 35,000 molecules/cell. The superior potency of DuoHexaBody-CD37 was also more prominent in primary patient cells rather than tumor cell lines, which may be attributed to differences in complement regulatory protein levels, receptor density, cell size, or the spatial organization of CD37 and associated proteins in tetraspanin-enriched micro domains in the cell membrane<sup>10,18,19</sup>. Furthermore, WT IgG1 antibodies generally require higher antigen expression levels for effective initiation of CDC<sup>17,20,21</sup>. These data suggests that multiple antibody engineering strategies including 1) enhancing IgG Fc-Fc interactions through the E430G mutation, 2) dual-epitope targeting, 3) monovalent antibody binding and 4) targeting multiple cell surface antigens or (5) a combination of these strategies, may enhance antibody and/or target clustering and thereby lower the threshold for complement activation (Figure 2). DuoHexaBody-CD37 uniquely combines the E430G Fc mutation and dual epitope targeting in a biparatopic (bispecific) antibody to potentiate CDC as an additional effector mechanism and illustrates how systematic evaluation of different antibody format technologies may positively impact the selection of lead compounds with broader mechanism of action and therapeutic function. The potent anti-tumor activity observed *in vitro*, *ex vivo* and *in vivo* provided the rationale to initiate a phase 1/2 first-in-human clinical trial to assess the clinical safety and preliminary efficacy of DuoHexaBody-CD37 in patients with hematologic malignancies (NCT04358458).

### **Enhancing therapeutic antibody function: ordered clustering as a tool for modular therapeutic design**

Despite their modular and highly adaptable architecture, the vast majority of current antibody engineering strategies are aimed at designing antibody therapeutics acting as single molecular entities. As reviewed in **Chapter 6**, the polyclonality of natural antibody immune responses that effectively exploit



◀ **Figure 2**

**Engineering strategies to enhance antibody (-mediated) clustering and complement activation.**

1) Enhancing IgG hexamerization using an E430G Fc mutation. 2) Dual-epitope targeting. 3) Monovalent antibody binding. 4) Targeting multiple cell surface antigens. (5) A combination of aforementioned engineering strategies, here illustrated as a biparatopic/dual-targeting hexamerization-enhanced antibody molecule.

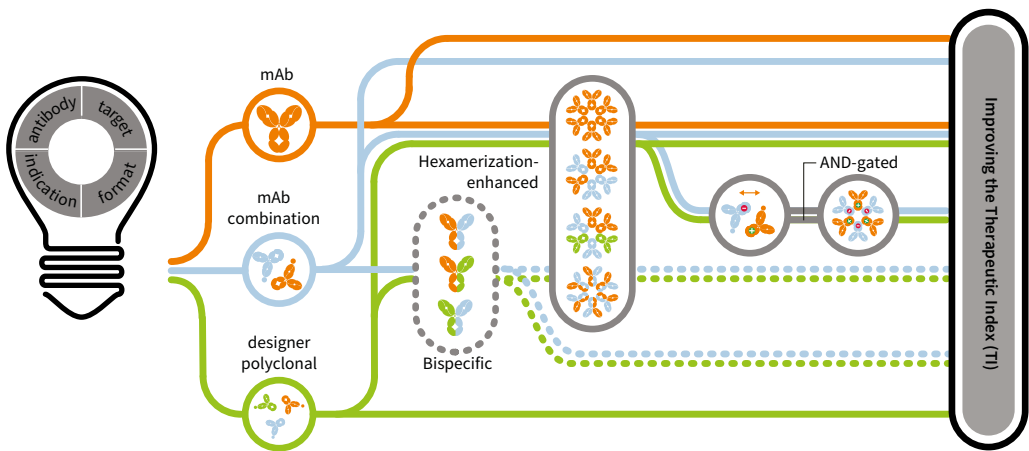
immune complexation by conjoining multiple affinities, valencies and binding specificities, argues for more effort towards rational design of combinatorial therapeutic approaches. Rational designer polyclonals for instance, represent a next frontier for therapeutic development. In **Chapter 2**, the therapeutic potential of such combinatorial approaches was illustrated by IgGs targeting different cell surface antigens that co-engaged in mixed hexameric complexes through non-covalent interactions between Fc domains. These observations laid the foundation for a novel antibody technology based on minimally engineered antibody combinations with molecular Fc interfaces designed to assemble into teams only if both components are bound to the same cell (**Chapter 5**). It is shown how IgG hetero-oligomerization and functional activation can be made dependent on the presence of two antibody components by introducing specific point mutations to modulate Fc-Fc interactions between these two components, C1q and Fc gamma receptor interactions. By requiring a combination of two input signals to license activation of a functional output signal, these antibody pairs act as a biologic equivalent of Boolean logic AND gates that allow for precisely tuning and restricting IgG avidity interactions and subsequent complex formation to preferred cell surfaces. Furthermore, this AND-gated approach may access a broader range of tumor or immune surface target molecules, of which expression is not sufficiently differentiated from healthy cells. A major challenge for potential therapeutic applications of mutually dependent antibody combinations is identifying cell surface receptors that co-localize and/or allow for antibody hetero-hexamerization after target binding. Compatibility with antibody hetero-hexamer formation is heavily influenced by individual target biological constraints including size, epitope, abundance, density, mobility, epitope-membrane distance and spatial organization<sup>9,11,20,22</sup>. While successful development of therapeutic antibodies relies on a thorough understanding of antibody and target biology, it is not trivial to predict which combination of antibody and format yields the most successful antibody drug candidate. The ‘plug and play’ nature of the Fc mutations that

form the basis of this antibody technology are readily applicable to combinatorial, high throughput screening of novel antibody target combinations to support drug development.

### Perspectives

As discussed in this thesis and reviewed in **Chapter 6**, efficient triggering of antibody effector functions requires multivalent target binding and clustering of IgG molecules on the cell surface. Clustering of IgG molecules may provide an 'avid docking surface' that serves as a threshold for the subsequent binding and activation of immune effector molecules. In natural biology, antibody immune responses are polyclonal and highly efficient at establishing avidity interactions through the generation of antibodies with different affinities, valencies and (multi-epitope) binding specificities. A broad spectrum of novel antibody engineering strategies and formats are emerging that exploit antibody clustering mechanisms to optimally engage 'classical' effector functions including activation of complement and Fc receptors and enable novel therapeutic mechanisms<sup>23-26</sup>. Engineering strategies focusing on some of the strengths offered by polyclonals, including valency tuning via enhanced IgG oligomerization or creating functionally monovalent antibodies and tuning binding specificities by targeting multiple cell surface receptors or epitopes, may allow for more precisely coordinating and potentiating antibody functional responses. It is additionally demonstrated that distinct avidity engineering approaches might be combined to optimally engage antibody effector functions to achieve 'incremental' avidity effects. Nonetheless, the development of increasingly complex antibody architectures and combinatorial designs requires close monitoring of the balance between efficacy and safety, also referred to as the therapeutic index (TI). The TI for antibodies exploiting classical effector functions including rituximab, ofatumumab, obinutuzumab and daratumumab is often broad and relatively well established, however the effect of potentiating such effector functions on the TI is not always known. The recently initiated first-in-human trial for DuoHexaBody-CD37 may provide novel insights into how effector function potentiation impacts the TI. By contrast, the TI is often small and less well characterized for increasingly complex antibody formats including CD3 bispecifics and antibody-drug conjugates, as well as antibodies directed towards immuno-oncology targets such as checkpoint inhibitors. Improving the TI by optimizing on-target efficacy and/or decreasing off-target toxicity may broaden the applicability of such antibody formats. Optimizing the antibody TI however, is challenging and requires a thorough understanding of the corresponding disease biology, its underlying mechanisms and targets, combined with antibody format characteristics. These factors are all regarded as critical components for transformative antibody therapeutics and emphasize the importance of studying antibody structure-function relations and antibody interactions with their antigen to

move product ideation. In this thesis, it was demonstrated that exploiting antibody clustering through Fc engineering and/or multi-targeting approaches represents a promising strategy to enhance antibody efficacy and/or decrease off-target toxicity. These different approaches have been summarized and presented as a road map for next-generation drug development in **Figure 3**. Improving the understanding of which type of targets and effector functions can be exploited by antibody clustering, as studied in this thesis, may pave the way for a new generation of improved antibody-based drugs for treating and curing human diseases.



▲ **Figure 3**

**Road map for next-generation antibody therapeutics.**

The basis of antibody drug discovery starts with a rational idea bringing disease biology, targets and antibody format/ backbone together. Improving the window between efficacy and/or safety of antibody drugs, also referred to as the therapeutic index (TI), requires engineering beyond the classical mAb format towards combinations or designer polyclonals and transforming the antibody backbone into a fit for purpose design. Different antibody engineering strategies discussed in this thesis are illustrated as stations within the road map leading towards improving and tailoring antibody function. Biologically focused drug discovery processes are crucial for the innovation of novel platform technologies that may broaden the road map towards the next generation of differentiated antibody therapeutics.

# REFERENCES

1. Melis JP, Strumane K, Ruuls SR, Beurskens FJ, Schuurman J, Parren PW. Complement in therapy and disease: Regulating the complement system with antibody-based therapeutics. *Mol Immunol* 2015; **67**(2 Pt A): 117-30.
2. Diebold CA, Beurskens FJ, de Jong RN, et al. Complement is activated by IgG hexamers assembled at the cell surface. *Science* 2014; **343**(6176): 1260-3.
3. de Jong RN, Beurskens FJ, Verploegen S, et al. A Novel Platform for the Potentiation of Therapeutic Antibodies Based on Antigen-Dependent Formation of IgG Hexamers at the Cell Surface. *PLoS Biol* 2016; **14**(1): e1002344.
4. de Weers M, Tai YT, van der Veer MS, et al. Daratumumab, a novel therapeutic human CD38 monoclonal antibody, induces killing of multiple myeloma and other hematological tumors. *J Immunol* 2011; **186**(3): 1840-8.
5. Teeling JL, French RR, Cragg MS, et al. Characterization of new human CD20 monoclonal antibodies with potent cytolytic activity against non-Hodgkin lymphomas. *Blood* 2004; **104**(6): 1793-800.
6. Xia MQ, Hale G, Waldmann H. Efficient complement-mediated lysis of cells containing the CAMPATH-1 (CDw52) antigen. *Mol Immunol* 1993; **30**(12): 1089-96.
7. Marshall MJE, Stopforth RJ, Cragg MS. Therapeutic Antibodies: What Have We Learnt from Targeting CD20 and Where Are We Going? *Frontiers in Immunology* 2017; **8**(1245).
8. Kumar A, Planchais C, Fronzes R, Mouquet H, Reyes N. Binding mechanisms of therapeutic antibodies to human CD20. *Science* 2020; **369**(6505): 793.
9. Rougé L, Chiang N, Steffek M, et al. Structure of CD20 in complex with the therapeutic monoclonal antibody rituximab. *Science* 2020: eaaz9356.
10. Golay J, Taylor RP. The Role of Complement in the Mechanism of Action of Therapeutic Anti-Cancer mAbs. *Antibodies (Basel, Switzerland)* 2020; **9**(4): 58.
11. Teeling JL, Mackus WJ, Wiegman LJ, et al. The biological activity of human CD20 monoclonal antibodies is linked to unique epitopes on CD20. *J Immunol* 2006; **177**(1): 362-71.
12. Barrena S, Almeida J, Yunta M, et al. Aberrant expression of tetraspanin molecules in B-cell chronic lymphoproliferative disorders and its correlation with normal B-cell maturation. *Leukemia* 2005; **19**(8): 1376-83.
13. Link MP, Bindl J, Meeker TC, et al. A unique antigen on mature B cells defined by a monoclonal antibody. *J Immunol* 1986; **137**(9): 3013-8.
14. Moore K, Cooper SA, Jones DB. Use of the monoclonal antibody WR17, identifying the CD37 gp40-45 Kd antigen complex, in the diagnosis of B-lymphoid malignancy. *J Pathol* 1987; **152**(1): 13-21.
15. Schwartz-Albiez R, Dörken B, Hofmann W, Moldenhauer G. The B cell-associated CD37 antigen (gp40-52). Structure and subcellular expression of an extensively glycosylated glycoprotein. *J Immunol* 1988; **140**(3): 905-14.
16. Beckwith KA, Byrd JC, Muthusamy N. Tetraspanins as therapeutic targets in hematological malignancy: a concise review. *Frontiers in physiology* 2015; **6**: 91-.
17. Strasser J, de Jong RN, Beurskens FJ, et al. Unraveling the Macromolecular Pathways of IgG Oligomerization and Complement Activation on Antigenic Surfaces. *Nano Letters* 2019; **19**(7): 4787-96.
18. Zuidschewoude M, Göttfert F, Dunlock VME, Figdor CG, van den Bogaart G, Spriel ABV. The tetraspanin web revisited by super-resolution microscopy. *Scientific Reports* 2015; **5**(1): 12201.

19. de Winde CM, Elfrink S, van Spriel AB. Novel Insights into Membrane Targeting of B Cell Lymphoma. *Trends Cancer* 2017; **3**(6): 442-53.
20. Hughes-Jones NC, Gorick BD, Howard JC, Feinstein A. Antibody density on rat red cells determines the rate of activation of the complement component C1. *Eur J Immunol* 1985; **15**(10): 976-80.
21. Derer S, Bauer P, Lohse S, et al. Impact of epidermal growth factor receptor (EGFR) cell surface expression levels on effector mechanisms of EGFR antibodies. *J Immunol* 2012; **189**(11): 5230-9.
22. Cragg MS, Morgan SM, Chan HT, et al. Complement-mediated lysis by anti-CD20 mAb correlates with segregation into lipid rafts. *Blood* 2003; **101**(3): 1045-52.
23. Deshaies RJ. Multispecific drugs herald a new era of biopharmaceutical innovation. *Nature* 2020; **580**(7803): 329-38.
24. Labrijn AF, Janmaat ML, Reichert JM, Parren PWHI. Bispecific antibodies: a mechanistic review of the pipeline. *Nature Reviews Drug Discovery* 2019; **18**(8): 585-608.
25. Wang Y, Yang S. Multispecific drugs: the fourth wave of biopharmaceutical innovation. *Signal Transduction and Targeted Therapy* 2020; **5**(1): 86.
26. Schuurman J, Parren PWHI. Editorial overview: Special section: New concepts in antibody therapeutics: What's in store for antibody therapy? *Current Opinion in Immunology* 2016; **40**: vii-xiii.





# SUMMARY

Owing to their high specificity and ability to engage multiple effector functions, combined with their modular and adaptable architecture fit for engineering approaches, antibodies have revolutionized drug development and treatment of human disease. Central to the mechanisms of action of many successful therapeutic antibodies are the affinity and avidity of binding interactions. Affinity can be defined as the strength of a single binding interaction between antibody and antigen, while avidity is determined by the accumulated binding strength of multiple individual non-covalent interactions including 1) Fab-mediated monovalent versus bivalent antigen binding (first order avidity), 2) Fc-mediated clustering and binding of immune effector molecules (higher order avidity) and 3) polyclonal binding interactions (cooperative avidity). Understanding and tuning these multidimensional avidity-based interactions formed the basis of this thesis. Special emphasis was placed on the role of Fc-mediated antibody clustering and how engineering strategies and platforms exploiting antibody clustering can be utilized for the design of novel and improved antibody therapeutics.

**Chapter 1** introduces the biology of antibody function including the role of antibody clustering in efficient activation of effector functions such as complement-dependent cytotoxicity (CDC), antibody-dependent cellular cytotoxicity and antibody-dependent phagocytosis. I highlighted the pioneering work of Diebold et al., who showed that CDC efficacy may be improved by introducing single point mutations in the Fc domain that enhance intermolecular Fc-Fc interactions between IgG molecules after cell surface antigen binding, thereby facilitating IgG hexamer formation. In **Chapter 2**, we demonstrated that combinations of antibodies targeting CD20 and CD37 cell surface receptors on malignant B cells, either as wild-type IgG1's or containing a hexamerization-enhancing Fc mutation (E430G), induced enhanced and synergistic CDC compared to the single agents alone. In depth analysis into the mechanism behind this synergy demonstrated that, upon antibody binding, both antibodies co-localized on the cell surface by forming mixed (hetero-) hexameric complexes and substantially enhanced C1q binding and recruitment, indicating more efficient complement activation.

In **Chapter 3**, we describe the preclinical development DuoHexaBody-CD37, a novel bispecific antibody targeting two non-overlapping CD37 epitopes (biparatopic) with an Fc domain engineered to allow enhanced target-dependent antibody hexamerization. Combining two approaches to increase antibody clustering into a single bispecific antibody molecule, including dual

epitope targeting and promoting antibody hexamerization by the E430G Fc mutation, proved to be the best strategy to optimally engage CDC and other Fc-mediated effector functions. In **Chapter 4**, the superior CDC efficacy of DuoHexaBody-CD37 was further demonstrated in primary tumor cells derived from patients with various B-cell malignancies. This research has led to Clinical Trial and Investigational New Drug applications for this molecule, as well as initiation of a first-in-human study in patients with relapsed or refractory B-cell non-Hodgkin lymphomas in the first half of 2020 (NCT04358458).

The observation that IgGs targeting different cell surface antigens can co-engage in mixed hexameric complexes inspired the design of AND-gated antibody pairs in **Chapter 5**, which require a combination of two input signals (dual antigen binding) to license activation of a functional output signal (effector functions such as complement activation or clustering-dependent target signaling). This research illustrated how modulating Fc-Fc-, C1q- and Fc gamma receptor interactions between two different antibody components may allow for precisely tuning and restricting IgG avidity interactions and subsequent complex formation to preferred cell surfaces, thereby potentially also improving the window between efficacy and/or safety.

The fundamental role of avidity as a central trigger for the overall efficacy of antibody functional responses was reviewed in **Chapter 6**. Herein, I comprehensively summarized how avidity interactions orchestrate both natural and therapeutic antibody mechanisms of action and highlighted how tuning avidity interactions may serve as a design principle for improving antibody function or introducing novel properties in next-generation antibody drugs. The detailed studies the biology on ordered antibody clustering provided in this thesis showed that there are multiple strategies to enhance antibody clustering and improve antibody function. The impact of these different approaches is discussed in **Chapter 7**. Overall, these studies emphasize that understanding antibody structure-function relations, as well as antibody interactions with both antigen and effector molecules or cells is crucial for designing novel and more efficacious antibody drugs to treat human disease.

# SAMENVATTING IN HET NEDERLANDS

## **Ons immuunsysteem**

Ons immuunsysteem (afweersysteem) beschermt ons tegen dagelijkse blootstelling aan ziekteverwekkers afkomstig van buiten het lichaam, zoals virussen en bacteriën. Ons immuunsysteem bestaat onder andere uit B cellen, een type witte bloedcellen, welke in staat zijn om antilichamen (eiwitten) te maken die deze ziekteverwekkers kunnen herkennen en eraan binden. Eenmaal gebonden dient een antilichaam als een herkenningspunt voor andere onderdelen van het immuunsysteem, welke vervolgens worden geactiveerd om de ziekteverwekker op te ruimen. Dit noemen we ook wel het opwekken van een immuunrespons. Tijdens een immuunrespons vermenigvuldigen B cellen zich en kunnen ze hun antilichamen moduleren om te zorgen dat deze de ziekteverwekker nog beter kunnen herkennen. Op deze manier past het immuunsysteem zich in rap tempo aan (adaptief) om binnen enkele dagen te evolueren tot een zeer specifieke afweer, welke in staat is om vele verschillende ziekteverwekkers te herkennen en te vernietigen.

## **Tumoren**

Naast blootstelling aan ziekteverwekkers afkomstig van buiten ons lichaam, kan ziekte ook ontstaan door lichaamseigen cellen die zich oncontroleerbaar gaan vermenigvuldigen en waaruit vervolgens een lokaal gezwel of tumor ontstaat. Daar waar gezonde cellen in het lichaam sterk worden gereguleerd en enkel delen wanneer dat nodig is, zoals bij cel vernieuwing of herstel, zijn bij de vorming van een gezwel of tumor één of meerdere cellen ontsnapt aan deze regulerende mechanismen. Men spreekt van kanker in het geval van kwaadaardig groeiende tumoren welke, in tegenstelling tot goedaardige of benigne tumoren, in staat zijn om het orgaan waarin ze zijn ontstaan te vernietigen en uit te kunnen zaaien (metastase) richting andere organen in het lichaam. Tumoren kunnen grofweg worden onderverdeeld in twee categorieën: hematologische (niet-solide) en solide tumoren. Hematologische tumoren ontstaan vaak uit witte bloedcellen of de voorlopers daarvan, zoals het beenmerg, of uit afweercellen die zich bevinden in lymfoïde organen zoals lymfeklieren. In tegenstelling tot hematologische tumoren, ontstaan solide tumoren in uit orgaan specifieke cellen, zoals cellen in de borst, longen en lever, en vormen een stevige tumormassa of gezwel.

De belangrijkste behandelingen voor kanker bestaan uit het chirurgisch verwijderen van de tumor, radiotherapie en chemotherapie. Voornamelijk radiotherapie en chemotherapie brengen ook vervelende bijwerkingen met

zich mee, omdat ze niet alleen de tumorcellen elimineren en/of hun groei beperken, maar ook schade toebrengen aan gezonde lichaamscellen. Nieuwe doelgerichte therapieën zijn daarom volop in ontwikkeling om specifiek de tumorcel te kunnen treffen en schade aan gezond weefsel zoveel mogelijk te beperken. Hierbij wordt steeds vaker het immuunsysteem ingezet om tumorcellen te bestrijden.

### **Antilichamen**

Antilichamen vormen een van de mogelijke doelgerichte therapieën om kanker te behandelen. Een antilichaam is een Y-vormig eiwitmolecuul en bevat twee domeinen; een Fab-domein bestaande uit twee fragmenten die binden aan een antigeen, ofwel een specifiek herkenningspunt op het oppervlak van een ziekteverwekker of tumorcel, en een Fc-domein welke kan interacteren met diverse moleculen en cellen van het immuunsysteem. De mens heeft vijf antilichaamklassen; IgA, IgD, IgE, IgG en IgM, waarbij Ig staat voor immunoglobuline en de toegevoegde letter staat voor de klasse. IgG is de meest voorkomende antilichaam klasse in bloed en kan verder worden onderverdeeld in vier typen; IgG1, IgG2, IgG3, en IgG4. Therapeutische antilichamen zijn meestal van het type IgG1 en kunnen op verschillende manieren zorg dragen voor het elimineren van de ziekteverwekker. Binding van het Fab-domein aan een antigeen op het oppervlak van een ziekteverwekker kan zijn functie blokkeren (neutralisatie), zoals bijvoorbeeld het infecteren van gezonde cellen. Daarnaast kan een gebonden antilichaam via zijn Fc-domein ook herkend worden door andere moleculen en cellen van het immuunsysteem, welke vervolgens worden geactiveerd om de ziekteverwekker te elimineren. Eliminatie kan bijvoorbeeld plaatsvinden door stoffen (aanwezig in bloed of geproduceerd door afweercellen) die gaatjes maken in de ziekteverwekker, waardoor deze sterft, of door een signaal te geven aan een afweercel om de ziekteverwekker op te eten en te verteren (fagocytose).

### **Promotieonderzoek**

Tijdens mijn promotieonderzoek heb ik bestudeerd hoe antilichamen samenwerken om ziekteverwekkers, en in het bijzonder tumor cellen, te elimineren. In **Hoofdstuk 1** wordt uitgelegd dat samenwerking tussen antilichamen plaats kan vinden door middel van clustering na binding aan receptoren (antigenen) die tot expressie komen op het oppervlak van een (tumor) cel. Cel-gebonden antilichamen kunnen onder andere clusters vormen via non-covalente interacties tussen Fc-domeinen, wat resulteert in hexameer-vormige complexen van zes antilichamen welke in staat zijn om efficiënter interacties aan te gaan met andere moleculen en cellen van het immuunsysteem. Een van die moleculen is genaamd C1q en vormt een onderdeel van een systeem aan factoren aanwezig in bloed, genaamd het complement systeem, die verantwoordelijk zijn voor eliminatie (lysis) van antilichaam-gebonden cellen. Antilichaam

hexamerizatie blijkt essentieel te zijn voor herkenning en binding van C1q en de daaropvolgende eliminatie van de cel. Daarnaast kunnen we hexamerizatie verder verbeteren door middel van puntmutaties in het Fc-domein van het antilichaam. Naast puntmutaties, ontdekten we in **Hoofdstuk 2** dat hexamerizatie ook verbeterd kan worden door antilichamen te combineren gericht tegen twee verschillende receptoren die tot expressie komen op dezelfde cel. We vonden dat deze antilichaam combinaties gemixte hexameer-vormige complexen kunnen vormen die leiden tot betere eliminatie van tumor cellen. Deze strategie brengt zodoende ook verschillende cel receptoren dicht bij elkaar en is daarom mogelijk ook relevant voor toekomstige combinatietherapieën.

De opgedane kennis over de rol van antilichaam clustering in het effectief elimineren van tumor cellen, zoals beschreven in dit proefschrift, kan ook bijdragen aan de ontwikkeling van nieuwe therapieën. In **Hoofdstuk 3** beschrijf ik de preklinische ontwikkeling van DuoHexaBody-CD37, een antilichaam gericht tegen het CD37 antigeen die tot expressie komt op tumor B cellen. De ontwikkeling van dit antilichaam was specifiek gericht op het optimaliseren van tumor cel eliminatie door middel van het activeren van het complement systeem. Naast het introduceren van een puntmutatie in het Fc-domein van dit antilichaam om hexamerizatie te verbeteren, ontdekten we dat het binden van twee verschillende herkenningspunten, ofwel epitopen, op hetzelfde CD37 antigeen leidde tot verdere verbetering van antilichaam hexamerizatie en complement-gemedieerde tumor cel lysis. DuoHexaBody-CD37 bevat daarom, naast een hexamerizatie-verbeterende puntmutatie in het Fc-domein, een Fab-domein welke twee verschillende CD37 epitopen bindt (bispecifiek). De preklinische activiteit van DuoHexaBody-CD37 werd verder bestudeerd in primaire tumor B cellen afkomstig van patiënten en is beschreven in **Hoofdstuk 4**. Momenteel wordt de veiligheid en voorlopige werkzaamheid van deze medicijn kandidaat getest in mensen met verschillende typen hematologische tumoren.

De ontdekking dat antilichamen gericht tegen verschillende cel receptoren samen kunnen werken door te clusteren in gemengde hexameer-vormige complexen, inspireerde het ontwerp van een nieuwe technologie om de functie van antilichamen te moduleren en verbeteren in **Hoofdstuk 5**. Deze technologie is gebaseerd op antilichaam combinaties die zijn ontworpen om alleen samen te werken in teams als beide componenten tegelijk zijn gebonden aan twee verschillende receptoren die tot expressie komen op dezelfde cel. Door het moduleren van interacties tussen twee verschillende antilichaam-componenten met behulp van puntmutaties in het Fc-domein, creëerden we 'AND-gated' antilichaam paren die een combinatie van twee invoersignalen (dubbele antigeenbinding) vereisen om activering van een functionele output

te licenseren (zoals bijvoorbeeld complement activatie). Op deze manier bleek het mogelijk om antilichaam clustering nauwkeurig af te stemmen en te beperken tot cellen van voorkeur, waardoor mogelijk ook het venster tussen werkzaamheid en/of veiligheid kan worden vergroot.

De fundamentele rol van antilichaam clustering als een centrale trigger voor de algehele functionaliteit van antilichamen wordt besproken in **Hoofdstuk 6**. Hierin vat ik uitgebreid samen hoe antilichaam clustering zowel natuurlijke als therapeutische antilichaam werkingsmechanismen orkestreert. Daarnaast wordt beschreven hoe antilichaam clustering kan dienen als een ontwerpprincipe voor het verbeteren van de antilichaam functie of het introduceren van nieuwe eigenschappen in de volgende generatie nieuwe antilichaam therapieën.

De gedetailleerde studies naar de biologie van antilichaam clustering, zoals beschreven in dit proefschrift, tonen aan dat er meerdere strategieën zijn om de clustering van antilichamen te versterken en de functie van antilichamen te verbeteren. De impact van deze verschillende strategieën wordt besproken in **Hoofdstuk 7**. De studies in dit proefschrift illustreren dat het begrijpen van antilichaam structuur en functie, evenals antilichaam interacties met zowel antigenen als effectormoleculen of cellen, cruciaal is voor het ontwerpen van nieuwe en effectievere antilichaam therapieën voor de behandeling van menselijke ziekten zoals kanker.

# DANKWOORD

Aan ieder begin komt een eind, zo ook aan dit proefschrift waar ik ontzettend trots op ben. Trots niet alleen op de inhoud, maar ook op degenen die gedurende de afgelopen jaren onmisbare stenen hebben bijgedragen aan dit proefschrift. Ik kan onmogelijk iedereen bij naam noemen die een rol heeft gespeeld in de totstandkoming van dit proefschrift, maar weet dat ik een ieder die zich aangesproken voelt enorm dankbaar ben.

Ik wil graag een aantal mensen specifiek bedanken. Te beginnen mijn promotor Paul Parren, bedankt dat je mij de kans hebt gegeven om mijn promotieonderzoek te doen binnen Genmab. Ik waardeer het ontzettend dat je ook na je vertrek bij Genmab jezelf hebt ingezet om mijn promotietraject te blijven begeleiden. Jouw passie voor de wetenschap, enorme schat aan kennis en je altijd scherpe blik hebben me geïnspireerd en gemotiveerd en zijn onmisbaar geweest in de totstandkoming van dit proefschrift.

Dan natuurlijk mijn copromotor Esther Breij, zonder jouw onvermoeibare steun had ik hier niet gestaan. Ondanks je volle agenda, kon ik altijd bij je terecht voor advies, nieuwe ideeën of gewoon een kop koffie en een goed gesprek.

Het begon allemaal bij het Antibody Research and Technologies team, ofwel ART. Frank (FBE) en Rob (RJO), bedankt voor het delen van jullie enthousiasme over HexaBody moleculen, het complement systeem en het oneindig aantal mogelijke variaties van IgG Fc puntmutaties. Marleen, bedankt voor het me wegwijs maken op lab en bovenal de gezelligheid tijdens koffie/lunch pauzes en buiten werktijd. Dan Janine, jouw deur staat altijd open en ik wil je bedanken voor de warme en inspirerende gesprekken. Ook bedankt aan andere (oud) ART teamgenoten: Bart-Jan, Gijs, Aran, Els, Xiaoguang, Kusai, Desiree, Jennifer, Klara, Tessa en Michel.

Ik vervolgde mijn promotietraject in het DuoHexaBody-CD37 team binnen Translational Research (TR). Marije, we begonnen als kamergenoten en al gauw werden we ook project teamgenoten. Bedankt voor alle gezelligheid en (PhD-gerelateerde) steun de afgelopen jaren, het is een feestje om met jou te werken! Juliette, de boemerang van Genmab; ik leerde je dubbel kennen als student en projectgenoot, vervolgens ook tijdelijk als collega, maar bovenal als super goede vriendin. Ik ben trots dat ik jou en Marije naast me mag hebben staan als paranimfen! Ook bedankt aan andere (oud) CD37- en TR

teamgenoten: Kristin, Ingrid (INI), Louise, Grietje, Laura (LVR), Berris, Laurens, Saida, Naomi, Kim, Wendy (WJA) en Barbara.

Dan mijn oud-kamergenoten Joyce, Ilse, Grietje, Maayke, Petra (PRB), Soeniel en Marije; bedankt voor de gezelligheid, eindeloze snoepvoorraden en fijne kerstsferen op de kamer. Studenten die ik heb mogen begeleiden; Lisa, Julie, Juliette, Janita en Sander: bedankt voor al het werk dat jullie me uit handen hebben genomen. Genmab oud-promovendi; Jeroen (JLA), Bart (BGO), Patrick (PEN) en Marije: bedankt voor het geven van het goede voorbeeld.

I also would like to thank Genmab colleagues at other departments, including LD&T (Rik (RRA), Marcel (MAR) and Dennis (DEV)), NAPR (Sandra (SVE), Jeroen (JBR), Ilse, Marcel (MBR), Patrick (PEN) and Bart (BGO)) and IPR/Medical Affairs (Monica, Bilge and Payal), for their one-team spirit and efforts to support this thesis. Daarnaast natuurlijk ook Joost Bakker en Laurant Blommers; bedankt voor de prachtige vormgeving van dit proefschrift.

In addition, I would like to thank colleagues at the University of Virginia (Ron and Margaret), Amsterdam Medical Centre (Hilma, Tuna and Martine), Radboud University Medical Centre (Annemiek and Simar) and Genentech (Greg), whom I have had the privilege to collaborate with during the past few years.

Natuurlijk valt geen promotietraject te voltooien zonder ontspanning. Liesbeth, zonder onze sauna uitjes ieder kwartaal had ik het niet volgehouden. Vriend(inn)en in en rondom Houten; bedankt voor de gezelligheid en de slapeloze nachten in de Ubica en omstreken.

Pap, mam, jullie onvermoeibare vertrouwen in mij zorgt ervoor dat ik iedere dag het beste uit mezelf kan halen, bedankt! Met vier kids is het ook altijd een gezellige boel aan tafel. Anouk, Joost en Manon, jullie zijn de leukste thuis!

Tot slot, lieve Jeroen: tussen de regels door ben jij degene die me heeft geholpen er een samenhangend verhaal van te maken. Dankzij jouw rotsvaste vertrouwen, oneindige geduld, luisterende oor, overzichtelijke Excelletjes en bovenal onvoorwaardelijke liefde is het me gelukt.



# PUBLICATIONS

1. van der Horst HJ, Oostindie SC, Cillessen S, et al. Potent Preclinical Efficacy of DuoHexaBody-CD37 in B-Cell Malignancies. *Hemasphere* 2021; **5**(1): e504.
2. Oostindie SC, van der Horst HJ, Kil LP, et al. DuoHexaBody-CD37<sup>\*</sup>, a novel biparatopic CD37 antibody with enhanced Fc-mediated hexamerization as a potential therapy for B-cell malignancies. *Blood Cancer J* 2020; **10**(3): 30.
3. Lubbers R, Oostindie SC, Dijkstra DJ, et al. Carbamylation reduces the capacity of IgG for hexamerization and complement activation. *Clin Exp Immunol* 2020; **200**(1): 1-11.
4. Engelberts PJ, Hiemstra IH, de Jong B, Schuurhuis DH, Meesters J, Beltran Hernandez I, Oostindie SC, et al. DuoBody-CD3xCD20 induces potent T-cell-mediated killing of malignant B cells in preclinical models and provides opportunities for subcutaneous dosing. *EBioMedicine* 2020; **52**: 102625.
5. Oostindie SC, van der Horst HJ, Lindorfer MA, et al. CD20 and CD37 antibodies synergize to activate complement by Fc-mediated clustering. *Haematologica* 2019; **104**(9): 1841-52.
6. Cook EM, Lindorfer MA, van der Horst H, Oostindie SC, et al. Antibodies That Efficiently Form Hexamers upon Antigen Binding Can Induce Complement-Dependent Cytotoxicity under Complement-Limiting Conditions. *J Immunol* 2016; **197**(5): 1762-75.
7. de Jong RN, Beurskens FJ, Verploegen S, Strumane K, van Kampen MD, Voorhorst M, Horstman W, Engelberts PJ, Oostindie SC, et al. A Novel Platform for the Potentiation of Therapeutic Antibodies Based on Antigen-Dependent Formation of IgG Hexamers at the Cell Surface. *PLoS Biol* 2016; **14**(1): e1002344.

# ABBREVIATIONS

AAALAC	association for assessment and accreditation of laboratory animal care	51Cr	chromium-51
7-AAD	7-aminoactinomycin	CRIB	charge repulsion induced bispecificity
Ab	antibody	CRP	complement regulatory protein
ABC	activated B cell	CTRL	control
(s)ABC	(specific) antibody bound per cell	DC	dendritic cells
ABC-DLBCL	activated B-cell diffuse large B-cell lymphoma	DLBCL	diffuse large B-cell lymphoma
ABTS	2,2'-azino-bis(3-ethylbenzothiazoline-6-sulfonic acid)	DMSO	dimethyl sulfoxide
ADC	antibody drug conjugate	DR5	death receptor 5
ADCC	antibody-dependent cellular cytotoxicity	DSMZ	Deutsche Sammlung von Mikroorganismen und Zellkulturen
ADCP	antibody-dependent cellular phagocytosis	EBV	Epstein-Barr virus
AF	Alexa Fluor®	EC	extra cellular
AGK	G237A, E430G, S440K	EC50	effective concentration 50%
AID	activation-induced deaminase	ECD	extra cellular domain
AKT	protein kinase B	EDTA	Ethylene Diamine Tetra-Acetic Acid
ALL	acute lymphoblastic leukemia	EGFR	epidermal growth factor receptor
AML	acute myeloid leukemia	ELISA	enzyme linked immuno sorbent assay
ANOVA	analysis of variance	ET	energy transfer
APC	allophycocyanin	E:T	effector to target ratio
ATCC	American Type Culture Collection	Fab	fragment antigen binding
AUC	area under the curve	FACS	fluorescence activated cell sorting
BaCa	Bispecific-Anchored Cytotoxicity Activator	Fc	Fragment crystallizable
BCR	B-cell receptor	FcR	Fc receptor
BL	Burkitt's lymphoma	FcRn	neonatal Fc receptor
BLA	Biologics license application	FCS	fetal calf serum
BMMC	bone marrow mononuclear cells	FcγR	Fc gamma receptor
bNAb	broadly neutralizing antibody	FDA	food and drug administration
B-NHL	B-cell non-Hodgkin's lymphoma	FELASA	European laboratory animal science associations
BSA	bovine serum albumin	FITC	fluorescein isothiocyanate
BV	brilliant violet	FL	follicular lymphoma
CAR	chimeric antigen receptro	FOLR-1	folate receptor-1
CAR-T cell	chimeric antigen receptor-bearing T-cell	FRET	Förster resonance energy transfer
CCR4	C-C Motif Chemokine Receptor 4	GC	germinal center
CD	cluster of differentiation	GCB	germinal center B cell
CDC	complement-dependent cytotoxicity	GC-DLBCL	germinal center diffuse large B-cell lymphoma
CDR	complementarity-determining region	gMFI	geometric mean fluorescence intensity
CDX	cell line-derived xenograft	HC	heavy chain
CFSE	carboxyfluorescein succinimidyl ester	HEK	human embryonic kidney
CH	heavy chain constant domain	HER(2, 3)	human epidermal growth factor receptor
CI	combination index	HERA	hexavalent receptor agonist
CL	light chain constant domain	HI-NHS	heat-inactivated normal human serum
CLL	chronic lymphocytic leukemia	HIV	human immunodeficiency virus
CODV-Ig	cross-over dual variable Ig-like protein	HLA	human leucocyte antigen
COVID-19	coronavirus disease 2019	hMDM	human monocyte-derived macrophage
		HRP	horseradish peroxidase
		Hx	hexamerization-enhanced

IC50	inhibiting concentration 50%	PerCP	peridinin chlorophyll
Ig	immunoglobulin (A, D, E, G, M)	Pen/strep	penicillin streptomycin
IgV	immunoglobulin variable region	PI	propidium iodide
IgC	immunoglobulin constant region	PI3K	phosphatidyl-4-5-biphosphate 3-kinase
IL	interleukin	PK	pharmacokinetics
IP	intraperitoneal	RGE	G236R, E430G, K439E
ITAM	immunoreceptor tyrosine-based activation motif	RLU	relative luminescence units
ITIM	immunoreceptor tyrosine-based inhibitory motif	RNA	ribonucleic acid
IV	intravenous	RR	relapsed/refractory
LC	light chain	RT	room temperature
LN	lymph node	SARS-CoV-2	severe acute respiratory syndrome coronavirus 2
mAb	monoclonal antibody	SC	subcutaneous
MAC	membrane attack complex	sdAb	single-domain antibody
MCL	mantle cell lymphoma	SCID	severely combined immunodeficient
mCRC	metastatic colorectal cancer	SD	standard deviation
mCRP	membrane complement regulatory protein	SEM	standard error of the mean
M-CSF	macrophage colony stimulating factor	SHM	somatic hypermutation
MESF	molecules of equivalent soluble fluorophores	SMIP	small immune-pharmaceutical protein
MET	tyrosine-protein kinase Met	SOCS3	suppressor of cytokine signalling 3
MFI	mean fluorescence intensity	TCR	T-cell receptor
MHC	major histocompatibility complex	TEM	tetraspanin-enriched microdomain
MM	multiple myeloma	TI	therapeutic index
MNC	mono nuclear cells	TI	test item
MPER	membrane-proximal external region	TNFR	tumor necrosis factor receptor
MoA	mechanism of action	TNFRSF	tumor necrosis factor receptor super family
MZL	marginal zone lymphoma	TRAIL	tumor necrosis factor-related apoptosis-inducing ligand
NC	negative control	WB	whole blood
ND	newly diagnosed	WT	wild type
ND	not determined	VHH	single domain antibody
NHS	normal human serum	ZEBOV	Zaire ebolavirus
NHL	non-hodgkin's lymphoma		
NK	natural killer		
NKT	natural killer T cell		
NOS	not otherwise specified		
NSCLC	non-small cell lung cancer		
OX40	tumor necrosis factor receptor superfamily member 4		
PBMC	peripheral blood mononuclear cells		
PBS	phosphate buffered saline		
PBST	phosphate buffer saline supplemented with tween		
PC	positive control		
PCD	programmed cell death		
PDX	patient-derived xenograft		
PE	R-Phycoerythrin		

# CURRICULUM VITAE

Simone Charlotte Oostindie was born on September 17, 1990 in Delft, The Netherlands. After finishing her high school at Lyceum de Hoven in Gorinchem in 2008, she studied Biology at Wageningen University & Research (WUR). In 2012, she received her Bachelor's degree and continued with her Master's degree Biology, which she received in 2014. During her Master's degree, she performed internships at The Walter and Eliza Hall Institute of Medical Research in Australia, where she studied the effect of regulatory signals on lymphocyte proliferation and survival and at Genmab, where she worked on synergistic antibody combinations targeting B-cell malignancies. In January 2015, she initially started as a research associate at Genmab in the Antibody Research and Technology department working on the discovery of novel technology platforms for the generation of differentiated therapeutic antibodies. She was then offered a PhD position under the supervision of Prof. Dr. Paul W.H.I. Parren and Dr. Esther C.W. Breij. During her PhD program, she worked in the Antibody Research and Technology department to study antibody clustering mechanisms to enhance therapeutic potency, as well as in the Translational Research department, where she was involved in the preclinical development of DuoHexaBody-CD37. The results of these studies are presented in this thesis.

